

Centre for Cell Signalling

Barts & The London School of Medicine and Dentistry

Queen Mary University of London

**THE ROLE OF PI3K p110 δ IN THE REGULATION OF GENE
EXPRESSION IN MURINE MACROPHAGES**

PhD Thesis

Postgraduate Student: Emily Burns

Supervisors: Prof. B. Vanhaesebroeck & Dr. B. Twomey

Sponsors: BBRSC and UCB

Abstract

PI3K are a family of lipid kinase enzymes that are involved in a broad spectrum of cellular, physiological and pathological processes. Notably, PI3K dysfunction is associated with cancer, inflammation and metabolism.

The PI3K family consists of three classes, Class I, Class II and Class III, which are defined according to their structure, function and lipid specificity. Class I is further subdivided into Class IA, which consists of p110 α , p110 β and p110 δ , and Class IB, which consists of p110 γ . Both p110 α and p110 β are ubiquitously expressed. Conversely, p110 δ and p110 γ have a restricted tissue distribution, limited mainly to leukocytes, where they are highly enriched.

In this work, we have focused on understanding the role of p110 δ in macrophages and specifically, on gaining insight into its role in genome-wide transcriptional regulation. Our results suggest that the contribution of p110 δ activity to transcriptional regulation in growing primary macrophages is very limited. Genetic or pharmacological inactivation of p110 δ resulted in differential regulation of less than twenty-five unique genes. Interestingly, at the level of genome-wide transcription, we have observed a significant difference between the effects of pharmacological and genetic inactivation. Indeed, none of the genes identified were differentially regulated as a result of both pharmacological and genetic inactivation of p110 δ . We discovered that the majority of the genes differentially regulated in p110 δ KI macrophages are located within close proximity to the *Pik3cd* gene. We propose that the differential regulation of these genes represents an artefact of the genetic engineering strategy employed to generate the p110 δ KI mice. We have confirmed that genetic inactivation of p110 δ results in reduced expression of *Rab6b*, a gene which is not linked to *Pik3cd*. We have confirmed that this does translate into a reduced level of rab6b protein in p110 δ KI macrophages.

Parts of this thesis have been published elsewhere:

Distinct roles of class IA PI3K isoforms in primary and immortalised macrophages

Evangelia A. Papakonstanti, Olivier Zwaenepoel, Antonio Bilancio, Emily Burns, Gemma E. Nock, Benjamin Houseman, Kevan Shokat, Anne J. Ridley and Bart Vanhaesebroeck, *Journal of Cell Science* [1]

Contents

LIST OF FIGURES	8
LIST OF TABLES	11
1. INTRODUCTION	16
1.1. THE PI3K FAMILY OF ENZYMES	16
1.1.1. <i>Class I PI3K</i>	17
1.2. CELLULAR SIGNALLING BY CLASS IA PI3K ISOFORMS.....	18
1.2.1. <i>Activation of Class IA PI3K isoforms</i>	18
1.2.2. <i>Signalling downstream of Class IA PI3K activation</i>	20
1.2.3. <i>Temporal regulation of PI3K signalling</i>	20
1.2.4. <i>Akt</i>	21
1.2.5. <i>Regulation of transcription downstream of PI3K-Akt pathway</i>	24
1.3. INVESTIGATING THE PHYSIOLOGICAL AND PATHOLOGICAL IMPLICATIONS OF PI3K ACTIVITY	31
1.3.1. <i>Tools and models for investigating PI3K functions</i>	31
1.3.2. <i>Non-redundant cell-specific functions of Class IA PI3K isoforms</i>	35
1.4. CELLULAR AND PHYSIOLOGICAL ROLES OF CLASS IA PI3KS.....	36
1.4.1. <i>Cellular and physiological roles of p110α</i>	36
1.4.2. <i>Cellular and physiological roles of p110β</i>	37
1.4.3. <i>Cellular and physiological roles of p110δ</i>	37
1.4.4. <i>Cellular and physiological roles of p110γ</i>	40
1.5. MACROPHAGES IN THE IMMUNE SYSTEM	42
1.5.1. <i>The components of the immune system and stages of immune response</i>	42
1.5.2. <i>Initiation of the adaptive immune response</i>	43
1.5.3. <i>Recognition of lipopolysaccharide and other pathogens by macrophages</i>	44
1.5.4. <i>The importance of a balanced immune response</i>	50
1.6. THERAPEUTIC POTENTIAL OF PI3K INHIBITION	52
1.6.1. <i>Therapeutic potential of targeting p110α</i>	52
1.6.2. <i>Therapeutic potential of targeting p110β</i>	52
1.6.3. <i>Therapeutic potential of targeting p110δ</i>	53
1.7. PROJECT AIMS AND OBJECTIVES	58
2. MATERIALS AND METHODS	59
2.1. MICE.....	59
2.1.1. <i>Genotyping of mice</i>	59

2.2.	REAGENTS, SOLUTIONS AND BUFFERS	61
2.2.1.	<i>Inhibitors</i>	62
2.2.2.	<i>Antibodies</i>	63
2.3	CELL CULTURE	64
2.3.1	<i>Macrophage cell lines</i>	64
2.3.2	<i>Isolation and differentiation of primary macrophages</i>	65
2.3.3	<i>Cell stimulation</i>	68
2.4	PROTEIN ANALYSIS AND DETECTION	68
2.4.1	<i>Western blot analysis</i>	68
2.4.2	<i>Semi-quantitative analysis of PI3K activation using p-Akt to Akt ratios</i>	71
2.5	FLUORESCENCE ACTIVATION CELL SORTING (FACS)	71
2.5.1	<i>Preparation and staining of cells</i>	71
2.5.2	<i>Analysis of stained cell by FACS</i>	71
2.6	EXTRACTION OF CELLULAR RNA AND QUALITY CONTROL.....	72
2.6.1	<i>Cell lysis</i>	72
2.6.2	<i>RNA extraction</i>	72
2.6.3	<i>RNA quantification and purity assessment</i>	72
2.7	QUANTITATIVE REAL-TIME PCR (qPCR)	73
2.7.1	<i>Reverse transcription</i>	74
2.7.2.	<i>qPCR</i>	75
2.7.3	<i>Data extraction and analysis</i>	77
2.7.4	<i>Semi-high throughput qPCR</i>	79
2.8	GENOME-WIDE EXPRESSION ANALYSIS.....	82
2.8.1.	<i>RNA integrity</i>	82
2.8.2.	<i>Affymetrix genome-wide expression analysis</i>	85
3.	INVESTIGATING THE FUNCTIONS OF CLASS IA PI3K ISOFORMS IN MACROPHAGES	90
3.1.	INTRODUCTION.....	90
3.2.	INVESTIGATING A CORRELATION BETWEEN IMMORTALISED STATE AND LOSS OF P110 DELTA DEPENDENCY IN MACROPHAGES.....	91
3.3.	THE CONTRIBUTIONS OF CLASS IA PI3K ISOFORM TO AKT ACTIVATION MACROPHAGE CELL LINES.....	92
3.4.	THE EFFECTS OF INHIBITING CLASS IA ISOFORMS IN RAW 264.7 MACROPHAGES.....	94
3.5.	INVESTIGATING THE UNCHARACTERISTIC DEPENDENCE OF BAC1.2F5 MACROPHAGES ON P110 ALPHA.....	96
3.6	CONCLUSION	97
3.6.	DISCUSSION	97
4.	INVESTIGATING THE EFFECTS OF PHARMACOLOGICAL INACTIVATION OF P110 DELTA ON THE TRANSCRIPTOME OF RAW 264.7 MACROPHAGES	103
4.1.	INTRODUCTION AND AIMS OF STUDY.....	103

4.2.	CHOOSING A MACROPHAGE LINE TO STUDY	104
4.3.	CHRONIC PRE-TREATMENT WITH IC87114 REDUCED AKT ACTIVATION.....	105
4.3.1.	<i>Final experiment design</i>	<i>106</i>
4.4.	EXTRACTION AND QUALITY CONTROL OF RNA.....	107
4.5.	OBTAINING EXPRESSION DATA.....	107
4.6.	MULTIVARIANCE ANALYSIS TO IDENTIFY SAMPLE CLUSTERS	108
4.6.1.	<i>Samples separate according to LPS-stimulation status.....</i>	<i>108</i>
4.7.	IDENTIFICATION OF INDIVIDUAL PROBE SETS AFFECTED BY IC87114 TREATMENT	109
4.8.	IDENTIFICATION ENRICHED FUNCTIONS AMONGST THE GENES AFFECTED BY IC87114.....	115
4.9.	IDENTIFICATION OF ENRICHMENT OF PATHWAY COMPONENTS AMONGST THE GENES AFFECTED BY IC87114.....	116
4.10.	IDENTIFICATION OF POTENTIAL BIOMARKERS OF P110 DELTA INACTIVATION.....	119
4.10.1.	<i>Biomarker characteristics.....</i>	<i>119</i>
4.10.2.	<i>Identification of potential biomarkers within the gene list</i>	<i>119</i>
4.10.3.	<i>Two potential biomarkers of p110δ inactivation.....</i>	<i>122</i>
4.11.	CONCLUSION	123
4.12.	DISCUSSION	124
5.	INVESTIGATING THE EFFECTS OF GENETIC INACTIVATION OF P110 DELTA ON THE TRANSCRIPTOME OF PRIMARY MACROPHAGES.....	127
5.1.	DEVELOPMENT AND VALIDATION OF A MODIFIED PRIMARY MACROPHAGE EXTRACTION AND DIFFERENTIATION PROTOCOL.....	127
5.1.1.	<i>Addressing difficulties with the differentiation of primary macrophages.....</i>	<i>127</i>
5.1.2.	<i>The modified protocol for production of differentiated macrophages.....</i>	<i>128</i>
5.1.3.	<i>Validation of macrophages generated using modified protocol.....</i>	<i>128</i>
5.2.	AIMS OF GENOME-WIDE EXPRESSION ANALYSIS OF P110 DELTA KI AND WT MACROPHAGES.....	131
5.3.	CONDITIONS USED FOR GENOME-WIDE EXPRESSION ANALYSIS.....	131
5.4.	OBTAINING GENOME-WIDE EXPRESSION DATA FOR WT AND P110 DELTA KI MACROPHAGES	133
5.4.1.	<i>Analysis of clustering within the dataset.....</i>	<i>133</i>
5.4.2.	<i>Identification of individual genes affected by p110δ inactivation.....</i>	<i>136</i>
5.4.3.	<i>Identification of functions enriched in the list of differentially genes</i>	<i>139</i>
5.4.4.	<i>Identification of most relevant networks using IPA</i>	<i>140</i>
5.5.	IDENTIFICATION OF POTENTIAL BIOMARKERS FOR P110 DELTA INACTIVATION.....	142

5.5.1.	<i>Identification of the differential regulation most representative of p110δ inactivation</i>	143
5.6.	VALIDATION OF THE DIFFERENTIAL EXPRESSION OF GENES IN P110 DELTA KI MACROPHAGES	144
5.6.1.	<i>The necessity to validate relationships identified by genome-wide analysis</i>	144
5.6.2.	<i>Validation of differential expression using Low Density Taqman Array (LDA)</i>	145
5.6.3.	<i>Validation confirmed differential regulation of seven genes in p110δ KI macrophages</i>	148
5.6.4.	<i>Summary of validation findings</i>	153
5.7.	VALIDATION OF P110 DELTA-REGULATED GENE EXPRESSION AT THE PROTEIN LEVEL	154
5.7.1.	<i>Rab6b protein was reduced in p110δ KI macrophages</i>	155
5.7.2.	<i>Normal expression of rab6b protein in whole brain tissue derived from p110δ KI mice</i>	156
5.7.3.	<i>Validation of the specificity of the commercial rab6b-specific antibody</i>	158
5.8.	CONCLUSION	158
6.	INVESTIGATING THE EFFECTS OF PHARMACOLOGICAL INACTIVATION OF P110 DELTA ON THE PRIMARY MACROPHAGE TRANSCRIPTOME	162
6.1.	INTRODUCTION	162
6.2.	THE EFFECT OF IC87114 TREATMENT ON AKT ACTIVATION	162
6.2.1.	<i>Activation of Akt in macrophages differentiated in the presence of IC87114</i>	163
6.3.	GENOME-WIDE EXPRESSION ANALYSIS EXPERIMENTAL DESIGN AND IMPLEMENTATION	163
6.4.	INVESTIGATING THE GENOME-WIDE EXPRESSION IMPACT OF IC87114 TREATMENT	164
6.4.2.	<i>Multivariate Analysis to determine sample clusters</i>	164
6.4.3.	<i>The expression of the classifier probe sets was not sufficient to identify inactivation of p110δ</i>	165
6.4.4.	<i>Identification of genes differentially regulated in WT macrophages differentiated in IC87114</i>	166
6.5.	COMPARISON OF PHARMACOLOGICAL AND GENETIC INACTIVATION OF P110 DELTA	168
6.5.1.	<i>The genes differentially regulated in p110δ KI macrophages were not affected by IC87114</i>	168
6.5.2.	<i>Analysis of the chromosomal locations of the genes identified</i>	171
6.5.3.	<i>Unlinked genes such as Rab6b are not affected by IC87114</i>	174
6.6.	CONCLUSION	176
7.	DISCUSSION	178
7.1.	THE EFFECTS OF GENETIC AND PHARMACOLOGICAL INACTIVATION OF P110 DELTA ON TRANSCRIPTIONAL REGULATION	178

7.1.1.	<i>Genetic inactivation of p110δ has a minimal effect on gene expression.....</i>	178
7.1.2.	<i>The genome-wide perspective.....</i>	182
7.2.	INVESTIGATING THE EFFECTS OF P110 DELTA ACTIVITY ON <i>RAB6B</i> EXPRESSION.....	185
7.2.1.	<i>Reduced expression of Rab6b in p110δ KI macrophages but not in p110δ KI brain tissue</i>	185
7.2.2.	<i>Possible functional consequences of reduced rab6b in p110δ KI macrophages</i>	186
7.3.	COMPARING THE EFFECTS OF PHARMACOLOGICAL AND GENETIC INACTIVATION OF P110 DELTA ON PRIMARY MACROPHAGE TRANSCRIPTOME	192
7.3.1.	<i>Pharmacological inactivation of p110δ results in minimal changes to the transcriptome</i>	192
7.3.2.	<i>Comparison of genetic and pharmacological inactivation of p110δ.....</i>	193
7.3.3.	<i>Enrichment of genes differentially regulated in p110δ KI macrophages flanking the Pik3cd locus</i>	194
7.4.	EXPLAINING PGE OF GENES DIFFERENTIALLY REGULATED IN P110 DELTA KI MACROPHAGES	195
7.4.1.	<i>Disruption to the expression of linked genes as an artefact of the D910A mutation</i>	196
7.4.2.	<i>Differential regulation represents the retention of 129-derived genetic material.....</i>	196
7.5.	LOCUS INDEPENDENT DIFFERENTIAL EFFECTS OF GENETIC AND PHARMACOLOGICAL INACTIVATION.....	205
7.5.1.	<i>Why are unlinked genes also not affected by differentiation in IC87114?</i>	206
7.6.	CONCLUDING REMARKS.....	208
8.	REFERENCES	210

LIST OF FIGURES

1. INTRODUCTION

Figure 1.1. Classification, domain structure and in vivo substrate preferences of PI3K enzymes	16
Figure 1.2. The classification of Class IA and Class IB PI3K isoforms	17
Figure 1.3. PI3K heterodimer recruitment to the membrane	19
Figure 1.4. Enzymatic conversion of PIP ₂ to PIP ₃ by PI3K activity and dephosphorylation to PIP ₂ by PTEN	21
Figure 1.5. Signalling Cascade initiated downstream of PI3K-Akt activation.....	22
Figure 1.6. Schematic illustration of PI3K signalling regulating transcription	26
Figure 1.7. Schematic representing the role of Class IA PI3K isoforms in CSF-1-induced responses in BAC1.2F5 macrophages	35
Figure 1.8. Illustration of the haematological cell lineage	42
Figure 1.9. LPS is recognised by macrophages via a PRR complex in association with an accessory protein	45
Figure 1.10. Illustration of the activation of NF- κ B-dependent transcription by LPS via the MyD88-dependent pathway.....	46
Figure 1.11. Schematic of the differential effect of PI3K activity on cytokine production mediated modulation of GSK-3 and mTORC1 activity	49

2. MATERIALS AND METHODS

Figure 2.1. Timeline of primary macrophage extraction and differentiation.....	66
Figure 2.2. Modified primary macrophage differentiation protocol	67
Figure 2.3. TaqMan [®] gene-specific probes	74
Figure 2.4. qPCR amplification plot features	78
Figure 2.5. Agilent Electropherogram	83
Figure 2.6. RNA integrity number	84
Figure 2.7. Schematic of the hybridisation of a labeled target sequence from the sample to a probe.....	85
Figure 2.8. A summary of the protocol for the GeneChip [®] 3' <i>In vitro</i> transcription (IVT) expression kit.....	87

3. RESULTS

Figure 3.1. CSF-1-induced p-Akt in primary macrophages is significantly reduced by inhibition of p110 δ , and is not significantly affected by inhibition of either p110 α or p110 β	91
Figure 3.2. BAC1.2F5 macrophages require p110 α activity for basal and CSF-1-induced p-Akt.....	92
Figure 3.3. Participation of Class IA PI3K isoforms in induction of p-Akt downstream of CSF-1 varies in J774.2 and IC-21 macrophage lines.....	93
Figure 3.4. Inhibition of individual Class IA PI3K isoforms does not reduce CSF-1-induced p-Akt in RAW 264.7 macrophages.....	94
Figure 3.5. Pan-PI3K inhibition reduced CSF-1-induced p-Akt in RAW 264.7 macrophages ...	95

Figure 3.6. Inhibition of p110 δ reduces CSF-1-induced p-Akt in RAW 264.7 macrophages in medium containing 10% FBS	96
---	----

4. RESULTS

Figure 4.1. Inhibition of p110 δ reduced basal and LPS-stimulated p-Akt in RAW 264.7 macrophages.....	105
Figure 4.2. Inhibition of p110 δ for 2 h or 72 h reduced basal and LPS-stimulated p-Akt in RAW 264.7 macrophages.....	106
Figure 4.3. RNA extracted from RAW 264.7 macrophages was intact and of high quality	107
Figure 4.4. Samples clustered according to treatment groups but there was variability within groups	109
Figure 4.5. The top ten molecular and cellular functions significantly enriched in the list of genes affected by IC87114-treatment.....	115
Figure 4.6. The top two networks found to be most relevant to our list of genes affected by IC87114-treatment	117
Figure 4.7. Subcellular view of top two networks relevant to the list of genes affected by IC87114-treatment	120

5. RESULTS

Figure 5.1. Photographs showing the normal range of morphology displayed by differentiated primary macrophages generated using the modified protocol	128
Figure 5.2. WT and p110 δ KI macrophages both express F4/80	129
Figure 5.3. WT and p110 δ KI macrophages express IA/IE at low levels in the unstimulated state and upregulate IA/IE significantly on LPS stimulation	130
Figure 5.4. Scheme of genome-wide expression analysis of p110 δ KI macrophages and WT macrophages.....	132
Figure 5.5. PCA revealed that the samples separated by genotype	133
Figure 5.6. Hierarchical clustering identified an outlier and a batch effect	135
Figure 5.7. Venn diagram of the twenty-five probe sets that were found to be differentially regulated in p110 δ KI macrophages compared to in WT macrophages	136
Figure 5.8. The top ten most statistically significant molecular and cellular functions enriched in the list of genes differentially regulated in p110 δ KI macrophages	139
Figure 5.9. IPA analysis revealed the Inflammatory Response, Antimicrobial Response, Cell-To-Cell Signalling and Interaction network as relevant to the list of genes differentially regulated in p110 δ KI macrophages	141
Figure 5.10. Classifier identified four genes (six probe sets) that were most representative of the four different conditions (WT basal, WT LPS, DK1 basal, DK1 LPS).....	144
Figure 5.11. Heatmap of comparative gene expression data obtained by LDA and Affymetrix.....	148
Figure 5.12. Expression of <i>Pdpm1</i> , <i>Fblim1</i> , <i>Plod1</i> and <i>Rab6b</i> was decreased in p110 δ KI macrophages.....	149
Figure 5.13. Expression of <i>Clstn</i> was increased in basal and to a lesser extent in LPS-stimulated p110 δ KI macrophages.....	150
Figure 5.14. Expression of <i>Mthfr</i> and <i>Ube4b</i> was decreased in LPS-stimulated p110 δ KI macrophages.....	151
Figure 5.15. Heatmap summary of the validation of the differential regulation of seven genes p110 δ KI macrophages compared to in WT macrophages in basal (-) and LPS-stimulated (+) conditions.....	153

Figure 5.16. Decreased expression of rab6b protein in p110δ KI macrophages compared to WT macrophages	155
Figure 5.17. Expression of rab6b is unaffected in p110δ KI brain tissue compared to expression in WT brain tissue	157
Figure 5.18. The Rab6b antibody detects a signal in the brain but not the liver samples whilst the Rab6a antibody detects a signal in both tissues	158

6. RESULTS

Figure 6.1. p110δ-selective inhibition reduced basal and LPS-induced p-Akt	162
Figure 6.2. Long-term pharmacological inactivation of p110δ in WT macrophages represses p-Akt	163
Figure 6.3. Schematic of the differentiation of WT macrophages in the presence of IC87114 or DMSO	164
Figure 6.4. PCA analysis revealed samples clustered according to LPS stimulation status rather than genotype	165
Figure 6.5. The classifier probe set produced by analysis of p110δ KI versus WT study did not classify WT IC87114 samples as p110δ KI	166
Figure 6.6. Comparison of the genome-wide expression analysis of the effects of genetic and pharmacological inactivation of p110δ	169
Figure 6.7. The concentration of IC87114 in the medium was within a suitable range throughout the course of the experiment	170
Figure 6.8. Positional gene enrichment analysis revealed a very highly statistically significant cluster of genes enriched on chromosome four, locus E1	173
Figure 6.9. Expression of rab6b protein is unaffected in WT macrophages differentiated in either 1 μM or 5 μM IC87114	175

7. DISCUSSION

Figure 7.1. Schematic of vesicle trafficking in the endomembrane system	187
Figure 7.2. Schematic of a nerve cell with extended axon and dendrites along which numerous cargo must be transported	189
Figure 7.3. PGE reveals a significant enrichment of genes differentially regulated in p110δ KI macrophages in the region proximal to <i>Pik3cd</i>	195
Figure 7.4. Schematic of the generation of genetically heterogenous/chimerical mice using 129-derived ES cell line and a C57BL/6 blastocyst	198
Figure 7.5. Schematic of strategy to generate congenic mutant mouse line	199
Figure 7.6. Increasing C57BL/6 allele homozygosity and concomitant decrease in heterozygosity for the donor 129 alleles with additional backcrosses	199

LIST OF TABLES

2. MATERIALS AND METHODS

Table 2.1. PCR master mix reagents and cycling conditions.....	60
Table 2.2. Expected fragment sizes from genotyping PCR	60
Table 2.3. Home-made reagents and buffers.....	61
Table 2.4. Small molecule inhibitors	62
Table 2.5. IC ₅₀ for PI3K inhibitors on Class I PI3K p110 isoforms	62
Table 2.6. IC ₅₀ for p110 δ -selective inhibitor IC87114.....	63
Table 2.7. Antibodies	63
Table 2.8. Macrophage cell lines, culture medium and starvation condition	64
Table 2.9. SDS-PAGE small gel components	69
Table 2.10. RT-PCR thermal cycling conditions.....	75
Table 2.11. qPCR master mix.....	75
Table 2.12. qPCR cycling conditions	76
Table 2.13. TaqMan® Inventoried gene expression assays.....	76-77
Table 2.14. Components of qPCR mix for analysis in TaqMan® Array Cards.....	81
Table 2.15. Hybridisation cocktail components.....	88

4. RESULTS

Table 4.1. List of eighty probe-sets with assigned gene symbols identified as differentially regulated in RAW 264.7 macrophages treated with IC87114	111-113
Table 4.2. List of fifty-nine probe-sets complementary to unassigned expressed sequences that were differentially regulated in RAW 264.7 macrophages treated with IC87114.....	113-114
Table 4.3. Potential biomarkers of p110 δ -inactivation identified by genome-wide expression analysis.....	122

5. RESULTS

Table 5.1. The expression of five genes was differentially regulated in p110 δ KI macrophages compared to in WT macrophages in basal conditions	137
Table 5.2. The expression of eight genes was differentially regulated in LPS-stimulated p110 δ KI macrophages compared to LPS-stimulated WT macrophages	137
Table 5.3. Differential regulation of twelve probe sets interrogating nine known genes and three RIKEN transcripts in p110 δ KI macrophages compared to WT macrophages in both basal and LPS-stimulated conditions	138
Table 5.4. Potential biomarkers identified include six genes encoding proteins that are either secreted or expressed on the plasma membrane	142-143
Table 5.5. List of fifteen genes chosen for validation by LDA	146
Table 5.6. Source of RNA and mice used for Affymetrix and LDA experiments.....	147
Table 5.7. Raw C _T values obtained for <i>Nin</i> expression in Wt and p110 δ KI macrophages.....	152

6. RESULTS

Table 6.1. Probe sets differentially expressed in basal WT macrophages differentiated and cultured in the presence of IC87114	167
Table 6.2. Probe sets differentially regulated in LPS-stimulated WT macrophages differentiated and cultured in the presence of IC87114	167
Table 6.3. Location of nineteen mapped probe sets differentially regulated in p110δ KI macrophages.....	171

7. DISCUSSION

Table 7.1. The expression of five genes was found to be differentially regulated in p110δ KI macrophages compared to WT macrophages in unstimulated conditions only	180
Table 7.2. The expression of eight genes was found to be differentially regulated in LPS-stimulated p110δ KI macrophages compared to LPS-stimulated WT macrophages.....	180
Table 7.3. The expression of twelve probe sets interrogating nine known genes and three RIKEN transcripts were differentially regulated in unstimulated as well as LPS-stimulated p110δ KI macrophages.	181
Table 7.4. Differential expression of eight probe sets was observed in unstimulated WT macrophages differentiated and cultured in the presence of IC87114 compared to WT control macrophages	193
Table 7.5. Differential regulation of three probe sets was detected in LPS-stimulated WT macrophages differentiated and cultured in the presence of IC87114 compared to WT control macrophages	193

ABBREVIATIONS

ABI	Applied Biosystems
ALL	Acute Lymphoblastic Leukaemia
AML	Acute Myeloid Leukaemia
APL	Acute Promyelocytic Leukaemia
AP1	Activator Protein 1
APC	Antigen Presenting Cell
aRNA	Amplified Ribonucleic acid
ATP	Adenosine-tri-phosphate
bp	Base Pair
BcR	B cell Receptor
B-H	Benjamini-Hochberg
BSA	Bovine Serum Albumin
bZip	Basic-region leucine-zipper
Cd28	Cd28 Antigen
CcO	Cytochrome c Oxidase
cDNA	Complementary DNA
CLL	Chronic Lymphocytic Leukaemia
cM	Centimorgans
CO ₂	Carbon Dioxide
CSF-1	Colony Stimulating Factor 1
Ct	Cycle threshold
CXCL2	Chemokine (C-X-C motif) ligand 2
CXCR2	Chemokine (C-X-C motif) receptor 2
DMSO	Dimethyl sulfoxide
DNA	Deoxyribonucleic acid
dNTP	Deoxynucleotide Triphosphate
DTT	Dithiothreitol
ECL	Enhanced chemiluminescence
EDTA	Ethylenediamine tetra-acetic acid
EGTA	Ethylene glycol tetra acetic acid
ELISA	Enzyme-linked immunosorbent assay
ER	Endoplasmic reticulum
ERK	Extracellular signal related kinase
ES cell	Embryonic stem cell
FACS	Fluorescence activated cell sorting
FBS	Foetal bovine serum
GC	Germinal Centre
GC-RMA	GeneChip-Robust Multiarray Averaging
GDP	Guanidine-di-phosphate
GPCR	G protein coupled receptor
GTP	Guanidine- tri-phosphate
IBD	Inflammatory bowel disease
IC ₅₀	Concentration giving 50% maximal inhibition

Ig	Immunoglobulin
I κ B	Inhibitor of κ B
IKK	I κ B Kinase
IRAK-M	IL-1 associated kinase
IRAK	IL-1 Receptor-associated kinase
IRF 8	Interferon Regulatory Factor 8
JNK	Jun N-terminal kinase
KI	Knockin
KO	Knockout
LBP	LPS binding Protein
LCCM	L-cell cultured medium
LDA	Low density array
LogFC	Log fold change
LPS	Lipopolysaccharide
MAL/TRAP	MyD88-adaptor-like/TIR domain containing adaptor protein
MAPK	Mitogen-activated protein kinase
MEK	Mitogen-activated-Erk Kinase
MHC	Major Histocompatibility Complex
mRNA	Messenger RNA
NF- κ B	Nuclear factor kappa-light chain-enhancer of B cells
mTORC1	mammalian target of rapamycin complex 1
mTORC2	mammalian target of rapamycin complex 2
Nt	Nucleotides
PAGE	Polyacrylamide gel electrophoresis
PAMP	Pathogen associated molecular pattern
PBC	Peripheral blood count
PBS	Phosphate buffered saline
PCA	Principal Component Analysis
PC	Principal Component
PCR	Polymerase chain reaction
PDGF	Platelet-derived growth factor
PGE	Positional gene enrichment
PH	Pleckstrin homology
PI3K	Phosphoinositide-3-kinases
PIP ₂	Phosphatidylinositol 4,5-bisphosphate
PIP ₃	Phosphatidylinositol (3,4,5)-trisphosphate
PDK1	Phosphoinositide-dependent kinase-1
PKB/Akt	Protein kinase B

p-Akt	Phospho-Akt
p-p38	Phospho-p38
PRRs	Pattern recognition receptors
PtdIns	Phosphatidylinositol
PTEN	Phosphatase and tensin homology deleted on chromosome ten
PVDF	Polyvinylidene fluoride
qPCR	Quantitative polymerase chain reaction
RA	Rheumatoid arthritis
RBD	Ras-binding domain
RTK	Receptor-tyrosine kinase
RIN	RNA integrity number
RNA	Ribonucleic acid
RNase	Ribonuclease
RNAi	RNA interference
RT	Room temperature
RT PCR	Real time-polymerase chain reaction
rRNA	ribosomal RNA
SDS	Sodium dodecyl sulphate
SH2	src homology 2
SHIP-2	SH2-domain-containing inositol 5-phosphatase
SOCS1	Suppressor of Cytokine signalling 1
S473	Serine-473
TCA	Trichloroacetic Acid
TCL	Total cell lysate
TcR	T cell Receptor
TFH cell	T Follicular Helper Cell
TGN	Trans Golgi network
TIR	Toll/IL-1 Receptor
TLR	Toll-like-Receptor
TNF	Tumour necrosis factor
TRAF6	TNF Receptor Associated factor 6
TRAM	TRIF related adaptor molecules
Treg	T Regulatory Cell
TRIF	TIR domain containing adaptor inducing IFN- β
TRIS	Tris hydroxyl methyl amino methane
TSC-2	Tuberous sclerosis complex-2
T308	Threonine-308
WT	Wild type

CHAPTER 1

1. INTRODUCTION

1.1. The PI3K family of enzymes

Phosphoinositide-3-kinases (PI3Ks) are a family of enzymes that play an important role in cellular signalling via their activation-dependent production of modified phosphatidylinositol (PtdIns). PI3K enzymes are subdivided into three classes according to their structure, lipid substrate specificity and regulation [Figure 1.1] [2-3]. The unifying feature of Class I, Class II and Class III PI3Ks is their highly homologous catalytic kinase domains, which consist of a kinase domain linked to a helical PIK (PI-Kinase homology) domain. This kinase domain interacts with Adenosine-triphosphate (ATP) and transfers a phosphate from ATP to Phosphatidylinositol 4,5-bisphosphate (PIP₂) generating Phosphatidylinositol 4,5-trisphosphate (PIP₃). All PI3K isoforms contain a PIK domain located next to the highly homologous kinase domain. In addition to these highly conserved regions, a number of auxiliary domains exist, which vary across the PI3K classes [Figure 1.1]. For example, Ras binding domains (RBD) are a common feature of the Class I and Class II isoforms, but are not present in Class III PI3K [Figure 1.1]. The presence of these variable domains is likely to contribute to differential functionality and regulation of the different Classes of PI3K enzymes.

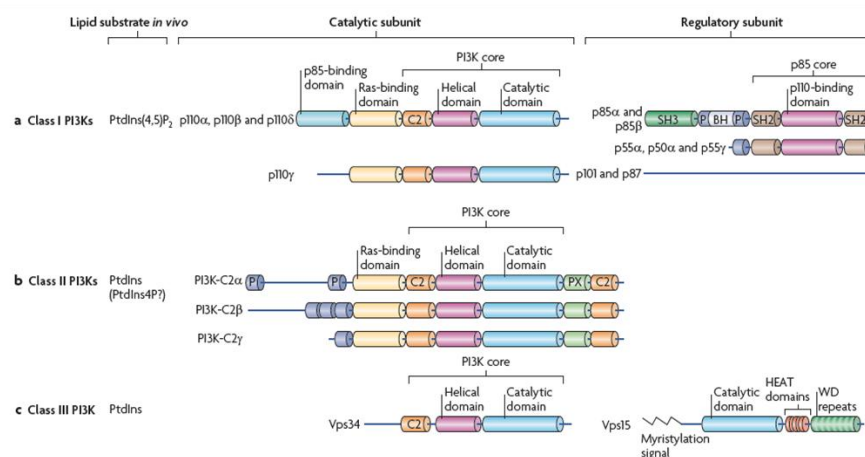


Figure 1.1. Classification, domain structure and in vivo substrate preferences of PI3K enzymes. PI3K enzymes are divided into three classes based on their structure, lipid specificity and the regulatory units which they associate [4].

1.1.1. Class I PI3K

The Class I PI3K isoforms, p110 α , p110 β , p110 δ and p110 γ , exist as heterodimers consisting of a catalytic p110 subunit constitutively associated with one of several regulatory subunits [5] that are described below. The *in vivo* phosphoinositide substrate preferred by Class I PI3K isoforms is PtdIns (4,5)P₂ (PIP₂), which is catalytically converted to PtdIns (3,4,5)₃ (PIP₃) [Figure 1.1].

1.1.1.1. Class IA and Class IB subdivision

Class I PI3Ks are further divided into Class IA, which consists of three isoforms, p110 α , p110 β and p110 δ , and Class IB, which encompasses only p110 γ [Figure 1.1 & 1.2] [6]. Class IA isoforms all signal downstream of Receptor Tyrosine Kinases (RTKs) and associate with p85-type regulatory subunits. The solitary Class IB isoform, p110 γ , is dissimilar to the Class IA isoforms in that it signals downstream of G protein-coupled receptors (GPCRs) and associates with unrelated p101 or p87 regulatory units [7-9]. Recent data has somewhat blurred this division within Class I as p110 β has been found to be capable of signalling downstream of GPCRs as well as RTKs [10-11]. Nevertheless, the structural difference between Class IA and Class IB PI3K heterodimers, with regard to their regulatory subunits, provides some rationale for maintaining the division.

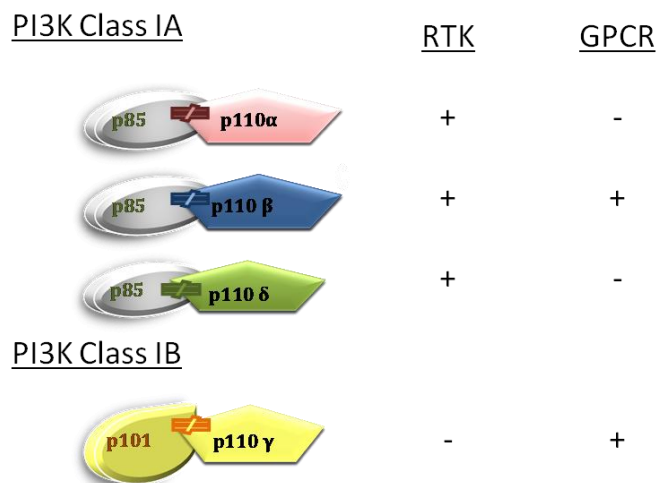


Figure 1.2. The classification of Class IA and Class IB PI3K isoforms. Class IA isoforms couple to a p85-type regulatory subunit, whereas Class IB p110 γ catalytic subunits couple to either p101 or p87 regulatory subunits. Class IA isoforms signal downstream of RTKs and associate with p85-type regulatory subunits, whilst p110 γ signals downstream of GPCRs. p110 β has been found to signal downstream of GPCRs as well as RTKs.

1.1.1.2. Class IA PI3K isoforms

1.1.1.2.1. Class IA PI3K catalytic subunits

Whilst p110 α and p110 β are ubiquitously expressed in mammalian tissue [10, 12] p110 δ has a more restricted expression pattern. Significant expression of p110 δ is observed predominantly in leukocytes [13-14] and to a lesser extent in neurons [15], melanocytes and breast cells [16].

1.1.1.2.2. Class IA PI3K regulatory subunits

The p110 subunits of Class IA isoforms associate with one of a number of related, structurally similar 'p85-type' regulatory subunits encoded by three genes. *PIK3RI* encodes subunits p85 α , p55 α and p50 α by alternative promoter usage, whilst *PIK3R2* and *PIK3R3* encode p85 β and p55 γ respectively. These Class IA regulatory subunits contain two (SH2) domains interspersed by an inter-SH2 domain through which the p110 subunits bind [2]. All of the p110 subunits are equally capable of binding to each of the p85-type regulatory subunits.

Within the PI3K enzyme, the regulatory subunit is necessary to maintain the structural stability of the p110 subunit and furthermore, to enforce a reversible steric inhibition upon catalytic activity in the absence of upstream stimuli [17-18]. This intra-dimer regulation appears to be bi-directional; the p110 subunits possess protein kinase activity that enables them to cross-phosphorylate their associated p85 regulatory subunit in the case of p110 α , rendering the PI3K enzyme inactive. In this respect, p110 δ and p110 β differ from p110 α in that they auto-phosphorylate themselves rather than its associated regulatory subunits [13, 19]. The effect of this auto-phosphorylation appears to be the same; the PI3K enzyme is rendered inactive.

1.2. Cellular signalling by Class IA PI3K isoforms

1.2.1. Activation of Class IA PI3K isoforms

Stimulation of PI3K activity occurs in response to activation of upstream transmembrane receptors that recognise and bind specific extracellular ligands. Receptor Tyrosine Kinases (RTKs) are a key class of receptor that initiate intracellular signalling, partially via the activation of PI3K enzymes. Upon ligand engagement, activated dimeric RTK receptor complexes are formed by monomer

oligomerisation [Figure 1.3]. This ligand-induced proximity between receptor monomers triggers cross-phosphorylation of the dimers on their intracellular domains [Figure 1.3 B]. These phosphorylated residues are recognised by the p85-type regulatory subunits via their SH2-domains [Figure 1.3 C][20]. Thus, the regulatory subunits act as adaptor proteins recruiting associated p110 subunits to active receptor complexes in a stimulus-dependent manner [Figure 1.3 C]. The documented inability of p110 γ to respond to RTK signalling is validated by the absence of SH2-binding domains in the Class IB regulatory subunits p101 and p84/87 [8].

Mechanistically, activation of PI3K upon recruitment to an activated RTK occurs in two ways. First, the conformational changes induced within the PI3K enzyme upon RTK-docking relieve the steric-inhibition imposed by the regulatory unit and secondly, the recruitment brings the enzyme into close proximity with its lipid substrate [Figure 1.3 C] [18]. PI3K production of PIP₃ from PIP₂ embodies the classic model of almost instantaneous signal amplification, which is reliant upon the rapid generation of a second messenger (PIP₃) from an existing precursor (PIP₂). Upon cellular stimulation, PIP₃ levels increase [Figure 1.3 C] and this localised concentration of PIP₃ initiates the next phase of PI3K signalling [Figure 1.3 D].

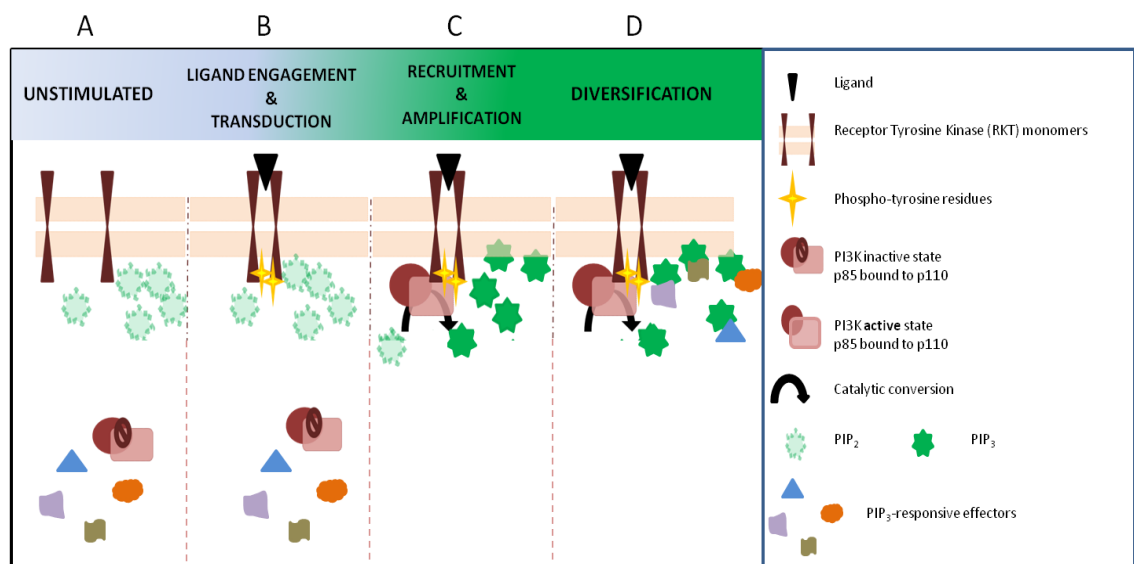


Figure 1.3. PI3K heterodimer recruitment to the membrane. Recruitment occurs via interaction with stimuli-induced phosphorylation sites on the intracellular domains of activated RTKs. Activated PI3K rapidly converts PIP₂ to PIP₃, which then recruits and regulates activity of Pleckstrin Homology (PH)-domain containing effectors.

1.2.2. Signalling downstream of Class IA PI3K activation

PIP₃ potentiates and diversifies the PI3K-RTK signal via interactions with a range of effector proteins [Figure 1.3 D] [21]. The selective capacity of these PIP₃-responsive proteins to interact with phosphoinositide species via their intrinsic PIP₃-binding Pleckstrin Homology (PH) domains facilitates their regulation by one of several mechanisms. Most apparently, the interactions of these proteins with PIP₃ results in their relocalisation into membrane proximal foci [Figure 1.3 D]. This spatial regulation often creates enhanced proximity between a protein and its substrates, regulators and or complexes with which it interacts [22]. Additionally, in some cases, the PIP₃-PH-domain interaction itself can induce conformational changes that alter the activity of the proteins.

1.2.3. Temporal regulation of PI3K signalling

The swift generation of second messengers, such as PIP₃, from existing precursors fulfils the necessity to rapidly transmit a signal in response to RTK activation. It is equally imperative that negative regulation acts to restrict and terminate this signal with comparable rapidity. Indeed, prompt generation and subsequent degeneration of second messengers enables tight temporal and signal-dependent control to be maintained over processes such as migration, metabolism and perhaps most importantly proliferation. Therefore, just as PIP₂ is rapidly catalysed to PIP₃, this PIP₃ must be rapidly catabolised upon signal termination [Figure 1.4]. Phosphatase and tensin homology (PTEN) is the main ubiquitous lipid phosphatase that limits PIP₃ levels. PTEN reduces PIP₃ levels by dephosphorylating the 3' position of its inositol ring returning it to its original PtdIns (4,5)P₂ form [23]. The high frequency of with which mutations that inactivate PTEN have been detected in a range of human solid tumours highlights the necessity of negative regulation of PI3K signalling.

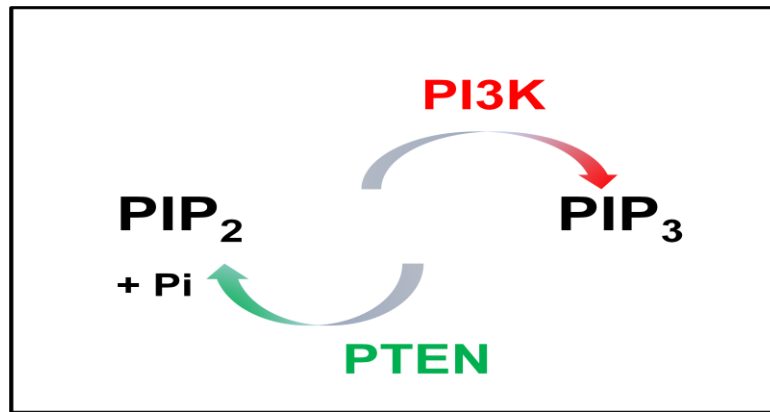


Figure 1.4. Enzymatic conversion of PIP₂ to PIP₃ by PI3K activity and dephosphorylation to PIP₂ (PtdIns 4,5)P₂ by PTEN.

Other lipid phosphatases that also regulate PI3K signalling include SH2-domain-containing inositol 5-phosphatase (SHIP-2) that is mainly restricted to haematopoietic cells [24] and SH2-domain-containing inositol 5-phosphatase 1 (SHIP-1), which is more widely expressed [25]. Unlike PTEN the SHIP phosphatases dephosphorylate the 5' position of the PIP₃ inositol ring and as a result they generate an alternative product PtdIns (3,4)P₂ [24]. Thus it is important to note that the SHIP phosphatase activities are not identical to PTEN by virtue of the different PtdIns product that they produce which has its own distinct associations and effects. The implications of the alternative products generated by PTEN and the SHIP phosphatases are still being investigated [26].

1.2.4. Akt

Akt (also known as Protein Kinase B [PKB]) is the most well characterised effector of PI3K signalling. Upon PI3K activation, Akt is rapidly redistributed from the cytoplasm to the plasma membrane via its high affinity interaction with PIP₃. Consequent activation of Akt occurs in a sequential manner, and is dependent first, upon the conformational changes induced upon binding PIP₃ and secondly, upon its co-localisation with two regulators.

The two independent regulators required to maximally activate Akt are 3-phosphoinositide-dependent kinase 1 (PDK1) and mammalian target of rapamycin complex 2 (mTORC2) [27]. Phosphorylation of Akt residue Threonine 308 (T308) by PDK1 appears to be the first step in Akt activation following PIP₃ binding and associated conformational changes [28]. Maximal activation of Akt requires an

additional phosphorylation event on Akt residue serine 473 (S473) and this is catalysed by mTORC2. The phosphorylation of S473 appears to require T308 phosphorylation as a prerequisite. Phosphorylation of Akt on S473 is considered indicative of complete activation of Akt [29]. Consequently, activated Akt is often referred to in the literature as phospho-Akt (p-Akt).

Akt is a serine/threonine protein kinase that recognises and phosphorylates substrates with a consensus Arg-X-Arg-X-X-Ser/Thr-φ sequence (X denotes any amino acid and φ a bulky hydrophobic residue). Activation of Akt has pleiotropic effects that can be summarised broadly as resulting in the promotion of a pro-survival, growth and proliferative phenotypes [30-32]. The mechanisms and downstream effectors through which Akt contributes to growth and survival are complex and far from completely elucidated. It is known that, Akt orchestrates changes to cellular composition and activity by targeting a broad range of effector proteins, which themselves have diverse downstream interactions [Figure 1.5].

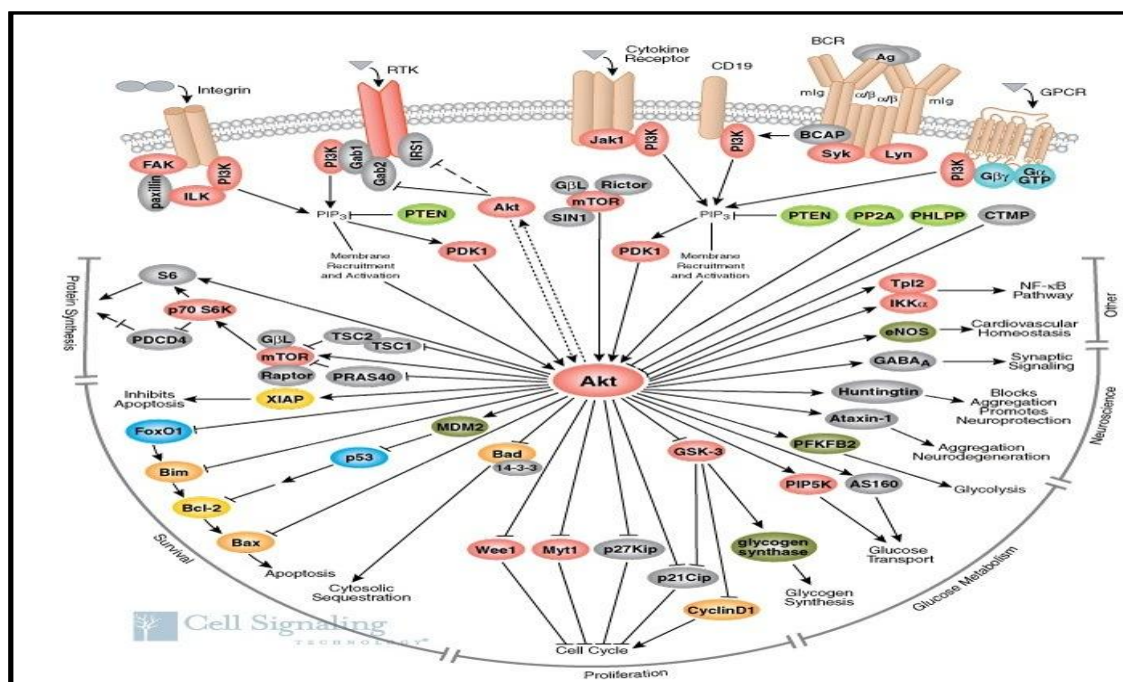


Figure 1.5. Signalling Cascade initiated downstream of PI3K-Akt activation. Akt phosphorylates a broad range of downstream effector proteins including several kinases resulting in phosphorylation cascades. The effects of Akt activation included alterations in protein synthesis, proliferation and metabolism. There is significant overlap and cross talk amongst the pathways that regulate these processes. This facilitates a coordinated response to the initial upstream extracellular signal that is acting in part via activation of PI3K-Akt signalling. [Pathway image reproduced courtesy of Cell Signalling Technology, Inc. (www.cellsignal.com)]

The balance between cell stasis and proliferation and fundamentally between apoptosis and survival are tightly regulated. In the absence of survival signals the cells default response is stasis and ultimately programmed cell death (apoptosis).

Akt appears to regulate many of its targets by means of multiple complementary mechanisms. If we consider the way in which Akt actively contribute towards a shift from cell stasis into a pro-proliferation state this phenomenon is very apparent. First, Akt alongside other regulators must actively promote progress through the cell cycle to facilitate proliferation. In order to do this Akt must also relieve the default cellular stasis that occurs in the absence of sufficient growth stimuli. One means by which Akt suppresses cell stasis is by targeting p27^{kip1} and p21^{cip1}. Akt limits the activity of both these proteins, which themselves act to block cell-cycle progression, first, by direct phosphorylation of these targets but also indirectly by suppressing the transcription of p27^{kip1} by the Forkhead related family type 0 (FOXO) transcription factors. Thus, Akt relieves cell-cycle blockade by inactivating p27^{kip1} and by concurrently reducing its *de novo* production through negative regulation of the FOXO family of transcription factors. We can observe a similar pattern of two-pronged regulation of Akt targets in terms of the contribution of Akt to the induction of growth and proliferation. Cyclin D, cyclin E and c-myc are required for cell-cycle progression and are marked for proteosomal degradation by Glycogen Synthase Kinase-3 (GSK-3) in the absence of growth and survival signals. Direct phosphorylation of GSK-3 by Akt inhibits its activity and thus promotes the stability of these pro-proliferation proteins [33]. Concurrently, Akt indirectly enhances translation of cyclin D and c-myc mRNAs by activating mTORC1, a pivotal regulator of protein synthesis and growth. Specifically, Akt inactivates tuberous sclerosis complex 2 (TSC-2) the complex that functions to repress the activity of mTORC1 in the absence of suitable upstream growth and survival signals. The activation of mTORC1 downstream of Akt activity has multiple effects beyond stimulating cap-dependent translation, which contribute to the proliferation and growth phenotype. In particular, the role of mTORC1 in the regulation of cellular metabolism has received a great deal of interest in relation to metabolic disorders and also in relation to cancer [reviewed in [34]. The mTORC1 pathway is just one of several pathways with which the PI3K-Akt pathway interacts. Indeed, cellular signalling pathways actually highly interconnected networks with many shared effectors, regulators and numerous feedback loops.

Thus, the effects and mechanisms of regulation through which Akt promotes growth, proliferation and survival are both complex and wide-ranging. The effects of inhibiting the “PI3K-Akt pathway” are often investigated in isolation, but should always be considered in the context of interconnected pathways. Complementary mechanisms and pathways synergise to facilitate rapid and dramatic changes in the location, concentration and activity of key effector proteins/complexes. Regulation occurs at all levels, including protein stability and post-translational modification, as well as translational and transcriptional regulation.

1.2.5. Regulation of transcription downstream of PI3K-Akt pathway

The effect of PI3K-Akt activity upon transcriptional regulation is of particular relevance to this thesis. The modulation of the activity of number of transcription factors occurs downstream of PI3K-Akt activation.

As mentioned above, Akt suppresses the transcription of p27^{kip} via its inhibitory actions towards the FOXO family transcription factors. Akt contributes to their signal-dependent regulation by directly phosphorylating them. Indeed, Akt is an important negative regulator of FOXO transcription factors and all but one members of the FOXO family contain three Akt consensus sites. The phosphorylation of FOXO proteins by Akt is thought to suppress their function primarily by the generation of docking sites for 14-3-3 proteins. Once tethered to 14-3-3 proteins the FOXO transcription factors are unable to shuttle into the nucleus or to bind DNA [35]. FOXO proteins are one of many p-Akt targets that are recognised by the 14-3-3 proteins. The possibility that the phosphorylation directly affects FOXOs capacity to bind DNA independent of 14-3-3 has not been ruled out.

Alongside the repression of pro-apoptotic genes, Akt has been shown to regulate positively the expression of the crucial pro-survival protein, BCL-2 [36]. By directly phosphorylating and activating the transcription factor cAMP-responsive element (CREB)-binding-protein (CPB/p300) Akt stimulates the expression of B Cell Lymphoma (BCL)-2 [36]. Activation of PI3K-Akt has been associated with enhanced activity of a Nuclear Factor- κ B (NF- κ B), a fundamental regulator of pro-survival and inflammatory gene expression. Like the FOXO transcription factors, NF- κ B is constitutively expressed but perpetually degraded or tethered in an inactive state in the cytosol. NF- κ B is held inactive via its sequestration in the

cytoplasm by inhibitory complexes known as I κ Bs. The canonical pathway through which NF- κ B is activated involves its release from the Inhibitor of κ B (I κ Bs) cytoplasmic tethers. Specifically, activated I κ B-kinases (IKKs) phosphorylates I κ B, which results in the liberation of NF- κ B from these tethers, allowing it to shuttle into the nucleus and to influence transcription [37] [38]. In addition, the capacity of NF- κ B to bind to DNA, which is stimulated by transactivators such as CPB/p300, has also been shown to be regulated in part by direct phosphorylation of NF- κ B [39]. The mechanisms through which PI3K-Akt activity modulates NF- κ B-dependent transcription are controversial. An early publication relating to the mechanism through which PI3K-Akt promotes NF- κ B-mediated transcription downstream of tumour necrosis factor (TNF)- α pointed to a direct phosphorylation of IKK by Akt, which resulted in NF- κ B release [Figure 1.6][40]. This finding was strongly refuted by the Karin group who proposed an alternative mechanism of enhanced NF- κ B-mediated transcription observed downstream of PI3K-Akt activity involving the regulation of a later stage of NF- κ B-mediated transcription [41]. Subsequently, Sizemore *et al.* showed that Akt activity downstream of IL-1 β may be involved in the induction of the stimulatory phosphorylation of the RelA/p65 NF- κ B dimer [Figure 1.6][42]. Supporting this role for PI3K-Akt activity in the stimulation of NF- κ B phosphorylation Madrid *et al.* also found PI3K-Akt activity contributed to the induction of NF- κ B phosphorylation [Figure 1.6]. Interestingly, this paper found evidence that this was dependent on the activation of the Mitogen-activated protein kinase (MAPK) p38 downstream of Akt. Thus, this brought together the previous observations that PI3K-Akt activation contributed to the promotion of NF- κ B-mediated activity [42-43] and that independent of nuclear translocation p38 activity also affects NF- κ B activity [44].

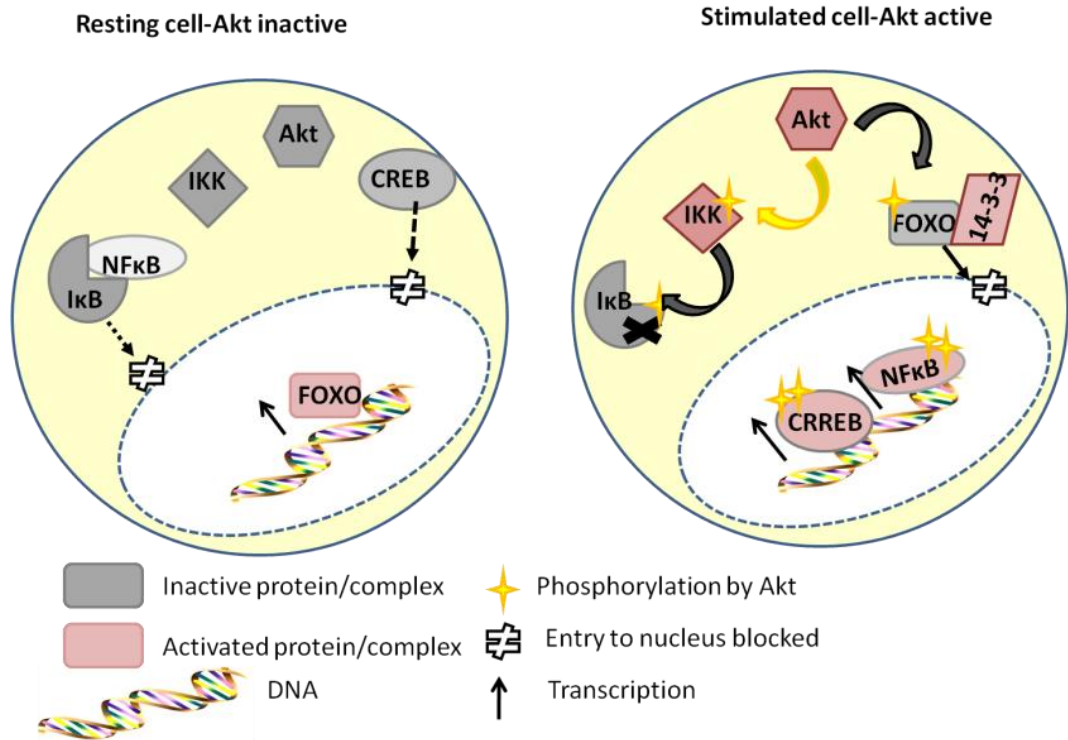


Figure 1.6. Schematic illustration of PI3K signalling regulating transcription. Activation of Akt positively regulates NF- κ B transcriptional activation. The mechanism through which this occurs is controversial, shown here are two possible mechanisms; firstly the activation of IKK by Akt resulting in the release of NF- κ B from cytoplasmic I κ B tethers or secondly by direct phosphorylation of NF- κ B, which enhances its transcriptional activities. Activation Akt suppresses FOXO-driven transcription: phosphorylation of FOXO proteins induces associated with 14-3-3 proteins which prevent them entering the nucleus. Activation of Akt results in activation of CREB and transcription of BCL-2.

In most cells, Akt activity was found to modulate not only NF- κ B but also AP-1 and Nuclear Factor of Activated T cells (NF-AT)-driven transcription in response to immunological stimulus. Overexpression of wild-type Akt was found to enhance the transcription of IL-10 and TNF- α , two inflammatory cytokines that are coordinately regulated by these transcription factors. In the case of NF-AT, it is the inactivation of GSK-3 by Akt, which appears to facilitate its activation by releasing it from inhibitory cytosolic interactions. Phosphorylation of GSK-3 is also predicted to facilitate the transcription of pro-proliferative AP-1-driven genes recognised by the cJun-fos complex. This is because GSK-3 negatively regulates cJUN by preventing it from forming a transcriptionally active complex with fos. Thus, it seems that the regulation of cellular phenotype by Akt potentially involves modulation at multiple levels including translation and transcription. GSK-3 appears to represent a common node in the regulation of transcription and translation downstream of Akt.

1.2.5.1. The PI3K-Akt transcriptome?

The majority of studies regarding regulation of transcription by PI3K-Akt have applied a reductionist approach, focusing on either individual transcription factors/families downstream of PI3K, or on individual genes regulated by PI3K. What are lacking in the literature are studies in which the effects of PI3K-Akt activity on genome-wide expression are determined. This unbiased systems biology approach has the potential to assist in better characterising and understanding the complex and multifaceted effects of PI3K-Akt signalling.

A limited number of studies have been published that identify a gene expression signature that is indicative of aberrant PI3K-Akt activation in malignant disease. The identified gene signatures have potential predictive value in determining the patients that are likely to be responsive to PI3K-Akt targeting strategies [45]. Yet, in terms of extracting the biological effects of PI3K-Akt activity on the transcriptome these disease-state based studies are less useful. The results are complicated by the presence of numerous other variable gene alterations and cancer associated dysfunctions.

To the best of our knowledge, at the time that we started this project, there were no publications regarding the genome-wide impact of PI3K inactivation on transcription. This is in spite of the availability of numerous mouse models and pan/selective-PI3K inhibitors. One group did investigate the modulation of gene expression in response to chronic Akt activation in heart tissue [46]. Akt activation was previously associated with a reduction in cardiomyocyte death and an increase in cardiac hypertrophy, which is in line with the well characterised pro-survival and growth activities of Akt. Based on this finding, the authors set out to identify genes downstream of Akt activation, which contribute to increased cardiomyocyte survival and growth. A comparison was made between genome-wide expression of WT heart tissue and heart tissue derived from transgenic mice expressing a cardiac-specific constitutively active Akt (myr-Akt) [46]. Only forty genes were found to be significantly deregulated by the constitutive expression of Akt, with roughly equivalent numbers increased *versus* decreased [46]. The authors validated ten of the genes identified using quantitative-PCR (qPCR) and found that all of them displayed a similar pattern but the data for only seven of them were statistically significant. Insulin growth factor-binding protein 5 was

identified as highly upregulated by both chronic and acute activation of Akt [46]. This upregulation was predicted to contribute to the pro-survival effect of Akt activation in cardiomyocytes. The results of this study, in particular the minimal number of genes affected provides some indication that the role of PI3K-Akt in the modulation of gene expression might be quite restricted, at least in this cell type. On the other hand, it is possible, had the study investigated the effects of loss of Akt, that many more Akt-regulated genes would be identified.

The Raes group later investigated the involvement of PI3K in LPS-induced transcriptional regulation, in particular focusing on comparing the effects of PI3K and NF- κ B inhibition [47]. This was of particular relevance because PI3K is upstream of NF- κ B activation but the LPS-induced MyD88 signalling pathway also independently activates NF- κ B. The authors analysed the expression of 233 well-characterised inflammatory genes in LPS-stimulated RAW 264.7 macrophages using a biased inflammatory-focused microarray. Their data, as predicted, revealed a significant overlap between the genes affected by pan-PI3K inhibition and NF- κ B inhibition [47]. The data also identified several genes that were regulated by PI3K and not NF- κ B and *vice versa* [47]. These findings suggest that the PI3K pathway contributes to LPS-induced gene regulation via its cross-talk with the NF- κ B pathway but also indicates that both PI3K and NF- κ B act independently as well.

During the course of this project, additional studies were published regarding the impact of PI3K inactivation on the transcriptome. The first was a second study by the Raes group that followed up the findings of Mendes *et al.* [47-48]. In order to delineate the separate contributions of PI3K and mTORC1, the effects of PI3K inhibition, NF- κ B inhibition and this time also inhibition of mTORC1 were investigated. With regards to the effects of NF- κ B inhibition, the authors identified a cluster of LPS-induced genes that were not affected by either PI3K or mTORC1 inhibition but were differentially expressed in the presence of an NF- κ B-inhibitor [48]. This was consistent with the findings of their earlier study and provides further evidence that PI3K regulation of transcription in response to LPS is not solely coordinated via regulation of NF- κ B. Interestingly, the results also revealed that PI3K and mTORC1 inhibition have different and in some cases opposing effects on LPS-induced gene regulation. For example, one set of genes observed to

be affected by PI3K inactivation were differentially affected by the pan PI3K inhibitor Wortmannin compared to the effects of LY294002. The genuine PI3K-dependent effect on these genes is likely to be represented by the effect of Wortmannin, which enhances the LPS-stimulated induction of these genes. It is probable that the observed repression of this set of genes by LY294002 is likely to be as a result of the dual inhibition of PI3K and mTORC1 occurring in response to the high dose of LY294002 used (25 μ M). Indeed, treatment with the mTORC1 inhibitor Rapamycin, similarly repressed the expression of these genes. Despite the fact that both NF- κ B and mTORC1 are downstream targets of PI3K, PI3K inhibition did not affect the same set of genes as inhibiting either NF- κ B or mTORC1 [48]. Not only were the effects overlapping yet far from identical, but in fact, the results of this study revealed that mTORC1 inhibition can actually have the inverse effect to PI3K inhibition [48]. These data, which reveal the disparate effects of pan-PI3K, mTORC1 and NF- κ B inhibition, highlight the fact that cell signalling “pathways” are really components within complex networks.

The first publication regarding the genome-wide impact of pan-PI3K inhibition on expression was published in 2010 [49]. Previous data had indicated that PI3K inactivation negatively impacted upon the growth of tibiae in mice. The authors therefore set out to identify genes that are affected by PI3K activity, which are involved in chondrocyte differentiation a key process in bone development. Treatment of primary mouse chondrocytes with LY294002 resulted in transcriptional changes that the authors describe as modest [49]. Indeed, the majority of genes were deregulated by less than 1.4-fold. In total 5035 probe sets were identified as differentially regulated in the presence of LY294002, but this list was generated without the application of filters for statistical significance, which would no doubt reduce the list considerably. Only 416 probe sets were upregulated by more than twofold and only 596 probe sets were downregulated by more than two fold [49]. These probe sets are likely to include duplicate probes interrogating the same gene and a number of false positives, thus the number of actual genes modulated by LY294002 is likely to be significantly lower. Based on the data and the analysis published one can assume that pan-PI3K inhibition modestly interferes with the transcriptional regulation of less than 1012 genes in these cells. The author cross-analysed these results with those obtained from analysis of differential gene expression in various regions of a micro-dissected

bone growth plate. In doing so, they identified biologically relevant genes that are regulated by PI3K in chondrocytes and differentially expressed in a specific region of the growth plate.

Towards the end of our project, the Okkenhaug group published the first paper detailing the effects of genetic inactivation of p110 δ on the transcriptome, using the p110 δ KI mouse model, in which p110 δ has been inactivated (see next section)[50]. Using genome-wide microarray expression analysis the transcriptome of p110 δ KI T regulatory cells (Tregs) was compared to that of wild-type Tregs. The authors aimed to identify deregulation of gene expression that might be responsible or contributing to the defective development, differentiation and suppressive function of Tregs derived from p110 δ KI mice. In total, 125 probe sets were found to be deregulated by twofold or more in the p110 δ KI Tregs ($p \leq 0.01$)[50]. This represents less than 0.3% of the transcripts interrogated by the microarray used. Within the 125 were twenty seven genes that belong to a previously published Treg gene signature, but none of the classic well-characterised Treg-associated genes were identified [50]. The authors validated around half of the genes identified as differentially regulated using qPCR. Only seven of these genes were confirmed as being twofold or more deregulated in p110 δ KI Tregs, whilst the majority of the others validated, showed a similar pattern but failed to meet the statistical criteria. It is possible that some of these unconfirmed genes identified in the gene array are genuinely modulated by PI3K activity but that this modulation is subtle as was mainly observed for genes affected by pan-PI3K inhibition in chondrocytes.

In summary, both at the start of this project and at the time of writing, surprisingly little data was available regarding the genome-wide impact of PI3K activity on transcription. The data so far, determined using overexpression of Akt, pan-PI3K inhibition and genetic inactivation of a specific PI3K isoform, all points to a relatively minor impact of PI3K activity on the transcriptome. As PI3K inhibitors are now entering clinical trials, fully appreciating their impact not just on signalling and translation but also on transcription seems all the more important. It will be interesting to see in the future if the effects of inhibition of different Class IA PI3K isoforms are similar or disparate and furthermore, whether some of the

functional diversity between the isoforms can be explained at the level of transcriptional regulation.

1.3. Investigating the physiological and pathological implications of PI3K activity

The extensive effects of PI3K-Akt activity on cellular processes naturally translate into numerous physiological effects. Indeed, PI3K-Akt signalling has been identified as a key regulator in a diverse and extensive range of physiological processes, including angiogenesis, metabolism and immunity [32, 51]. Moreover, the PI3K-Akt pathway has been implicated in the aetiology or progression of a vast array of pathological conditions. Cancer was perhaps the first human condition in which dysfunctional PI3K was found to play a key role. Indeed, mutations in *PIK3CA* the gene encoding p110 α , and also in the PTEN gene are in fact, some of the most common somatic mutations in solid tumours [31, 52-57].

Investigation into the physiological and pathological processes in which PI3K partakes has been greatly aided by the use of mouse models generated using a variety of gene-targeting strategies. Details regarding the generation of these models and highlights from the wealth of information obtained from these models are discussed below, alongside a summary of available pharmaceutical tools.

1.3.1. Tools and models for investigating PI3K functions

1.3.1.1. Pharmacological tools available to disrupt PI3K function

1.3.1.1.1. Pan-PI3K inhibitors

Much of the initial and indeed continuing investigations into PI3K function have utilised inhibitors that are broadly effective against multiple PI3K isoforms. The two commonly used pan-PI3K inhibitors are LY294002 [58] and Wortmannin [59], both of which inhibit all Class I PI3K isoforms. Obviously, when using pan-PI3K inhibitors, it is not possible to distinguish which of the individual isoforms are responsible for any phenotypic changes observed in their presence. It is also important to recognise that LY294002 has been found to inhibit a number of non-PI3K targets including mTORC1, DNA-dependent protein kinase and casein kinase-2 [60-61]. Further complicating the interpretation of the effects of pan-PI3K inhibitors is the differential inhibitory effects of LY294002 and Wortmannin across

the PI3K family. Wortmannin has an IC₅₀ of around 5 nM across the PI3K family with a similar inhibitory effect on Class I, II and III PI3K enzymes, but a ten-fold lower inhibitory effect on the PI3K-C2 α enzyme. LY294002 is less potent than Wortmannin but is much more soluble and has an IC₅₀ of around 1 μ M across the Class I and III PI3K enzymes but has a negligible effect on Class II PI3K enzymes. Despite their off-target effects the use of pan-PI3K inhibitors has provided valuable insights into the processes in which PI3K enzymes as a family are integral. Pan-PI3K inhibitors also provide useful controls when used alongside isoform-selective inhibitors.

1.3.1.1.2. Isoform-selective PI3K inhibitors

There is now a broad selection of small molecule isoform-selective inhibitors, which have varying selectivity for one or a sub-group of the PI3K isoforms. All currently available PI3K inhibitors are reversible competitive inhibitors, which inhibit Class I PI3K lipid activity by interacting with and thereby occluding access to the ATP-binding pocket of PI3K catalytic subunits. IC87114, which selectively targets p110 δ , was the first of these PI3K isoform-selective drugs to be used in published work [62], and is still used today to probe for p110 δ functions *in vitro* and *in vivo* in animal models [63-64].

Recent advances have been made regarding the development of isoform-selective inhibitors. These advances were driven by the observation of a conformational change adopted by p110 δ and p110 γ but rarely adopted by p110 α or p110 β [65]. Specifically, based on these findings a number of inhibitors that are highly selective for both p110 δ and p110 γ (p110 δ/γ) as compared to the other PI3K Class I isoforms, have been developed [66].

1.3.1.2. Genetic strategies for disrupting PI3K activity

A number of genetic models for PI3K inactivation have been generated in order to fully appreciate and delineate the range of cellular, physiological and pathological roles of PI3K enzymes. Initial strategies involved targeting the regulatory subunits in an attempt to assess the effects of pan-Class I PI3K inactivation. More recently

research has moved towards the investigation of more targeted isoform-specific disruption.

1.3.1.2.1. Targeting of the regulatory subunit

Two groups developed mouse lines in which the p85 regulatory units were targeted, with the aim of investigating the effects of abrogating Class IA PI3K activity *in vivo* [67-68]. Both of these mouse lines were found to have defective B cell development and one of the lines failed to survive in normal environments as a result of this. No defects in T cell development were reported by either group, which at the time implied that PI3K activity is essential for B cell but not T cell development and function. Paradoxically, when non-immunological responses were assessed in the regulatory subunit knockout (KO) mice, insulin-responsive signalling was found to be enhanced [57]. Further analysis of cells derived from these regulatory subunit knockout mice revealed serious problems with the deletion strategies, which may well be responsible for this phenotype. First, the expression of untargeted regulatory subunits was enhanced (increased expression of p85 β in the pan-p85 α KO model, for example) and secondly the expression of the Class IA catalytic subunits was decreased.

1.3.1.2.2. Targeting of the catalytic subunits

Initially, isoform-specific mouse models for each Class IA isoform were generated using the traditional deletion strategy. Analysis of cells derived from these mice revealed that this strategy, as with the regulatory subunit KO models, causes off-target effects. The expression of untargeted p110 isoforms is affected and furthermore, a notable disruption to the expression of the regulatory subunits was observed [69]. The compensatory changes that occur in response to deletion of the regulatory or catalytic subunit highlights the complexity of targeting a multiple isoform family, in particular, one that functions in a heterodimeric form. The mechanism by which these compensatory effects occur remains unknown. As a result of these compensation mechanisms, the gene deletion/KO models have now largely been superseded by an improved targeting strategy.

This novel knock-in (KI) strategy results in the expression of an inactive, lipid kinase-dead form of the p110 of interest. Abrogation of lipid kinase activity is achieved by the engineering of a point mutation into the gene, which alters the conserved DFG motif to AFG. This results in the translation of the protein with a single amino acid substitution at a functionally important residue located in the mouth of the ATP-binding pocket. The expression of untargeted p110 subunits is unaffected in all KI mice analysed, as is the expression of the regulatory subunits [70]. Analysis and comparison of the phenotypes of the p110 KI lines to the p110 null lines revealed that certain phenotypes observed in the PI3K KO mouse lines were not due to the loss of lipid kinase activity. For example, the p110 γ KO mice had a prominent cardiac phenotype which was absent in the p110 γ KI mice [71] and was due to loss of a scaffolding function performed by p110 γ in a cyclic-AMP regulatory complex [70].

In summary, the KI model abrogates the need to delete the entire catalytic subunit gene and thus does not induce compensatory changes in the expression of the untargeted regulatory or catalytic subunits. The model is a more representative of pharmacological inhibition as the targeted isoform is still translated, present in the cell and able to interact normally with regulatory subunits and other proteins, but is simply catalytically inactivate. The phenotypic effects of genetically inactivating the lipid kinase activity of p110 α , p110 β and p110 γ are summarised below, alongside a more detailed analysis of the effects of loss of p110 δ lipid kinase activity.

1.3.1.2.3. Additional models for studying PI3K function

Indeed, a wide range of mutant mouse lines have been generated to study the effects of both loss and gain of PI3K activity *in vivo*. These include conditionally inactivated models that utilise targeted DNA cleavage strategy to delete a particular PI3K gene [72]. This can be used to remove a particular isoform at a certain stage of development or in a certain cell type/cell lineage only. The effects of increased uncontrolled PI3K activity have been studied in *Pten*-inactivated mice, and in mice where *Pik3ca*, the gene encoding p110 α , is mutated so that it encodes a constitutive active form of p110 α . A homozygous mutation activating or inactivating *Pik3ca* or *Pten* respectively, are both embryonic lethal *in vivo* [12, 73-74]. The lethality observed in these mutant mouse lines, in which PI3K activity is

rendered independent of upstream signalling, emphasises the importance of tightly controlled and signal responsive-PI3K signalling.

1.3.2. Non-redundant cell-specific functions of Class IA PI3K isoforms

Recent research has focused on distinguishing between the individual functions of the PI3K isoforms, with the ultimate aim of discerning how selective inhibition could be clinically useful. The interest in isoform-specific functions has been enhanced by the expectation that isoforms-specific inhibitors may have improved toxicity profiles compared to pan-PI3K inhibitors.

A solid body of evidence now indicates that there are functions performed solely or predominantly by a particular isoform in a certain cell type or downstream of a specific stimulus [1, 75-79]. Vanhaesebroeck *et al.* published one of the earlier examples of this functional division [80]. The authors used microinjection of isoform-selective antibodies to illustrate that in BAC1.2F5 macrophages, the various cellular responses to Colony Stimulating Factor (CSF-1) were regulated by different isoforms. Chemotaxis induced by CSF-1 was found to be dependent on p110 δ and p110 β activity, whereas proliferation induced by CSF-1 was strongly dependent on p110 α activity [Figure 1.7] [80]. These data indicate that the differential functionality can occur downstream of a single stimulus in a particular cell type. Subsequent investigations into the non-redundant roles of Class IA PI3K isoforms in primary bone marrow-derived macrophages revealed that p110 δ regulates CSF-1-driven chemotaxis as it does in BAC1.2F5 macrophages, but that in primary macrophages p110 δ is also necessary for a normal proliferative response to occur [1]. This finding revealed that the contributions of the Class IA PI3K isoforms are influenced by cell state, i.e. primary *versus* immortalised.

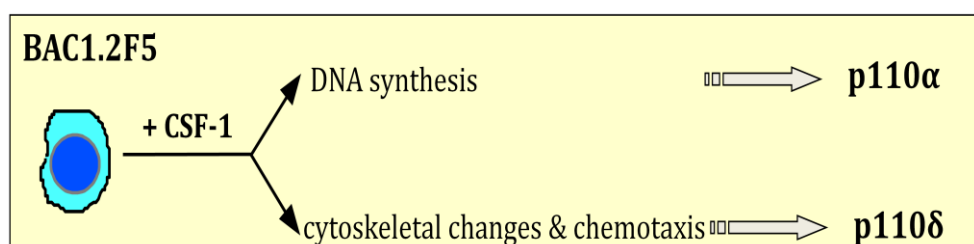


Figure 1.7 Schematic representing the role of Class IA PI3K isoforms in CSF-1-induced responses in BAC1.2F5 macrophages. Blockade of p110 α resulted in inhibition of CSF-1-induced proliferation, whilst blockade of p110 δ and to a lesser extent p110 β resulted in inhibition of CSF-1

induced chemotaxis and associated cytoskeletal changes. [Altered with permission from Prof. Vanhaesebroeck]

1.4. Cellular and physiological roles of Class IA PI3Ks

1.4.1. Cellular and physiological roles of p110 α

Both p110 α KO and p110 α KI (p110 α ^{D933A/D933A}) mutations are embryonic lethal [12, 32]. Staining of p110 α KO embryos at a stage prior to lethality exposed a severe proliferation defect. This effect of p110 α inactivation on proliferation was confirmed by the incapacity of explanted murine embryonic fibroblasts (MEFs) to proliferate *ex vivo* [12]. Subsequent cellular studies using p110 α -specific antibodies and RNA interference (RNAi) have revealed that p110 α has a crucial role in cell cycle progression, which may represent the mechanism underlying the proliferative defects of p110 α KO cells [78].

Substantial angiogenic abnormalities were detected in the p110 α KI embryos, including failure to form and expand a normal vascular network [51]. Graupera *et al.* subsequently created an endothelial-specific model for genetic inactivation of p110 α , and in doing so established that the observed p110 α -dependent angiogenic abnormalities were sufficient to cause embryonic lethality. Heterozygous p110 α KI mice were found to be viable, but tissues from the adult mice have defects in angiogenic responses. This indicates that the role of p110 α in angiogenesis is not limited to developmental embryonic angiogenesis, and might therefore be relevant to tumour-induced angiogenesis [51].

Further investigation of the heterozygous p110 α KI mice revealed a major role for p110 α in metabolic regulation; significant metabolic deregulation was observed in both the mice and cells derived from them [32]. Foukas *et al.* attributed this to disruption of a positive role performed by p110 α in signalling downstream of several metabolic regulators, including insulin and leptin [32].

1.4.2. Cellular and physiological roles of p110 β

Investigation into the effects of p110 β loss of function were initially precluded by the early embryonic lethality of the p110 β KO mutant mice and the failure of MEFs derived from p110 β KO embryos to proliferate in culture [81]. Subsequently, a mutant p110 β mouse model was developed which encoded a deletion in the catalytic domain of the p110 β gene (p110 $\beta^{\Delta 21,22/\Delta 21,22}$) [10]. Two p110 β KI mouse lines have since been generated and in both cases a partial lethality has been observed [[82], Dr Guillermet-Guibert, The Centre for Cell Signalling, unpublished data]. MEFs and bone marrow-derived macrophages extracted from p110 β KI mice are able to proliferate [Guillermet-Guibert, Centre for Cell Signalling, unpublished data]. Together these data suggest that the kinase activity of p110 β is in fact not essential for proliferation but p110 β certainly appears to contribute in some way, perhaps by assisting p110 α in driving the cell to enter S phase, as shown by Marques *et al.* [78].

Physiologically, p110 β plays an important role in haemostasis and in particular in thrombus formation. Activation and aggregation of platelets in response to shear-stress appears to require p110 β activity. In the absence of p110 β activity, platelet aggregation is reduced *in vitro* and this translates to a reduction of thrombus formation *in vivo* [83]. Mechanistically, the absence of p110 β activity seems to abrogate the capacity of integrin $\alpha_{IIb} \beta_3$ complexes to form the stable adhesion contacts that facilitate platelet aggregation.

1.4.3. Cellular and physiological roles of p110 δ

p110 δ KI (p110 $\delta^{D910A/D910A}$) mice have been generated and they are not only viable, and fertile but also have no gross anatomical or behavioural defects [84]. As stated earlier, p110 δ has a very limited tissue distribution and is highly enriched in leukocytes and, as a result, the genetic inactivation of p110 δ primarily impacts upon the function of immune cells. In the section below, I have summarised the effects of p110 δ inactivation on some of the immune cell types. I have introduced macrophage function and immunity in greater detail in a subsequent section.

1.4.3.1. The role of p110 δ in macrophage biology

The effects of p110 δ inhibition on macrophage function are of particular relevance to my project. As with most immune cells, an ability to migrate and specifically, to move in a directional manner (chemotax) towards a stimulus, is essential for macrophage function. As described above, Vanhaesebroeck *et al.* showed that p110 δ regulates chemotaxis downstream of CSF-1 in BAC1.2F5 macrophages [80]. Subsequent in depth analysis of the role of p110 δ in macrophage migratory/chemotaxis has revealed that p110 δ inactivation in primary macrophages results in a reduction of actin polymerisation, membrane ruffling and cell spreading [79]. The underlying molecular mechanism of these cytoskeletal and motility defects was found to be caused by deregulation of two key regulators: RhoA and Rac1. Rac1 and RhoA are both small guanidine tri-phosphate (GTP)-ases that cycle from an inactive guanidine di-phosphate (GDP)-bound state to an active GTP-bound state with the help of regulatory molecules, which either stimulate the proteins' own intrinsic GTP hydrolysis activity or enhance GTP binding. Rac1 activity was found to decreased upon p110 δ inactivation, and conversely RhoA activity is increased in both basal and CSF-1-stimulated macrophages in the absence of p110 δ activity. This increased RhoA-GTP activity was found to be the crux of the migratory problem in these macrophages [79].

In primary macrophages, p110 δ has been found to play a far more extensive role downstream of CSF-1 than it does in immortalised BAC1.2F5 macrophages. Indeed, in primary macrophages, p110 δ is the major isoform responsible for CSF-1-induced p-Akt induction and its inhibition represses CSF-1 induced proliferation as well as chemotaxis [1, 79]. p110 δ activity has been shown to be necessary for normal proliferation of many other immune cells including B cells, T cells. It should be noted that, unlike the B cell defects in the p110 δ KI mice, macrophages derived from these mice differentiate into phenotypically normal macrophages *in vivo* and *ex vivo* [79]. Thus, these data indicate that although p110 δ plays a significant role in regulation of macrophage proliferation, its activity is not necessary for macrophage development and differentiation.

1.4.3.2. The role of p110 δ in mast cell biology

Mast cells, which reside *in situ* in tissues, play a central role in allergic response. Mast cells detect allergens through the Immunoglobulin E (IgE) molecules on their surface and upon repeat exposure, allergen binding to surface-IgE initiates a signalling cascade. This cascade induces the release of mast cell granular contents, which includes histamine amongst other inflammatory mediators. Ali *et al.* found that mast cells derived from p110 δ KI mice are partially unable to degranulate and release inflammatory mediators in response to allergic stimulus [75]. This cellular defect translates into attenuated allergic responses *in vivo* in p110 δ KI mice [75].

1.4.3.3. The role of p110 δ in T and B cell biology

Signalling downstream of the T cell Receptor (TcR) was observed to be affected in p110 δ KI mice. This causes a reduction in T cell proliferation in response to anti-CD3 stimulation [84] but despite this T cells retain their capacity to differentiate into the main mature T cell subtype, effector T cells.

When the p110 δ KI mice were first generated the initial publication focused on both *ex vivo* and *in vivo* evidence of serious defects in B cell Receptor (BcR) as well as TcR signalling [68, 84]. B cell defects in the p110 δ KI mice are wide ranging and include a vastly diminished ability to produce antigen-specific antibodies in response to immunological challenge [84]. The production of antibodies in response to immunological challenge requires the formation of micro-anatomical structures known as germinal centres (GCs) in secondary lymphoid organs. In these GCs, B cells undergo division, antibody class switching, somatic hypermutation and ultimately differentiation into either memory B cells or plasma B cells. The plasma B cells that differentiate in the GCs are responsible for the production of antigen-specific antibodies. Histological analysis of lymphoid tissue revealed that the inability of p110 δ KI mice to produce antigen-specific antibodies was associated with a complete absence of GCs. The GC reaction involves also involves antigen-presenting cells (APCs) and specialist type of T cells known as follicular T helper (T_{FH}) cells, which support the differentiation of B cells. A recent publication has revealed that it is the absence of p110 δ activity in T cells rather than B cells, which is responsible for the lack of GC formation and associated low antibody titres in p110 δ KI mice [85]. Rolf *et al.* showed that selective deletion of

p110 δ in B cells did not result in the same blockade of GC formation or antibody production as observed in the p110 δ KI mice [85]. Yet, selective deletion of p110 δ in T cells did result in these GC-related phenotypes mimic [85]. Specifically, the inability of p110 δ KO T cells to expand and differentiate into a normal T_{FH} cell population was found to be the limiting factor preventing GC formation [85].

Tregs are another important T cell population that are reduced in p110 δ KI mice. Tregs as their name suggests, perform an important regulatory function; they maintain peripheral tolerance by limiting both the activity and expansion of effector T cells. Tregs extracted from these mice have been found to have reduced suppressive capacities and do not produce the anti-inflammatory cytokine IL-10 *ex vivo* [86].

In summary, inactivation of p110 δ has a significant impact on the adaptive immune cell population. This includes abnormal B cells differentiation and severely disrupted function resulting in poor humoral responses. This B cell dysfunction appears to be primarily a T cell-intrinsic effect rather than a direct result of the loss of p110 δ activity in the B cells themselves. T cells derived from p110 δ KI mice have distortions in their subpopulations, which affects the spectrum of T cell activity and also p110 δ KI Effector T cells have attenuated TcR signalling.

1.4.4. Cellular and physiological roles of p110 γ

Like the p110 δ KI mice, the p110 γ null mice are viable, fertile and display with no gross anatomical or behavioural defects [71, 84]. Similarly, as observed in the p110 δ KO and p110 δ KI mice, p110 γ KO mice have a range of immunological defects that are apparent *in vitro* and *in vivo* [71]. A p110 γ KI mouse line has also been generated, which closely replicate the p110 γ KO mice phenotypes, with the exception that the cardiac phenotype observed in the p110 γ KI mice that was absent. This was attributed to disruption of a p110 γ scaffolding function in the p110 γ null mice [87].

Analysis of leukocytes derived from p110 γ null mice revealed a number of defects, which can mostly be traced back to lack of p110 γ signalling downstream of GPCR agonists. This concurs with the hypothesis that p110 γ couples primarily to GPCRs. In particular, the *in vitro* migratory responses to GPCR-linked chemo-attractants

such as complement component C5a were defective in both macrophages and neutrophils [71]. This migratory defect has been shown to translate into reduced neutrophil migration to a site of viral infection *in vivo* p110 γ null mice [71]. Other GPCR-dependent immunological responses were found to be affected by loss of p110 γ activity, including GPCR-stimulated oxidative burst in neutrophil [71]. Unlike p110 δ KI mice, p110 γ null mice appear to have no defects in B cell developmental or functionality [71].

Some groups have presented evidence for a role of p110 γ in T cells; effector T cells were found to migrate inefficiently and this was attributed to downstream dysfunction in migratory responses caused by loss of p110 γ activity [88]. More recent data suggest that the defects in T cell function in p110 γ null could actually be attributed to an impairment of TcR signalling. Although the TcR is an RTK and p110 γ is known to function downstream of GPCRs, p110 γ was nevertheless found to be activated in response to TcR engagement [89]. Loss of p110 γ activity reduced the capacity of T cells to interact with APCs by forming immunological synapses, a crucial step in the activation of T cells by APCs [89]. In summary, p110 γ activity appears to be necessary for GPCR-ligand-driven migration and activation of both innate and adaptive immune cells. Furthermore, loss of p110 γ attenuates the capacity of these cells to perform their normal functions in infected tissues such as cytotoxic killing of pathogens.

1.5. Macrophages in the immune system

1.5.1. The components of the immune system and stages of immune response

The mammalian immune system consists of a diverse range of functionally distinct cell types [Figure 1.8]. The complete immune response is a complex and coordinated tri-phasic response.

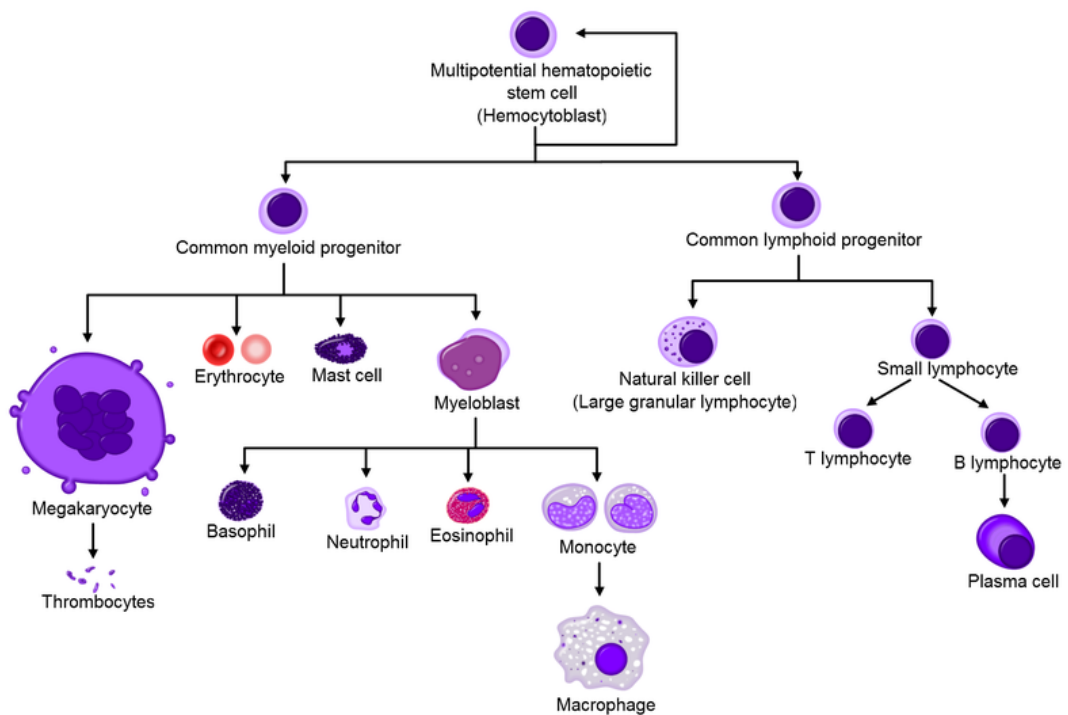


Figure 1.8. Illustration of the haematological cell lineage. Haematopoietic cells derive from pluripotent stem cells in the bone marrow and then differentiate into a range of cells either belonging to the lymphoid or the myeloid lineage. Each cell has a specialised function. Macrophages are differentiated from monocytes and belong to the myeloid lineage. [Image reproduced with permission from Wikimedia Commons, original illustration by A. Rad.]

1.5.1.1. Macrophages and the innate immune response

Rapid detection of a pathogenic threat and subsequent activation of innate immune cells, including macrophages and neutrophils is the first stage of any immune response. The innate immune cells are the first line of defence, utilising search and destroy tactics to clear pathogen. Further to this, the innate immune cells must call to arms the adaptive immune cells that are capable of providing

more pathogen-specific immunity. Macrophages reside *in situ* in most solid tissues and are primarily derived from circulating monocytes [Figure 1.8] [90]. Macrophages perform their search and destroy duties first, by employing highly sensitive detection mechanisms and secondly, by engulfing pathogenic material using a specialised endocytotic process known as phagocytosis.

1.5.2. Initiation of the adaptive immune response

Activated macrophages induce adaptive immunity by releasing a wide range of inflammatory mediators including cytokines and chemokines [91]. The cocktail of inflammatory mediators released recruits adaptive immune cells to the site of infection and also contribute to the process of adaptive cell activation. The combined pathogen-specific cytotoxic and antibody/humoral functions performed by T and B cells are necessary to clear a tissue of pathogens and cells infected with them. To direct the adaptive immune cells to initiate the appropriate programme the macrophages must present fragments of the pathogen to the incoming cells. To do this they first engulf pathogens or pathogen fragments using a specialised endocytosis process known as phagocytosis. This material is processed internally and displayed on the surface of the macrophages in complex with Major Histocompatibility Complex Class II (MHC Class II). The MHC II-antigen complex engages with antigen recognition receptors such as the TcR on adaptive immune cells and stimulates the formation of immunological synapses [92]. This interaction between APCs and T cells is affected by loss of p110 γ inactivation [89]. In the case of T cells, interaction of naive T cell MHC-antigen receptors with MHC-antigen complexes induces proliferation and differentiation of the cells into effector T cells or helper T cells. The effector T cells are then able to identify host cells infected by the pathogen and destroy them by cytotoxic mechanisms. Meanwhile, primed B cells that have been previously exposed to a particular pathogen proliferate and in the presence of T_{FH} cell stimulation differentiate into plasma B cells. The reduced numbers of T_{FH} cells in the p110 δ KI mice was found to be responsible for the drastically reduced production of pathogen-specific antibodies in these mice.

1.5.3. Recognition of lipopolysaccharide and other pathogens by macrophages

Macrophages are able to achieve an exquisite sensitivity to the presence of a wide range of pathogens [93]. This is achieved by expressing an array of highly selective pattern recognition receptors (PRRs) that recognise specific molecular patterns in pathogenic material, known as pathogen-associated molecular patterns (PAMPs).

Lipopolysaccharide (LPS), the major component of gram-negative bacteria cell walls, is of particular clinical significance because to its capacity to induce life-threatening endotoxic shock syndrome (also known as Septic Shock). Following recognition by macrophages LPS induces an immune response as described above. The production of a cocktail of macrophage-derived inflammatory mediators is thought to be a major element in the development of endotoxic shock syndrome. Several of these mediators, including $\text{TNF}\alpha$, stimulate local vasodilation in order to facilitate entry of leukocytes into the infected tissue [94-96]. If systemic vasodilation occurs due to excess soluble vasodilators in to the blood stream a rapid drop in blood pressure. This can cause insufficient tissue perfusion and hypoxia and ultimately can result in multi-organ failure and death [97].

1.5.3.1. Recognition of LPS by macrophages

Recognition of LPS and initiation of intracellular signalling requires the formation of multi-protein complexes. LPS itself forms a complex with LPS binding protein (LPB) in the plasma [Figure 1.9]. This LPS-LBP complex is presented to Toll-Like-Receptor 4 (TLR4) by the membrane-anchored protein CD14. [Figure 1.9] [93, 98-100]. This CD14-TLR4 complex also requires another extracellular accessory protein MD-2 [Figure 1.9] in order to respond appropriately to LPS-LBP. Deletion of TLR4, MD-2 or CD14 in mice results in hypo-responsiveness to LPS and concomitant resistance to endotoxic shock [98, 100-103].

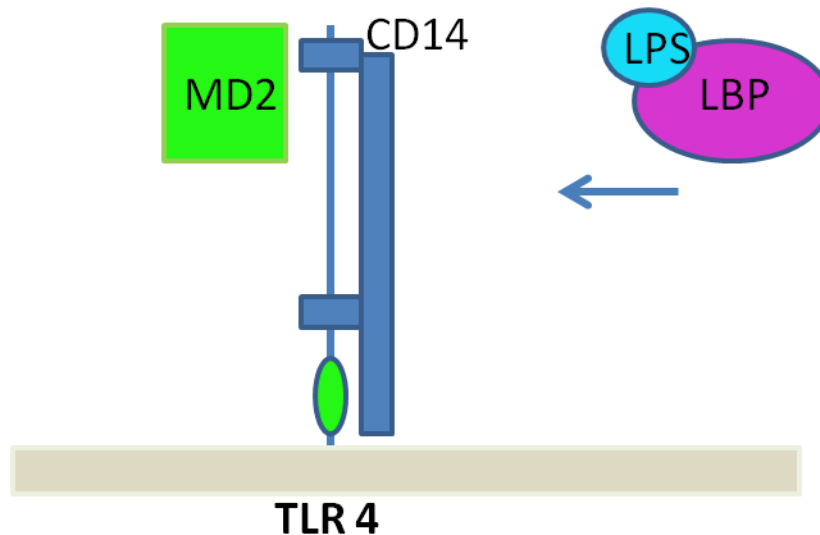


Figure 1.9. LPS is recognised by macrophages via a PRR complex in association with an accessory protein. LPS in complex with plasma LBP binds to the macrophage surface complex consisting of TLR4-CD14 in association with the accessory protein MD2. The TLR4 component of this complex is then activated.

1.5.3.2. LPS-induced signalling downstream of TLR4-CD14-MD-2 complex

LPS signalling is initiated via adaptor proteins that interact with the intracellular Toll/IL-1 Receptor (TIR) domain of TLR4 [Figure 1.10]. The details of the exact components, pathways and mechanisms contributing to LPS-induced signalling are not yet fully elucidated. It is clear that LPS activates a number of canonical signalling pathways including the MAPK, NF- κ B and the PI3K-Akt pathways. The classical LPS-signalling pathway activated directly downstream of TLR4 is the myeloid differentiation primary response gene 88 (MyD88)-dependent pathway. MyD88 is recruited to activated TLR4 receptors and acts as an adaptor recruiting kinases, which then initiates downstream signalling. Deletion of MyD88 is sufficient to abrogate LPS-induced signalling and cytokine production [104]. IL-1 Receptor-associated kinase 4 (IRAK4) is the main kinase recruited to TLR4 by MyD88 [105]. IRAK4 facilitates the formation of a downstream effector complex composed of kinase TNF-Receptor-Associated Factor 6 (TRAF6) and IRAK1. The TRAF6-IRAK1 complex then propagates the signal via phosphorylation of downstream proteins [Figure 1.10][105].

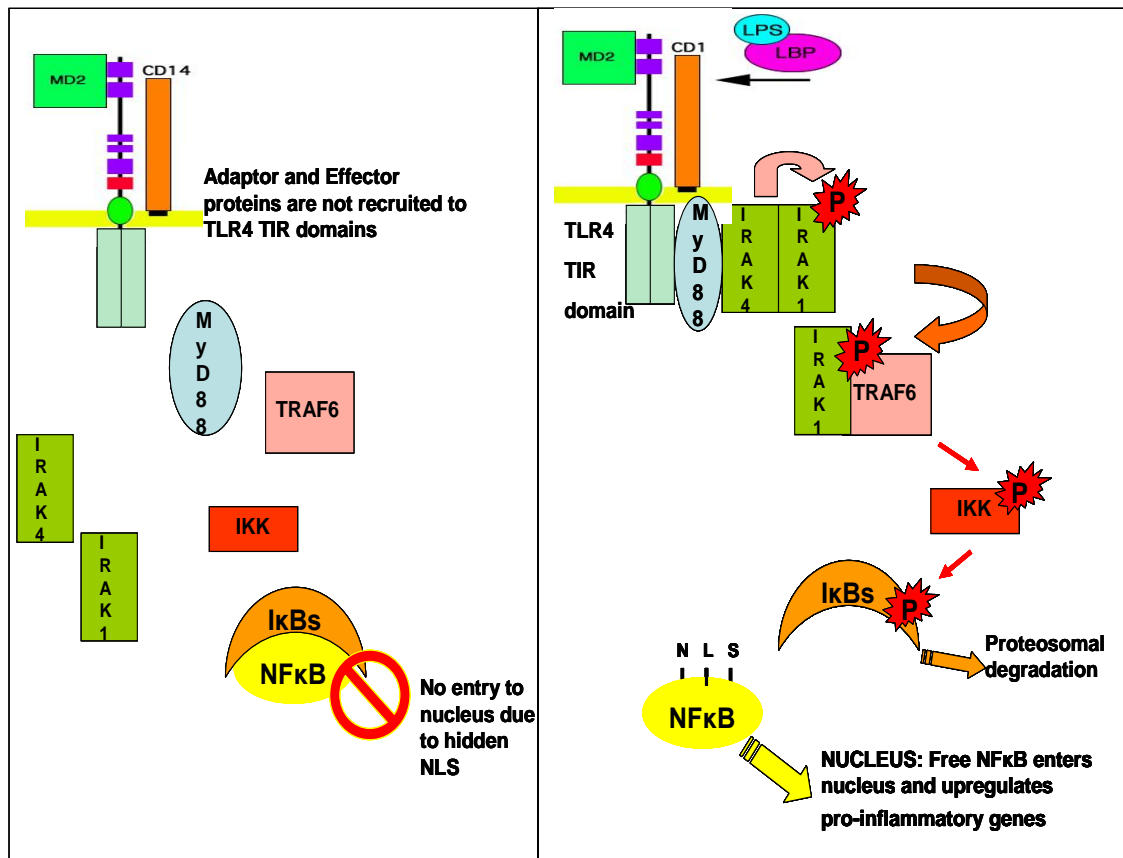


Figure 1.10. Illustration of the activation of NF- κ B-dependent transcription by LPS via the MyD88-dependent pathway. LPS recognition results in recruitment of the adaptor protein MyD88 to the TLR4 TIR domain and initiates a cascade of signalling via several kinases. Downstream kinase activity results in the release of NF- κ B from its inhibitory partner I κ B. Release of NF- κ B reveals its NLS and allows it to enter the nucleus and upregulate expression of pro-inflammatory genes.

1.5.3.3. LPS induces a shift in the macrophage transcriptome

LPS has profound effect upon the transcriptome of macrophages and this transcriptional regulation appears to play a central role in the induction of the activated inflammatory phenotype. LPS alters the expression of thousands of genes including the induction of a wide range of inflammatory mediators such as chemokines and cytokines.

One of the most well characterised transcription factors regulated by LPS signalling is NF- κ B. As described earlier, Akt activity promotes the activation of NF- κ B but downstream of LPS independent pathways also potently induce NF- κ B. The presence of inactive NF- κ B tethered in the cytosol, allows LPS and other

immunological stimuli to rapidly initiate transcriptional changes by inducing the liberation and activation of NF- κ B. The MyD88 pathway rapidly initiates activation of NF- κ B downstream of TLR4-LPS engagement. Specifically, IRAK1 activity induces the activation of NF- κ B-driven transcription indirectly by the activation of IKKs. As described above, activated IKK phosphorylates I κ B and this results in the release NF- κ B [37] [38]. This activation of NF- κ B results in the upregulation of early NF- κ B-driven pro-inflammatory genes, which contribute to LPS-driven macrophage functions. Further to this, a second delayed wave of transcriptional change is initiated via the *de novo* expression of NF- κ B-regulated transcription factors or their regulators. This deferred response allows the cells to modulate macrophage phenotype to suit the stage of the infection and plays a role in the induction of tolerance.

A second pathway downstream of TLR4 activation, the so-called “MyD88-independent” pathway, has been identified and its components are necessary for optimal induction of inflammatory genes, including those encoding cytokines [106]. The components and mechanisms of action of the MyD88-independent pathway are poorly characterised. Two adaptor proteins, TIR domain-containing adaptor inducing IFN- β (TRIF) and TRIF-related adaptor molecules (TRAM), are known to bind the TLR TIR domain. In the absence of MyD88 activity, these components have been found to facilitate LPS-induced activation of NF- κ B and also induce the activity of the MAPK pathway (p38 activation) in dendritic cells [104, 106]. How this pathway functions in concert with MyD88 signalling is not yet fully characterised.

1.5.3.4. Regulation of LPS responses by PI3K

PI3K dependent phosphorylation of Akt at S473 and T308 occurs rapidly in response to LPS-stimulation [107-108]. The mechanism by which PI3K activity and downstream Akt activation are coupled to LPS stimulation is currently unclear. We know that PI3K p85 regulatory subunits can be recruited to another member of the TLR family, TLR2 upon activation and that this recruitment was sufficient to activate PI3K activity [109]. This recruitment was suppressed by site-directed-mutagenesis of specific tyrosine residues on TLR2 indicating direct recruitment and its aberration had functional significance [109]. Whether direct recruitment of PI3K to the TLR4 complex occurs in response to LPS remains an open question.

PI3K has been reported to interact with MyD88 upon LPS stimulation, which suggests that PI3K may be recruited to the TLR4 complex rather than directly to TLR4 [110]. It is also possible that PI3K is activated by LPS in an autocrine manner by ligands secreted by LPS-stimulated macrophage or alternatively by an intracellular effector of LPS. Indeed, it is not inconceivable that multiple mechanisms contribute to the activation of PI3K in response to LPS.

There is a significant body of evidence that indicates PI3K activity plays a role in LPS-induced responses [107-108, 111-112]. Early data and indeed much of the current data attributes a negative regulatory role to PI3K activity downstream of LPS [107, 111-112]. Contrary to evidence discussed above indicating a positive regulatory role for PI3K-Akt upstream of NF- κ B [42, 113], the inhibition of PI3K in monocytic cells has been shown to increase NF- κ B activity [107]. Importantly, an increased production of pro-inflammatory cytokines was concomitantly observed, alongside enhanced NF- κ B activity upon PI3K inhibition [107]. Indeed, PI3K-dependent suppression of TNF α induction has been observed *in vivo* in p85 α KO mice. The p85 α KO mice have higher TNF α serum levels than their wild-type counterparts when challenged with LPS. On the other hand, contradictory studies have shown a profound reduction in the secretion of TNF α from p110 δ KI leukocytes including macrophages [114-115]. In macrophages, this was attributed to a defect in the secretion of TNF α , whilst its production remained unaffected [114-115]. It remains possible that another PI3K Class IA isoforms negatively regulates the transcription or translation of TNF α in these cells, which could account for the increased production upon pan-PI3K inhibition. Alternatively, the increased TNF α secretion observed in p85 KO mice could be as a result of a compensatory mechanism and perhaps should not be taken at face value.

Data is increasingly pointing to the differential regulation of cytokine production or secretion downstream of PI3K-Akt upon LPS-stimulation. mTORC1 and GSK-3 are two central nodes downstream of PI3K-Akt that both appear to play significant role in differential regulation of cytokine/chemokine production. GSK-3, which is inactivated by Akt activity as described above, negatively regulates the production of the important immuno-modulator cytokine IL-10, whilst also positively regulating the production of a number of potent pro-inflammatory cytokines including TNF α , IL-12 [116]. Thus, Akt activation results in a suppression of TNF α ,

IL-12 whilst enhancing the production of IL-10 through GSK-3 inactivation [Figure 1.11][116]. In contrast, Akt activates mTORC1 activity downstream of PI3K by inactivating TSC1/TSC2 and mTORC1 has the polar opposite effect on the production of these same cytokines [Figure 1.11].

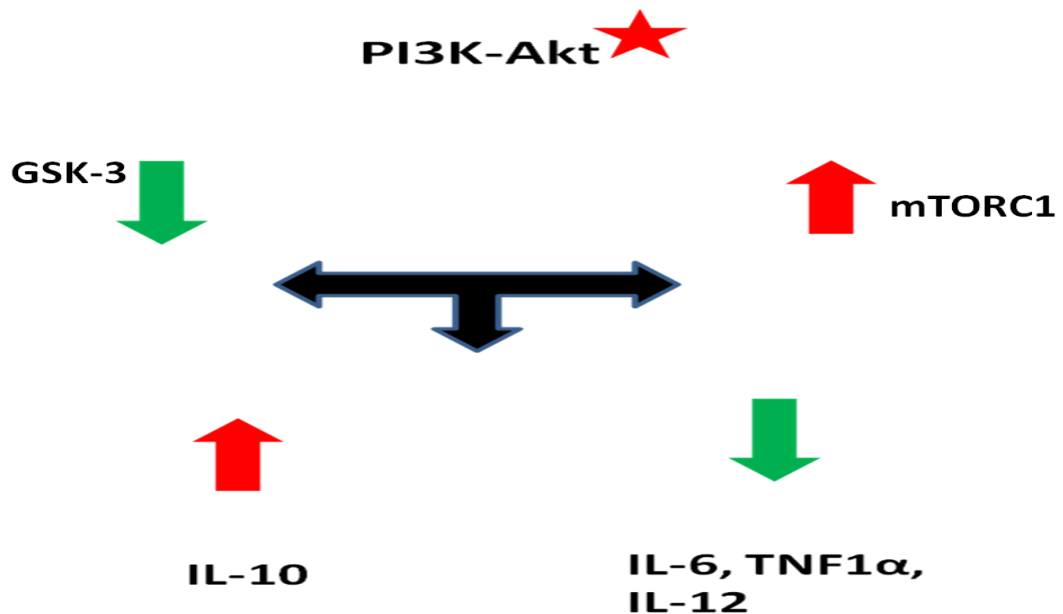


Figure 1.11. Schematic of the differential effect of PI3K activity on cytokine production mediated modulation of GSK-3 and mTORC1 activity. Inactivation of GSK-3 and activation of mTORC1 results in enhanced production of immune-modulatory IL-10 and suppression of pro-inflammatory mediators including IL-12, IL-6 and TNF α .

Thus, by the inhibition of GSK-3 and the activation of mTORC1, PI3K-Akt signalling suppresses the production of several pro-inflammatory cytokines, whilst simultaneously enhancing the production of the key immune-regulatory cytokine IL-10 [Figure 1.11]. The potential *in vivo* immune-regulatory effects of IL-10 have been demonstrated *in vivo* by the improved symptoms of patients with Crohn's disease who were treated with bacteria encoding a recombinant IL-10 [117]. Furthermore, IL-10 has been shown to suppress NF- κ B activity, which might in part explain why the inhibition of PI3K-Akt in monocytic cells resulted in enhanced production of some cytokines whilst also enhancing NF- κ B transcriptional activity [107].

There is also evidence to suggest that PI3K may function in the later stages of LPS responses. After an initial exposure to LPS, the immune system responds less vigorously to a second LPS exposure. This so-called endotoxin tolerance that blunts the immune systems activation in response to LPS is thought to be safety mechanism that prevents an unnecessarily and potentially damaging maximal response being initiated [96, 118]. In RAW 264.7 macrophages, inhibition of PI3K was found to increase TNF α and Nitric Oxide production in response to a second exposure to LPS. These data suggest that tolerance was not properly induced or was overcome in the absence of PI3K activity. The potential importance of PI3K-Akt in the induction of tolerance was also apparent in Akt null mice, which had hyper-inflammatory phenotypes and concurrently failed to develop endotoxin tolerance. Thus, evidence points to a role for PI3K in LPS responses both in the initial stages and in longer-term responses such as the induction of tolerance [119].

Together, these data suggest that PI3K-Akt activity primarily functions to negatively regulate the induction of LPS-induced responses. There is conflicting data that suggests that certain LPS-induced inflammatory responses require PI3K activity in macrophages. Despite this, the primary role of PI3K appears to be the induction of mediators that suppress or limit the activation of LPS-responses. It is not unheard of for the same effector to activate signalling whilst also downstream initiating negative regulators of the same signalling and indeed this represents a capacity to modulate rather than simply switch on or off responses. It therefore seems plausible that PI3K may act to modulate responses by maintaining some degree of homeostasis, rather than simply by repressing inflammation.

1.5.4. The importance of a balanced immune response

It is vital that when the immune system responds to infections the response is both balanced and appropriate; otherwise it can do considerably more harm than the pathogen itself. The loss of peripheral tolerance and resulting misdirected immunity can be extremely harmful [120]. The importance of a balanced and appropriate immune response and the role p110 δ plays in achieving this balance is apparent in the p110 δ KI mice. These mice develop inflammatory bowel disease (IBD) in the form of inflammatory colitis, which ultimately causes rectal prolapse

in a certain proportion of the female mice. The colitis has been attributed to an inappropriate immune response to commensal enteric bacteria [84, 121]. This phenotype suggests that the observed negative regulation of bacterial responses by PI3K does indeed translate into a deregulation *in vivo*. The data implies that p110 δ may play a negative regulatory role in suppressing responses to commensal bacteria in the gut. Indeed, p110 δ maps to the human IBD sensitivity locus [122], although it must be noted that to date, there is no direct evidence that inactivation of p110 δ in humans results in IBD. The inappropriate inflammatory reaction to commensal bacteria has been partly attributed to the reduced population of Treg cells in these mice. In support of this, in adoptive transfer experiments Treg cells derived from p110 δ KI mice were unable to protect against experimental colitis induced in WT mice [86]. A more recent publication has provided evidence that the loss of p110 δ in macrophages also contributes to the IBD in the p110 δ KI mice [123]. Thus PI3K and specifically p110 δ does appear to contribute to the regulation of the immune responses to bacteria in innate and adaptive immune cells.

1.6. Therapeutic potential of PI3K inhibition

Whilst considering the phenotypes observed in the various PI3K mouse models, it is apparent that inhibition of the PI3K Class I enzymes represents an opportunity to modulate a range of physiological and pathological processes. Indeed, at the time of writing, there were at least eighteen clinical trials underway using a wide range of PI3K inhibitors [124].

1.6.1. Therapeutic potential of targeting p110 α

The high prevalence of *PIK3CA* and *PTEN* mutations in human solid tumours has revealed that PI3K and specifically p110 α are targets worthy of attention in pharmaceutical/translational research [125]. A large proportion of the clinical trials currently underway are testing the efficacy of PI3K inhibition in the treatment of human solid tumours. Initially, it was thought that p110 α -selective inhibitors could represent a “magic bullet” in the treatment of human malignancies. This was not purely based on the frequency of the *PIK3CA* mutations, but also on supporting data that indicated p110 α plays a pivotal role not just in proliferation, metabolism and angiogenesis [32, 51, 53, 125]. Recent data has suggested that inhibition of p110 α and even pan-Class I PI3K inhibition may not be sufficient to kill cancer in the majority of cases [126-127]. Instead, if we wish to utilise PI3K-targetted inhibitors to improve clinical outcome in oncology, it may be necessary to combine them with conventional chemotherapies or inhibitors of other deregulated pathways.

1.6.2. Therapeutic potential of targeting p110 β

The role of p110 β in the regulation of platelet formation makes it an interesting potential anti-thrombosis target. Thrombosis, often occurring as the result of the rupture of atherosclerotic lesions, is a major health concern as it can lead to heart attacks and strokes. Current anti-thrombotic therapies interfere with the capacity of platelets to aggregate and thus reduce thrombus formation but also interfere with normal haemostasis. As a result, standard therapies prolong bleeding and can result in serious bleeding complications. Inhibition of p110 β holds particular promise as a therapeutic strategy because it appears to specifically affect shear stress-induced activation of platelets and thus does not have a detrimental impact

upon bleeding times [83, 128]. This potential capacity to reduce sheer-stress induced thrombus formation in at-risk patients without prolonged bleeding time would be a major step forward in the field of prophylactic treatment for heart attack and strokes.

A potentially important discovery regarding p110 β function in tumours has recently been made [129-130]. As described above, the PI3K pathway is commonly deregulated in cancer, predominantly by activation of p110 α or by inactivation of PTEN [125, 131-132]. Wee *et al.* found that whilst tumours harbouring *PIK3CA* mutations were responsive to inactivation of p110 α those harbouring *PTEN* mutations were not [130]. The authors found that whilst inactivation of p110 α and also p110 δ had little impact on proliferation of PTEN null cell lines, downregulation of p110 β reduced PI3K activity and concordantly reduced cell growth [130]. These finding highlights the importance of understanding the isoform specific roles of the PI3K family members if we are to target them successfully for maximum therapeutic benefit.

1.6.3. Therapeutic potential of targeting p110 δ

As this project focuses on p110 δ , I have concentrated on detailing a number of representative conditions in which p110 δ -selective inhibition may address unmet medical needs.

1.6.3.1. Treatment of immune disorders and inflammatory conditions

There is a vast array of chronic human conditions in which inappropriate activity of the immune system maintains an unnecessary and damaging inflammatory state. Consequently, selective inhibition of p110 δ and also p110 γ represents an exciting opportunity to treat such conditions by disrupting a number of immune functions that drive inflammation.

1.6.3.2. The leukocyte PI3K isoforms p110 γ and p110 δ

The therapeutic potential of dual inhibition of p110 γ and p110 δ has received much attention as they are both enriched in leukocytes and particularly, because their

inactivation *in vivo* results in different but complementary immunological phenotypes. It is hypothesized that, by inhibiting both isoforms, it may be possible to more completely disrupt the dysfunctions associated with chronic inflammatory or autoimmunity conditions. On the other hand, when the individual immunological dysfunctions resulting from either p110 δ or p110 γ are considered, it seems predictable that dual inhibition could also result in an unacceptable degree of immune-compromise [71, 84, 133-134]. Indeed, a p110 γ null-p110 δ KI mouse line was generated and the mice were very sickly with severely compromised immune systems that prevented it surviving in a normal environment [134].

Research over the past decade has identified an ever-increasing list of conditions in which inflammation is at least a contributing factor to the pathogenesis, such as cancer, neuro-degeneration and cystic fibrosis. Thus, the breadth of possible therapeutic applications for p110 δ / γ -selective inhibitors is potentially considerably broader than one might initially anticipate.

Below I have focused on the potential clinical benefits of p110 δ -selective inhibitors in two classic immune disorders: Asthma and Rheumatoid Arthritis. Subsequently, I provide a summary of the data regarding the use of p110 δ -selective inhibitors in the treatment of haematological malignancies.

1.6.3.3. Allergic disorders and chronic inflammation

Allergic disorders are increasingly prevalent in the western world and remain a cause of significant morbidity. As described previously, Ali *et al.* first delineated a cellular mechanism by which p110 δ KI mice had significantly attenuated allergic responses [75]. The mast cells of these mice fail to degranulate efficiently in response to allergen-IgE stimulation, significantly attenuating the release of a range of inflammatory mediators as well as smooth muscle constrictors. The authors subsequently showed that p110 δ but not p110 γ is required for maximal IgE-dependent hypersensitive responses to an allergen *in vivo* [135]. Following these publications, the area of p110 δ and allergy has received considerable interest from the public domain <http://news.bbc.co.uk/1/hi/health/7247600.stm> and the pharmaceutical/translation research community. It has been observed that p110 δ inactivation also reduces macrophage infiltration to the lungs in

murine asthma models (and other chronic respiratory inflammatory conditions) [63]. Indeed, the ability to reduce inflammatory infiltration of the lung tissue, attenuate mast cell degranulation and consequently, to decrease inflammatory mediators, together indicates p110 δ -selective inhibitors could be utilised as potent anti-asthma drugs.

1.6.3.4. Rheumatoid Arthritis

As with severe asthma, chronic inflammatory disorders such as Rheumatoid Arthritis (RA) are characterised by a milieu of inflammatory cells that have infiltrated the diseased tissue. These inflammatory cells continue to drive active inflammation in absence of pathogenic stimuli and this chronic inflammation causes swelling, pain, functional impairment and eventually results in physical damage to the joint structures. The pathology of RA involves a major auto-immune humoral response; primed B cells produce auto-antibodies that drive cytotoxic T cell action, which erodes the joint. As described above, both the differentiation and activation of B cells is impaired in p110 δ KI mice, as the capacity of T cells to activate in response to TcR ligation. Furthermore, Randis *et al.* found that inactivation of p110 δ substantially reduced neutrophil infiltration and importantly reduced joint erosion in a mouse model of serum-induced arthritis [136]. This reduction was found to be comparable to the reduction observed when p110 γ was inhibited. Importantly, the reduction in joint swelling and destruction was greatly enhanced by combined inactivation of both isoforms [136]. Thus, targeting p110 δ activity alone or in combination with p110 γ -selective inhibitors may represent a novel method for interfering with both the infiltration of immune cells and humeral element of the pathogenesis of RA.

1.6.3.5. Haematological malignancies

PIK3CA is rarely mutated in haematological malignancies and therefore, p110 α -selective inhibitors are unlikely to address the aberrant proliferation inherent to these conditions [137-138]. Similarly, mutations in *PIK3CD* have not been identified in haematological malignancies. Despite the absence of mutations, PI3K-Akt signalling has been found to be constitutively active in a large proportion of

haematological malignancies [138-140]. Importantly, this constitutive activation of Akt correlates with poor survival of patients with acute myeloid leukaemia (AML) [140].

The expression of p110 δ is consistently high in AML blasts, whilst the expression of the other Class I PI3K isoforms varies widely between patients [64]. Consistent with this, in the majority of leukaemia subtypes, p110 δ appears to be the key, if not sole isoform upstream of constitutively active Akt. The dominance of p110 δ upstream of constitutively active Akt is demonstrated by the fact that both constitutive and FLT-3-stimulated p-Akt in primary AML blast cells was equally repressed by treatment with a pan-PI3K inhibitor or a p110 δ -selective inhibitor [64]. Crucially, the observed suppression of p-Akt levels correlated with an almost complete blockade of proliferation, whilst the treatment of normal haematological progenitors did not affect their proliferation [64].

Pharmaceutical companies have been quick to pursue the potential of p110 δ inhibition in the treatment of leukaemia. The capacity to repress aberrant growth of haematological malignancies by targeting an enzyme that is not expressed in the majority of tissues is particularly desirable because this should translate to lower toxicity *in vivo*. Gilead, who bought out Calistoga, are currently undertaking clinical trials to test the efficacy of a novel p110 δ -selective inhibitor, CAL-101, in the treatment refractory leukaemia. Preclinical *in vitro* work revealed that CAL-101 efficiently blocked proliferation of primary chronic lymphocytic leukaemia (CLL) cells and also induced apoptosis in these cells [141]. In addition, Lannutti *et al.* found that treating T-acute lymphoblastic leukaemia (ALL) and B-ALL cells with CAL-101 *in vitro* resulted in decreased proliferation and a reduction in phosphorylation of Akt and its downstream targets [142].

The initial results from the CAL-101 trial have been extremely promising; especially with regards to the CLL patient group [143-144]. The therapeutic benefit of CAL-101 was expected to be due to suppression of survival and growth signalling in the leukaemic cells. Interestingly, the clinical activity of CAL-101 is not in keeping with the predicted mode of action. Specifically, patients display rapid lymph node shrinkage and concomitant but transient lymphocytosis, alongside a notable reduction of circulating CCL-3, CCL-4 and CXCL13 [143]. *In vitro* investigation of these observations revealed a reduced migratory and

chemotactic capacity of CLL cells in the presence of CAL-101 and confirmed that the secretion of chemokines was reduced [143]. Thus, it appears that CAL-101 has a dual mechanism of action against CLL. First, as expected, CAL-101 suppresses survival signals in the CLL cells. Secondly, it interferes with the stromal cell interaction that facilitates leukaemic cell accumulation in the lymph nodes and suppresses the secretion of inflammatory mediators. In line with this additional anti-inflammatory effect, the clinical trial coordinators have reported that the best responders to CAL-101 treatment are those patients whose disease has the most inflammatory characteristics [144]. Whether or not CAL-101 and other similar agents will need to be combined with cytotoxic drugs to achieve long-term remission is yet to be clarified, but certainly, the capacity to induce rapid lymphocytosis could represent an opportunity to enhance the efficacy of traditional therapies.

1.7. PROJECT AIMS AND OBJECTIVES

The fundamental objective of this project was to better understand the role that p110 δ plays in macrophage biology. Initially, we focused on comparing the role of p110 δ to that of the other PI3K Class IA isoforms in macrophage signalling. Following this, we have focused on addressing the unanswered question, to what degree does p110 δ activity contribute to the regulation of macrophage transcription? At the time we started, this study there were no publications describing the effects of inactivating p110 δ on the transcriptome of macrophages, or any other cell. We therefore set out to determine the effects of p110 δ inactivation on the macrophage transcriptome, and whilst doing so hoped to identify potential biomarkers of p110 δ inactivation. The initiation of several clinical trials testing p110 δ -selective inhibitors has made this task all the more relevant. Additionally, we wanted to observe whether genetic and pharmacological inactivation of p110 δ have similar effects on gene expression.

1. To compare the roles of the Class IA isoforms in macrophage signalling
2. To investigate the effects of inactivation of p110 δ on the macrophage transcriptome
3. To compare the effects of genetic and pharmacological inactivation of p110 δ on the transcriptome of macrophages
4. To identify potential biomarkers of p110 δ inactivation

CHAPTER 2

2. MATERIALS AND METHODS

2.1. Mice

Maintenance of mouse colonies: Mouse colonies were maintained in accordance with Home Office Guidelines with the help of a qualified Animal Technician. p110 δ ^{D910A/D910A} mice are viable fertile and have no gross anatomical or behavioral defects and have been described previously in Okkenhaug *et al.* [84]. The p110 δ ^{D910A/D910A} mice (p110 δ KI) are usually bred using heterozygous crosses as the female homozygous mice frequently suffer from anal prolapses as a result of severe colitis [86, 123]. The mice used in the Affymetrix experiment and in the subsequent TaqMan[®] validation were obtained from a separate colony from Cambridge, which was maintained as a homozygous line. WT controls were obtained from a WT colony bred in house, which itself was original derived from a commercial breeder.

2.1.1. Genotyping of mice

2.1.1.1. Sample digestion

An ear clipping or tail snip were digested by incubation in 100 μ l NaOH at 100°C for 10 min, followed by 10 min incubation at Room Temperature (RT). The reaction was stopped by the addition of 16.6 μ l of Tris-HCl pH 8.8 and the samples were vortexed and stored at -20°C.

2.1.1.2. Polymerase chain reaction (PCR)

PCR master mix as detailed in Table 2.1 was prepared for n+2 samples and was aliquoted into autoclaved PCR tubes containing 5 μ l of digested DNA. Amplification of target templates was achieved using the cycling conditions detailed below.

PCR Master Mix	1n (µl)	Step	Amplification conditions	Time
DNA	2	1	94°C	3 min
10X PRIMER MIX	5	2	94°C	30 sec
10X PCR BUFFER	5	3	65°C	30 sec
dNTP	5	4	72°C	30 sec
PCR H ₂ O	32.75	5	Return to 2 and repeat x 39	
50XTaq polymerase	0.25	6	72°C	7 min

Table 2.1. PCR master mix reagents and cycling conditions. a. Constituents of PCR master mix.
b. PCR cycling conditions.

2.1.1.3. Primers

Forward primer used at a final concentration of 0.2 µM: D148
(AGGGAACCGCCGTATGAC)

Reverse primer used at a final concentration of 0.2 µM: D146
(AATGCTTTCGTCCCACGTCC)

Expected fragment size		
Genotype	Abbreviation	Base pairs (bp)
Wild type	WT	426
Heterozygous	Het	426 and 554
p110δ ^{D910A/D910A}	p110δ KI	554

Table 2.2. Expected fragment sizes from genotyping PCR.

2.2. Reagents, solutions and buffers

Reagents	
Buffers and reagents	
Tris buffered saline (TBS)	20 mM Tris HCl pH 7.5, 137 mM NaCl in ddH ₂ O
TBS-Tween (TBS-T)	0.1% (v/v) TWEEN 20 in TBS
Tris EDTA (TE) buffer	10 mM Tris HCl pH 7.5, 1 mM ethylenediamine tetra-acetic acid (EDTA)
Cell lysis buffer (to obtain protein)	50 mM Tris-HCl pH 7.4, 100 mM NaCl, 50 mM NaF, 5 mM EDTA, 2 mM ethylene glycol tetra acetic acid (EGTA), 40 mM β-glycerophosphate, 10 mM sodium pyrophosphate, 1% (v/v) Triton X-100
Running buffer	0.25 M Tris-HCl, 0.192 M glycine, 0.1% (w/v) SDS, pH 8.3
Transfer buffer	48 mM Tris-HCl pH 8.5, 0.39 M glycine, 0.1% (w/v) SDS, 20% (v/v) ethanol
Stripping buffer	5% (w/v) Trichloroacetic acid (TCA) dissolved in ddH ₂ O
Enhanced chemiluminescence (ECL) solution	
Mix equal volumes of solution A and solution B	
Solution A	20 mM Tris-HCl pH 8.5, 0.02% (v/v)H ₂ O ₂
Solution B	20 mM Tris-HCl pH 8.6, 13.2 mg coumaric acid, 0.868 mg luminal

Table 2.3. Reagents and buffers.

2.2.1. Inhibitors

Powdered inhibitors were solubilised in Dimethyl sulfoxide (DMSO) to a standard concentration of 10 mM. The diluted inhibitors were stored at -20°C in small aliquots (5-10 µl/tube) aliquots to avoid repeat freeze-thaw cycles of inhibitors.

For use the inhibitors were diluted by 1 in 100 in medium to generate a concentration of 10 µM and were subsequently diluted further in medium to a final concentration as required for experiments. As a negative control the equivalent volume of DMSO was diluted 1 in 100 and subsequently diluted further as per the inhibitor used.

Inhibitor	Target	Source	Cat. No.	Solvent
PW12 ("Paul Workman-12")	p110α	Prof. K Shokat (PIramed compound)	N/A	DMSO
TGX155	p110β	Collaborator	N/A	DMSO
IC87114	p110δ	Calbiochem	528118	DMSO
LY294002	pan- PI3K	Calbiochem	440202	DMSO
Wortmannin	pan- PI3K	Calbiochem	681676	DMSO

Table 2.4. Small molecule inhibitors.

Inhibitor	IC ₅₀ S (µM) of PI3K inhibitors on Class I PI3K p110 isoforms			
	p110α	p110β	p110δ	p110γ
PW12	0.015	0.83	0.73	0.97
TGX155	>20	0.03	0.34	>20
IC87114	> 200	16	0.13	61
LY294002	9.3	2.9	6.0	>20
Wortmannin	0.57	2.33	0.40	0.089

Table 2.5 IC₅₀S of PI3K inhibitors on Class I PI3K p110 isoforms.

IC87114 IC ₅₀ (μM)	
Class IA PI3K isoform	IC ₅₀ (μM)
p110α	>200
p110β	16
p110δ	0.13
p110γ	61

Table 2.6. IC₅₀ for p110δ-selective inhibitor IC87114. IC87114 was the first isoform-selective small molecule inhibitor to be used in published research [62].

2.2.2. Antibodies

Antigen	Manufacturer	Cat. Number
Primary antibodies for immunoblotting		
p110δ	Santa Cruz	sc-7176
Phospho-Akt (S473)	Cell Signalling Technology	4060
Phospho-p-38 (T180/Y182)	Cell Signalling Technology	9215
Akt	Cell Signalling Technology	9272
Rab6b (KT79)	Abcam	ab95374
Rab6a	Abcam	ab55660
GAPDH	Abcam	ab8245
Vinculin	Sigma	V9131
β-actin	Sigma	A5441
Primary antibodies for Fluorescence Activated Cell Sorting		
F4/80-PE	eBiosciences	12480182
IA/IE-PE	BD Biosciences	557000
PE-IgG _{2a} , κ, isotype control	BD Biosciences	553930
FITC-IgG _{2a} , κ, isotype control	BD Biosciences	11432181

Table 2.7. Antibodies.

Primary antibodies were diluted in 3% (w/v) Bovine Serum Albumin (BSA)-TBS-T to the appropriate dilution (usually 1 in 1000). Aliquots were stored at -20°C and were re-used up to four times, depending on their potency.

2.3 Cell culture

2.3.1 Macrophage cell lines

Cell Line	Medium	Growth Supplements	Starvation conditions	Source of cells
BAC1.2F5 [145]	DMEM	10% serum* (v/v) 2 mM L-glutamine, 0.15 mM L-asparagine, 50 nM 2-mercaptoethanol, antibiotics & 10 ng/ml Colony Stimulating Factor-1 (CSF-1)	Remove CSF-1 for 12-48 h	Frozen vials (passage 5) Division of Cell and Molecular Biophysics Kings College London
J774.2 [146]	RPMI	10% (v/v) serum, 1 mM sodium pyruvate, 1X non-essential amino acids, 50 nM 2-mercaptoethanol & antibiotics.	Reduce serum from 10% to 5% (v/v) in complete medium for 12-24 h	Frozen vials (passage 5) Division of Cell and Molecular Biophysics Kings College London
IC-21 [147]	RPMI	As per J774.2	Reduce serum from 10% to 5% (v/v) in complete medium for 12-24 h	Frozen vials (passage 5) Division of Cell and Molecular Biophysics Kings College London
RAW 264.7 [148]	DMEM	As per J774.2	Reduce serum from 10% (v/v) to 0.1-5% (v/v) in complete medium for 12-24 h	Frozen vials (passage 5) Division of Cell and Molecular Biophysics Kings College London

Table 2.8. Macrophage cell lines, culture medium and starvation conditions. Serum refers to heat-inactivated foetal bovine serum (FBS) which was been tested in vitro to ensure macrophages generated in its presence were endotoxin-responsive.

2.3.1.1 Maintenance of cell lines

Cells were maintained in a humidified incubator containing 5% CO₂ at 37°C in the medium detailed in Table 2.8. The cells were passaged in accordance with standard sterile conditions every two to three days.

2.3.1.2 Passage procedure

Cells were washed with pre-warmed calcium- and magnesium-free Phosphate Buffered Solution (PBS) and were subsequently detached by incubation in 5 ml of Versene per 75 cm² flask at 37°C for 5-10 min. Versene contains EDTA which disrupts cellular adhesions by sequestering calcium ions. The detached cells were then resuspended and diluted in the appropriate pre-warmed medium and seeded into fresh tissue culture-treated flasks.

2.3.2 **Isolation and differentiation of primary macrophages**

Macrophages can be derived from mice in two main ways. First, differentiated tissue macrophages can be purified from the spleen or after thyoglycolate stimulation, from the peritoneum. Alternatively, precursor cells can be extracted from the marrow in mouse leg bones and differentiated *ex vivo* in the presence of recombinant Colony Stimulating Factor-1 (CSF-1) or CSF-1-containing L cell conditioned medium (LCCM). We chose to extract bone marrow precursor cells and differentiate them *ex vivo* because this generates much higher yields of macrophages per mouse.

2.3.2.1 Macrophage growth medium

RPMI 1640, 10% (v/v) heat-inactivated low endotoxin FBS, 1 mM sodium pyruvate, 1x non-essential amino acids, 0.029 mM 2-mercaptoethanol. The above was supplemented with either 20 ng/ml recombinant CSF-1 or 10% (v/v) LCCM.

2.3.2.2 Isolation of precursor cells

Bone marrow precursor cells were extracted from femur and fibula bones from the hind legs of mice following cervical dislocation and dissection. The detached legs were dipped in ethanol and cleared of soft tissue before cutting the bones at both ends. Subsequently, the marrow was flushed out of the bones with pre-warmed medium using a 25G needle attached to a syringe. The exudates were homogenized and spun at 5000 x g for 5 min at RT. After resuspension the cells were counted and seeded at a concentration of 1×10^6 cells per ml in macrophage growth medium containing either 20 ng/ml of CSF-1 or 10% (v/v) LCCM on 10 cm² Petri dishes.

2.3.2.3 Original macrophage differentiation protocol

This protocol was used to generate macrophages used in experiments detailed in Chapter 3. After three days culture, non-adherent cells were collected and re-seeded at $3-5 \times 10^5$ cells/ml on 10 cm² Petri dishes and were allowed to differentiate in complete medium containing 20 ng/ml CSF-1 for a further four days before use [Figure 2.1]. Primary macrophages were detached for passage using the same method described above for the macrophage cell lines. The cells were re-plated on fresh Petri dishes in complete medium containing 20 ng/ml CSF-1 and allowed to grow and differentiate for a further four days at which pointed they were harvested for use in experiments [Figure 2.1].

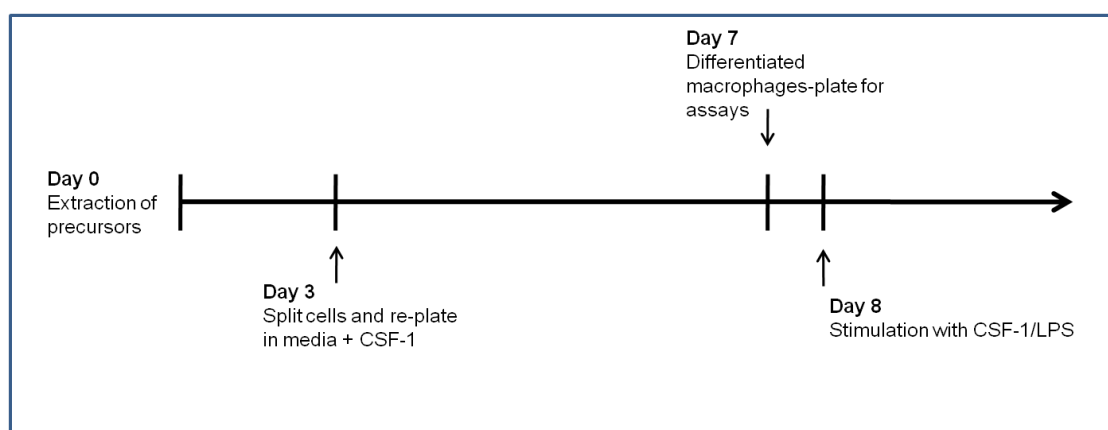


Figure 2.1. Timeline of primary macrophage extraction and differentiation. Precursor cells were split on day 3 and differentiated macrophages were harvested on day 7.

2.3.2.4 Modified macrophage differentiation protocol

All primary macrophages used in Chapter 5 and 6 (all microarray analysis and associated experiments) were generated using a modified protocol. This was due to a problem with the original protocol.

The precursor cells were plated as described above, except the concentration of CSF-1 was increased from 20 ng/ml to 30 ng/ml. One day after isolation the cells were fed 5 ml of fresh complete medium supplemented with 30 ng/ml of CSF-1. After a further three days of culture the medium was removed from plates and fresh medium supplemented with 20 ng/ml of CSF-1 was added. The removed medium was spun down to collect the non-adherent cell population, which was then re-plated in fresh medium supplemented with 20 ng/ml CSF-1 [Figure 2.2]. If the original dishes were 80 to 100% confluent on this third day some of the adherent cells were removed along with the non-adherent population by gently pipetting medium over the mono-layer of cells using a p1000 pipette. The following day (day 4) and on the sixth day after isolation all dishes were fed with 5 ml of medium supplemented with 20 ng/ml of CSF-1 [Figure 2.2]. Seven days after isolation the cells were harvested for use in experiments using the standard splitting procedure described above [Figure 2.2].

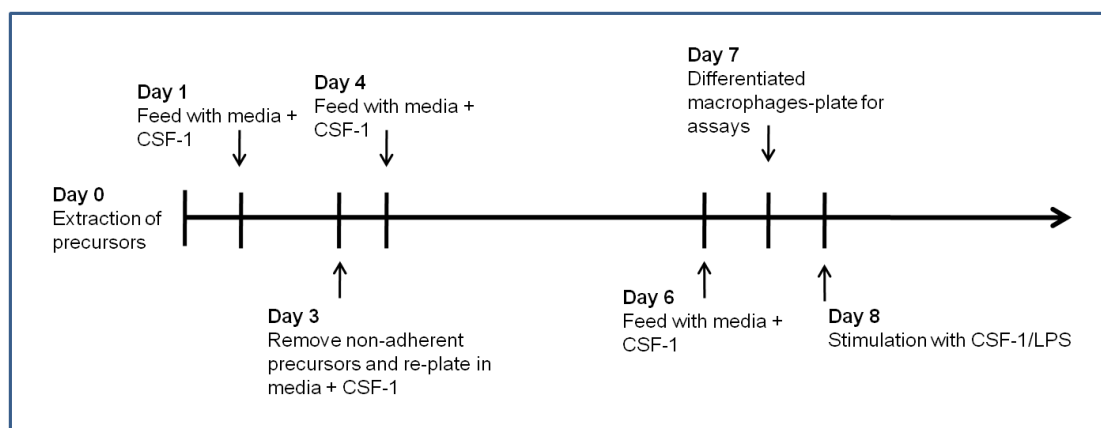


Figure 2.2. Modified primary macrophage differentiation protocol. Precursor cells were fed on day 1 after isolation, split on day 3 and fed again on day 4 and day 6. Differentiated macrophages were harvested on day 7.

2.3.2.5 LCCM production

LCCM was obtained by culturing fibrosarcoma L-cells, which secrete CSF-1. The cells were cultured in large flasks and were sealed using parafilm to induce hypoxic conditions after they had reached approximately 70% confluency. The

medium was removed after approximately two weeks and was tested to confirm its capacity to support the generation of primary macrophages from bone marrow precursor cells at 10% (v/v) of complete medium.

2.3.3 Cell stimulation

2.3.3.1 Stimulation with CSF-1

After starvation by depletion or reduction of either FBS or CSF-1 (as described in Table 2.7) cells were stimulated with 30 ng/ml of CSF-1 for 10 min at 37°C. Stimulation was stopped by placing the plates on ice, removing of the medium and washing the cells with ice-cold PBS. The cell lysates were then prepared as described below.

2.3.3.2 Stimulation with Lipopolysaccharide (LPS)

Cells were stimulated with 1 µg/ml LPS for 30 min at 37°C in complete medium containing 10% FBS. Stimulation was stopped by placing the plates on ice, removing of the medium and washing the cells with ice-cold PBS. The cell lysates were then prepared as described below.

2.4 Protein analysis and detection

2.4.1 Western blot analysis

2.4.1.1 Cell lysis and sample preparation

Cells were lysed with lysis buffer supplemented with a protease inhibitor cocktail (Sigma, P2714) and two phosphatase inhibitor cocktails (Sigma, P2850 & P0044). The wells were scraped and their contents transferred into Eppendorf tubes for incubation on ice for 30 min with intermittent vortexing. Cellular debris was separated and removed from the samples by centrifugation 8000 x g for 10 min at 4°C. Supernatants were transferred to ice-cold Eppendorf tubes and protein concentrations were measured using the Bio-Rad protein assay Bradford reagent to measure the absorbance at 595 nm. Finally, sample concentrations were equalized by the addition of appropriate volumes of lysis buffer prior to addition of

5X sample buffer containing Dithiothreitol (DTT). The samples were denatured by boiled at 95°C for 5 min prior to use or storage at -80°C.

2.4.1.2 Sodium Dodecyl Sulphate-polyacrylamide Gel Electrophoresis (SDS-PAGE)

	Resolving		Stacking
Ingredient	8%	15%	
1.5 M Tris-HCl pH 8.8	3.75 ml	3.75 ml	-----
1 M Tris-HCl pH 6.8	-----		0.625 ml
H ₂ O	6.95 ml	4.25 ml	3.4 ml
30% Acrylamide Solution	4.0 ml	7 ml	0.85 ml
10% SDS	0.15 ml	0.15 ml	0.05 ml
10% APS (ammonium persulfate)	0.15 ml	0.15 ml	0.05 ml
TEMED (tetramethylethylenediamine)	0.01 ml	0.015 ml	0.005 ml

Table 2.9. SDS-PAGE small gel components.

Gel preparation: Small gels were hand poured using the BioRad system. Briefly, resolving gel mix was prepared as described in Table 2.9, poured into the mould and allowed to set. Subsequently the stacking gel mix was poured onto of the set resolving gel with a ten or fifteen tooth comb in place.

2.4.1.3 Loading and separation of protein samples

The gels were placed in an electrophoretic tank containing running buffer, the combs were removed and the denatured samples were loaded alongside a protein molecular weight marker. The proteins were subsequently separated by SDS-PAGE for 90 min at 100 Volts (V). Following separation, the proteins were transferred to an ethanol-activated polyvinylidene fluoride (PVDF) membrane (Immobilon™-P, Millipore) by electroblotting at 100 V for 1 h at 4°C.

2.4.1.4 Antibody incubation and protein detection

Following transfer, PVDF membranes were blocked in 5% Milk powder TBS-Tween (TBS-T) for 20 min to reduce non-specific binding of antibodies to the membrane. Membranes were subsequently washed and incubated overnight at 4°C in the appropriate antibody diluted in 3% BSA-TBS-T. Excess antibody was washed off the membrane using TBS-T prior to addition and incubation for 1 h at RT with horseradish peroxidase-conjugated secondary antibodies diluted in 5% Milk-TBS-T.

2.4.1.5 Visualisation of bands

Membranes were washed with TBS-T and subsequently incubated for 2-3 min in a home-made ECL solution. Finally, exposure of medical X-ray film to the membranes was performed using a standard film cassette in a dark room facility. The exposed films were chemically developed and fixed. Densities of bands were quantified using either ImageJ software or a densitometer (GS-800 Calibrated Densitometer, Biorad). Densitometry provides quantification of the density of bands but density of bands does not actually correlate in a linear manner with HRP-signal. Thus, caution should be applied when analyzing results and comparisons across multiple experiments is not advisable. The results can be considered as semi-quantitative.

2.4.1.6 Stripping membranes

Membranes were washed thoroughly with ddH₂O prior to incubation in 5% (w/v) TCA stripping buffer for 20 min at RT. The membranes were washed and re-blocked before storage or further probing.

2.4.2 Semi-quantitative analysis of PI3K activation using p-Akt to Akt ratios

Direct measurement of changes in the PI species that are generated by active PI3K enzymes requires the use of either radioactivity activity assays or imaging using PIP₃ specific fluorescent probes, both of which are technically challenging and time consuming. In *in vitro* research the level of p-Akt or the ratio of p-Akt over Akt, as detected by antibodies and quantified using a densitometer is commonly used as a proxy read-out for PI3K activity [149].

2.5 Fluorescence activation cell sorting (FACS)

2.5.1 Preparation and staining of cells

Cells were scraped into 200 µl ice cold 1% BSA-PBS and collected in chilled 15ml tubes with 1 ml of 1% (w/v) BSA-PBS prior to spinning at 5000 x g for 5 min at 4°C. Following an additional wash step, the cells were incubated on ice for 30 min and subsequently resuspended in 450 µl 1% (w/v) BSA-PBS. The samples were divided into polystyrene round-bottom tubes and incubated with 1 µl of the two appropriate antibodies for 1 h at RT in the dark. The stained cells were washed to remove unbound antibody as described above and resuspended prior to analysis.

2.5.2 Analysis of stained cell by FACS

Analysis of staining and data acquisition was performed using a FACS machine (DAKO Cyan ADP FACS). Viable cells were gated according to their forward scatter and side scatter profiles. Data was analysed using FlowJo software (TreeStar).

2.6 Extraction of cellular RNA and quality control

2.6.1 Cell lysis

Cells were washed with ice-cold PBS and lysed in RLT Plus buffer (Qiagen, 74104) containing 10 μ l of Beta-Mercaptoethanol (β -MCE)/1 ml. The inclusion of β -MCE in the RLT Plus buffer improved the consistency with which RNA of high quality was obtained. Plates were snap-frozen and stored at -80°C .

2.6.2 RNA extraction

Thawed lysates were homogenized using QIAshredder columns in accordance with the manufacturer's instructions (Qiagen, 79656). Total cellular RNA was subsequently isolated using the RNeasy Plus Mini Kit (Qiagen, 74104) in accordance with the manufacturer's instructions. Purified RNA was eluted in the maximum recommended volume of 50 μ l RNase-free H_2O .

N.B. The RNeasy Plus Mini Kit was used as it includes columns that eliminate genomic DNA from RNA samples, which the RNeasy Mini Kits do not include.

2.6.3 RNA quantification and purity assessment

Total RNA was analysed using a NanoDrop® ND-100 Spectrophotometer to determine concentration and to assess purity. The NanoDrop calculates concentration by measuring the absorbance of a sample at 260 nm; absorbance correlates with concentration in a linear manner (Beer-Lambert law). RNA absorbs strongly at 260 nm, whereas contaminants such as phenol and ethanol absorb around 280 nm. The ratio of absorbance at 260 nm over 280 nm can therefore be used to determine purity; a ratio of 2.0 or above is indicative of a pure RNA sample. Other contaminants such as proteins and EDTA strongly absorb at 230 nm and therefore the A_{260}/A_{230} nm ratio can also be used to monitor RNA sample purity.

2.7 Quantitative real-time PCR (qPCR)

Real-time qPCR is a two-step method used to quantify the expression of a gene of interest by measuring PCR amplification of a target sequence within a sample. First, the RNA is reverse transcribed to generate cDNA and the cDNA sequence of interest is subsequently amplified by PCR using sequence-specific primers. This sequence-specific amplification is measured in real time (after each cycle) throughout the PCR. Measurement of amplification is performed using one of two main methods.

1. The SYBR Green method utilises a fluorescent dye that intercalates in a non-specific manner into newly synthesized DNA. The fluorescence emitted is positively correlated with the amount of amplified DNA and therefore, with the concentration of the target sequence in the sample.
2. The TaqMan method utilises gene-specific probes covalently linked to a fluorescent reporter dye at the 5'-end and a fluorescence quencher at the 3'-end measure target-specific amplification. These probes anneal within the region amplified by the gene-specific primers. During amplification the probe is cleaved by the 5'-nuclease activity of the advancing polymerase resulting in the separation of the reporter from the quencher resulting in emission of fluorescence. The fluorescence detected in this method is directly correlated with the concentration of the target DNA sequence [Figure 2.3].

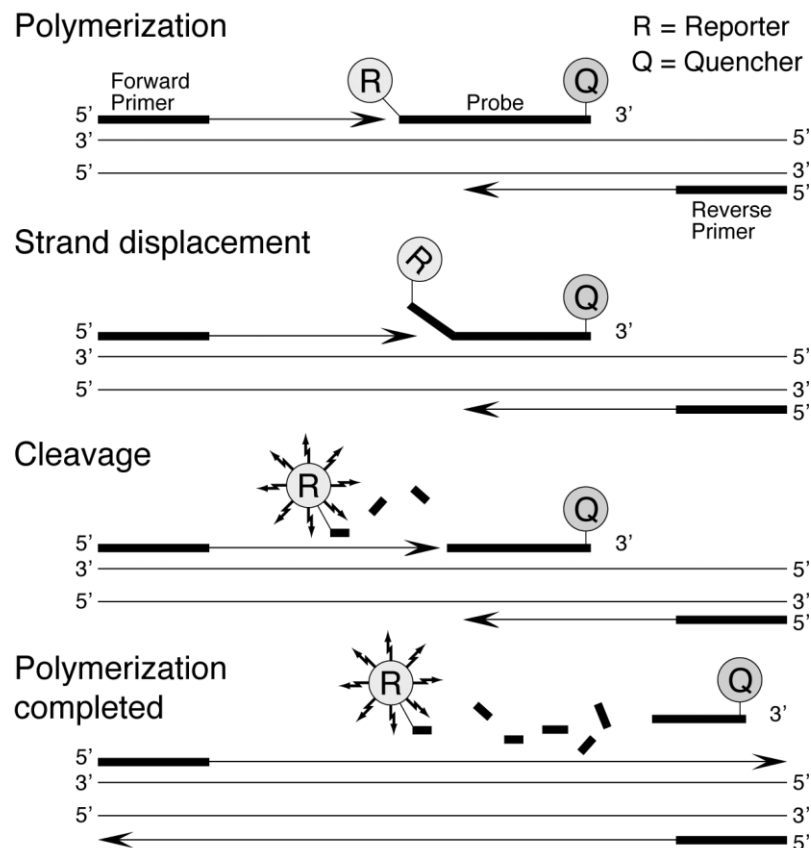


Figure 2.3. TaqMan® gene-specific probes. The advancing polymerase displaces the reporter from the 5'-end of the bound probe resulting in its separation from the quencher and concomitant emission of fluorescent signal. Image reproduced with permission from Applied Biosystems. [www.appliedbiosystems.com].

2.7.1 Reverse transcription

Reverse transcription was performed using the TaqMan® Reverse Transcription Reagents Kit (Applied Biosystems, N8080234) in accordance with the manufacturer's instructions. Briefly, 1-5 µg of RNA was reverse transcribed using Multiscribe Reverse Transcriptase at 2.5 U/µl, in the presence of random-hexamer primers at 2.5 µM, mixed dNTPs at 0.5 mM, MgCl₂ at 5.5 mM plus 5 µl 10X PCR buffer and sufficient H₂O to make the mix up to 50 µl per reaction. The reaction was then performed in a thermal cycler [Table 2.9]. The cDNA generated was either processed or stored at -80°C.

Reverse transcription thermal settings	
Temperature	Time
25°C	10 min
37°C	60 min
95°C	5 min
4°C	-----

Table 2.10. RT-PCR thermal cycling conditions.

2.7.2. qPCR

We utilised the TaqMan method to measure the relative expression of genes of interest in control samples compared to samples derived from treated or mutant cells. Inventoried TaqMan Gene Expression Assays (part number, 433182) containing gene-specific primers and probe sets that had been pre-designed and validated by Applied Biosystems were used in accordance with manufacturer's instructions qPCR method. In addition to assays for the genes of interest, assays for endogenous controls such as beta-actin or 18S were included in every experiment to allow for normalisation across samples. Briefly, a master mix was made for each assay as described in Table 2.10, and aliquoted into appropriate wells of a 384-well plate before the addition of 2 µl of cDNA produced by Reverse Transcription.

qPCR master mix	1n
Universal Master Mix (4364338)	5 µl
ddH ₂ O	2.5 µl
Taqman primers/probe 20X	0.5 µl

Table 2.11. qPCR master mix.

Each reaction was performed in triplicate. In order to account for contamination and non-specific amplification a negative control of additional replicates containing no added cDNA (RT negative) were included for each assay. 40 cycles of amplification was performed using an Applied Biosystems Prism 7900HT Sequence Detection System using the cycling conditions detailed in Table 2.11.

Step	Time	Temp.	Ramp rate	Notes
PCR activation	15 min	95°C	20°C/s	Activates hot start polymerase
2-step cycling				
Denaturation	0 s	95°C	20°C/s	
Annealing & extension	60 s		20°C/s	Fluorescence data collection
Number of cycles	33-55			Dependent on amount of template DNA

Table 2.12. qPCR cycling conditions.

Amplicon	TaqMan Assay ID
Housekeeping genes	
18S rRNA	Hs99999901_m1
GAPDH	Mm99999915_g1
β -actin	Mm00607939_s1
TBP	Mm00446971_m1
Targets	
<i>Clstn1</i>	Mm00502631_m1
<i>Efcab1</i>	Mm00523825_m1
<i>Efhd2</i>	Mm00482568_m1
<i>Fblim1</i>	Mm00505298_m1
<i>Fst</i>	Mm00514982_m1
<i>Htatsf1</i>	Mm00459252_m1
<i>Kif1b</i>	Mm00801813_m1

<i>Mthfr</i>	Mm00487784_m1
<i>Nin</i>	Mm01265284_m1
<i>Pdpr</i>	Mm00494716_m1
<i>Plod1</i>	Mm01255760_m1
<i>Rab6b</i>	Mm00620651_m1
<i>Rex</i>	Mm03029904_g1
<i>Ube4b</i>	Mm00502528_m1
<i>Ubiad1</i>	Mm00503616_m1

Table 2.13. TaqMan Inventoried gene expression assays

2.7.3 Data extraction and analysis

Obtaining raw data: Before obtaining values from amplification plot two parameters must be set; the base line and the threshold. Both are set automatically by the Sequence Detection Software (SDS) Relative Quantification (RQ) Manager, but should be checked manually to ensure correct positioning.

Baseline: Background fluorescent signal accounts for the majority of the signal detected during early thermal cycles prior to substantial amplification. The baseline threshold must be set across a range exceeding this level of background fluorescence; the SDS RQ Manager software automatically sets the baseline from cycles 3-15. If the baseline is set appropriately the initial amplification will occur one or more cycles after the end of this base line (i.e. after 16 cycles if the automatic baseline is left in place). If the target is particularly abundant, as is usually the case for housekeeping genes such as 18S rRNA, the initial amplification will occur earlier than cycle 15. The baseline must then be manually adjusted to 1-2 cycles prior to the initiation of amplification.

Cycle threshold (Ct) value: The final value obtained for each replicate is the cycle threshold (Ct) value. The Ct is the cycle of the PCR reaction at which the detected fluorescence crosses the threshold [Figure 2.4]. Transcripts of low abundance

have larger the C_t values as the number of cycles taken to reach the fluorescence threshold is greater.

Threshold: In order to obtain an accurate C_t value the appropriate threshold must be set. The threshold must be above the initial linear region and below the plateau region, i.e. within exponential linear region. The threshold is automatically set at 10 standard deviations above the baseline and this should be within the region of exponential amplification in all plots [Figure 2.4]. The position of the threshold is best assessed in the log view of an amplification plot in which the region of exponential amplification appears linear. Identifying where the replicates are the least variable within this linear region assists in the identification of the optimal position for the threshold. To assess the precision of the replicates the x-axis of the amplification plot can be widened.

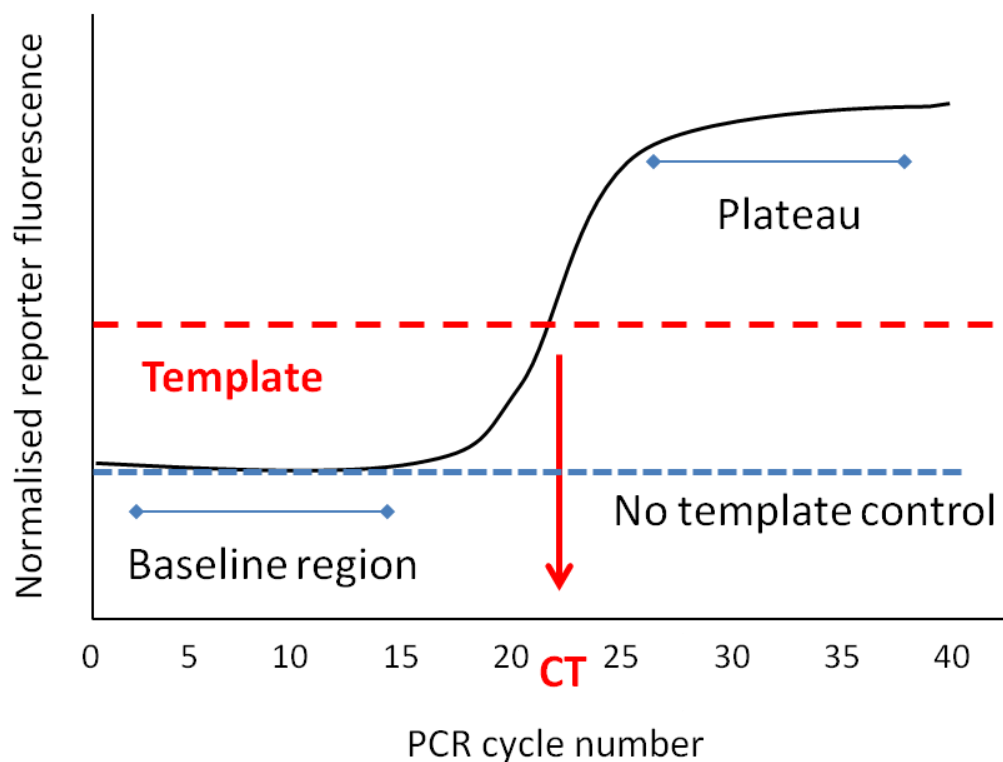


Figure 2.4. qPCR amplification plot features. Baseline automatically set from 3-15 cycles and the threshold is automatically set 10 standard deviations above the end of the baseline. C_t value is read off the graph from the intercept of the amplification line through the threshold.

2.7.3.1 Relative quantification of gene expression

The Comparative Ct method allows the user to determine relative expression of a gene of interest in two or more conditions and subsequently to calculate folds change from these values. This method abrogates the need to generate a standard curve of transcript copy number, but as a result cannot be used for absolute quantification. This method relies upon the fact that the amplification efficiencies of the target amplification and the endogenous control amplification are equivalent. 100% amplification efficiency denotes a doubling of PCR product/amplicon at every PCR cycle, i.e. exponential amplification. All TaqMan Gene Expression assays have been validated by the manufacturer and are reported to have an average efficiency of 100% (-/+ 10%).

Having obtained a Ct value for each well the **delta Ct (Δ Ct) equation** can be used to calculate fold change relative to the control sample, known as the calibrator. In this project WT unstimulated was set as the calibrator sample. First, the Ct value is normalized to the housekeeping control to account for any sample to sample variation to generate the **Δ Ct value**. The Δ Ct value can then be normalized to the Δ Ct of the calibrator sample, producing the **$\Delta\Delta$ Ct value** which is negative. Finally, the $\Delta\Delta$ Ct value can be converted into a fold change using the formula (treatment over calibrator) $2^{-\Delta\Delta Ct}$.

Calculations for comparative Ct method

1. Ct target gene - Ct endogenous control = Δ Ct
2. Δ Ct sample - Δ Ct calibrator = $\Delta\Delta$ Ct
3. Apply the formula: $2^{-\Delta\Delta Ct}$ = **fold change relative to calibrator sample**

2.7.4 **Semi-high throughput qPCR**

2.7.4.1 TaqMan Array Microfluidic cards

Applied Biosystems offer TaqMan assays in a semi-high throughput format containing multiple TaqMan assays. These TaqMan Array Microfluidic cards are a form of low density arrays (LDAs) contained within microfluidic 384 well-cards. The arrays are available either as custom cards in which the included assays are

selected by the customer or alternatively as pre-designed gene-signature cards. The array cards allow for standardized relative quantification of the expression of a selection of genes across multiple unique samples in a semi-high throughput format.

2.7.4.2 LDA formats

TaqMan Array Microfluidic cards are available in ten different formats which allow the user to determine relative expression of between eleven and 380 genes depending on the number of samples analysed per card, the number of replicates per reaction and the number of endogenous control assays included. We choose to use format 32 (part number, 4346799) which can include up to 31 unique assays alongside at least one mandatory endogenous control assay with three replicates per assay. This format allows the relative quantification of all thirty unique assays and one control to be determined in four unique samples per array card. We included four endogenous controls.

2.7.4.3 LDA method

The custom-made array cards were used in accordance with the manufacturer's instructions. Briefly, total RNA was reverse transcribed as described above except that a High Capacity RT Kit (Applied Biosystems, 4368813) was used instead of the standard RT kit.

The cDNA was then mixed with TaqMan PCR Master Mix and RNase-free water as described in Table 2.13; twice the volume of this master mix was made for each sample as each sample was loaded into two reservoirs. The volume of master mix made was increased to ensure there was enough to load 100 µl/reservoir. The manufacturer recommends that between 30 and 1000 ng of total RNA should be included per sample/reservoir, we used 250 ng/reservoir.

Component	Vol (μl)/reservoir	Vol (μl)/sample
cDNA sample + Rnase free H₂O	50	120
TaqMan universal PCR Master Mix	50	120
Total	100	140

Table 2.14. Components of qPCR mix for analysis in TaqMan Array Cards.

100 μl of each sample mix was pipetted into two of the eight loading reservoirs at the top of the cards. The cards were spun and sealed using the array card sealer. The arrays were then run on an Applied Biosystems Prism 7900HT Sequence Detection System with a TaqMan Array Card file pre-loaded.

Manufacturer's video demonstrating loading and processing of TaqMan arrays:

http://www2.appliedbiosystems.com/lib/multimedia/taqman_tlda/tlda_1.cfm

2.7.4.4 LDA data analysis

Analysis of TaqMan array card data is identical to analysis of individual TaqMan assays. The data for all cards from one experiment must be loaded into the SDS RQ Manager software together to allow baselines and thresholds to be set consistently across all cards for each assay.

Manufacturer's video demonstrating analysis of TaqMan array data:

http://media.invitrogen.com.edgesuite.net/ab/videos/TMArrayCard_iw_360.swf

2.8 Genome-wide expression analysis

Genome-wide expression analysis allows the user to rapidly identify the effects of a certain perturbation such as an inhibitor or mutation, on global transcriptional regulation. The expression of every gene can be determined and compared in a control and treatment sample. There are now a number of microarray platforms available which enable rapid analysis of the entire transcriptome in multiple samples.

In the case of two-colour arrays, the control and treatment samples are processed so that the final samples are labeled with two different fluorophores. The differently labeled samples are then mixed and hybridized to a single microarray. This method can be used to identify genes that are either up- or down-regulated in the treatment sample compared to the control sample can be determined. Alternatively, one-colour arrays are available that allow the user to obtain an expression value for each gene/transcript in the microarray in multiple independent samples, which are each hybridized to a separate array. This allows for the comparison of expression of a gene of interest across many samples and even across multiple experiments if batch effects are taken into account. A comparison of the expression of different genes within a sample cannot be made because factors such as hybridization efficiency of probes-target sequences effect the final expression value. Both of these approaches have allowed scientists to identify lists of individual genes affected by particular treatments, mutations or disease states and have also provided a more global perspective on the effects.

2.8.1. RNA integrity

RNA is highly susceptible to degradation because ribonucleases (Rnases) are ubiquitous in the environment and can easily contaminate a sample. Significant degradation of RNA can affect whole-genome expression analysis. Therefore, in addition to the assessment of purity of samples RNA integrity must also be checked to confirm quality.

The abundance of two ribosomal RNA (rRNA) species, 18S and 28S, is used as a marker to assess the integrity of RNA. The abundance of these rRNA species in a sample can be measured by running RNA samples labeled with an intercalating

fluorescent dye on an electrophoretic gel. 28S and 18S rRNA exist in equal concentrations in cells, but twice as much fluorescent dye intercalates into 28S rRNA than into 18S resulting in a 28S band with double the fluorescent intensity of the 18S band. Furthermore, 28S rRNA is degraded before the 18S rRNA in samples exposed to ribonucleases and thus, a ratio significantly less than two indicates degradation of RNA species has occurred within the sample. Significant shifts in the ratio of 28S to 18S are normally observed alongside smearing on the gel due to the presence of fragmented RNA.

2.8.1.1 Agilent Bioanalyser

RNA quality can now be determined with improved accuracy using technology developed by Agilent. The Agilent Bioanalyser applies the standard electrophoretic technique in a chip format with software that utilises an algorithm to assess RNA integrity. The algorithm takes into account the 18S to 28S rRNA ratio alongside additional factors that are also predictive of RNA quality [150]. The software generates an electropherogram on which the two distinct peaks, which correspond to the 18S and 28S rRNA can be seen alongside the 25 nucleotide marker [Figure 2.5].

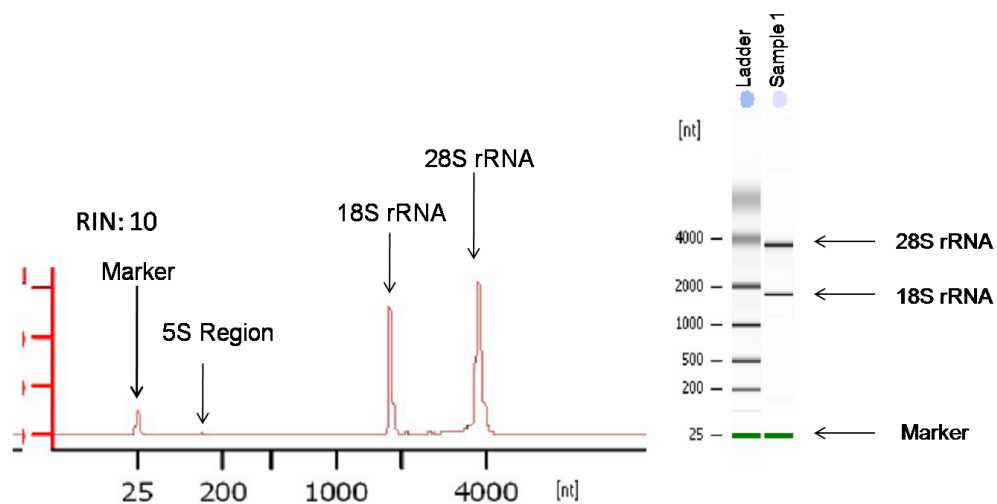


Figure 2.5. Agilent Electropherogram. Agilent Bioanalyser produces an electropherogram on which the fluorescence signal from labelled 28S and 18S rRNA species is plotted alongside a 25 nucleotide marker. The x-axis (25-4000) represents nucleotides (nt). 18S rRNA at around 1400 nt and 28S rRNA at around 4000nt. Based on the area under the peaks for the 18S and 28S rRNA a ratio of 2.0 is calculated, and no smaller fragments are apparent indicating no degradation products were present in this sample. To the right the gel image of the sample; the upper band is the 28S rRNA, the lower is the 18S rRNA and the green band represents the marker which can also be seen as a small peak.

An RNA Integrity Number (RIN) is assigned to each sample; the RIN scale ranges from ten to one and in some cases highly degraded samples are not assigned a RIN. A RIN of ten indicates an optimal intact sample to a RIN, whereas a RIN below eight is indicative of moderate degradation and RIN below 7 is indicative of highly degraded RNA [Figure 2.6] [150].

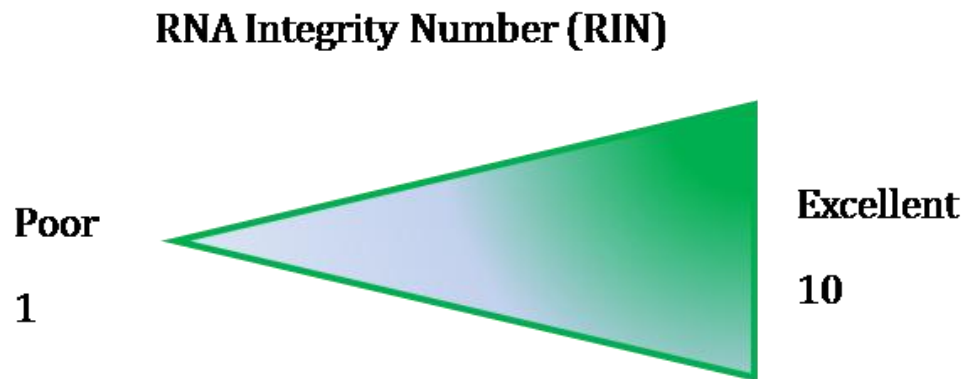


Figure 2.6. RNA integrity number. Agilent Bioanalyzer assigns a RIN to each sample analysed based on a number of parameters including the 18S to 28S ratio and the presence of small RNA fragments that represent degradation products.

Ideally samples to be analysed by microarray should have a RIN of 8 or more and the RIN across a sample set should also be relatively consistent within an experiment.

2.8.1.1.1 Agilent method

RNA samples were analysed to determine integrity using an Agilent Bioanalyser in accordance with the manufacturer's instructions. Briefly, 1 μ l of each sample was loaded into the wells of the RNA 6000 Nanochip pre-loaded with a sieving polymer and fluorescent dye. A 25 nucleotide marker and a ladder of RNA fragments were also loaded. The chip was vortexed using an IKA vortex mixer (Model MS2-S8/S9) at 2400 rpm and then analysed using the Agilent Bioanalyzer. All samples used in our microarray studies were assigned a RIN of between 9.8 and 10, with 18S to 28S ratios of between 1.8 and 2.0.

2.8.2. Affymetrix genome-wide expression analysis

Affymetrix is a world-leader in the field of whole-genome expression analysis as the most frequently used microarray platform in published work. Affymetrix microarrays are in the form of GeneChips® that encompass one-colour oligonucleotide arrays. In oligonucleotide arrays the probes (complementary sequences that hybridise to labeled target sequences) are synthesized in clusters *in situ* on a glass surface using the photolithographical method.

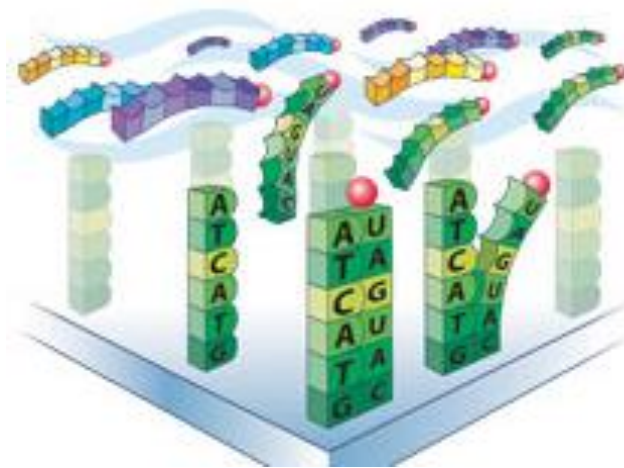


Figure 2.7. Schematic of the hybridisation of a labeled target sequence from the sample to a probe. Labeled RNA samples are added to chip and allowed to hybridise with complementary fixed probes. [Image reproduced with permission from Affymetrix Image Library].

Highly complementary labeled target sequences will form multiple non-covalent bonds with the corresponding probe and will thus remain hybridized after washes remove those partially complementary sequences.

2.8.2.1. The Affymetrix Mouse Genome GeneChip® 430 2.0 Array

The Affymetrix Mouse Genome GeneChip® 430 2.0 Array that we used in this study provides complete coverage of the mouse genome with over 39,000 transcripts interrogated by over 45,002 probe sets. The clusters of probes synthesised on a GeneChip® are made up of probe sets, which each consist of eleven probes that together are designed to interrogate a particular sequence. Each probe is twenty-five base pairs long and is complementary to a different segment of the 3' region of a given sequence. Each probe set includes a number of mismatch probes that enable a value for non-specific binding to the transcript of interest to be

determined. The expression value for each probe set is the mean value of all the probes within that set normalised to the non-specific binding detected. The probe sets allow multiple independent measures to be obtained for a single gene or transcript, which increases the accuracy and reproducibility of the final probe set expression value. Furthermore, some genes/transcripts are represented by multiple probe sets, which target different sequence regions and the presence of these redundant multiple probe sets spotted at different locations increases the reliability of the data obtained. Multiple probe sets can in some cases assist in the identification of regulatory events affecting part but not all of the sequence being interrogated.

2.8.2.2. GeneChip® 3' IVT Expression Kit

2.8.2.2.1. RNA Amplification, Fragmentation and Labelling

The total RNA was processed using the GeneChip® 3' *In Vitro* Transcription (IVT) Expression Kit in accordance with manufacturer's instructions. The GeneChip® 3' IVT Expression Kit utilizes poly-A directed primers to produce fragmented amplified RNA (aRNA) [Figure 2.8; steps 1-5].

Briefly, first-strand and second-strand cDNA were synthesised from total RNA [Figure 2.8; steps 1-3]. Subsequently *in vitro* transcription was performed using biotinylated Ribonucleotide Analogs [Figure 2.8: step 4]. The biotinylated aRNA generated was purified and quantified using the NanoDrop® ND-100 Spectrophotometer [Figure 2.8: step 5]. The RNA 6000 Nano Kit with an Agilent 2100 Bioanalyser were employed to confirm the size of aRNA samples were between 250-5500 nucleotides long.

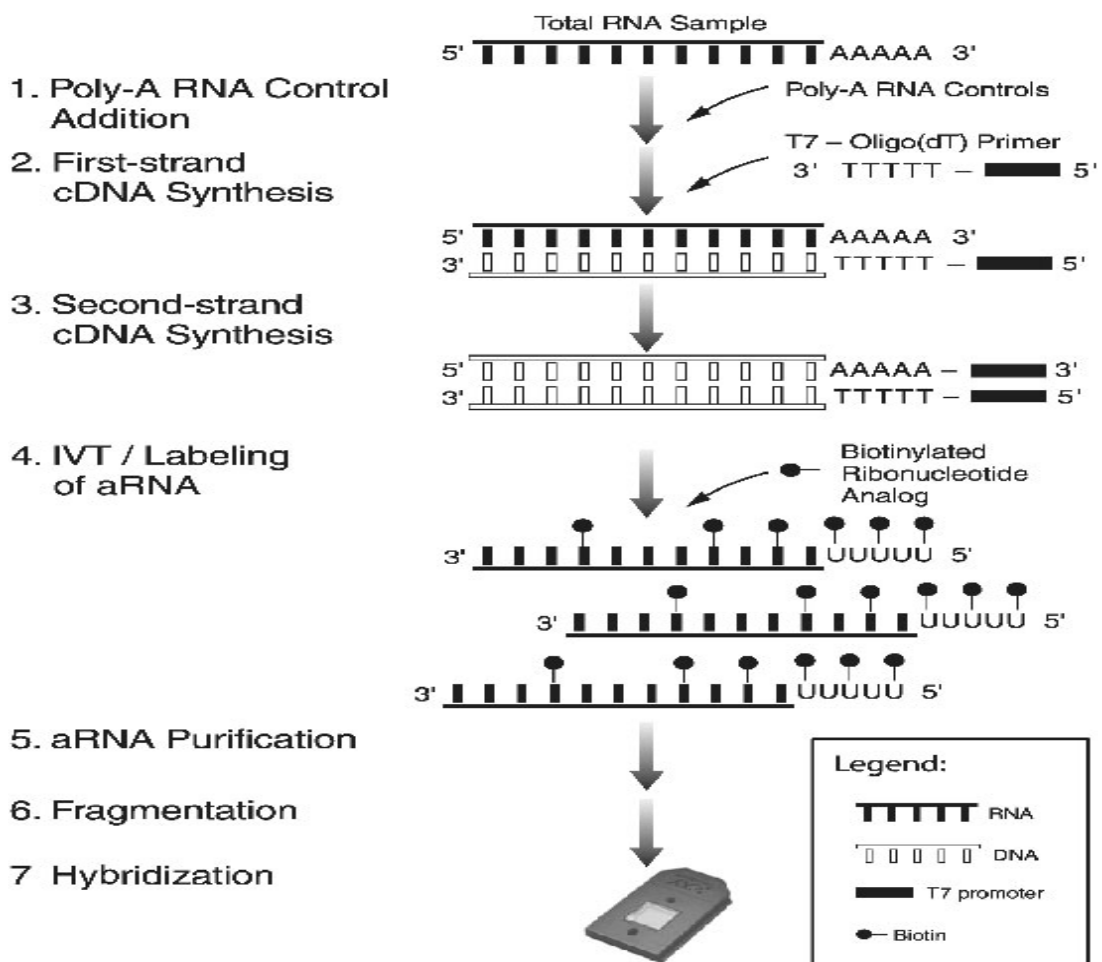


Figure 2.8. A summary of the protocol for the GeneChip® 3' *In vitro* transcription (IVT) expression kit. First and Second Strand cDNA are synthesised from total RNA for each sample, and subsequently *in vitro* transcription is performed using biotinylated ribonucleotide Analogs to generate aRNA. aRNA is purified from the mixture and subsequently measured and fragmented prior to hybridisation to a GeneChip® Mouse Genome 430 2.0 Array chips. [Image from the Affymetrix GeneChip® 3'IVT Express Kit User Manual, reproduced with permission from the Affymetrix GeneChip® 3' IVT Express Kit User Manual, part 901228 [www.affymetrix.com].

The biotinylated amplified RNA (aRNA) was then fragmented [Figure 2.8: step 6]. A hybridization cocktail was then made including the fragmented labeled aRNA and a number of hybridization controls as described in Table 2.15. This was then injected into the GeneChip® Mouse Genome 430 2.0 arrays and left to hybridise on a rotor in a hybridization oven at 45°C for 16 h [Figure 2.8: step 7].

Component	Volume/array	Final dilution
Fragmented and labeled aRNA	12.5 µg (33.3 µl)	0.05 µg/L
Control Oligonucleotide B2	4.2 µl	50 pM
20X Hybridization Controls (bioB, bioC, bioD, cre)	12.5 µl	1.5, 5, 25, 100 pM respectively
2X Hybridisation Mix	125 µl	1X
DMSO	25 µl	10%
Nuclease free water	50 µl	-----
Total volume	250 µl	-----

Table 2.15. Hybridisation cocktail components.

After 16 h incubation with the labeled fragmented aRNA the chips were washed and stained according to the IVT kit protocol in a GeneChip® Fluidics Station 450 (according to the manufacturer's Fluidics protocol FS450_0001). Washed chips were subsequently scanned in the Affymetrix GeneChip® Scanner 3000.

2.8.2.3. Analysis of Affymetrix data

Analysis of expression data is described in further detail in Chapter 4. Briefly, the data for all chips was extracted and normalized using the GeneChip-Robust Multiarray Averaging (GC-RMA) algorithm. The data was reduced by filtering to include only the top 10,000 most variable probe sets.

Genome-wide expression analysis produces expansive data sets and thus, mathematical models must be employed to drastically reduce the dimensionality of the data in order to obtain useful information.

We employed Principal Component Analysis (PCA) to reduce the data in order to obtain information on clustering and to identify outliers. Subsequently, the data was analysed to identify affected genes and pathways or processes that were enriched with those genes identified.

Differentially regulation was determined by calculating the ratio of the average expression data of each probe set in the IC87114 samples compared to in the DMSO samples. This ratio was converted into a log fold change using a log to the

base 2 conversion. The statistical significance of fold changes was calculated and the p values were subsequently adjusted hypotheses using the Benjamini-Hochberg (B-H) Correction formula [151]. The B-H correction controls for the false discovery rate thus reducing the number of false positives likely to occur within a dataset. This correction is required as a result of the multiple hypotheses testing that is intrinsic to microarray data analysis and which inflates Type I statistical errors.

2.8.2.3.1. Network and gene ontology enrichment analysis

Ingenuity Pathway Analysis (IPA) software (Ingenuity Systems®) was used to test for an enrichment of genes associated with a particular gene ontology or network within our data sets. The software automatically excludes duplicate probe sets from analysis and also only excludes those probe sets mapped to a particular gene or function in analysis. Top pathways and gene ontologies are identified and the statistical significance of the enrichment is provided by the software as a score. A score of 20 indicates the relevance of the network to the gene list has a statistical significance of $p = 10^{-20}$.

CHAPTER 3

3. INVESTIGATING THE FUNCTIONS OF CLASS IA PI3K ISOFORMS IN MACROPHAGES

3.1. Introduction

Previous investigations into the contributions of the individual Class IA PI3K isoforms in immortalised BAC1.2F5 macrophages revealed that the isoforms perform distinct roles downstream of CSF-1 stimulation. Specifically, in these cells inhibition of p110 δ activity blocks CSF-1-induced cytoskeletal rearrangements and chemotaxis, whilst blockade of p110 α activity has no effect on these processes but instead significantly reduces proliferation and p-Akt generation [80]. Based on these data it appears that in BAC1.2F5 macrophages, p110 δ is required to drive CSF-1-induced actin cytoskeleton rearrangements and chemotaxis whilst p110 α alone regulates proliferation [80]. These findings showed that the Class IA PI3K isoforms can fulfil distinct roles downstream of a single stimulus. Furthermore, these data revealed that the uninhibited PI3K isoforms do not compensate for the loss of activity of an inhibited isoform in these cells downstream of CSF-1, at least not upon acute inhibition in the conditions tested.

In order to establish whether the observed non-redundancy of Class IA PI3K isoform function is a common feature of macrophage-like cells, Dr Papakonstanti a former postdoctoral fellow in the laboratory, compared their contributions downstream of CSF-1 in primary macrophages. The data indicated that all observed responses to CSF-1 including induction of p-Akt, proliferation and chemotaxis are repressed by inhibition of p110 δ but not by the inhibition of p110 α or p110 β [p-Akt data are shown in Figure 3.1, data regarding proliferation and chemotaxis are not shown]. First, these data confirmed that the functions of the isoforms are also non-redundant in primary macrophages as they are in BAC1.2F5 macrophages. Secondly, these data revealed a significant disparity between the isoform contributions in primary macrophages compared to BAC1.2F5

immortalised macrophages. Specifically, primary macrophages are much more dependent on p110 δ activity than BAC1.2F5 macrophages. The observed dominance of p110 δ in primary macrophages is consistent with its reported dominance in primary mast cells and primary lymphocytes [75, 84, 152].

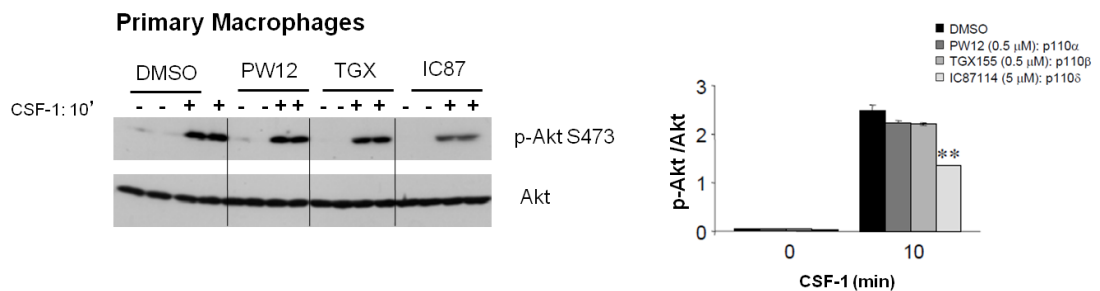


Figure 3.1. CSF-1-induced p-Akt in primary macrophages is significantly reduced by inhibition of p110 δ , and is not significantly affected by inhibition of either p110 α or p110 β . Dr Papakonstanti starved the macrophages of CSF-1 overnight prior to 1 h pre-treatment with the indicated inhibitors: PW12 (0.5 μ M), TGX155 (0.5 μ M), IC87114 (5 μ M). Subsequently the macrophages were stimulated by the addition of CSF-1 (33 ng/ml) and the p-Akt to Akt ratios were then measured using western blotting [1]. Graph presents data for the mean \pm s.e.m. of two experiments performed in duplicate (* p < 0.05; ** p < 0.01; *** p < 0.001).

It is of interest to note that inhibition of p110 δ in primary macrophages does not result in the complete repression of CSF-1-induced p-Akt and in fact the reduction represents approximately 50% of the uninhibited CSF-1-induced p-Akt level [Figure 3.1]. Nevertheless, inhibition of the other isoforms had no significant impact on CSF-1-induced p-Akt.

3.2. Investigating a correlation between immortalised state and loss of p110 delta dependency in macrophages

We reasoned that the observed dominance of p110 α in the induction of CSF-1-induced p-Akt in BAC1.2F5 macrophages, whilst p110 δ was primarily responsible for this in primary macrophages, might be related to the immortalised state of the former cells. We therefore set out to clarify whether the shift to dominance of p110 α is common to macrophage cell lines and thus is correlated with the immortalised state. To do this we compared the involvement of the Class IA PI3K isoforms in the generation of CSF-1-induced p-Akt in additional macrophage cell lines. We acknowledge that it could also have been informative to determine the

involvement of p110 γ in CSF-1-induced p-Akt. This was not done primarily as this work was performed within the constraints of a body of work that had already been performed by Dr Papakonstanti. In addition, p110 γ is thought to only act downstream of GPCRs rather than RTKs such as CSF-1 unlike p110 α and p110 δ which are recruited and activated by RTKs and p110 β that can couple to GPCRs and also to RTKs.

Before embarking on this task, we confirmed the previous unpublished data that identified p110 α as the principal isoform responsible for CSF-1-induced p-Akt in BAC1.2F5 macrophages [Figure 3.2].

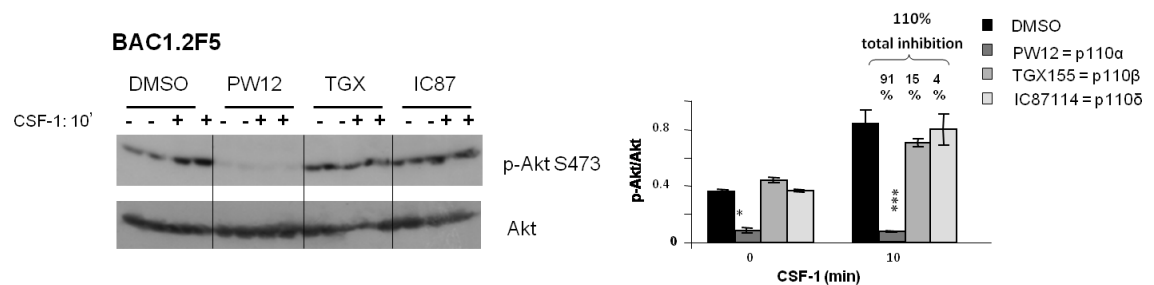


Figure 3.2. BAC1.2F5 macrophages require p110 α activity for basal and CSF-1-induced p-Akt. BAC1.2F5 were starved of CSF-1 overnight prior to pre-treatment for 1 h with indicated inhibitors the following day: PW12 (0.5 μ M), TGX155 (0.5 μ M) or IC87114 (5 μ M). The cells were subsequently stimulated with CSF-1 (33 ng/ml) for 10 min. The graph and western blot are representative of results of two experiments. Graph presents data for the mean \pm s.e.m. of these two experiments performed in duplicate (* p < 0.05; ** p < 0.01; *** p < 0.001). Percentages represent percentage decrease in p-Akt in the inhibitor treated sample compared to the p-Akt levels in the CSF-1-stimulated DMSO control.

3.3. The contributions of Class IA PI3K isoform to Akt activation macrophage cell lines

First, we determined the Class IA PI3K isoforms necessary for generation of CSF-1-induced p-Akt in two additional macrophage cell lines; IC-21 and J774.2. We observed decreased CSF-1-induced p-Akt in both of these cell lines after pre-treatment with p110 α , p110 β or p110 δ -selective inhibitors, but only the decrease observed in response to inhibition of p110 α was found to be significant [Figure 3.3]. Our data indicated that in IC-21 and J774.2 macrophages, p110 α and not p110 δ was the principal isoform responsible for CSF-1-induced p-Akt. The contribution of p110 α observed in the IC-21 and J774.2 macrophages was not as substantial as the contribution of p110 α in BAC1.2F5 macrophages. When we

calculated the percentage inhibition of p-Akt in the stimulated state we found a 91% decrease in the presence of a p110 α -selective inhibitor in BAC1.2F5 macrophages [Figure 3.2] whereas in J774.2 and IC-21 we observed a 39% and 56% decrease, respectively [Figure 3.3]. The percentage reduction in CSF-1 induced p-Akt in the IC-21, J774.2 and the BAC1.2F5 macrophages in response to p110 β inhibition was relatively consistent and appeared to be minimal with a decrease of between 15-17% observed across the cell lines [Figure 3.2, 3.3].

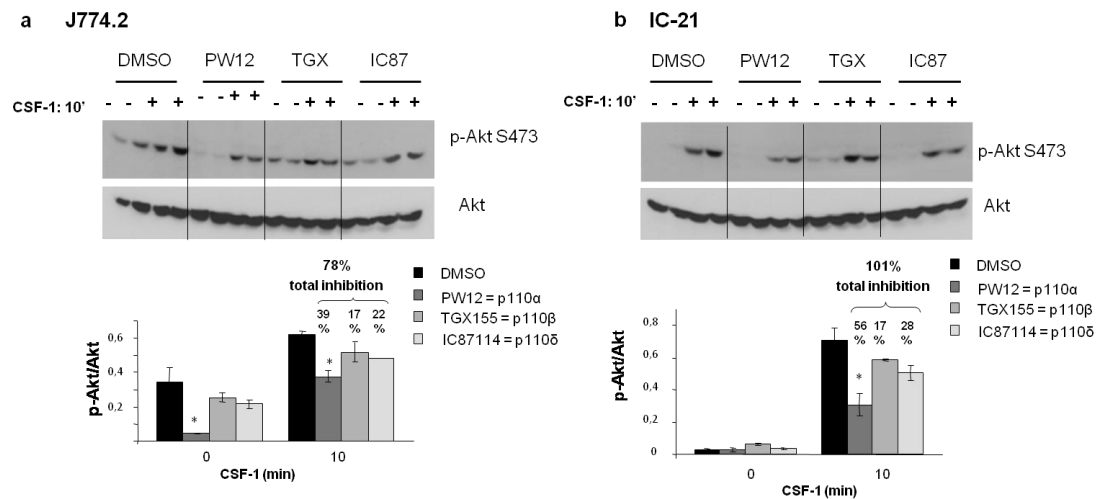


Figure 3.3. Participation of Class IA PI3K isoforms in induction of p-Akt downstream of CSF-1 varies in J774.2 and IC-21 macrophage lines. a. J774.2 cells cultured overnight in complete medium with FBS reduced from 10% to 5% prior to 1 h pre-treatment for with either DMSO or inhibitors the following day: PW12 (0.5 μ M), TGX155 (0.5 μ M) or IC87114 (5 μ M). The cells were stimulated with CSF-1 (30 ng/ml) for 10 b. IC-21 cells treated as described in a. Graphs and western blots are representative of results of multiple experiments. Graphs presents data for the mean \pm s.e.m. of two experiments performed in duplicate (* p <0.05; ** p <0.01; *** p <0.001). Percentages represent percentage decrease in p-Akt compared to the p-Akt levels in the CSF-1-stimulated DMSO control.

In contrast to the BAC1.2F5 macrophages, which were only very minimally affected by p110 δ -selective inhibition, there was a greater p-Akt reduction in IC-21 and J774.2 macrophages treated with a p110 δ -selective inhibitor.

In a few instances, we noted that treatment with the p110 β -selective inhibitor (TGX155) resulted in an elevated CSF-1-induced p-Akt signal in the IC-21 macrophages [Data not shown]. Another member of the laboratory has also observed this stimulatory effect of p110 β -selective inhibitors in other cell types and their data also indicates it is a highly variable/inconsistent effect of p110 β -inhibition. The reason for this is currently unclear and is currently being investigated in the laboratory as part of a separate project. In the majority of

experiments performed by either Dr Papakonstanti or myself, we observed a slight reduction of p-Akt in the presence of this inhibitor as illustrated in the graphical representation of our results [Figure 3.3b].

3.4. The effects of inhibiting Class IA isoforms in RAW 264.7 macrophages

We next proceeded to determine the contributions of the Class IA PI3K isoforms downstream of CSF-1 in one more macrophage cell line, RAW 264.7. The data that we obtained was unexpected in that we found that in most experiments (n=2) that the individual isoform selective inhibitors were unable to suppress CSF-1-induced p-Akt in these cells [Figure 3.4].

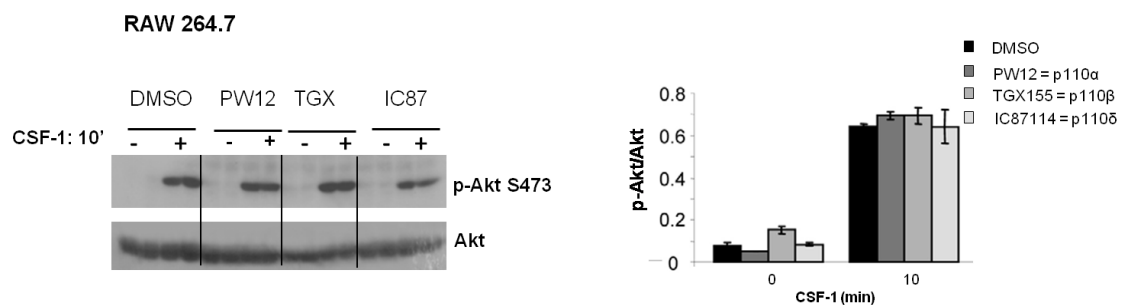


Figure 3.4. Inhibition of individual Class IA PI3K isoforms does not reduce CSF-1-induced p-Akt in RAW 264.7 macrophages. RAW 264.7 macrophages were cultured overnight in a complete medium with FBS reduced from 10% to 5% before pre-treatment with the indicated inhibitors for 1 h: PW12 (0.5 μ M), TGX155 (0.5 μ M) or IC87114 (5 μ M). The cells were subsequently stimulated with CSF-1 (30 ng/ml) and the p-Akt to Akt ratio was determined by western blotting. The graph and western blot are representative of results of multiple experiments. Graph presents data for the mean \pm s.e.m. of two experiments performed in duplicate (* p < 0.05; ** p < 0.01; *** p < 0.001).

At this point this part of the project was coming to a close, but we performed a few exploratory experiments to investigate the unexpected resistance of the RAW 264.7 p-Akt to each of the Class IA inhibitors. First, in order to determine whether the p-Akt could be reduced by targeting multiple PI3K isoforms we repeated the experiment but with the inclusion of a pan-PI3K inhibitor. Indeed, pre-treatment with the pan-PI3K inhibitor LY294002 resulted in a substantial decrease (more than 50%) in the CSF-1-induced p-Akt [Figure 3.5]. Also, in this experiment we observed a reduction in p-Akt in response to individual inhibitors [Figure 3.5]. The quality of this blot is not ideal and thus no conclusions can be confidently made regarding the effects of the individual inhibitors.

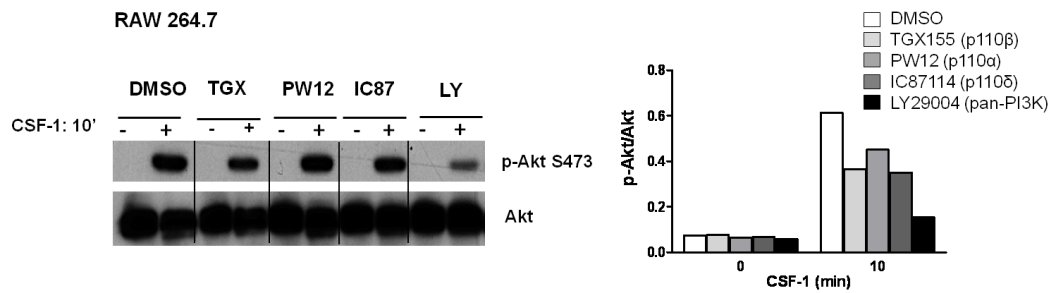


Figure 3.5. Pan-PI3K inhibition reduced CSF-1-induced p-Akt in RAW 264.7 macrophages. RAW 264.7 macrophages were cultured overnight in a complete medium with FBS reduced from 10% to 5% (v/v) prior to pre-treated for 1 h with the indicated inhibitors the following day: PW12 (0.5 μ M), TGX155 (0.5 μ M), IC87114 (5 μ M) or LY294002 (5 μ M). The cells were then prior to stimulation with CSF-1 (30 ng/ml). The graph illustrates quantification of p-Akt to Akt ratio from the western blot presented.

We performed another experiment alongside the one presented above in which we tested whether a dependence of p-Akt on individual isoforms could be observed in RAW 264.7 macrophages in normal culture conditions (10% (v/v) FBS in complete medium as opposed to 5% (v/v) FBS in complete medium used in the previous experiments). The results of the experiment performed provide some evidence that in these conditions the inhibition of the individual Class IA isoforms was sufficient to reduce CSF-1-induced p-Akt and that in these conditions the RAW 264.7 macrophages were more sensitive to the effects of these inhibitors [Figure 3.6]. In this experiment we used the pan-PI3K inhibitor Wortmannin rather than LY294002, as we were aware that the latter has significant off-target effects in particular on the activity of mTOR. These preliminary data suggest that the individual isoforms all contribute to the generation of p-Akt in RAW 264.7 macrophages in normal culture conditions. Further replicates would be needed before a firm conclusion could be drawn. The mechanism behind the apparent variable redundancy of Class IA PI3K isoforms in RAW 264.7 macrophages remains unclear.

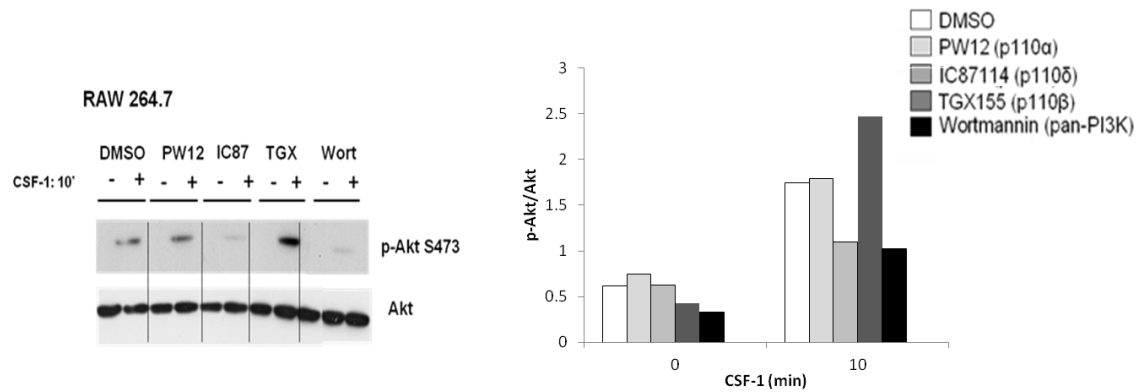


Figure 3.6. Inhibition of p110 δ reduces CSF-1-induced p-Akt in RAW 264.7 macrophages in medium containing 10% (v/v) FBS. RAW 264.7 macrophages were plated in 10% FBS complete medium and pre-treated for 1 h the following day with inhibitors as indicated: PW12 (0.5 μ M), TGX155 (0.5 μ M), IC87114 (5 μ M) or Wortmannin (50 nM). The cells were then stimulation with CSF-1 (30 ng/ml). The graph illustrates quantification of p-Akt to Akt ratio from the western blot presented. Western blot and graph are from a single experiment.

3.5. Investigating the uncharacteristic dependence of BAC1.2F5 macrophages on p110 alpha

We reasoned that the unrepresentative dependence of BAC1.2F5 macrophages on p110 α downstream of CSF-1 could be indicative of a mutation in *Pik3ca*, the gene encoding p110 α . Therefore, a member of the laboratory (Dr G. Nock) sequenced the *Pik3ca* gene in the BAC1.2F5 macrophages. This sequence analysis did not reveal any mutations in the *Pik3ca* gene [1].

3.6 Conclusion

Primarily, these data support the hypothesis that p110 α plays a greater role in the induction of CSF-1-induced p-Akt in macrophage cell lines compared to its minimal role in primary macrophages. Thus, these results suggest that the two main isoforms responsible for generating CSF-1-induced p-Akt in macrophages are p110 α and p110 δ , and that their relative contributions are affected by cell state, with p110 α dominating in the immortalised state and p110 δ dominating in the primary state. In addition, we have shown that in general, the inhibition of one isoform cannot be compensated for by the remaining uninhibited isoforms. On the other hand, our data regarding RAW 264.7 macrophages, in which individual inhibitors were not always able to reduce CSF-1-induced p-Akt, gives the impression that in certain conditions uninhibited Class IA PI3K isoforms may have the capacity to compensate. This apparent capacity to compensate for the loss of other isoforms seems to be the exception rather than the rule.

3.6. Discussion

The main conclusions of this part of the project are:

1. The dependence of the immortalised BAC1.2F5 macrophage cell line on p110 α is atypical of immortalised macrophages and is not due to a mutation in the *Pik3ca* gene
2. The dominance of p110 δ observed in primary macrophages is reduced in immortalised macrophages
3. The contributions of the Class IA PI3K isoforms are variable across macrophage cell lines and are generally non-redundant

With the generation and analysis of several mouse models of PI3K inactivation, it became clear that the Class I PI3K isoforms perform distinct, although at times overlapping, functions in cellular and physiological processes[3, 12, 81, 83, 133, 153]. Delineating the distinct roles of the individual Class IA PI3K isoforms remains an area of intense research, which attempts to address several questions. First, which isoforms are associated with which processes and how do the isoforms couple to them? Secondly, can remaining un-inhibited isoforms

compensate for the loss of function of an inhibited isoform? This question of redundancy of function is fundamental to the capacity to selectively targeting specific disease-associated processes with isoform-selective inhibitors. Indeed, isoform-selective inhibitors are now in clinical trials targeting a wide range of disease-related dysfunctions and are largely reported to have low toxicity.

In line with the observations of distinct and non-redundant roles of PI3K isoforms, Dr Papakonstanti, a former member of the Centre for Cell Signalling, observed that in primary macrophages signalling downstream of CSF-1 was most dependent upon p110 δ activity, whilst inactivation of p110 β or p110 α had minimal impact [1]. In immortalised BAC1.2F5, this dominance of p110 δ was lost and replaced with a striking degree of reliance upon p110 α [1]. We reasoned that this switch from p110 δ - to p110 α -dependence could be related to the immortalised state of the BAC1.2F5 macrophages. We wanted to determine whether the state of a cell is correlated with the functionality of the PI3K Class IA isoforms. To address this question, we compared the effects of each of the Class IA PI3K inhibitors on CSF-1-induced p-Akt in three additional immortalised macrophage cell lines, namely J774.2, IC-21 and RAW 264.7. We first confirmed that in BAC1.2F5 macrophages, CSF-1-induction p-Akt is highly dependent upon p110 α activity. Data obtained in J774.2 and IC-21 supported the correlation between a loss of p110 δ dependency and immortalised status, but also revealed that the almost total reliance of BAC1.2F5 macrophages upon p110 α to signal downstream of CSF-1, was not representative of the norm. Indeed, the contributions of each of the PI3K Class IA isoforms were quite variable across the cell lines tested. Interestingly, we observed a consistent low-level contribution of p110 β activity across all of the macrophages tested, including the primary macrophages. These data support the hypothesis that loss of p110 δ dominance is correlated with immortalisation but reveal that the involvement of other isoforms in immortalised macrophages is variable. With regards to non-redundancy, we have observed that in general, inhibition of individual PI3K Class IA isoforms is sufficient to partially suppress CSF-1-induced p-Akt. The ability to suppress p-Akt induction with a single isoform-selective PI3K inhibitor led us to conclude that uninhibited isoforms are unable to compensate for the loss of the inhibited isoform's activity. We found it particularly interesting that this inability to compensate occurs even when the

other isoforms appear to be contributing alongside the inhibited isoform to CSF-1-induced p-Akt production.

Results obtained for the RAW 264.7 macrophage cell line were not consistent with those obtained for the other cell lines, in that these macrophages had an unusual insensitivity to inhibition of individual Class IA PI3K isoforms. Indeed, in a later experiment we observed a minimal effect upon inhibition of individual isoforms. This result was observed only once and additionally the quality of the blot was poor, thus we can only state that we saw some indication that selective-isoform inhibition could affect p-Akt generation in these cells but generally we observed no effect. These data suggested that either these cells are somewhat resistant to PI3K inhibition or that the uninhibited isoforms were capable of compensation. We began a preliminary investigation into this insensitivity and acquired some preliminary evidence that pan-PI3K inhibition was sufficient to repress p-Akt induction. This, if proven, would support the theory that the individual isoforms are functioning in a redundant manner. We also observed a capacity for isoform-selective inhibitors to repress p-Akt induction in different culture conditions to those in which their effects were originally tested. Conclusions cannot be drawn confidently from these final experiments on RAW 264.7 macrophages because there were insufficient replicates and furthermore, the qualities of the blots were not suitable for reliable quantification. Whilst working with the RAW 264.7 macrophages in our main project we observed a decrease in basal and LPS-stimulated p-Akt upon p110 δ -selective inhibition when the macrophages were grown in complete medium containing 10% FBS. We therefore suspect, but cannot conclusively state, that the observed insensitivity to PI3K inhibitors is not representative of PI3K functionality in RAW 264.7 macrophages.

We noted that there was also a variation between the macrophage cell lines in terms of apparent basal Akt activation, as determined by p-Akt levels. The primary macrophages, IC-21 and RAW 264.7 macrophages appear to have very little p-Akt in the unstimulated conditions whilst the J774.2 macrophages and the BAC1.2F5 macrophages appear to have higher levels. The p-Akt levels in the unstimulated BAC1.2F5 macrophages in fact appear similar to the stimulated levels. This could indicate that the starvation conditions of 5% (v/v) FBS instead of the 10% used in

normal culture conditions were insufficient to reduce activation of Akt in these cells. In relation to this observation we have also noted that the effects of the isoform-selective inhibitors on this variable unstimulated p-Akt also differ. In the BAC1.2F5 the stimulated and high basal p-Akt are both repressed by treatment with the p110 α -selective inhibitor PW12, whereas PW12 blocked unstimulated p-Akt but did not fully inhibit stimulated p-Akt in J774.2 macrophages. We are unable to explain this finding based on our data, but we acknowledge that although the apparent differences in basal levels of p-Akt across the cell lines could represent genuine cell line variability it may also be an artefact of differences in the exposure of x-ray films during the development of blots or other technical inconsistencies. In order to confirm a difference in basal p-Akt levels or the differing effects of the inhibitors on unstimulated versus stimulated cells a quantitative method would be required.

Ideally, in order to prove a causal relationship between immortalisation and the loss of p110 δ dominance, one would need to observe this shift directly during and following immortalisation of primary macrophages. It would be particularly interesting if it were possible to follow the process of immortalisation and transformation and observe at what point(s) the dependence on p110 δ decreased. Assuming immortalisation directly results in a shift away from p110 δ dominance, it would be useful to determine whether other changes in cellular signalling are correlated with this shift. In the Centre for Cell Signalling, Dr G. Nock previously attempted to immortalise primary murine mast cells which retained functional c-kit receptor dependence. In the case of immortalisation by introduction of the Hox11 homeobox gene, the cells became growth factor (IL3)-independent and displayed undifferentiated characteristics including a lack of expression of the c-kit receptor [154]. A second mast cell line immortalised by expression of polyoma middle T remained growth factor-dependent (like BAC1.2F5 macrophages) and maintained the differentiated mast cell characteristics including c-kit receptor expression, but unfortunately the line could not be recovered after freezing [154]. In principle, similar studies could be carried out for mouse macrophages in order to help elucidate the effects of immortalisation on isoform function. We note that the documented ability of polyoma middle T expression to activate PI3K could render this method of immortalisation unsuitable for our PI3K-focused

investigations [155-157]. Below we summarize what is known in this context, and which strategies could be used.

With regards to existing macrophage cell lines, J774.2 and RAW 264.7 were both derived from murine tumours [146, 148]. The IC-21 and BAC1.2F5 macrophage cell line were published as a macrophage line immortalised by SV40 infection *in vitro* [145, 147]. In the case of the BAC1.2F5 macrophages, we have been informed that this was later found to be incorrect [Pollard, personal communication to Prof. Vanhaesebroeck]. The BAC1.2F5 cells were found to lack SV40 DNA and may instead have arisen as a result of spontaneous immortalisation, potentially due to inactivation of the INK4a/Arf locus [Personal communication to Prof Vanhaesebroeck, J.W. Pollard]. In line with this, a later publication revealed that inactivation of INK4a can induce primary macrophage immortalisation [158]. This is therefore a strategy that could be attempted to immortalise primary mouse macrophages.

We could perhaps have use previously published cell lines from the Pollard group. Indeed, Pollard *et al.* studied BAC1.2F5-derived mutants and compared these to the original BAC1.2F5 cells, which are dependent on CSF-1 for survival and proliferation [159]. The authors studied mutants with varying degrees of transformed character and observed a capacity of cells to separate the requirement for CSF-1 for survival and for proliferation [159].

1. Cells survive and proliferate in culture but only in the presence of CSF-1
2. Cells survive but do not proliferate in the absence of CSF-1
3. Cells survive and proliferate in the absence of CSF-1 but proliferate faster in the presence of CSF-1
4. Cells that are entirely independent of and unresponsive to CSF-1

We considered that these mutants with their varying degrees of immortalisation and transformation might potentially be excellent models in which to investigate the effect of cellular state upon PI3K Class IA isoform contributions. We did not proceed with this primarily because this project was coming to an end, but also because of the unusual dependence on p110 α in the BAC1.2F5 macrophages compared to the other macrophages cell lines, which made this otherwise ideal system unsuitable. Of course, it is possible that had we investigated the effects of inhibiting each Class IA PI3K isoform in the BAC1.2F5-derived mutant lines that

are independent of CSF-1 for survival, we would observe a pattern more similar to that seen in the CSF-1-independent J744.2 and IC-21 macrophage cell lines. Had we proceeded with this project we would certainly have attempted to immortalise primary macrophages, probably using INK4a inactivation, in order to follow any changes in PI3K Class IA isoform contributions during the transitions.

The ability of either p110 α or p110 δ to be the predominant isoform, which induces p-Akt downstream of CSF-1 in different murine macrophages, suggests that the capacity of these isoforms to act downstream of CSF-1 is not dependent on a fixed and intrinsic factor. Instead, the ability of the isoforms to function downstream of a particular stimulus appears to be affected by the state of the macrophages. Based on these results we would advise that when investigating the role of a particular PI3K isoform or investigating the effects of isoform-selective inhibition, the cell type and perhaps, the growth conditions used, might have a substantial impact upon conclusions drawn.

We conclude that this work contributed to the knowledge regarding the capacity of PI3K Class I isoforms to perform distinct and non-redundant functions in cultured cells. Furthermore, our work highlighted the fact that the distinct roles played by each isoform are not fixed to one role in one cell type but are also influenced by the state of the cell. Finally, in macrophages we found evidence that the dominance of p110 δ is reduced in immortalised cells and that multiple isoforms can contribute in absence of p110 δ dominance. The contributions of the isoforms were generally found non-redundant and as such p-Akt was reduced by inhibition of any single isoform.

CHAPTER 4

4. INVESTIGATING THE EFFECTS OF PHARMACOLOGICAL INACTIVATION OF P110 DELTA ON THE TRANSCRIPTOME OF RAW 264.7 MACROPHAGES

4.1. Introduction and aims of study

From here on in, the focus of the project shifted to investigating the role of p110 δ in transcriptional regulation. At the time that we initiated this investigation, information regarding the role of PI3K in transcriptional regulation at the whole genome level was very limited. In fact, there were no published studies detailing the effect of p110 δ inactivation on the whole transcriptome of any cell type.

We had intended to investigate the role of p110 δ in transcriptional regulation in primary macrophages. Unfortunately, at this point in the project the generation of differentiated primary macrophages was causing difficulties. This challenge was overcome using a systematic problem solving approach, as described briefly in the next chapter. In the mean time, we designed and performed a pilot genome-wide expression analysis using a macrophage cell line treated with the p110 δ -selective inhibitor IC87114. We hoped that this study would provide the first indication as to the magnitude and range of transcriptional deregulation that occurs in response to inactivation of p110 δ in macrophages. We reasoned that this was also an excellent opportunity to familiarise ourselves with microarray experiments and analysis. This was particularly important as we were primarily performing the microarray experiment ourselves, with guidance from our pharmaceutical sponsor. The preliminary work leading up to this genome-wide expression analysis and the results of the experiment are detailed below.

This and all subsequent experiments were designed in collaboration with our pharmaceutical sponsor UCB. Being a pharmaceutical company, their interests naturally lay in translational rather than more fundamental scientific questions. With this borne in mind, experiments were designed with consideration for the potential translational relevance of resulting data. In particular we considered one element of experimental design; the culture conditions of the cells prior to RNA extraction. When considering the culture conditions, we proposed that performing these experiments in normal culture conditions (complete medium including 10% FBS) rather than pre-starving the cells might be preferable. We reasoned that withdrawal of growth factors and or nutrients induces cellular and metabolic stress is not likely to be representative of the *in vivo* conditions that may occur in a clinical blood sample, for example. We therefore made the decision to assess the genome-wide impact of p110 δ inactivation on macrophages in the basal unstimulated exponentially growing state. We also choose to reduce the concentration of IC87114 used in these and all subsequent experiments (unless clearly stated) from the 5 μ M we had used in earlier experiments to 1 μ M. IC87114 was originally published as a p110 δ -selective drug when used a 5 μ M *in vitro* but tests performed on p110 δ KI cells revealed that above 1 μ M IC87114 affects the function of other Class I isoforms [135]. Based on this new isoform selectivity data and our desire to minimise off-target effects we therefore choose to reduce the concentration of IC87114 that we used in all subsequent experiments to 1 μ M.

4.2. Choosing a macrophage line to study

It was imperative that we performed this investigation in a macrophage cell line that is dependent on p110 δ activity to some degree in the basal. From the outset, UCB had a preference for the use of the RAW 264.7 cell line because this is the macrophage cell line that they commonly use in their own immunological research. We were cautious about using this cell line based on our findings described in Chapter 3. Consequently, before proceeding we tested whether inhibition of p110 δ affected p-Akt levels in RAW 264.7 macrophages. We included samples treated with a pan-PI3K inhibitor in order to compare the level of inhibition to that resulting from p110 δ inhibition. We included LPS-treated samples as a control to

check that the basal cells were not in an activated state and blotted for phospho-p38 (p-p38) to confirm which samples had been stimulated with LPS.

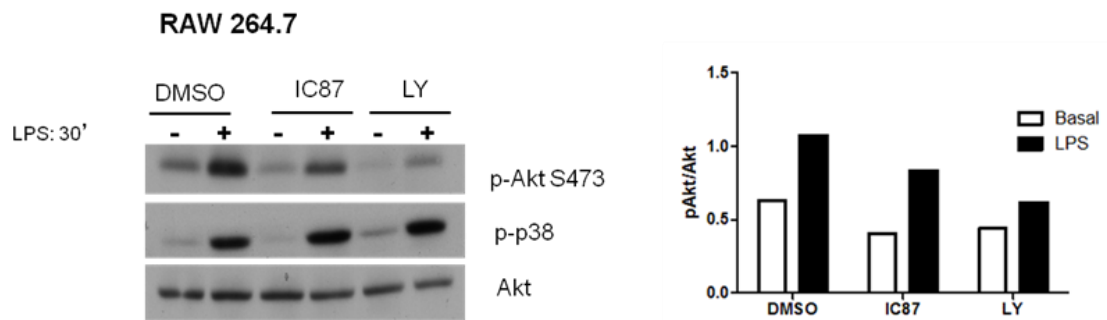


Figure 4.1. Inhibition of p110 δ reduced basal and LPS-stimulated p-Akt in RAW 264.7 macrophages. RAW 264.7 macrophages were plated in complete medium including 10% FBS. The following day the cells were pre-treated with either DMSO, p110 δ -selective IC87114 (1 μ M) or pan-PI3K inhibitor LY294002 (5 μ M) prior to stimulation with LPS (1 μ g/ml) for 30 min.

Our results indicated that RAW 264.7 basal p-Akt is reduced by pharmacological inactivation of p110 δ as is LPS-induced p-Akt [Figure 4.1]. The p-p38 confirmed that only the LPS-stimulated samples (+) had been exposed to LPS and showed that activation of p38 is unaffected by treatment with a pan-PI3K inhibitor or with a p110 δ -selective inhibitor.

Based on these results we felt confident to proceed with our genome-wide expression analysis using RAW 264.7 macrophages pre-treated with 1 μ M of IC87114.

4.3. Chronic pre-treatment with IC87114 reduced Akt activation

We reasoned that in order to best mimic chronic administration of p110 δ -selective inhibitors in a clinical setting it would be more representative to have an extended IC87114 treatment prior to sample extraction. We performed a final preliminary experiment to compare the effects of 2 h IC87114 treatment to the effect of 72 h IC87114-treatment on the basal and also LPS-induced p-Akt. A 2 h pre-treatment with LY294002 was also included to enable the effects of long-term p110 δ -selective inhibition to be compared to the effects of pan-PI3K inhibition [Figure 4.2].

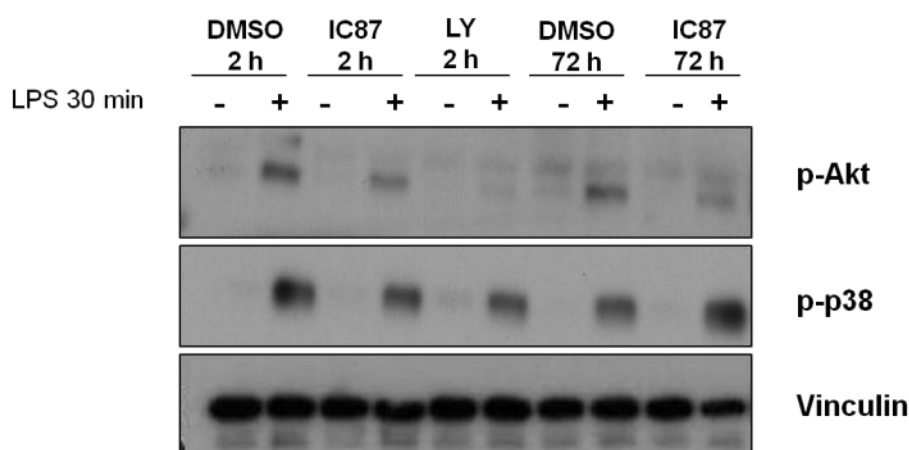


Figure 4.2. Inhibition of p110 δ for 2 h or 72 h reduced basal and LPS-stimulated p-Akt in RAW 264.7 macrophages. RAW 264.7 macrophages were plated in complete medium containing 10% FBS and pre-treated with DMSO or p110 δ -selective IC87114 (1 μ M) or pan-PI3K inhibitor LY294002 (5 μ M) for the times indicated. DMSO and IC87114 were added to the medium every 24 h during the 72 h period. Following 2 or 72 h incubation the cells were stimulated with LPS (1 μ g/ml) for 30 min prior to extraction of cell lysates. Lysates were processed and analysed for the indicated proteins using standard immunoblotting techniques.

These data confirmed that IC87114-treatment for 2 or 72 h both repressed basal and LPS-induced p-Akt levels in RAW 264.7 macrophages [Figure 4.2]. Based on this data we felt confident to pre-treat the RAW 264.7 macrophages with 1 μ M of IC87114 for 72 h in order to represent chronic inactivation *in vitro*.

4.3.1. Final experiment design

We finalised our plans and set out to perform genome-wide transcriptional analysis on RAW 264.7 macrophages in the basal state grown in complete medium. We pre-treated RAW 264.7 macrophages with either DMSO or IC87114 for 72 h and then extracted RNA from six plates of grown in normal culture conditions (complete medium including 10% FBS).

4.4. Extraction and quality control of RNA

The quality of the six RNA samples was confirmed using the Agilent Bioanalyser in accordance with the protocol described in the Materials and Methods section [Chapter 2, section 2.8.1.1]. All of the samples were assigned a RIN between 9.8 and 10 indicating that they consisted of high quality RNA. An example electropherogram is shown in Figure 4.3.

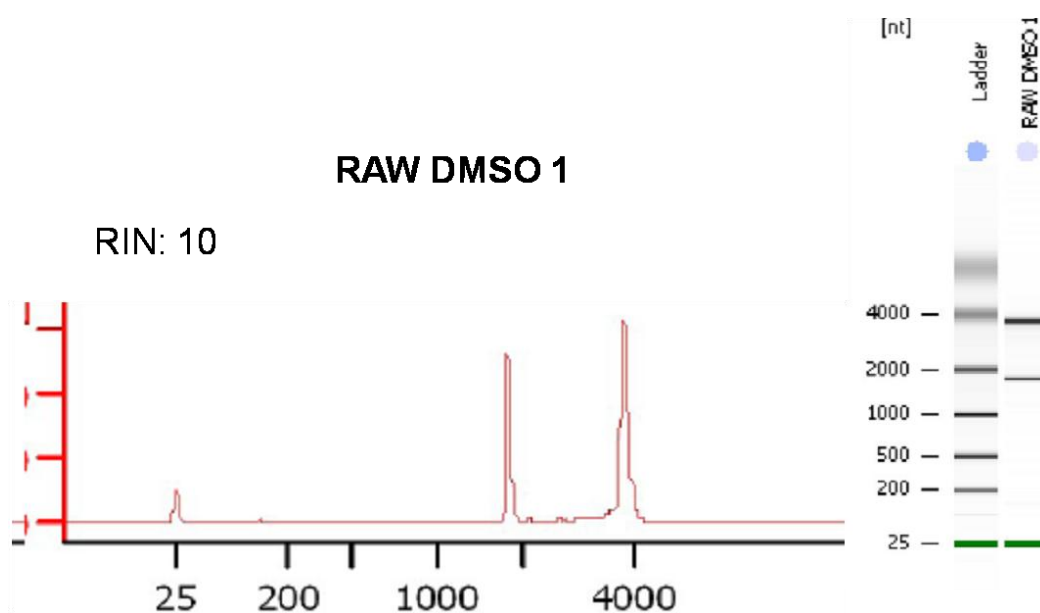


Figure 4.3. RNA extracted from RAW 264.7 macrophages was intact and of high quality. A representative electropherogram of the electrophoretic trace of sample DMSO 1 which was assigned a RIN of 10. The axis 25-4000 represents nt with a peak representing the 18S rRNA at approximately 1500 nt and second larger peak representing 28S rRNA at approximately 4000 nt. Based on the area under the two main peaks an 18S to 28S ratio of 2.0 was calculated. The gel image is shown to the right. The upper band represents the 28S rRNA whilst the lower represents the 18S rRNA and the green band at 25bp is the marker which can also be seen as a small peak on the electropherogram.

4.5. Obtaining expression data

The genome-wide expression of the three samples treated with DMSO and the three samples treated with IC87114 was determined using the 3' IVT GeneChip® protocol and Affymetrix Mouse Genome GeneChip® 430 2.0 microarrays. Each processed sample was hybridized to an individual chip, stained and subsequently scanned to obtain fluorescence data. A visual check of the raw data image for each chip was performed and all Affymetrix GeneChip® internal controls and standards were checked and found to be satisfactory. In order to obtain comparative expression data for the samples included in the experiment we first had to

normalise across the entire experiment to account for chip to chip variation. This chip to chip normalisation was performed on our behalf by three bioinformaticians Dr H. Edwards, Dr P. Hales and Ms E. Gadaleta using the standard GC-RMA algorithm. With the help of these bioinformaticians the data set was subsequently reduced from the full 45,002 probe sets by filtering to extract the top 10,000 most variant probe sets.

4.6. Multivariate analysis to identify sample clusters

With the assistance of Dr H. Edwards, Dr P. Hales and Ms E. Gadaleta we employed PCA to reduce the dimensionality of the data in order to group samples and identify outliers. PCA is a mathematical model that enables the most prominent variation within a data set to be identified, whilst retaining and representing as much of the original data as feasible [160-161]. This is achieved first, by taking all the values per sample and shrinking them into a smaller set of values, which still represent the variability within the original data set. Secondly, the algorithm identifies the most apparent feature within the smaller set of values, which represents the greatest degree of variation between samples. This feature is assigned as the Principal Component 1 (PC1), and PC2 is determined based on the feature creating the second greatest variation, which is not already explained by PC1. PC3 represents other sources of variation not represented by either PC1 or PC2. The algorithm identifies any remaining variability within the data set that is not accounted for by the three major PCs. The two main PCs can be represented on a graph, on which the samples can be located to represent visually which PC each sample is best aligned with and their relationship, if any, with the other PC.

4.6.1. Samples separate according to LPS-stimulation status

The PCA revealed two clusters of samples, which represented the DMSO and IC87114-treated samples [Figure 4.4a]. This analysis also revealed variability within the treatment groups; the samples within the groups did not cluster tightly on a single principal component. In fact, two outliers were identified based on the plot obtained and the values for each PC [Data not shown]. In fact PCA 1 was independent of the treatment effect in this PCA. Consequently, the data from these

two outlier samples (DMSO 1 and IC87114 1) were excluded from further analysis. The PCA was re-run on the reduced data excluding the outliers to confirm that in their absence the PC1 was dependent on the IC87114-treatment [Figure 4.4b]. The removal of two outliers reduced the data to two replicates per condition which was sufficient to continue analysis but reduced the confidence with which any results can be presented. Unless otherwise stated all subsequent analysis was performed on the dataset generated after the exclusion of the outlier samples data.

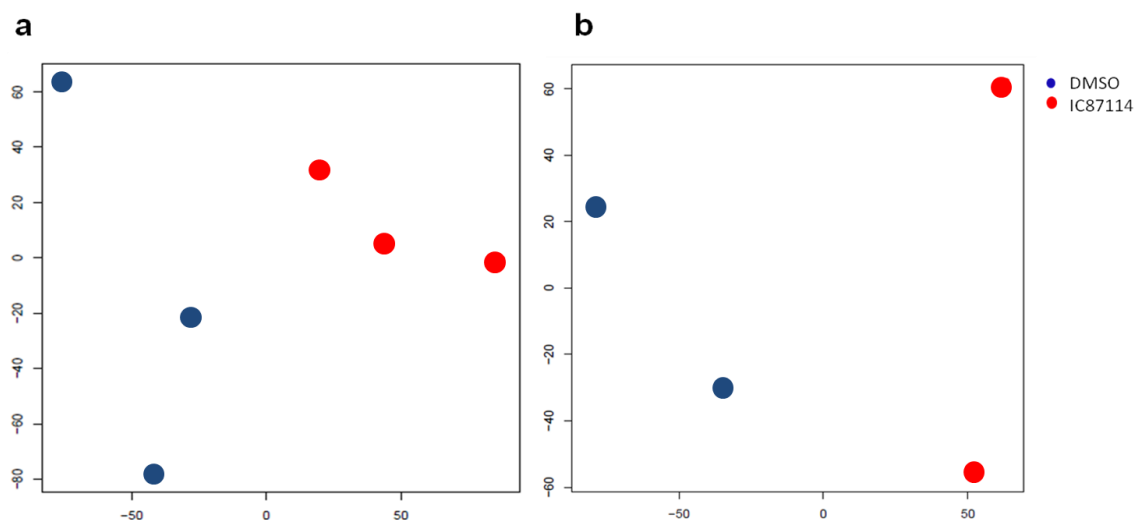


Figure 4.4. Samples clustered according to treatment groups but there was variability within groups. PCA was performed on the data set acquired. **a.** The original PCA including the outlier samples. **b.** The PCA after removal of the two outlier samples. After the exclusion of the two outliers, the greatest degree of variation represented by PC1 was dependent on treatment effects.

4.7. Identification of individual probe sets affected by IC87114 treatment

We next obtained a list of probe sets differentially regulated in the IC87114-treated RAW 264.7 macrophages by applying a minimum threshold of 1 Log Fold Change (LogFC, calculated as the log to the base 2) to the list of the top 10,000 most variably expressed probe sets. The statistical significance of the changes were subsequently calculated using a standard two-tailed t-test. The p values obtained were adjusted to take into account the multiple hypothesis testing that is inherent in genome-wide expression analysis. This adjustment was performed using the B-H formula to generate an adjusted p value ($_{adj}p$ value)[151].

Application of the cut off of a minimum logFC of greater than or equal to (\geq) 1 and an adjusted p value of less than or equal to (\leq) 0.05 reduced this list to 139 probe sets that were differentially regulated in RAW 264.7 macrophages treated with IC87114 compared to those treated with DMSO [Table 4.1]. Increasing the statistical stringency to $p \leq 0.001$ did not eliminate any of these 139 probe sets, which indicated that the differential regulation detected for these 139 probe sets was very significant. Within the 139 probe sets fifty-nine were specific to transcripts that were not associated with known genes and therefore lack gene symbols and protein names (designated NA). These probe sets are complementary to sequences that have been found to be expressed sequences by the expressed sequence tag (EST) method. ESTs are short DNA sequences generated from cDNA sequences that are generated by reverse transcribing cellular mRNAs into DNA sequences that do not contain intronic sequences. As such they should represent sequences that are expressed within the cell from which the mRNA sequence was derived. Scientists can search for sequence similarity to a gene or sequence of interest and as the sequences are mapped to the genome ESTs are assigned to chromosomal regions and known genes. The probe sets interrogating EST sequences may therefore be associated with a known gene or protein product in the future and this will be linked to the relevant Affymetrix probe set identification numbers. We have therefore included two tables, one including only those probe sets assigned a gene symbol or some other relevant annotation such as a RIKEN name [Table 4.1] and a further table includes those unassigned probes [Table 4.2]. We have chosen to list these assigned probe sets because the information regarding unassigned expressed transcripts and RIKEN clones is continuously expanding.

With regards to the assigned probe sets we found eighty that were differentially regulated in IC87114-treated RAW 264.7 macrophages. Affymetrix GeneChips® include multiple redundant probe sets for some but not all genes. This increases the reliability of data obtained by providing multiple independent measures of expression. The number of unique differentially regulated genes or transcripts identified is often inflated by the detection of differential regulation by duplicate probe sets. Multiple probe sets were identified for *Cd28*, *Trib3*, *Cox6a* and *Orly*. The identification of multiple probe sets increases the confidence with which the effect of IC87114 on the expression of these genes can be presented.

Probe set ID	Gene Symbol	Protein name	logFC	adj.p value
1433283_s_at	<i>Orly</i>	oppositely-transcribed, rearranged locus on the Y	-4.647	2.90E-92
1460500_at	5033421C21Rik	RIKEN cDNA 5033421C21 gene	-4.572	2.52E-89
1444668_at	<i>Astx</i>	amplified spermatogenic transcripts X encoded	-4.288	1.76E-78
1442812_at	Gm10482	predicted gene 10482	-4.094	1.79E-71
1456340_at	<i>Mettl11a</i>	methyltransferase like 11A	-4.059	2.69E-70
1425881_at	<i>Psg28</i>	pregnancy-specific glycoprotein 28	-3.903	5.25E-65
1449832_at	1700091H14Rik	RIKEN cDNA 1700091H14 gene	-3.466	3.44E-51
1459564_at	Gm4670	predicted gene 4670	-2.971	1.76E-37
1454437_at	<i>Orly</i>	oppositely-transcribed, rearranged locus on the Y	-2.785	7.71E-33
1430441_at	4933438K21Rik	RIKEN cDNA 4933438K21 gene	-2.759	3.18E-32
1438620_x_at	<i>Sfrp1</i>	secreted frizzled-related protein 1	-2.53	5.66E-27
1421496_at	<i>Acer2</i>	alkaline ceramidase 2	-2.515	1.16E-26
1458854_at	C78891	expressed sequence C78891	-2.202	2.52E-20
1430324_x_at	1700049E17Rik1	RIKEN cDNA 1700049E17 gene, gene 1	-2.077	5.16E-18
1431117_x_at	1810029B16Rik	RIKEN cDNA 1810029B16 gene	-2.013	6.86E-17
1458243_at	Gm7844	predicted gene 7844	-1.987	1.96E-16
1422875_at	<i>Cd84</i>	CD84 antigen	-1.876	1.33E-14
1422726_x_at	<i>Speer4a</i>	spermatogenesis associated glutamate (E)-rich protein 4a	-1.702	6.39E-12
1427514_at	LOC624295	hypothetical protein LOC624295	-1.667	2.08E-11
1452418_at	1200016E24Rik	RIKEN cDNA 1200016E24 gene	-1.63	6.75E-11
1447749_at	<i>Smyd5</i>	SET and MYND domain containing 5	-1.595	2.07E-10
1433163_at	6230414M07Rik	RIKEN cDNA 6230414M07 gene	-1.587	2.60E-10
1447182_at	C77815	expressed sequence C77815	-1.562	5.63E-10
1443213_at	Gtdc1	glycosyltransferase-like domain containing 1	-1.553	7.43E-10
1432590_at	4930573021Rik	RIKEN cDNA 4930573021 gene	-1.551	7.79E-10
1426243_at	<i>Cth</i>	cystathionase (cystathionine gamma-lyase)	-1.542	1.01E-09
1416298_at	<i>Mmp9</i>	matrix metalloproteinase 9	-1.538	1.12E-09
1426065_a_at	<i>Trib3</i>	tribbles homolog 3 (Drosophila)	-1.524	1.72E-09
1453668_at	3110052M02Rik	RIKEN cDNA 3110052M02 gene	-1.5	3.48E-09
1456225_x_at	Trib3	tribbles homolog 3 (Drosophila)	-1.425	3.09E-08
1428046_a_at	<i>Zfx</i>	zinc finger protein X-linked	1.322	5.08E-07
1438050_x_at	Gm9222	predicted gene 9222	-1.314	6.14E-07
1422504_at	<i>Glrβ</i>	glycine receptor, beta subunit	-1.266	2.10E-06
1441414_at	<i>Sfi1</i>	Sfi1 homolog, spindle assembly associated (yeast)	-1.264	2.18E-06
1423072_at	6720475J19Rik	RIKEN cDNA 6720475J19 gene	-1.255	2.69E-06

Probe set ID	Gene Symbol	Protein name	logFC	adj.p value
1438802_at	<i>Foxp1</i>	forkhead box P1	1.253	2.83E-06
1456504_at	<i>Zfp182</i>	zinc finger protein 182	1.251	2.91E-06
1456282_at	6720457D02Rik	RIKEN cDNA 6720457D02 gene	-1.249	3.01E-06
1451382_at	<i>Chac1</i>	ChaC, cation transport regulator-like 1 (E. coli)	-1.238	3.92E-06
1423524_at	<i>Mastl</i>	microtubule associated serine/threonine kinase-like	1.224	5.37E-06
1441565_at	LOC100039111	similar to cadherin 11	-1.222	5.66E-06
1457633_x_at	<i>Cox6a2</i>	cytochrome c oxidase, subunit VI a, polypeptide 2	-1.213	6.86E-06
1440144_x_at	C330046E03	hypothetical protein C330046E03	-1.211	7.20E-06
1441829_s_at	<i>Akap10</i>	A kinase (PRKA) anchor protein 10	1.192	1.15E-05
1455900_x_at	<i>Tgm2</i>	transglutaminase 2, C polypeptide	-1.185	1.33E-05
1438874_at	<i>Nme7</i>	non-metastatic cells 7, protein expressed in (nucleoside-diphosphate kinase)	-1.179	1.50E-05
1442453_at	<i>Fcho2</i>	FCH domain only 2	1.178	1.51E-05
1445047_at	C79246	expressed sequence C79246	-1.158	2.43E-05
1429717_at	<i>Ipo11</i>	importin 11	1.153	2.68E-05
1428827_at	<i>Whsc1</i>	Wolf-Hirschhorn syndrome candidate 1 (human)	1.151	2.79E-05
1459760_at	<i>Ndufs4</i>	NADH dehydrogenase (ubiquinone) Fe-S protein 4	1.147	3.06E-05
1437923_at	AI314760	expressed sequence AI314760	-1.145	3.14E-05
1425177_at	<i>Shmt1</i>	serine hydroxymethyltransferase 1 (soluble)	-1.138	3.71E-05
1460304_a_at	<i>Ubtf</i>	upstream binding transcription factor, RNA polymerase I	-1.134	4.03E-05
1460469_at	<i>Tnfrsf9</i>	tumor necrosis factor receptor superfamily, member 9	-1.129	4.45E-05
1419985_s_at	<i>Ccdc69</i>	coiled-coil domain containing 69	1.122	5.07E-05
1423467_at	<i>Ms4a4b</i>	membrane-spanning 4-domains, subfamily A, member 4B	1.104	7.63E-05
1460722_at	<i>Soat2</i>	sterol O-acyltransferase 2	-1.089	1.06E-04
1456296_at	5830418K08Rik	RIKEN cDNA 5830418K08 gene	1.073	1.50E-04
1458667_at	<i>Ninl</i>	ninein-like	1.07	1.56E-04
1419721_at	<i>Niacr1</i>	niacin receptor 1	-1.068	1.61E-04
1449984_at	<i>Cxcl2</i>	chemokine (C-X-C motif) ligand 2	-1.063	1.79E-04
1444677_at	C77673	expressed sequence C77673	1.048	2.43E-04
1417262_at	<i>Ptgs2</i>	prostaglandin-endoperoxide synthase 2	-1.048	2.43E-04
1417607_at	<i>Cox6a2</i>	cytochrome c oxidase, subunit VI a, polypeptide 2	-1.048	2.43E-04
1417597_at	<i>Cd28</i>	CD28 antigen	1.047	2.43E-04
1437285_at	1110020G09Rik	RIKEN cDNA 1110020G09 gene	1.047	2.44E-04
1460474_at	2610028L16Rik	RIKEN cDNA 2610028L16 gene	-1.043	2.64E-04

Probe set ID	Gene Symbol	Protein name	logFC	adj.p value
1435728_at	<i>Tyw3</i>	tRNA-yW synthesizing protein 3 homolog (<i>S. cerevisiae</i>)	1.042	2.67E-04
1442311_at	<i>Zfr</i>	zinc finger RNA binding protein	1.034	3.12E-04
1451577_at	<i>Zbtb20</i>	zinc finger and BTB domain containing 20	1.032	3.22E-04
1443703_at	<i>Cd28</i>	CD28 antigen	1.029	3.41E-04
1428010_at	<i>Timm9</i>	translocase of inner mitochondrial membrane 9 homolog (yeast)	1.024	3.75E-04
1432885_at	4632432E15Rik	RIKEN cDNA 4632432E15 gene	-1.024	3.79E-04
1438831_at	<i>Cdk12</i>	cyclin-dependent kinase 12	1.022	3.83E-04
1433016_s_at	<i>Orly</i>	oppositely-transcribed, rearranged locus on the Y	-1.021	3.88E-04
1456667_at	<i>Htt</i>	huntingtin	1.019	4.07E-04
1438063_at	<i>Mphosph9</i>	M-phase phosphoprotein 9	1.012	4.68E-04
1437025_at	<i>Cd28</i>	CD28 antigen	1.01	4.82E-04
1434798_at	<i>Atp6v0d2</i>	ATPase, H+ transporting, lysosomal V0 subunit D2	-1.008	5.01E-04

Table 4.1. List of eighty probe-sets with assigned gene symbols identified as differentially regulated in RAW 264.7 macrophages treated with IC87114. The probe sets are ranked based on largest to smallest LogFC. Those increased in RAW 264.7 macrophages pre-treated with IC87114 (1 μ M) for 72 h are highlighted in red whilst those that were found to be decreased are highlighted in green.

Probe set ID	Gene Symbol	Protein name	logFC	adj.p value
1420310_at	NA	NA	-6.194	4.72E-164
1458382_a_at	NA	NA	-5.611	1.38E-134
1447329_at	NA	NA	-5.096	6.62E-111
1446017_at	NA	NA	-4.693	6.13E-94
1457657_at	NA	NA	-4.659	1.22E-92
1428301_at	NA	NA	-3.957	8.59E-67
1434280_at	NA	NA	-3.915	2.19E-65
1452731_x_at	NA	NA	-3.804	9.44E-62
1447059_at	NA	NA	-3.768	1.36E-60
1439920_at	NA	NA	-3.748	5.94E-60
1448022_at	NA	NA	-3.655	5.37E-57
1426060_at	NA	NA	-3.402	2.72E-49
1426061_x_at	NA	NA	-3.38	1.10E-48
1434279_at	NA	NA	-3.377	1.31E-48
1427346_at	NA	NA	-3.23	2.00E-44
1417838_at	NA	NA	-3.061	8.01E-40
1440815_x_at	NA	NA	-2.504	1.96E-26
1424609_a_at	NA	NA	-2.409	2.03E-24
1452433_at	NA	NA	-2.305	2.68E-22

Probe set ID	Gene Symbol	Protein name	logFC	adj.p value
1424607_a_at	NA	NA	-2.292	4.71E-22
1459989_at	NA	NA	-2.269	1.32E-21
1440508_at	NA	NA	-2.23	7.50E-21
1445267_at	NA	NA	-2.117	9.85E-19
1460084_at	NA	NA	-2.018	5.75E-17
1424608_a_at	NA	NA	-1.98	2.45E-16
1438237_at	NA	NA	-1.938	1.26E-15
1458543_at	NA	NA	-1.86	2.37E-14
1442493_at	NA	NA	-1.838	5.34E-14
1429993_s_at	NA	NA	-1.834	6.17E-14
1447044_at	NA	NA	-1.814	1.24E-13
1420073_s_at	NA	NA	-1.813	1.27E-13
1447408_at	NA	NA	1.645	4.28E-11
1442947_x_at	NA	NA	-1.605	1.54E-10
1447410_at	NA	NA	-1.562	5.63E-10
1443649_at	NA	NA	1.5	3.48E-09
1452452_at	NA	NA	-1.483	5.69E-09
1457022_at	NA	NA	-1.468	8.68E-09
1445389_at	NA	NA	-1.393	7.66E-08
1435158_at	NA	NA	1.371	1.39E-07
1448018_at	NA	NA	1.37	1.40E-07
1441131_at	NA	NA	1.367	1.51E-07
1445518_at	NA	NA	1.345	2.72E-07
1446661_at	NA	NA	-1.313	6.31E-07
1442547_at	NA	NA	1.296	9.70E-07
1449652_at	NA	NA	-1.278	1.53E-06
1441391_at	NA	NA	1.244	3.37E-06
1437534_at	NA	NA	-1.241	3.66E-06
1440925_at	NA	NA	1.233	4.34E-06
1447123_at	NA	NA	-1.185	1.33E-05
1458018_at	NA	NA	1.179	1.51E-05
1441584_at	NA	NA	1.178	1.51E-05
1439813_at	NA	NA	1.131	4.28E-05
1457053_at	NA	NA	1.127	4.63E-05
1435708_at	NA	NA	1.11	6.73E-05
1447461_at	NA	NA	-1.072	1.51E-04
1439944_at	NA	NA	-1.071	1.55E-04
1460416_s_at	NA	NA	-1.065	1.70E-04
1455759_a_at	NA	NA	1.022	3.83E-04
1447575_at	NA	NA	1.006	5.15E-04

Table 4.2. List of fifty-nine probe-sets complementary to unassigned expressed sequences that were differentially regulated in RAW 264.7 macrophages treated with IC87114. The probe sets are ranked based on largest to smallest LogFC. Those increased in RAW 264.7 macrophages pre-treated with IC87114 (1 μ M) for 72 h are highlighted in red whilst those that were found to be decreased are highlighted in green.

4.8. Identification enriched functions amongst the genes affected by IC87114

We employed Ingenuity Pathway Analysis (IPA) software (Ingenuity Systems) to determine whether the list of genes that we had found to be affected by IC87114 treatment were enriched with genes involved in a particular molecular or cellular function. The analysis was performed on the list of genes affected by 1 logFC or more and with a statistical significance of $p \leq 0.001$ [Table 4.1]. IPA calculated the number of genes in the uploaded list that are associated with a molecular function and then calculated the statistical significance of any enrichment. Enrichment is deemed statistically significant if there are more genes in the list associated with a particular function that would be expected by chance based on the total number of genes associated with that function. IPA software identified several molecular functions including cellular compromise, cell signalling and molecular transport that were enriched in our gene list [Figure 4.5].

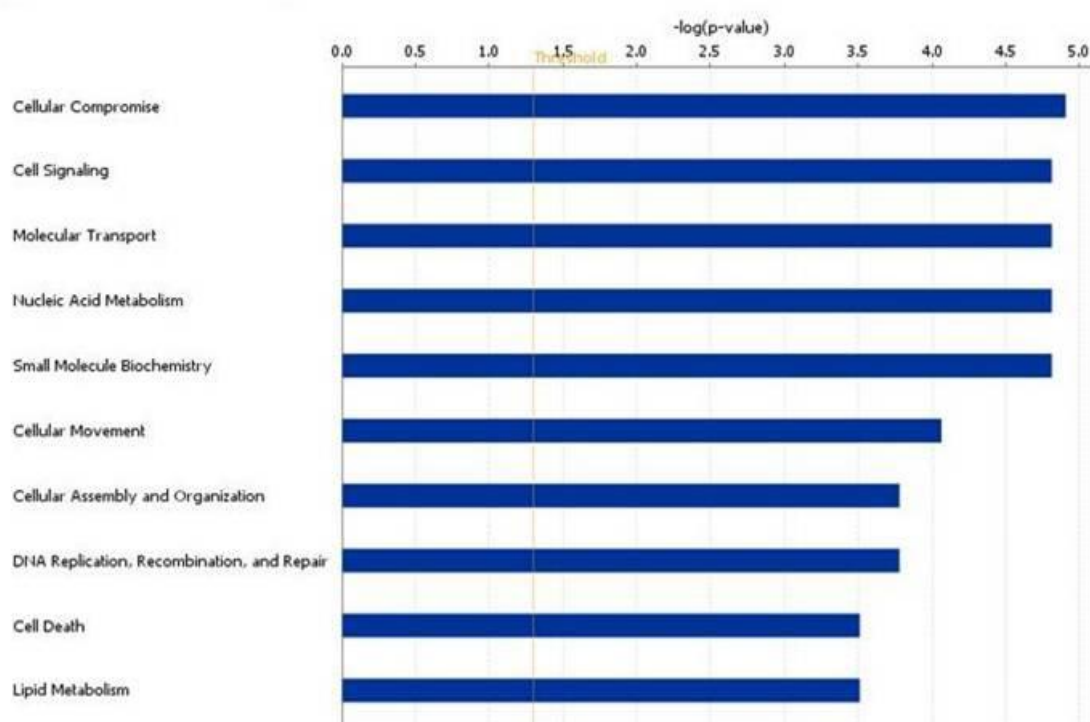


Figure 4.5. The top ten molecular and cellular functions significantly enriched in the list of genes affected by IC87114-treatment. Functional enrichment analysis was performed using IPA software on the complete list of genes differentially regulated in RAW 264.7 macrophages chronically treated with p110 δ -selective IC87114 (1 μ M) for 72 h. The statistical significance of the enrichment of genes associated with each listed molecular processes are indicated by the length of the position of the bar against the Y axis, which represents log p values determined using Fisher's exact test. The statistical significance threshold set at $p \leq 0.05$ is indicated by the thin grey line.

Cellular compromise was identified as the most statistically significantly enriched function in the list of differentially regulated genes. This was calculated based on the number of genes in this functional category in the input list with reference to the total number of genes in the category (Fisher's exact test). Six of the known genes found to be differentially regulated in RAW 264.7 macrophages treated with IC87114 are associated with cellular compromise in IPA's database (p value 2.24×10^5).

Cellular compromise is defined by Ingenuity as including "any functions that are associated with the damage or degradation of cells or any process that might compromise the functions of a cell" [IPA Help Manual 5.5 v1]. We were interested to note from the list of six genes (*Mmp9*, *Ubtf*, *Htt*, *Ndufs4*, *Ptgs2* and *Tgm2*) that IPA assigned to this ontology four were associated with the subcategory of neurological damage or degeneration; *Htt*, *Ndufs4*, *Ptgs2* and *Tgm2*. Notably, the *Htt* gene, which encodes the huntingtin protein that is mutated in sufferers of the terminal neurodegenerative disorder Huntingdon's disease, was included in this category. The expression of *Htt* was increased by 1 logFC in the IC87114-treated samples according to our Affymetrix data. The predominance of neuronal-related genes in our list that belong to this cellular compromise function could be of interest as p110 δ is also expressed in neurons and might therefore regulate these genes affecting neuronal integrity in these cells.

4.9. Identification of enrichment of pathway components amongst the genes affected by IC87114

IPA software also allows users to place their results within the context of molecular networks. We next set out to determine whether the components of any pathway or biological network were enriched within the genes that we had found in our study to be affected by IC87114-treatment. This analysis highlighted two biological networks that may be relevant to our list of genes affected by IC87114 treatment. The most relevant network that was assigned a score of 20 consisted of Nutritional disease, Cellular movement, Haematological System Development and Function. The second network scored 18 and also encompassed genes belonging to Haematological System Development and Function alongside Cellular Growth and Proliferation, and Cell death [Figure 4.6b].

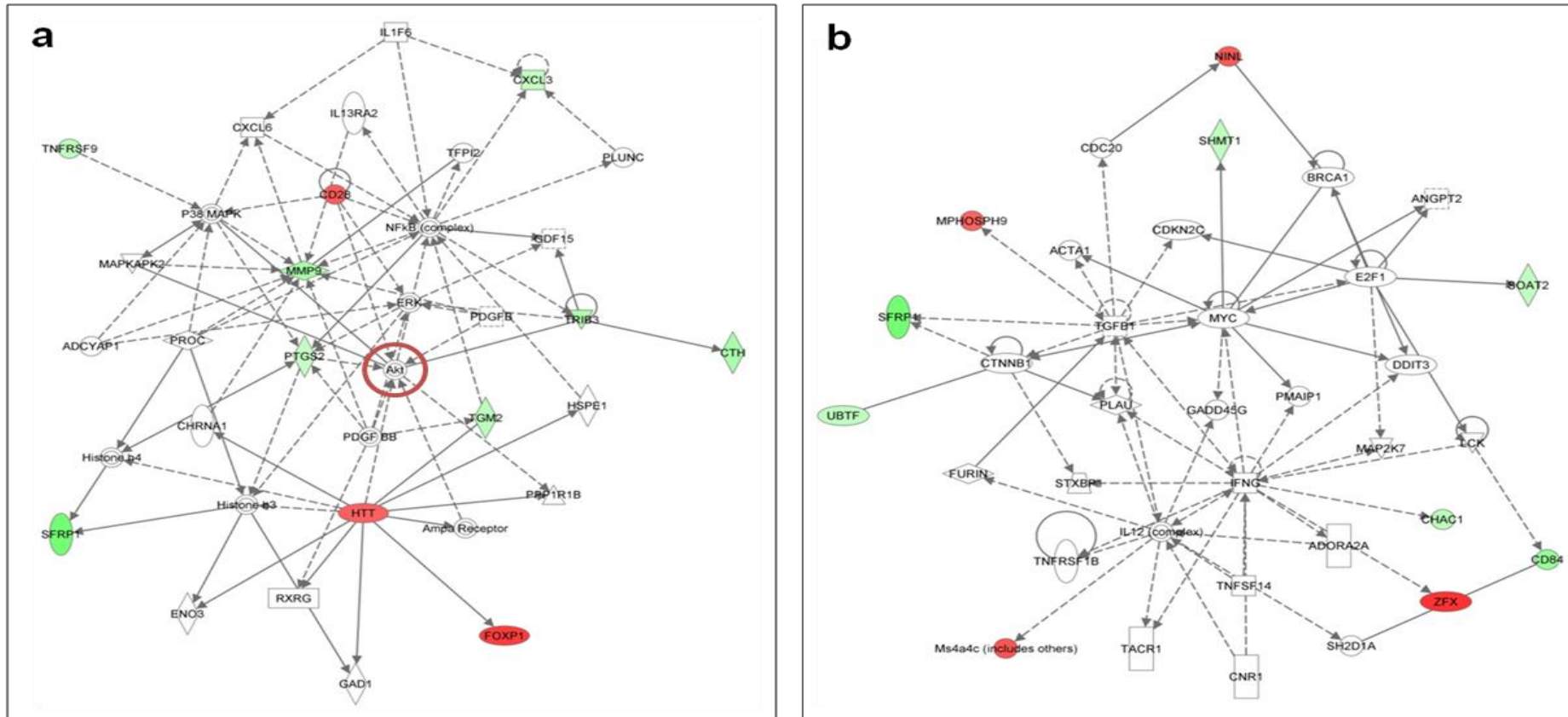


Figure 4.6. The top two networks found to be most relevant to our list of genes affected by IC87114-treatment. The list of genes affected by IC87114-treatment was uploaded into IPA software and core analysis was performed to as determined by IPA software. Scores were attributed based on a right tailed t test of the enrichment of genes in our list in these networks. A score of 20 represents a p value of 10^{-20} . Direct relationships are represented by full lines whilst indirect relationships or connections are indicated with a dashed line. Genes from the input list are indicated either in red or green for an increased or decreased expression in IC87114-treated cells respectively. **a.** The highest scoring network (20) was Nutritional disease, Cellular movement, Haematological System Development and Function **b.** Cellular Growth and Proliferation, Haematological System Development and Function, Cell death was the second most relevant network which was designated a score of 18.

We noted that Akt was one of the central nodes in the top network identified [Figure 4.6a Akt is circled in red]. Moreover, Akt was shown to have reported direct or indirect relationships with several of the genes in our list [Figure 4.6a]. In addition, the network revealed that within this network the transcription factor NF- κ B has reported indirect or direct relationships with the majority of the genes from the list, as well as with many of the other genes in the network [Figure 4.6a][162-165]. This could indicate that NF- κ B is one of the transcription factors through which p110 δ may regulate the expression of genes.

Further investigations revealed that the relationships between the input genes and Akt were largely spurious. For example, the relationship designated between Akt and Htt is based on a publication which showed, amongst other things, that Akt activity was not affected by MK-801 [166]. Thus, this publication has triggered IPA to link Akt and HTT despite in fact stating the opposite, that MK-801, which affects Htt, does not affect Akt activation [166]. On the other hand, the direct relationship between Akt and TRIB3 is made in reference to a publication showing that Akt has been found bound to TRIB3 in human cells [167]. This does have possible functional implications but they are unlikely to be relevant to the regulation of *Trib3* gene expression by p110 δ , which is suggested by our data. These findings highlights the caution with which these enrichment analyse must be analysed. This network analysis has perhaps not highlighted anything particularly pertinent to our analysis, except that it has identified NF- κ B as a transcription factor associated with several of our affected genes. Indeed, even this potential link with NF- κ B may need to be treated with caution. The fact that NF- κ B and also PI3K-Akt are areas which are highly covered in the literature may result in their over-representation in IPA networks. Having said that, *Mmp9* one of the genes identified in this study and in network one [Figure 4.6a] as discussed below, appears to be a genuine target of NF- κ B in a manner that is at least partially dependent on PI3K activity. Thus, the link between the genes we have identified in NF- κ B may be relevant but perhaps not to the exclusion of other transcription factors that are less well covered in the literature.

4.10. Identification of potential biomarkers of p110 delta inactivation

4.10.1. Biomarker characteristics

Biomarkers must be not only consistently correlated with a particular state or treatment such as IC87114 treatment, but ideally should also be relatively straightforward to measure. For that reason, cell surface molecules that can be rapidly measured using FACS are considered as ideal biomarkers. Secreted proteins can also often be easily monitored and quantified using ELISA techniques to determine their concentration in supernatant taken from cells. In fact, in some instances, it may be possible to monitor the concentration of secreted products in blood plasma using an ELISA.

4.10.2. Identification of potential biomarkers within the gene list

IPA software allows users to view enriched networks in either the standard view [Figure 4.6] or in a subcellular view [Figure 4.7]. This view allows the user to rapidly identify which subcellular location (extracellular, cytoplasm, plasma membrane, extracellular or unknown) each protein resides within.

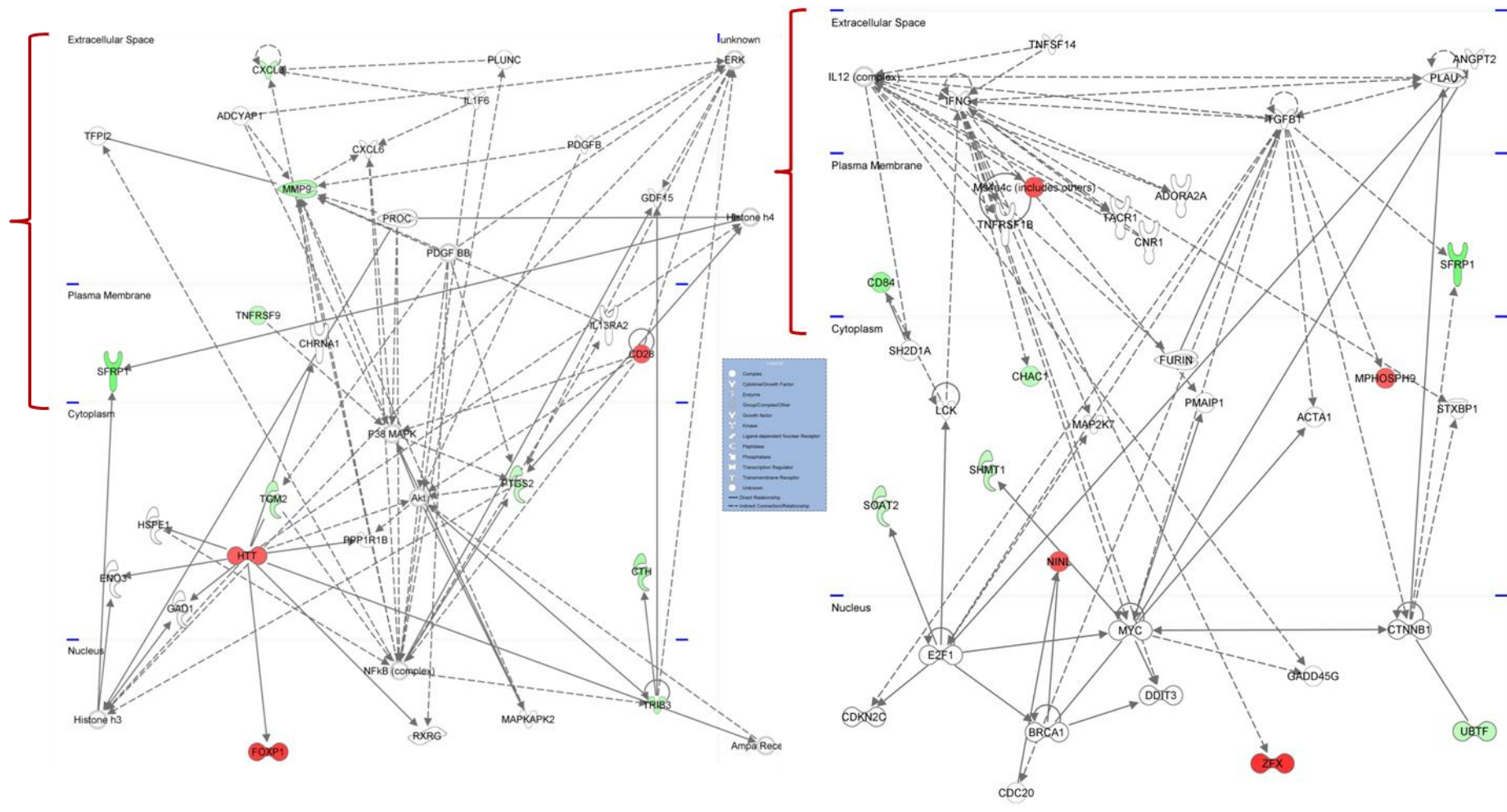


Figure 4.7. Subcellular view of top two networks relevant to the list of genes affected by IC87114-treatment. Red brackets indicate areas encompassing extracellular space and the plasma membrane.

We can observe six unique proteins encoded by a gene derived from our list that reside within either the extracellular space or the plasma membrane as highlighted by red brackets [Figure 4.7]. These proteins include Cd84, Cd28, Sfrp1 and Tnfrsf9 and which are located in the plasma membrane and therefore can be, quantified rapidly using FACS [Figure 4.7]. In addition, in the first network there are two genes encoding secreted proteins *Mmp9* and *Cxcl2*, which can be measured by ELISA [Figure 4.7]. Thus, just by examining the subcellular location of the genes in the top two networks relevant to our gene list we have identified seven genes that represent potential biomarkers for p110 δ inactivation. We proceeded to analyse our complete list of genes affected by IC87114 treatment and identified a further three genes that were not included in the top two networks, which also encode proteins that are either located in the plasma membrane or are secreted into the extracellular space. The nine genes in the complete list were *Sfrp1*, *Tnfrsf9*, *Cd84*, *Cd28*, *Ms4a4c*, *Cxcl2*, *Mmp9*, *Glrp* and *Niacr1* [Table 4.3]. Although it should be pointed out that proteins located within the cytosol or nucleus can usually be measured by immunoblotting and it is also not out of the question for the differential expression of an mRNA to be measured as a biomarker using qPCR. The remaining genes if found to be reproducibly affected by IC87114 treatment could therefore, in principle also be validated and developed into biomarkers.

Gene Symbol	Protein	Sub-cellular location	Method of detection	logFC
<i>Cd28</i>	Cd28 Antigen	Plasma membrane	FACS	1.029
<i>Cd84</i>	Cd84 Antigen	Plasma membrane	FACS	-1.876
<i>Cxcl2</i>	Chemokine	Extracellular	ELISA	-1.063
<i>Glrp</i>	Glycine receptor, beta subunit Sf1 homolog	Plasma membrane	FACS	-1.266
<i>Mmp9</i>	Matrix metalloproteinase 9	Extracellular	ELISA/Zymography	-1.538
<i>Ms4a4c</i>	membrane-spanning 4-domains, subfamily A, member 4C	Plasma membrane (?)	FACS (?)	1.104
<i>Niacr1</i>	Niacin R1	Plasma membrane	FACS	-1.068
<i>Sfrp1</i>	Secreted frizzled-related protein 1	Plasma membrane	FACS	-2.530
<i>Tnfrsf9</i>	TNF receptor superfamily, member 9	Plasma membrane	FACS	-1.129

Table 4.3. Potential biomarkers of p110 δ -inactivation identified by genome-wide expression analysis. Genes identified were grouped according to sub-cellular locations and those found to be expressed on the plasma membrane or in the extracellular space were considered to be the most promising biomarker candidates. *Ms4a4c* is a predicted protein encoded on chromosome 19 and for this reason the location of the protein is uncertain (symbolised by ?). The proteins predicted structure indicates it would be located within the plasma membrane.

4.10.3. Two potential biomarkers of p110 δ inactivation

Below I have briefly outlined the functions of two of the genes that we have found to be affected by IC87114 treatment. The two genes chosen have the potential to be used as biomarkers for the rapid determination of the p110 δ activity status of macrophages.

4.10.3.1. *Cd28* expression was increased by IC87114 treatment

Data obtained from three probe sets revealed that *Cd28* expression was increased by greater than 1 logFC in IC87114-treated RAW 264.7 macrophages compared to control cells [Table 4.1 & 4.2]. These data would suggest that p110 δ is a negative regulator of the expression of *Cd28* in RAW 264.7 macrophages. This result is puzzling because *Cd28* is a T cell marker, which recognises cell surface molecules

expressed on APCs and is to the best of our knowledge, not known to be expressed by macrophages. Specifically, Cd28 functions as a co-stimulatory molecule for the TcR and activation of the TcR. In the absence of this co-stimulation from bound CD28, TcR activation actually suppresses the activity of the T cells by inducing anergy [168]. Assuming *Cd28* expression is induced to a detectable level in IC87114-treated RAW 264.7 macrophages, this could be a useful marker of p110 δ inactivation. The expression of Cd28 on RAW 264.7 macrophages could be measured using Cd28-specific immune-fluorescent antibodies and FACS analysis.

4.10.3.2. *Mmp9* expression was reduced by IC87114 treatment

Mmp9 is a matrix metallo proteinase (mmp9) that is secreted during the inflammatory reaction by a range of immune cells including macrophages. Mmp9 has dual gelatine and collagen degradation activity and as such, degrades extracellular matrix components including collagen IV, which is a major component of the basement membrane. Secretion of Mmp9 remodels the extracellular matrix to facilitate leukocytes transmigration, which is necessary for immune cell recruitment to and entry into a site of infection. We consider that this differential expression of *Mmp9* in IC87114-treated RAW 264.7 macrophages may warrant further investigation and potentially could be measured using a simple gelatine zymography experiment.

4.11. Conclusion

As a consequence of the exclusion of two outlier samples (one from each treatment group), our results have been generated based on data obtained from only two replicates per condition. This small number of replicates certainly reduces the confidence with which these results can be presented. Statistical analysis was nevertheless performed and revealed that 139 probe sets were differentially regulated in IC87114-treated RAW 264.7 macrophages by 1 logFC or more with a $p \leq 0.001$ [Table 4.1]. Within this 139 probe sets were fifty-four known genes, including several that encode proteins that are expressed on the surface of the cell or are secreted. These genes represent potential biomarkers of p110 δ inactivation but we would of course need to validate the effect of IC87114 on their expression

in an independent experiment. By the time we had acquired these results, we were ready to perform a microarray to test the effect of p110 δ inactivation on primary macrophages. Thus, we decided not to validate any of the potential hits in this pilot study at this stage.

4.12. Discussion

Before proceeding with our main microarray study on primary macrophages, we performed a pilot microarray study to determine the impact of inactivating p110 δ on the RAW 264.7 transcriptome. Specifically, we compared the genome-wide expression of RAW 264.7 macrophages chronically (72 h) treated with IC87114 to RAW 264.7 macrophages treated with vehicle control. This study provided an excellent opportunity to familiarise ourselves with RNA work and especially with microarray studies both at a practical level but also in terms of data analysis.

All of the results from this study are presented with one major caveat, in consequence of which, we have been cautious not to draw any firm conclusions from them. The caveat is this: the results are based on a data set consisting of just two replicates per condition, after the removal of one outlier from each condition. The necessity to remove one outlier per condition is in itself somewhat troubling, especially as these replicates are derived from a single cell line source. We were nevertheless advised that it was acceptable to perform statistical analysis on the remaining data. This statistical analysis revealed that the differential regulation of the 139 probe sets is very highly significant ($p \leq 0.001$). It may be relevant that we originally analysed these data with the outlier samples' data included and in fact, in this original analysis we also identified *Cd28*, *Tgm2* and *Mmp9* as genes amongst many others that were differentially regulated in IC87114-treated RAW 264.7 macrophages. Indeed, if one were keen to follow up these results, without performing another microarray, it would be useful to obtain a list of the probe sets identified irrespective of the inclusion or exclusion of outliers. This problem of outliers certainly highlighted the importance of including sufficient replicates in a microarray experiment, in order to retain statistical power even if samples need to be excluded as outliers. Specifically, based on this experience, we decided that any future arrays that we perform should include at least four replicates per condition.

Briefly, we found that 139 probe sets were differentially regulated in RAW 264.7 macrophages chronically treated with IC87114 compared to their control counterparts. Within the list of probe sets identified were a number of genes that potentially represent useful biomarkers of p110 δ activity, including *Cd84*, *Cd28* and *Mmp9*.

Mmp9 is secreted by cells in response to a wide range of stimuli including TNF- α and LPS [169-170]. The available literature points to a requirement for NF- κ B activity for the induction of *Mmp9* expression in response to immunological stimuli, which is in keeping with the presence of several NF- κ B binding sites within the *Mmp9* promoter. Interestingly, induction of *Mmp9* expression and the subsequent increase in the secretion of *mmp9* have been reported to be significantly repressed by pan-PI3K inhibition [169, 171]. This involvement of PI3K was shown to occur alongside other LPS-activated signalling pathways such as the MAPK (p38 activation) or the Notch signalling pathways [169, 171]. These publications support our finding regarding decreased *Mmp9* expression in RAW 264.7 macrophages treated with IC87114. In light of our result it is tempting to speculate that p110 δ is responsible for the regulation of *Mmp9* expression, but without further investigation we cannot rule out a contribution of other PI3K isoforms. Interestingly, Mendes *et al.* found that Rapamycin treatment, which inhibits mTORC1 had a resulted in significantly increased expression of *Mmp9* in RAW 264.7 macrophages stimulated with LPS [48]. These publications also highlight that immunological stimuli are potent activators of *Mmp9* expression. We therefore speculate that a more substantial and importantly more easily detectable deregulation of *Mmp9* expression might be observed in response to IC87114 treatment if RAW 264.7 macrophages were stimulated with LPS. In theory, enhancing the differential regulation of *Mmp9* in RAW 264.7 macrophages treated with IC87114 by stimulation with LPS could improve its usefulness as a biomarker of p110 δ inactivation.

The identification of the *Cd28* as a gene differentially regulated in these macrophages was somewhat unexpected because *Cd28* is a T cell marker. To our knowledge *Cd28* is not expressed in macrophages and it is possible that this regulation is functionally irrelevant as *Cd28* is not actually transcribed, translated or expressed on the surface of these cells. Alternatively, we speculate that this

could be a clue to indicate that these cells have, as a result of transformation or prolonged culture, lost their macrophage phenotype to some degree or aberrantly express T cell genes. We recognise that this may also be an indication of cross-contamination within this cell line.

Despite the limitations of this study, we propose that the data could provide a useful starting point for the development of an assay to validate the activity of potential p110 δ -selective inhibitors. Before developing an assay it would be necessary to validate the results. Validation would require the effect(s) to be observed consistently in at least three additional samples at the RNA level and preferably, depending on the final assay design, at the protein level. To ensure that the effect of IC87114 on the gene expression is related to its inhibition of p110 δ , the effect(s) would also need to be observed consistently in response to treatment with several other p110 δ -selective inhibitors. The development of novel p110 δ -selective agents is ongoing within the pharmaceutical industry and consequently, the ability to screen agents reliably and rapidly for p110 δ -selective activity is much sought. We suggest that, subject to validation, the differential regulation of one or a number of the genes identified could be developed into an *in vitro* assay to screen for agents that inactivate p110 δ . The potential to perform this type of assay using a fast-growing, readily-cultured cell line has advantages for development into the high throughput format, which is preferred by pharmaceutical companies. We conclude that despite some major limitations, the results of this study could potentially be of use in the development of an *in vitro* assay for the inactivation of p110 δ activity. Furthermore, we gained useful experience in genome-wide expression analysis and have learned valuable lessons and as such we feel this study fulfilled its role as a pilot study.

CHAPTER 5

5. INVESTIGATING THE EFFECTS OF GENETIC INACTIVATION OF P110 DELTA ON THE TRANSCRIPTOME OF PRIMARY MACROPHAGES

5.1. Development and validation of a modified primary macrophage extraction and differentiation protocol

At the beginning of this project we had substantial difficulties culturing primary macrophages. This had to be resolved before we could proceed with our genome-wide expression analysis using primary macrophages. As such this caused some delay to the start of our work with primary macrophages, but during this delay we performed the study described in Chapter 4. The problem and its resolution are briefly described here. Several consecutive cultures failed to differentiate and cells appeared to be dying within three days of extraction.

5.1.1. Addressing difficulties with the differentiation of primary macrophages

Initially we replaced all reagents with fresh bottles to ensure none of the reagents were contaminated and changed all plastic-ware to certified endotoxin-free products. Unfortunately these measures did not resolve the issue. Initially we checked with a more experienced member of the Centre for Cell Signalling, that the original protocol was being performed appropriately to eliminate any technical errors. No technical errors or good lab practice concerns were identified. The current protocol was therefore deemed to be no longer suitable and we decided to develop a modified protocol.

5.1.2. The modified protocol for production of differentiated macrophages

The most substantial difference between the modified and original protocol is the increased addition of CSF-1. The modified protocol requires addition of CSF-1 to the progenitors more frequently and at a higher dose during the differentiation period. We also adjusted the method of splitting the cells to reduce stress caused during differentiation. The original and the modified protocol are described in detail in Materials and Methods alongside the original protocol [Chapter 2, section 2.3.2].

We consistently obtain differentiated primary macrophages using the modified protocol. Moreover, we have significantly increased the yield of macrophages produced from each mouse from an average of around ten million to an average of between thirty and forty million. We now suspect/infer that the original protocol may have become ineffective due to altered potency in the commercially produced CSF-1.

5.1.3. Validation of macrophages generated using modified protocol

Photographs of differentiated macrophages have been included here to record the macrophage-like morphology of the cells generated [Figure 5.1]. Two pictures are included in order to illustrate the range of morphologies observed in primary macrophages including more rounded and more extended cell shapes [Figure 5.3].

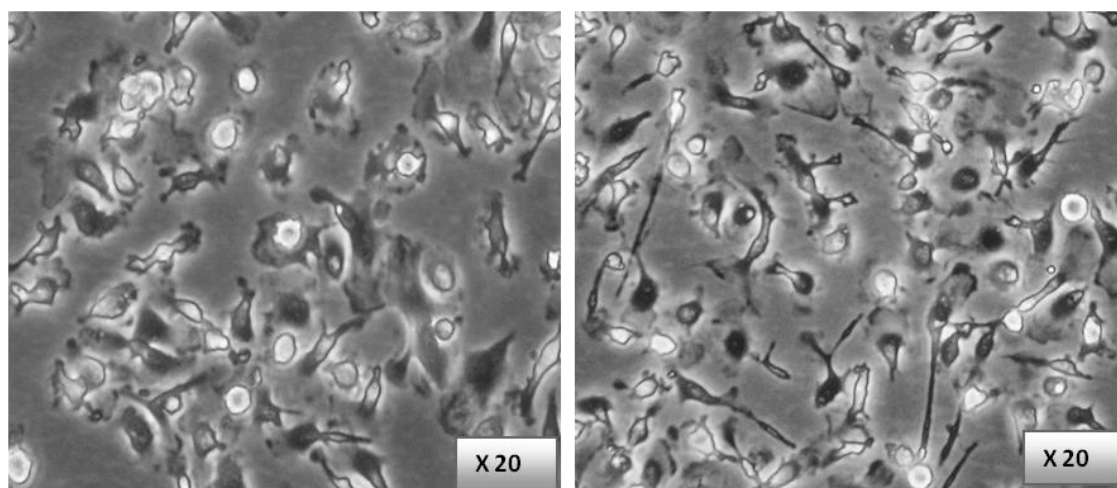


Figure 5.1. Photographs showing the normal range of morphology displayed by differentiated primary macrophages generated using the modified protocol. Macrophages were extracted and differentiated in accordance with the modified protocol. Photographs of macrophages in the presence of CSF-1 on Petri dishes were taken seven days after extraction using a digital camera and a light microscope (objective 20X).

5.1.3.1. Phenotypic analysis of macrophages generated with modified protocol

We performed basic phenotypic analysis using FACS to assess the expression of the classic macrophage surface marker F4/80 on the cells generated using the modified protocol to confirm that they were indeed macrophages. We observed expression of F4/80 in both the WT and p110 δ KI macrophages [Figure 5.2]. It has previously been shown that surface expression of F4/80 is normal in p110 δ KI macrophages [79]. These data indicated that there was modest difference between the expression of F4/80 on the WT and p110 δ KI macrophages [Figure 5.2]. The experiment would need to be repeated to confirm this, but we suggest the difference is not sufficient to be of any importance.

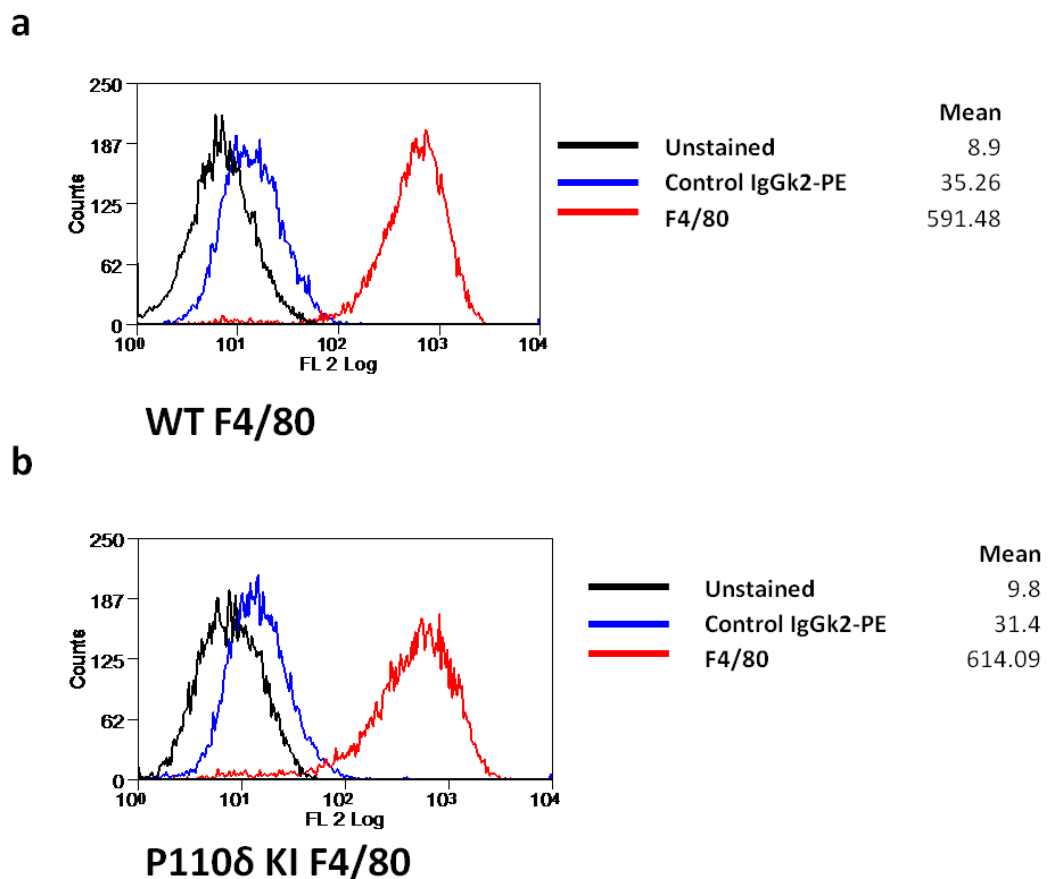


Figure 5.2. WT and p110 δ KI macrophages both express F4/80. **A.** WT macrophages were allowed to adhere overnight and the following day were scraped into FACS buffer, washed and stained at RT for 1 h with an F4/80 specific-PE conjugated antibody. **B.** p110 δ KI macrophages were prepared and treated as described in A. **C.** WT BMMs were treated with LPS at 1 μ g/ml overnight and prepared as described in A. The histograms are representative of results of two samples for both WT and p110 δ KI macrophages.

5.1.3.2. Testing the LPS-responsiveness of the differentiated macrophages

To test whether the cells are responsive to LPS, we assessed the expression of IA/IE (the mouse homolog of MHC II). Unstimulated immature macrophages express low levels of IA/IE and upon LPS-stimulation, LPS-responsive macrophages, i.e. ones that have not been tolerised to LPS by previous exposure, upregulate expression of the antigen presenting complex IA/IE. We observed that the unstimulated-macrophages of both genotypes were IA/IE-low and that they did indeed upregulate IA/IE surface expression following stimulation with LPS [Figure 5.3].

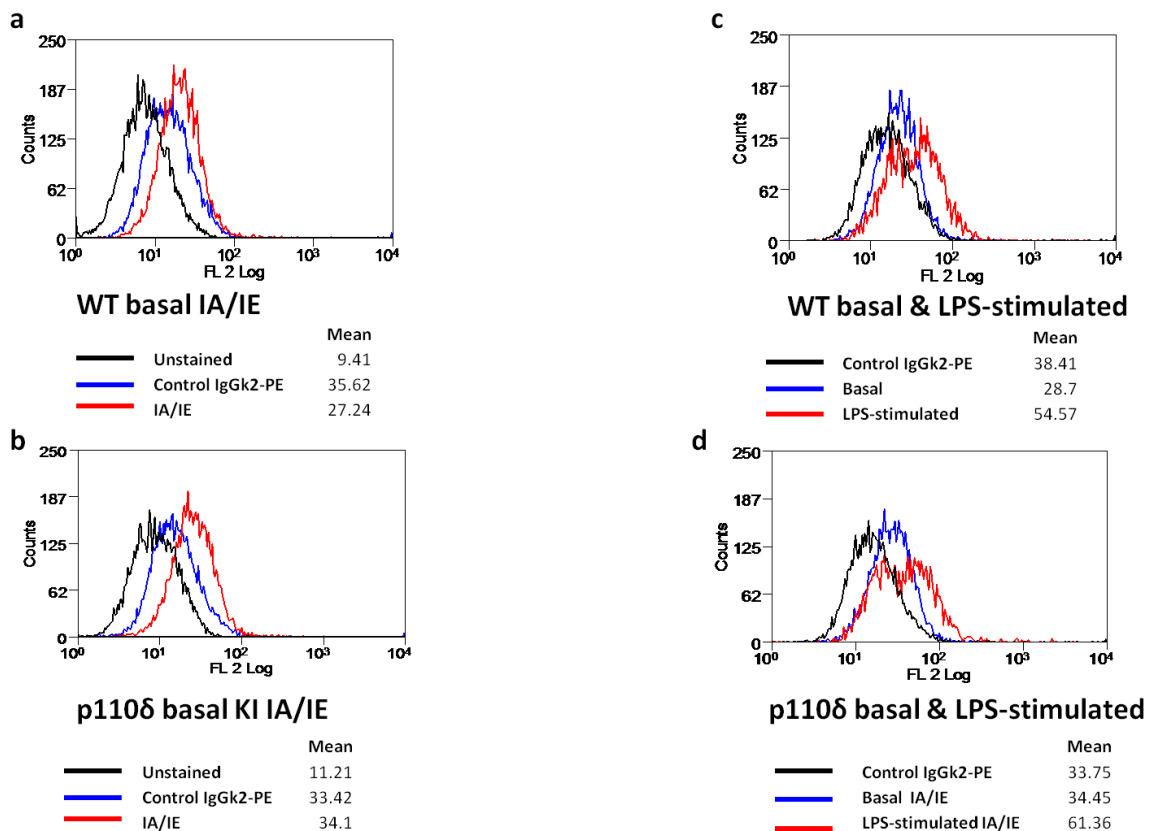


Figure 5.3. WT and p110δ KI macrophages express IA/IE at low levels in the unstimulated state and upregulate IA/IE significantly on LPS stimulation. Cells were stimulated with either control or LPS (1 µg/ml) for 24 h. The following day cells were scraped into FACS buffer and washed, before staining at RT for 1 h with F4/80 and IA/IE specific antibodies and were subsequently analysed. Histograms shown are representative of results of two samples for both WT and p110δ KI macrophages.

These two findings, regarding F4/80 and IA/IE expression, are consistent with the expected profile of immature macrophages, and therefore, based on these results we are confident that the modified protocol can be used to produce a pure population of LPS-responsive macrophages.

5.2. Aims of genome-wide expression analysis of p110 δ KI and WT macrophages

After completing the pilot genome-wide expression analysis study and concurrently solving our problems with primary macrophage culture we were ready to proceed with our main experiment. Our objectives remained the same, first, to gain insight into the contribution and role of p110 δ activity in transcriptional activation and secondly, to identify potential biomarkers of p110 δ inactivation. We reasoned that primary macrophages derived from p110 δ KI mice would be an ideal model with which to address these questions. Primary cells are often preferable to cell lines when work being performed has a translational element because the inherent abnormalities in cell lines can complicate the interpretation of results. The p110 δ KI mutation is considered to be an excellent model of selective pharmaceutical inactivation of p110 δ . We were interested to observe whether any of the genes affected by chronic IC87114 treatment in RAW 264.7 macrophages, would also be differentially regulated in p110 δ KI primary macrophages.

5.3. Conditions used for genome-wide expression analysis

We wanted to assess the contribution of p110 δ to transcriptional regulation in normal culture conditions that we deemed most relevant to physiological conditions. Primary macrophages are dependent on CSF-1 for growth and survival and are ubiquitously exposed to CSF-1 *in vivo*. Assessment of genome-wide expression analysis in primary macrophages was therefore performed on primary macrophages in complete media containing 10% FBS and CSF-1 (20 ng/ml). We chose to expand our investigation to include the identification of changes to the transcriptome of primary macrophages lacking p110 δ activity in an activated as

well as basal state. Specifically, we decided to determine the transcriptome of p110 δ KI macrophages compared to WT macrophages in the basal and LPS-stimulated state [Figure 5.4]. LPS has a rapid and dramatic impact on the macrophage transcriptome and PI3K inactivation has been shown to impact upon this transcriptional regulation induced by LPS in macrophages and other immune cells [96]. We predicted that if the impact of p110 δ inactivation on basal macrophages was minimal in terms of magnitude of deregulated expression that these effects might be amplified in the presence of LPS. We therefore felt that the inclusion of paired samples treated with LPS would assist us in gaining a greater insight into the contributions of p110 δ to macrophage transcriptional regulation. Furthermore, our pharmaceutical sponsors proposed that if an altered expression of a certain gene identified in LPS-stimulated p110 δ KI macrophages translated to LPS-stimulated human monocytes that this would represent a suitable biomarker.

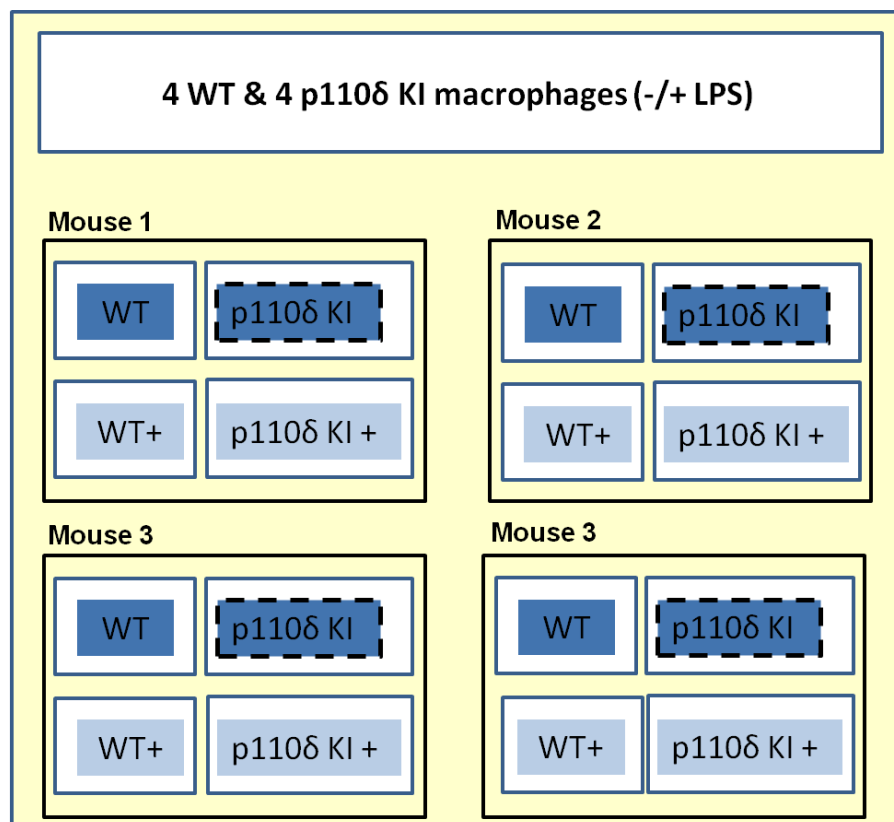


Figure 5.4. Scheme of genome-wide expression analysis of p110 δ KI macrophages and WT macrophages. Primary macrophages derived from four WT mice and four p110 δ KI mice were plated in complete media containing 10% FBS and 20 ng/ml of CSF-1. The following day the cells were stimulated with LPS (1 μ g/ml) for 6 h and the RNA was extracted for genome-wide expression analysis.

5.4. Obtaining genome-wide expression data for WT and p110delta KI macrophages

Macrophages were derived from four WT mice and four p110 δ KI mice and treated with control or LPS for 6 h. Genome-wide expression data was subsequently obtained for each of the sixteen samples using Affymetrix GeneChip® Mouse Genome 430 2.0. Firstly we visually appraised the data image files and all Affymetrix internal controls were checked and found to be satisfactory. We then processed the data in the same way as described in Chapter 4 with assistance from Dr H. Edwards, Dr P. Hales and Ms E. Gadaleta [Chapter 4, section 4.5]. Briefly, this included chip to chip normalisation using the GC-RMA algorithm and subsequently reducing the data set from the full 45,002 probe sets by filtering to extract the top 10,000 most variant probe sets.

5.4.1. Analysis of clustering within the dataset

5.4.1.1. Samples clustered by LPS-stimulation status and not genotype

We performed PCA, which revealed that the key principal component (PC1) represented the variation between the basal and LPS-stimulated samples [Figure 5.5]. Thus the samples clustered according to LPS-stimulation status and not by genotype.

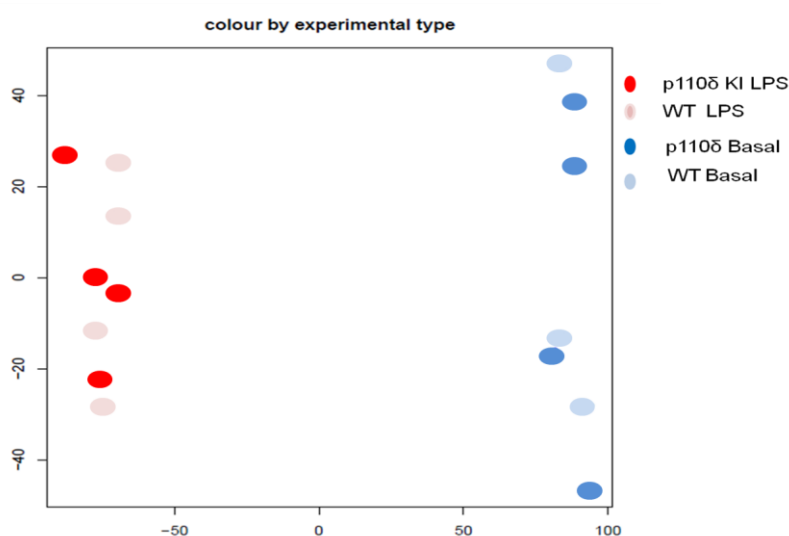


Figure 5.5. PCA revealed that the samples separate by LPS-stimulation status and not by genotype. PCA was performed on expression data to determine separation of samples. Samples separate according to basal and LPS-stimulated status and not according to genotype (WT versus p110 δ).

5.4.1.2. Hierarchical clustering reveals an outlier and a batch effect

Bearing in mind the impact of LPS on the transcriptome, it was not surprising to us that basal *versus* LPS-stimulated status represents the greatest differential within our data set. Furthermore, our ability to detect this LPS-driven effect provided a useful internal control for the power of the Affymetrix to identify biologically relevant changes in gene expression within our samples. We subsequently employed hierarchical clustering and confirmed that LPS-stimulation represents the biggest differential in our data set and that the samples did not cluster according to their genotype [Figure 5.6]. In fact, whilst the samples did not cluster by genotype within the basal and LPS branches, we noticed that they did cluster by day of extraction or effectively by batch [Figure 5.6]. Hence WT 2 clusters with DKI 2 as the mice from which the macrophage precursors were extracted on the same day and were subsequently differentiated over the same seven day period [Figure 5.6]. Batch effects are caused by systemic errors which result from non-biological experimental variation introduced when samples are not processed together, as in our experiment. Whilst every effort was made to make sure that batches were treated according to an identical protocol, with consistent reagents used throughout, the only way to completely eliminate intra-array variation is to process all samples together. Thus, ideally all the macrophages should have been extracted on the same day and consequently differentiated over the same period and finally processed on the same day. We reason that this batch effect is not a significant problem as we are aiming to identify differences that can potentially be used as biomarkers in clinical work, which therefore must be apparent despite background variation. In fact if anything we would expect a much higher variation in both sample processing and also individual variation associated with collection of clinical samples.

Experiment
 ■ wild type
 ■ DK1
 ■ wild type + LPS
 ■ DK1 + LPS

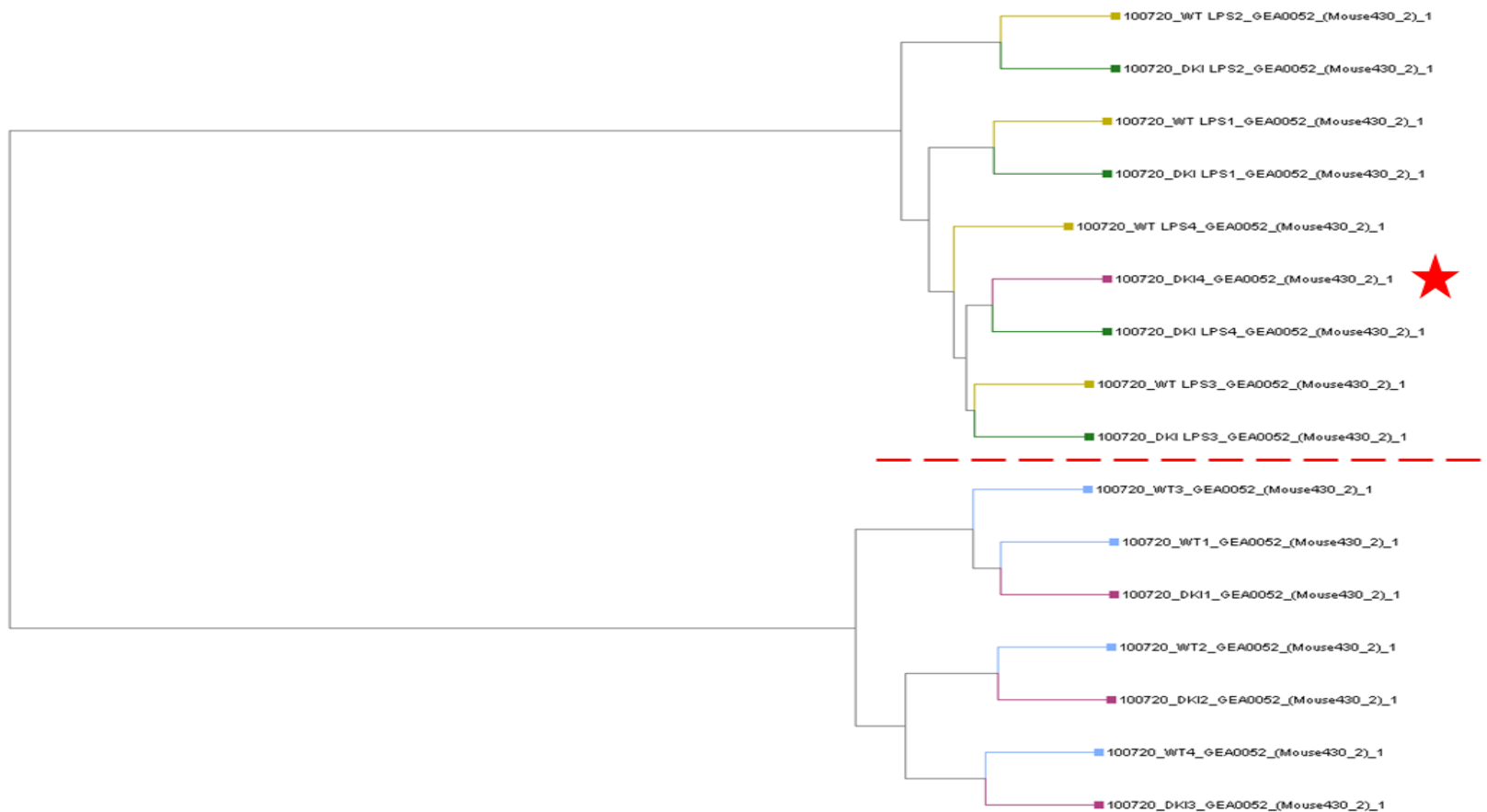


Figure 5.6. Hierarchical clustering identified an outlier and a batch effect. Hierarchical clustering was employed to identify the relationships between the samples. Samples separated into two main branches, unstimulated and LPS-stimulated and did not cluster according to genotypes. One outlier sample was identified; DK1 4 (indicated by the red star) an unstimulated sample clustered with the LPS-stimulated samples. A batch effect where samples extracted on the same day clustered together.

The HCA analysis also revealed that sample p110 δ KI 4 (DKI4-indicated by red star) was an outlier as it was aligned with the LPS-stimulated samples in the hierarchical tree [Figure 5.6]. This sample may have been accidentally exposed to LPS or some other stimulant. The data set from this outlier was excluded from further analysis, unless otherwise stated.

5.4.2. Identification of individual genes affected by p110 δ inactivation

We proceeded to extract the probe sets that were differentially regulated by a logFC of 1 or more and a statistical significance of $p \leq 0.05$. We found twenty-five probe sets that met these criteria; seventeen probe sets including fourteen known genes and three RIKEN sequences were affected in the basal state [Table 5.1 & 5.3], whilst twenty probe sets including the same three RIKEN sequences were affected in the LPS-stimulated state [Table 5.2 & 5.3]. The proportion of increases compared to decreases in expression was relatively balanced with 54.2% of the probe sets decreased and 45.8% increase overall. Within these probe sets twelve were affected irrespective of the LPS-stimulation status, whilst five were affected only in basal macrophages and eight were only identified as differentially regulated in LPS-stimulated genes [Figure 5.7]. A summary of these probe sets is provided in Tables 5.1, 5.2 & 5.3.

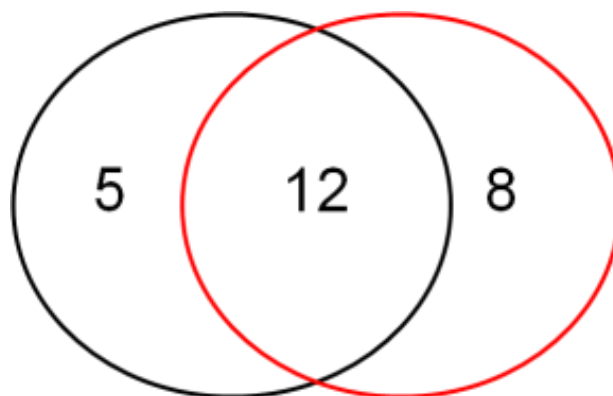


Figure 5.7. Venn diagram of the twenty-five probe sets that were found to be differentially regulated in p110 δ KI macrophages compared to in WT macrophages. Twelve probe sets (nine known genes and three RIKENs) are differentially expressed irrespective of LPS treatment. Five known genes are only differentially regulated in basal p110 δ KI macrophages and eight only in LPS-stimulated p110 δ KI macrophages. The probe sets within the black ring were identified in the basal state and those within the red ring were identified in the LPS-stimulated state

Probe Set ID	Gene Symbol	Protein	Basal	
			logFC	adjP value
1434914_at	Rab6b	RAB6B, member RAS oncogene family	-2.368	2.14E-05
1419078_at	Nin	Ninein	2.316	2.14E-05
1421861_at	Clstn1	calsyntenin 1	1.737	7.60E-03
1423024_at	Sh2d1b1	SH2 domain protein 1B1	1.286	4.02E-02
1417120_at	Miip	migration and invasion inhibitory protein	-1.092	3.05E-02

Table 5.1. The expression of five genes was differentially regulated in p110 δ KI macrophages compared to in WT macrophages in basal conditions. The expression of two genes (*Rab6b* and *Miip*) was decreased in basal p110 δ KI macrophages. The expression of three genes (*Clstn1*, *Sh2d1b1* and *Nin*) was increased in basal p110 δ KI macrophages. Genes are ordered by magnitude of change irrespective of the direction of logFC and red and green highlighting indicate whether expression of the gene is increased or decreased in p110 δ KI macrophages respectively.

Probe Set ID	Gene Symbol	Protein	LPS-stimulated	
			logFC	adjPValue
1450498_at	Mthfr	5,10-methylenetetrahydrofolate reductase	-2.194	1.70E-04
1432499_a_at	Ube4b	ubiquitination factor E4B, UFD2 homolog (S. cerevisiae)	-1.802	1.38E-04
1425270_at	Kif1b	Kinesin family member 1b	1.409	1.72E-02
1438239_at	Mid1	midline 1	1.408	1.64E-02
1421365_at	Fst	Follistatin	1.305	1.07E-03
1416995_at	Pacsin3	protein kinase C and casein kinase substrate in neurons 3	1.304	3.10E-03
1442140_at	Tnn	tenascin N	-1.083	3.47E-02
1454760_at	Htatsf1	HIV TAT specific factor 1	1.078	4.33E-02

Table 5.2. The expression of eight genes was differentially regulated in LPS-stimulated p110 δ KI macrophages compared to LPS-stimulated WT macrophages. The expression of three genes, (*Mthfr*, *Ube4b*, *Tnn*) was decreased in LPS-stimulated p110 δ KI macrophages. The expression of five genes was increased in LPS-stimulated p110 δ KI macrophages (*Kif1b*, *Mid1*, *Fst*, *Pacsin3* and *Htatsf1*). Genes are ordered by magnitude of LogFC irrespective of the direction of change. Known genes are highlighted in bold and red and green highlighting indicate whether expression of the gene is increased or decreased in p110 δ KI macrophages respectively

Probe Set ID	Gene Symbol	Protein	Basal		LPS-stimulated	
			logFC	adjPValue	logFC	adjPValue
1419309_at	<i>Pdgn</i>	Podoplanin	-3.629	2.14E-05	-3.321	2.71E-05
1425521_at	<i>Paip1</i>	polyadenylate binding protein-interacting protein 1	3.110	6.79E-06	3.350	8.71E-07
1449141_at	<i>Fblim1</i>	filamin binding LIM protein 1	-2.927	3.61E-04	-3.892	4.42E-03
1453145_at	<i>Pisd-ps3</i>	phosphatidylserine decarboxylase, pseudogene 3	2.230	2.24E-03	1.849	4.57E-03
1431106_a_at	9530053H05Rik	RIKEN cDNA 9530053H05 gene	2.157	1.20E-02	1.329	2.04E-02
1416289_at	<i>Plod1</i>	procollagen-lysine, 2-oxoglutarate 5-dioxygenase 1	-1.886	5.93E-04	-1.771	4.08E-04
1424213_at	<i>Ubiad1</i>	UbiA prenyltransferase domain containing 1	1.811	9.11E-03	2.345	2.95E-04
1437478_s_at	<i>Efhd2</i>	EF hand domain containing 2	-1.782	4.66E-04	-1.541	7.10E-04
1436574_at	1700029I01Rik	RIKEN cDNA 1700029I01 gene	-1.685	6.82E-03	-1.752	1.83E-03
1439279_at	3110007F17Rik	RIKEN cDNA 3110007F17 gene	-1.662	2.24E-03	-1.230	1.33E-02
1451349_at	<i>Efcab7</i>	EF-hand calcium binding domain 7	-1.583	4.08E-03	-1.409	4.57E-03
1437708_x_at	<i>Vamp3</i>	vesicle-associated membrane protein 3	-1.088	3.05E-02	-1.121	1.11E-02

Table 5.3. Differential regulation of twelve probe sets interrogating nine known genes and three RIKEN transcripts in p110 δ KI macrophages compared to WT macrophages in both basal and LPS-stimulated conditions. Six known genes and two RIKEN clones (*Fblim1*, *Pdgn*, *Plod1*, *Efhd2*, *Efcab7* and *Vamp-3*) were found to be decreased in basal and LPS-stimulated p110 δ KI macrophages. Three known genes and one RIKEN were found to be increased in basal and LPS-stimulated p110 δ KI macrophages. Probe sets are ordered by magnitude of logFC irrespective of the direction of change and known genes are in bold and red and green highlighting indicate whether expression of the gene is increased or decreased in p110 δ KI macrophages respectively

The most substantial deregulation was a logFC of -3.89 *Fblim1* in LPS-stimulated p110 δ KI macrophages compared to WT macrophages. This is equivalent to a decrease of *Fblim1* transcription by 14.8 times compared to its transcription in WT macrophages. Although this is a very substantial decrease the majority of the logFCs were relatively modest. The mean increase in expression of genes affected by 1 logFC or more ($p \leq 0.05$) was a logFC of 1.79 (3.45 times more) and the average decrease was 1.9 logFC (3.73 less).

5.4.3. Identification of functions enriched in the list of differentially genes

We next employed IPA software to determine which, if any, molecular and or cellular functions were enriched in the list of genes differentially regulated in p110 δ KI macrophages. The results indicated that a number of functions were enriched including amino acid metabolism, cell cycle, and cell-to-cell signalling and interaction [Figure 5.8]. The majority of the enriched functions do not overlap with those identified as most enriched in the RAW 264.7 gene list. Although, one of the enriched functions in the RAW 264.7 gene list was cellular compromise and we note that there is also an enrichment of genes differentially regulated in p110 δ KI macrophages belonging to this category [Figure 5.8]. Four of the genes differentially regulated in p110 δ KI macrophages are categorised by IPA under cellular compromise: *Ube4b*, *Mid1*, *Plod1* and *Nin*.

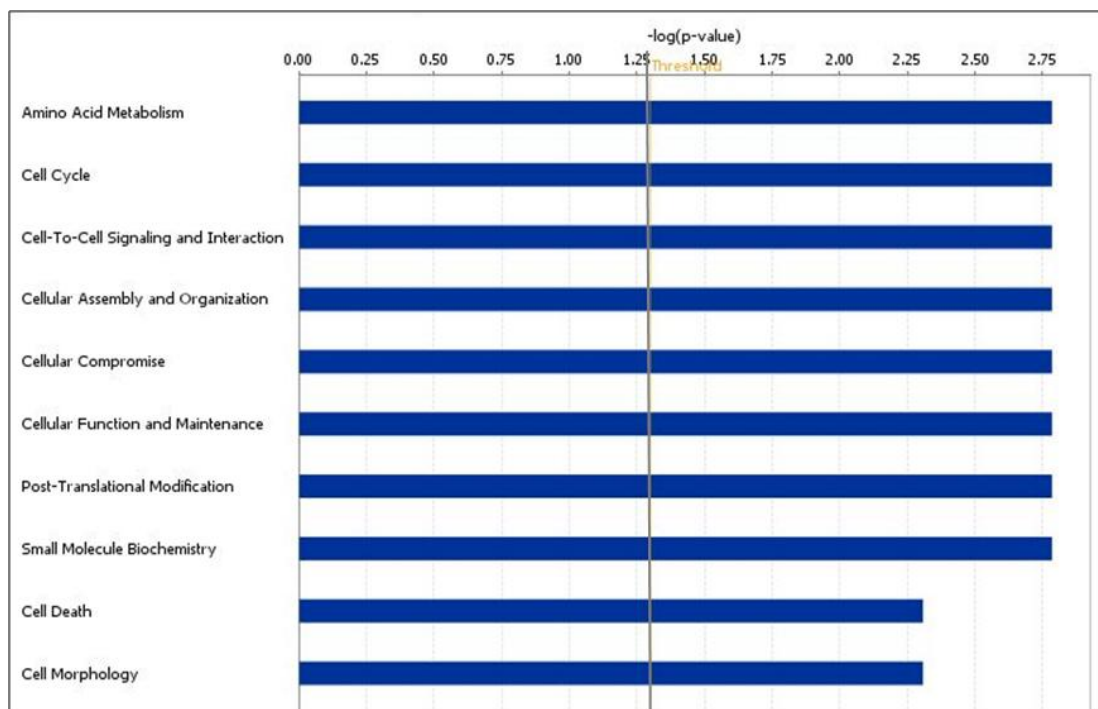


Figure 5.8. The top ten most statistically significant molecular and cellular functions enriched in the list of genes differentially regulated in p110 δ KI macrophages. Functional enrichment analysis was performed using IPA software on the complete list of genes differentially regulated in basal and/or LPS-stimulated p110 δ KI macrophages. The statistical significance of the enrichment of genes associated with each listed molecular processes are indicated by the length of the position of the blue bar against the Y axis, which represents log p values determined using Fisher's exact test. The statistical significance threshold set at $p \leq 0.05$ is indicated by the thin grey line.

5.4.4. Identification of most relevant networks using IPA

Although we only identified twenty-five unique genes or transcripts, we were nevertheless interested to determine whether this list of genes was enriched for any particular molecular networks. We found that the scores assigned to the top two networks relevant to the gene list were much smaller than those assigned to the top two networks relevant to the RAW 264.7 gene list [Chapter 4, Figure 4.11]. The most relevant network identified by IPA was inflammatory response, antimicrobial response, cell-to-cell signalling and interaction network [Figure 5.9]. This network was assigned a score of 6 (equivalent to $p \leq 10^{-6}$) based on the relationships between five of the genes in the input list (*Fblim1*, *Vamp3*, *Htatsf1*, *Pdpr*, *Tnn* and *Fst*) and other network components [Figure 5.9].

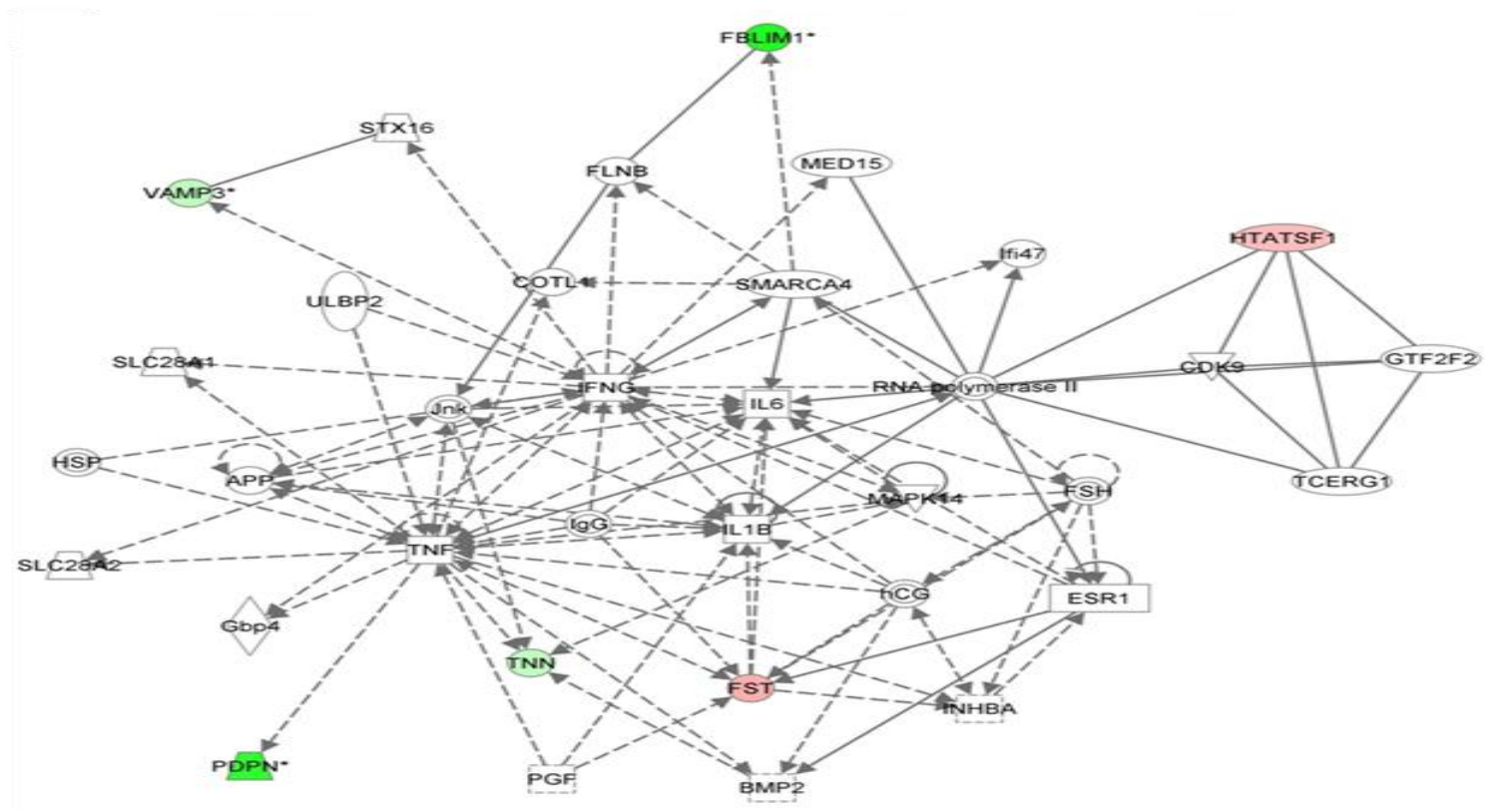


Figure 5.9. IPA analysis revealed the Inflammatory Response, Antimicrobial Response, Cell-To-Cell Signalling and Interaction network as relevant to the list of genes differentially regulated in p110δ KI macrophages. IPA identified the most relevant molecular networks based on the twenty-five probe sets differentially regulated in basal and or LPS-stimulated p110δ KI macrophages. Scores were assigned based on right tailed t tests of the enrichment of genes in the list in the networks. Full and dashed lines represent direct relationships and indirect relationships or connections respectively. Red or green indicates increased or decreased expression respectively. The network of Inflammatory Response, Antimicrobial Response, Cell-To-Cell Interactions was identified as most relevant network to the gene list and was assigned a score of 6.

The second network IPA software identified as most relevant to the gene list was cancer, embryonic development and tissue morphology. On closer inspection, despite a score of three, the network consisted of just two components *Rab6b* and a micro RNA miR122. Although this result serves to highlight the possible regulation of *Rab6b* by miR122, the classification of this as a network seems a little spurious. Indeed, this rather limited “network” and the statistical significance assigned to it despite its composition of just two components, highlights the caution with which IPA results should be treated.

5.5. Identification of potential biomarkers for p110 delta inactivation

We observed a lack of overlap between the genes differentially regulated in p110 δ KI primary macrophages with those genes found to be differentially regulated in RAW 264.7 macrophages chronically treated with IC87114. Had any gene(s) been identified in both studies, they would have represented prime candidates for development as p110 δ biomarkers. The absence of overlap raised several questions, which are discussed in the subsequent chapter and in the discussion in the context of later results. We reasoned that it was still important to proceed with validation and to choose genes that represented the most promising candidates for development as potential biomarkers. Within the gene list there were six genes encoding proteins that are identified by IPA as encoding proteins that are located in the plasma membrane or extracellular space; *Clstn1*, *Fst*, *Fblim1*, *Pdpn*, *Tnn* and *Vamp3* [Table 5.4].

Gene Symbol	Protein	Location (IPA)
<i>Fst</i>	Follicle-stimulating hormone	Secreted*
<i>Clstn1</i>	Calsyntenin	Plasma membrane
<i>Fblim1</i>	filamin binding LIM protein	Plasma membrane
<i>Pdpn</i>	Podopalin	Plasma membrane

<i>Tnn</i>	Tenascin N	Plasma membrane
<i>Vamp3</i>	Vesicular-associated membrane protein 3	Plasma membrane*

Table 5.4. Potential biomarkers identified include six genes encoding proteins that are either secreted or expressed on the plasma membrane. The sub-cellular locations of the twenty-five unique probe sets were identified using *in silico* analysis. *Fst* encodes a secreted protein, whilst *Clstn1*, *Fblim1*, *Pdpm*, *Tnn*, and *Vamp3* all encode proteins expressed on the plasma membrane. * denotes that the subcellular location stated may not be the exclusive location of this protein.

In fact, although the proteins may associate with the plasma membrane, they are in fact intracellular and for the purposes of a biomarker we ideally wanted to identify genes encoding transmembrane proteins that can be measured using FACS. One of the genes, *Fst*, encodes follicle-stimulating hormone which is indeed secreted, although we are not confident based on what is known about its function, that it will actually be secreted by macrophages.

5.5.1. Identification of the differential regulation most representative of p110 δ inactivation

With the help of Dr P. Hales, we employed GeneData Expressionist Software to aid us in the unbiased identification of the genes that are most representative of p110 δ inactivation in primary macrophages. Classifier analysis distils large data sets down to a number of key changes in expression that are the most representative of the states investigated. The algorithm performed on our complete dataset (excluding outlier DKI4) identified that the expression values of six probe sets are necessary and sufficient for separation of samples into the four categories; WT basal, WT LPS, DKI basal or DKI LPS [Figure 5.10]. The six probe sets consisted of two duplicate probe sets for *Paip1*, two duplicate probe sets for *Fblim1*, a probe set for *Pdpm* and a probe set for RIKEN sequence A430071A18Rik. This would suggest that the expression values of just three known genes and one RIKEN sequence would be sufficient to confidently distinguish between p110 δ KI and WT samples and furthermore, also to differentiate basal from LPS-stimulated samples within those genotypes.

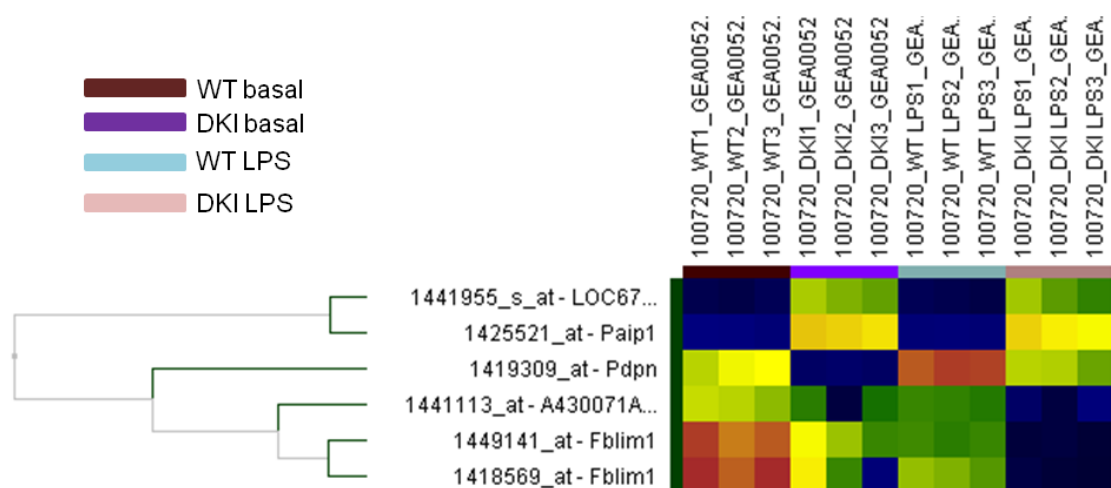


Figure 5.10. Classifier algorithm identified four genes (six probe sets) that were most representative of the four different conditions (WT basal, WT LPS, DKI DKI LPS). GeneData Expressionist software was used to perform a classifier analysis that identified the top variations between the four groups of samples. The expression of six probe sets specific to three unique genes, *Paip1*, *Fblim1*, *Pdpm* and one RIKEN sequence was identified as highly indicative of p110 δ KI status.

We had anticipated that a larger number of probe sets would be necessary to categorise the sample groups particularly in light of the lack of clustering by genotype that was identified by PCA and hierarchical clustering [Figures 5.5 & 5.6]. The results of the classifier suggest that despite the lack of clustering and the relatively small number of genes differentially regulated by p110 δ inactivation, it is possible to distinguish between genotypes. We reasoned that the three genes identified could, following further validation, be used as biomarkers for p110 δ inactivation.

5.6. Validation of the differential expression of genes in p110 delta KI macrophages

5.6.1. The necessity to validate relationships identified by genome-wide analysis

Affymetrix GeneChips®, alongside other microarrays are excellent tools for gaining a global perspective of the impact of a mutation or treatment on gene expression. Validation of the identified “hits” is usually considered to be necessary before any further conclusions can be confidently drawn. In particular, with regard to the

differential regulation of individual genes as a result of the investigated variable validation is important. To state with any confidence that the genes identified in our genome-wide analysis are genuinely differentially regulated in p110 δ KI macrophages we therefore needed to perform validation analyses.

5.6.2. Validation of differential expression using Low Density Taqman Array (LDA)

We chose to perform our validation using low density TaqMan[®] arrays (LDAs) [Materials and Methods]. LDAs allow semi-high throughput comparative expression analysis of up to twenty-eight genes (chosen by the end-user) across multiple samples simultaneously. Despite the semi-high throughput format the enhanced dynamic range of TaqMan compared to Affymetrix GeneChip[®] arrays is maintained. We had already identified three unique genes that were found by an unbiased computer algorithm to be representative of the p110 δ KI genotype [Figure 5.10]. We were keen to validate more than three genes as potential biomarkers and we therefore ranked all the unique probe sets found to be differentially regulated in p110 δ KI macrophages by 1 logFC or more ($p \leq 0.05$). Magnitude of deregulation, irrespective of the direction of change, was prioritised as larger differences in protein concentration will usually be easier to reliably detect and quantify. The list of fifteen genes/transcripts to validate based on this ranking included the two of the three genes identified by the classifier algorithm as most representative of the four categories [Table 5.5. & Figure 5.10]. The third gene identified by the classifier algorithm, *Paip1* was not available in the LDA format at the time we designed and ordered our LDA cards. We recognise that it would be of interest to validate this gene independently to confirm whether it is genuinely differentially regulated in p110 δ KI macrophages compared to their WT counterparts.

Gene symbol	Protein	Basal Fold Change (p110δ/WT)	logFC	adjp value
<i>Fblim1</i>	filamin binding LIM protein 1	-13.12	-3.71	1.36E-02
<i>Pdpn</i>	Podoplanin	-12.73	-3.63	2.14E-05
<i>Mthfr</i>	5,10-methylenetetrahydrofolate reductase	-6.39	-2.80	2.66E-05
<i>Ubiad1</i>	UbiA prenyltransferase domain containing 1	5.08	2.34	2.95E-04
<i>Rab6b</i>	RAB6B, member RAS oncogene family	-5.07	-2.37	2.14E-05
<i>Nin</i>	Ninein	4.98	2.32	2.14E-05
<i>Rex2</i>		4.54	2.16	9.93E-03
<i>Plod1</i>	procollagen-lysine,2-oxoglutarate 5-dioxygenase 1	-3.70	-1.89	5.93E-04
<i>Clstn1</i>	calsyntenin 1	3.33	1.74	7.60E-03
<i>Efhd2</i>	EF hand domain containing 2	-2.91	-1.54	7.10E-04
<i>Efcab7</i>	EF-hand calcium binding domain 7	-2.66	-1.41	7.10E-04
<i>Kif1b</i>	kinesin family member 1B	2.66	1.41	4.13E-05
<i>Fst</i>	Follistatin	2.47	1.31	1.07E-03
<i>Htatsf1</i>	HIV TAT specific factor 1	2.11	1.08	4.33E-02
<i>Ube4b</i>	ubiquitination factor E4B, UFD2 homolog (<i>S. cerevisiae</i>)	-1.80	-3.49	1.38E-04

Table 5.5 List of fifteen genes chosen for validation by LDA. The probe sets listed were chosen as candidates for further validation. The unique probe sets were ranked first, by magnitude of fold change and then secondarily to that by p value using Microsoft Office Excel software. Red represents an increase and green a decrease in expression in the p110δ KI macrophages compared to the WT macrophages. The two genes identified by classifier analysis that were also found to be expressed at the plasma membrane are highlighted in red.

5.6.2.1. Validation of differential regulation of chosen genes using additional samples

We reasoned that it was important to perform validation on fresh RNA samples, i.e. not the ones that were used for the original Affymetrix experiment. We therefore decided to perform validation on new samples from additional WT and p110 δ KI mice derived from the same colony as those mice used for the Affymetrix experiment. We reasoned that using additional samples would increase our confidence in any validation results and in the relationships between the identified genes and p110 δ [Table 5.6].

Assay	p110 δ KI mice	Mouse source	WT control mice	Mouse source
Affymetrix	RNA from four p110 δ KI mice	Source A [Lymphocyte Signalling and Developments Laboratory, Babraham Institute, Cambridge] <u>Colony:</u> homozygous x homozygous	RNA from four WT mice	Source A <u>Colony:</u> Separate WT x WT line originally derived from commercial breeder
LDA	RNA from three p110 δ KI mice & RNA set from Affymetrix assay	Source A <u>Colony:</u> homozygous x homozygous	RNA from three WT mice	Source A <u>Colony:</u> Separate WT x WT line

Table 5.6. Source of RNA and mice used for Affymetrix and LDA experiments. Mice were sourced from the Lymphocyte Signalling and Developments Laboratory, Babraham Institute, Cambridge. p110 δ KI mice were bred as a homozygous line and the WT control mice were obtained from a separate WT C57BL/6 line, which was started using mice obtained from a commercial breeder (Charles River).

We compared the genome-wide expression of the chosen fifteen genes in WT and p110 δ KI macrophages in the basal and the LPS-stimulated state using three new sets of samples [Table 5.6]. Alongside these, we included a set of the original Affymetrix samples to provide a reference point and gain information regarding the reproducibility of Affymetrix data by LDA TaqMan[®].

5.6.3. Validation confirmed differential regulation of seven genes in p110 δ KI macrophages

Using LDA comparative expression analysis we obtained quantitative data to substantiate the effect of p110 δ inactivation on the expression of seven of the fifteen genes tested. The data obtained for these genes and a summary of the data obtained by LDA is presented below [Figure 5.11].

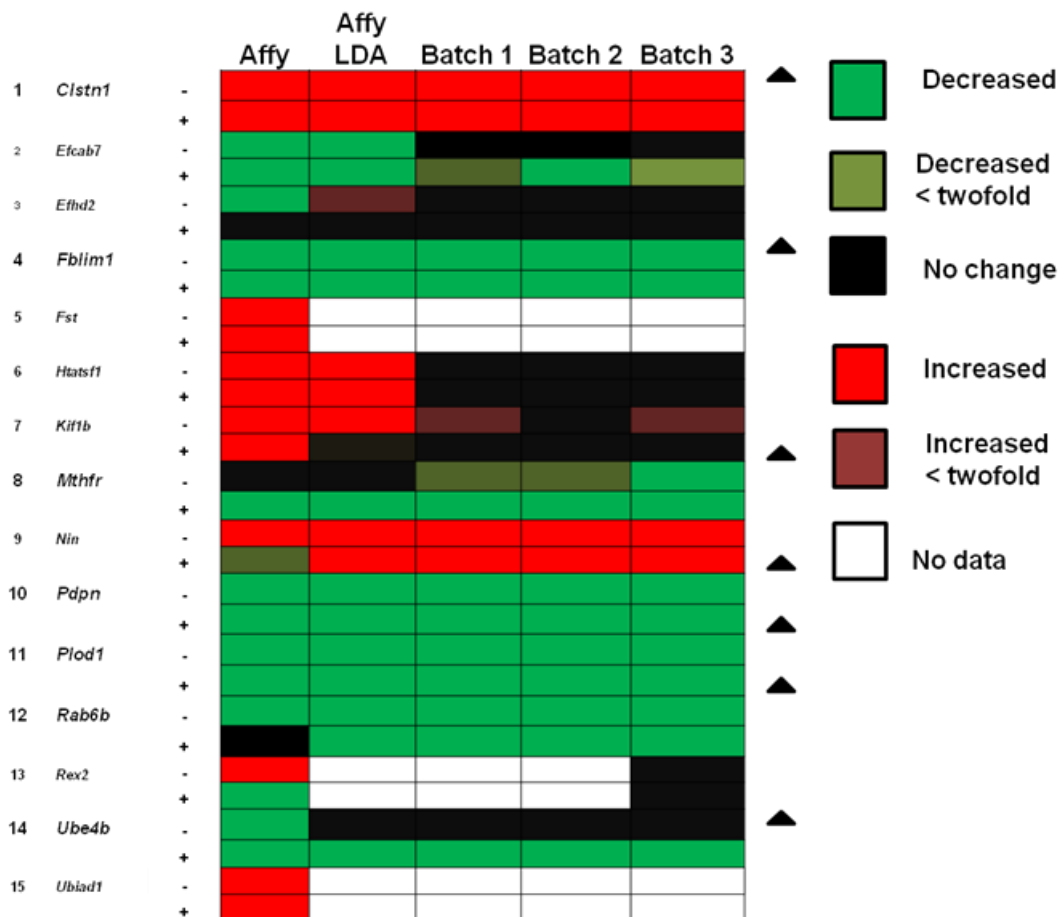


Figure 5.11. Heatmap of comparative gene expression data obtained by LDA and Affymetrix. LDA analysis of fifteen genes validated the effect of p110 δ inactivation on seven of the genes. The increased expression of *Clstn1* in p110 δ KI macrophages was confirmed. The decreased expression of *Clstn1*, *Fblim1*, *Mthfr*, *Pdpm*, *Plod1*, *Rab6b* and *Ube4b* in p110 δ KI macrophages was confirmed. Data qualitatively indicated that *Nin* expression was also decreased in p110 δ KI macrophages but quantitative data was not obtained due to variation between technical replicates.

5.6.3.1. The expression of *Pdpm1*, *Fblim1*, *Plod1* and *Rab6b* was decreased in p110 δ KI macrophages

The validation confirmed that the expression of *Pdpm*, *Fblim1*, *Plod1* and *Rab6b* was decreased in p110 δ KI macrophages [Figure 5.12]. Specifically, consistent with the data from the Affymetrix analysis we found that *Pdpm1* expression was reduced in

both the basal and LPS-stimulated p110 δ KI macrophages [Figure 5.12a]. The expression of *Fblim1* was decreased in both basal and LPS-stimulated macrophages, with a more substantial repression in the LPS-stimulated state [Figure 5.12b]. This result is consistent with the decreased expression of *Fblim1* identified in the basal and LPS-stimulated p110 δ KI macrophages in the original Affymetrix experiment [Table 5.3]. Furthermore, the same pattern of a more substantial decrease in the LPS-stimulated state (logFC -3.89) compared to in the basal state (logFC -2.95) was observed in the Affymetrix experiment [Table 5.3 & Figure 5.12].

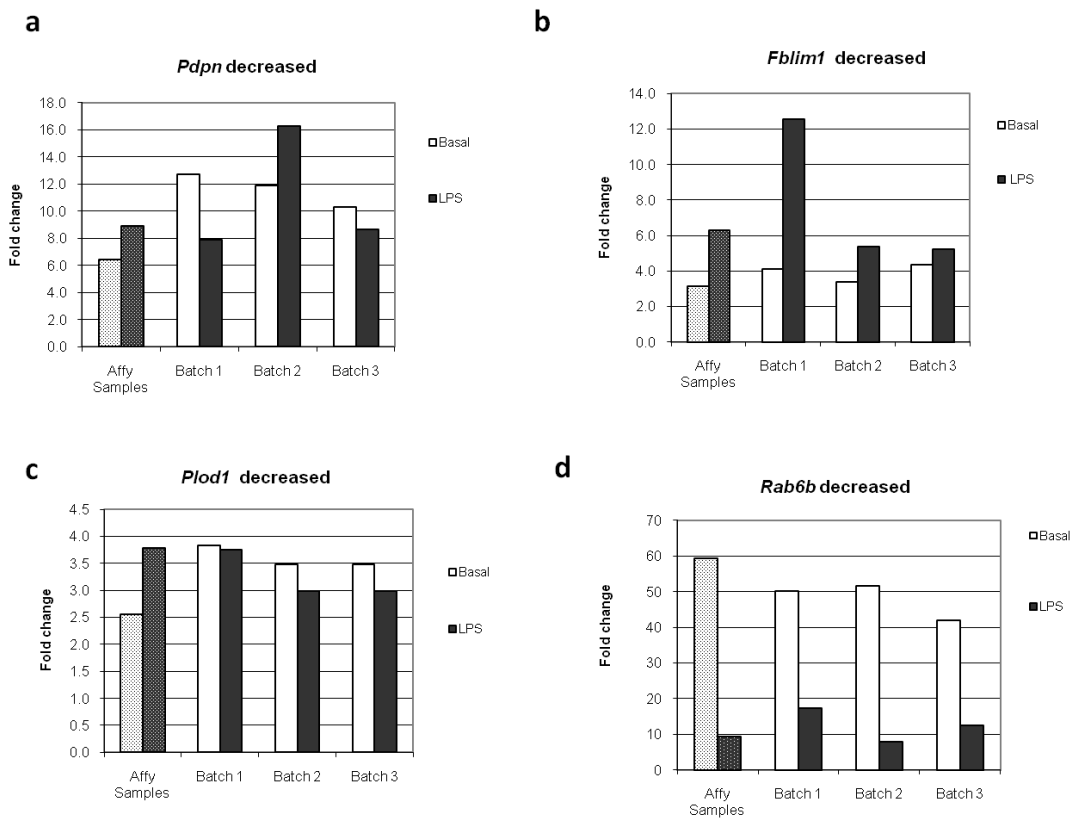


Figure 5.12. Expression of *Pdpn1*, *Fblim1*, *Plod1* and *Rab6b* was decreased in p110 δ KI macrophages. RNA samples derived from three batches of WT and p110 δ KI macrophages stimulated with control or LPS (1 μ g/ml) for 6 h and an additional set of samples from the original Affymetrix (Affy samples) experiment were analysed on a LDA microfluidics card to determine gene expression. Expression data were obtained using SDS RQ Manager Software. Data are presented as a ratio of the expression in the p110 δ KI macrophages to WT macrophages.

The data obtained regarding the expression of *Rab6b* in p110 δ KI macrophages confirmed that *Rab6b* expression is decreased in p110 δ KI basal macrophages and also revealed that the magnitude of change may be greater than was initially suggested by Affymetrix data. Additionally, these data revealed that *Rab6b* expression may also be affected to a lesser extent in LPS-stimulated than in p110 δ

KI basal macrophages. This difference in magnitude of change compared to the Affymetrix data and the observation of an effect in the LPS-stimulated state are both likely to be as a result of the enhanced sensitivity and dynamic range of TaqMan assays compared to Affymetrix GeneChips®. Together these results confirm our Affymetrix results and strongly suggest that p110δ activity positively regulates the expression of *Pdpm*, *Fblim1*, *Plod1* and *Rab6b* in macrophages.

5.6.3.2. Expression of *Clstn1* was increased in basal and LPS-stimulated p110δ KI macrophages

Our validation has confirmed the increased expression of *Clstn1* in p110δ KI macrophages in the basal state that was observed in the Affymetrix experiment [Figure 5.13]. In the Affymetrix experiment we identified *Clstn1* as differentially regulated in basal but not LPS-stimulated p110δ KI macrophages. This data is therefore consistent with the original Affymetrix data. We noticed that there was also an increase in the LPS-induced state in all samples tested including those from the original Affymetrix experiment [Figure 5.13 & 5.15]. Therefore, the increased expression of *Clstn1* may also occur in LPS-stimulated p110δ KI macrophages but to a lesser extent [Figure 5.13]. As with the detection of differential regulation of *Rab6b* in LPS-stimulated p110δ KI macrophages, we suggest that this difference to the Affymetrix data reflects the enhanced sensitivity of qPCR compared to Affymetrix microarrays.

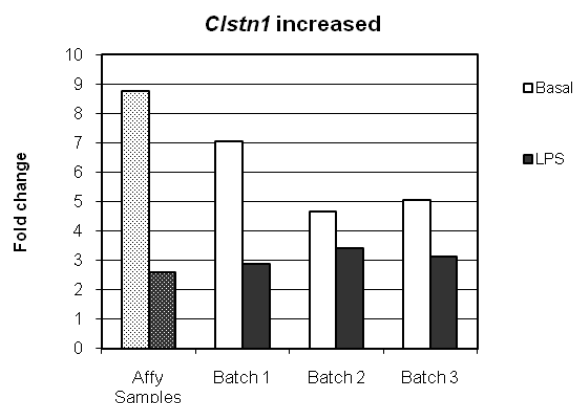


Figure 5.13. Expression of *Clstn* was increased in basal and to a lesser extent LPS-stimulated p110δ KI macrophages. RNA samples derived from three batches of WT and p110δ KI macrophages stimulated with control or LPS (1 µg/ml) for 6 h and an additional set of samples from the original Affymetrix (Affy samples) experiment were analysed on a LDA microfluidics card

to determine gene expression. Expression data was obtained using SDS RQ Manager Software. Data are presented as a ratio of the expression in the p110 δ KI macrophages to WT macrophages.

5.6.3.3. Expression of *Mthfr* and *Ube4b* was decreased in LPS-stimulated p110 δ KI macrophages

Our validation study also confirmed that both *Mthfr* and *Ube4b* were unaffected in basal p110 δ KI macrophages but were decreased in LPS-stimulated p110 δ KI macrophages [Figure 5.14]. In fact in both cases there does seem to be a minimal effect in the basal state but this is below the threshold of twofold (1 log FC) [Figure 5.14]. These data together with the original Affymetrix data suggest that p110 δ activity may be required for the LPS-induced expression of *Mthfr* and *Ube4b* in macrophages.

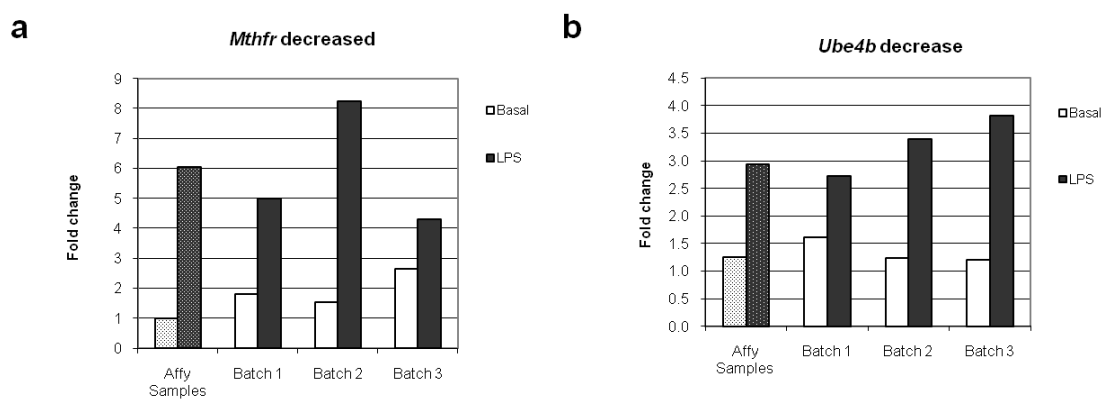


Figure 5.14. Expression of *Mthfr* and *Ube4b* was decreased in LPS-stimulated p110 δ KI macrophages. **a.** RNA samples derived from three batches of WT and p110 δ KI macrophages stimulated with control or LPS (1 μ g/ml) for 6 h and an additional set of samples from the original Affymetrix (Affy samples) experiment were analysed on a LDA microfluidics card to determine comparative expression of *Mthfr*. Expression data were obtained using SDS RQ Manager Software. Data are presented as a ratio of the expression in the p110 δ KI macrophages to WT macrophages. **b.** Samples were prepared and analysed as described in **a.** to determine comparative expression of *Ube4b*.

5.6.6.3. The differential expression of *Nin* in p110 δ KI macrophages was not confirmed

The data obtained regarding the expression of *Nin* were inconclusive. We did not perform fold change calculations on the data obtained for the expression of this gene as the C_T values were not sufficiently tight across the three technical replicates. We suspect this is as a result of very low expression of this gene, which was outside of the range of accurate quantification by TaqMan. Nevertheless, the

raw C_T values provided some qualitative evidence that the expression of this gene may be affected by p110 δ inactivation [Table 5.7].


Stimulation	WT sample	WT C_T	p110 δ KI sample	p110 δ KI C_T
Control	Affymetrix 5	35.02	Affymetrix 11	30.31
Control	Affymetrix 5	36.48	Affymetrix 11	33.27
Control	Affymetrix 5	33.13	Affymetrix 11	33.54
LPS	Affymetrix 6	32.3	Affymetrix 12	33.51
LPS	Affymetrix 6	32.90	Affymetrix 12	37.55
LPS	Affymetrix 6	39.35	Affymetrix 12	33.24
Control	WT 1	32.94	p110 δ KI 1	33.17
Control	WT 1	34.14	p110 δ KI 1	35.94
Control	WT 1	29.41	p110 δ KI 1	36.37
LPS	WT 1	30.85	p110 δ KI 1	33.78
LPS	WT 1	Undetermined	p110 δ KI 1	35.64
LPS	WT 1	35.05	p110 δ KI 1	33.56
Control	WT 2	32.67	p110 δ KI 2	32.58
Control	WT 2	28.96	p110 δ KI 2	34.26
Control	WT 2	32.61	p110 δ KI 2	32.41
LPS	WT 2	29.80	p110 δ KI 2	32.37
LPS	WT 2	31.68	p110 δ KI 2	35.82
LPS	WT 2	35.16	p110 δ KI 2	33.80
Control	WT 3	31.49	p110 δ KI 3	32.11
Control	WT 3	30.58	p110 δ KI 3	33.07
Control	WT 3	31.64	p110 δ KI 3	35.70
LPS	WT 3	30.53	p110 δ KI 3	34.22
LPS	WT 3	35.29	p110 δ KI 3	35.84
LPS	WT 3	31.21	p110 δ KI 3	37.37


Table 5.7 Raw C_T values obtained for *Nin* expression in Wt and p110 δ KI macrophages. Raw C_T values were obtained for the expression in *Nin* in four Wt basal sample, four WT LPS-stimulated samples alongside four p110 δ KI basal and p110 δ KI LPS-stimulated samples. The C_T values were all “flagged” by the SDS RQ software indicating that they should not be used for data analysis.


5.6.4. Summary of validation findings

In summary, we have confirmed that the expression of seven genes was differentially regulated in p110 δ KI macrophages in the same manner as observed in our Affymetrix study [Figure 5.15]. The expression of *Clstn1* was increased in p110 δ KI macrophages in the basal state and to a lesser extent in the LPS-stimulated state [Figure 5.13 & 5.15]. *Fblim1*, *Pdpn*, *Plod1*, and *Rab6b* were found to be decreased in both basal and LPS-stimulated macrophages [Figure 5.12 & 5.15]. Two of the genes, *Ube4b* and *Mthfr* were found to be affected by p110 δ inactivation only in LPS-stimulated cells, suggesting p110 δ activity may contribute to the induction of these genes by LPS [Figure 5.14 & 5.15].

	Affy		Affy			
	Affy		LDA	B1	B2	B3
<i>Clstn1</i>	3.6	-	8.8	7.0	4.7	5.1
			2.6	2.9	3.4	3.1
<i>Fblim1</i>	7.6	-	3.2	4.1	3.4	4.4
	13.1	+	6.30	12.6	5.4	5.2
<i>Mthfr</i>				1.8	1.5	2.6
	6.4	+	6.1	5.0	8.2	4.3
<i>Pdpn</i>	12.7	-	6.4	12.7	11.9	10.3
	10.0	+	8.9	7.9	16.2	8.6
<i>Plod1</i>	3.8	-	2.6	3.8	3.6	3.5
	4.2	+	3.8	3.8	2.5	3.0
<i>Rab6b</i>	5.1	-	60.3	50.2	51.9	41.6
			10.2	18.1	8.7	12.3
<i>Ube4b</i>	2.8	-				
	2.9	+	2.9	2.7	3.4	3.8

 Decreased

 Increased

 Decreased < twofold


 No change

Figure 5.15. Heatmap summary of the validation of the differential regulation of seven genes p110 δ KI macrophages compared to in WT macrophages in basal (-) and LPS-stimulated (+) conditions. Data obtained by LDA confirmed the differential expression of seven genes (*Clstn1*, *Fblim1*, *Mthfr*, *Pdpn*, *Plod1*, *Rab6b* and *Ube4b*) in p110 δ KI macrophages compared to their WT counterparts.

5.7. Validation of p110 delta-regulated gene expression at the protein level

We decided to focus our attention on the relationship between *Rab6b* expression and p110 δ activity for a number of reasons. First, there is a correlation between the highly restricted tissue distributions of *Rab6b* and of *PIK3CD* expression. *Rab6b* is reported to be highly expressed in the brain and is apparently absent or minimally expressed in other major organs [172]. Besides from in brain tissue, *Rab6b* cDNA was found to be abundant in human melanocytes suggesting it may be highly expressed in these cells [172-173]. Likewise, p110 δ is also expressed in both melanocytes and neurons [15-16]. In addition, the SK-N-SH neuroblastoma cell line that Fransen's group found is also highly enriched with *Rab6b* mRNA also expresses significant levels of p110 δ [172]. In fact, melanocytes and brain cells are two of the non-immunological cell types in which p110 δ is expressed at detectable levels. A second reason that we chose to focus on *Rab6b* was that at the time we obtained our LDA validation results, an independent laboratory identified *Rab6b* as a gene affected by p110 δ inactivation [50]. The authors identified reduced expression of *Rab6b* in p110 δ KI Tregs in a genome-wide expression analysis [50].

There was a final compelling reason that directed us to focus on the link between p110 δ activity and *Rab6b* expression as opposed to following up one of the genes we have highlighted as promising biomarker candidates. We had significant reason to believe that unlike the majority of the genes that we had validated with regards to their differential expression in p110 δ KI macrophages, *Rab6b* may be genuinely affected by the loss of p110 δ activity. The evidence leading us to doubt the genuine effect of inactivation of p110 δ on the expression of the other genes but not *Rab6b* are discussed in detail in the subsequent chapter. Here we simply state that we discovered that the majority of the genes identified are located within very close proximity (within or next to) of the locus where the *Pik3cd* gene encoding p110 δ is located, whilst *Rab6b* is encoded on a separate chromosome. The potential implications of this finding are the discussed alongside its discovering in the following chapter.

5.7.1. Rab6b protein was reduced in p110 δ KI macrophages

There were no published data regarding the expression of *Rab6b* in leukocytes and so our first task was simply to confirm whether rab6b protein is expressed at detectable levels in macrophages. We used a commercially available antibody that the manufacturers claimed is specific to rab6b. Using the antibody we were able to detect a band at the appropriate molecular weight in macrophage lysates [data not shown]. We subsequently compared the levels of rab6b in WT and p110 δ KI macrophages derived from three mice per genotype, and we found it was consistently decreased in the later genotype [Figure 5.16]. This result is consistent with both our Affymetrix and subsequent LDA data, which indicated that *Rab6b* expression was reduced in p110 δ KI macrophages. Moreover, we have shown that this decrease in gene expression translates into a significant decrease in protein expression. We included both basal and LPS-stimulated samples and found that that LPS-stimulation had no impact upon the expression of *Rab6b* [Figure 5.16]. We also probed the membrane for rab6a and found it was expressed at similar levels in both WT and p110 δ KI macrophages [Figure 5.16]. These results strongly suggest that in primary murine macrophages p110 δ regulates *Rab6b* expression and does not affect *Rab6a* expression.

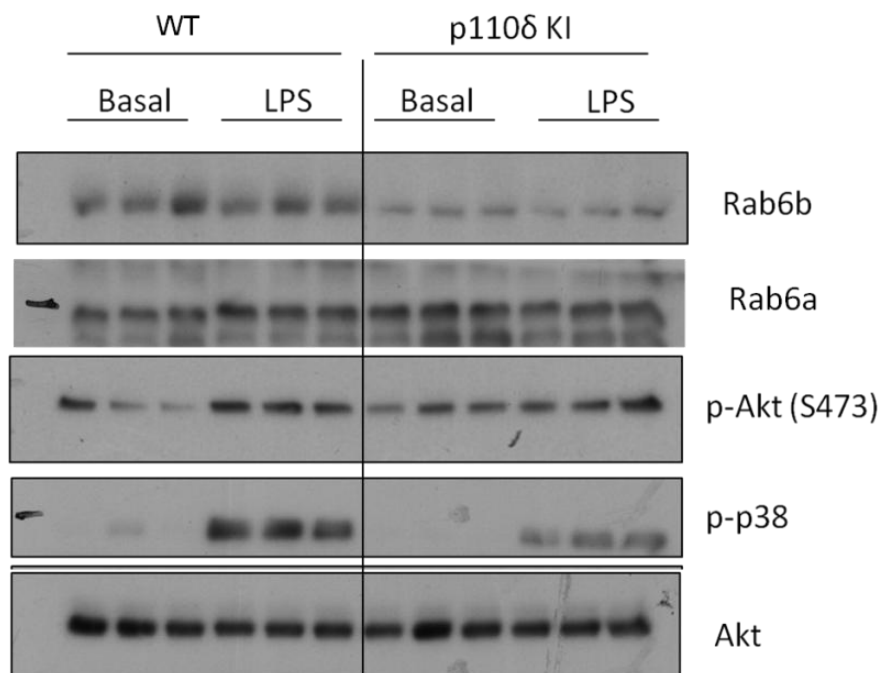


Figure 5.16. Decreased expression of rab6b protein in p110 δ KI macrophages compared to WT macrophages. Primary macrophages were plated in complete medium containing CSF-1. The following day the cells were stimulated with LPS for 30 min and cell lysates were extracted and immunoblotting was used to measure the indicated proteins.

We note that the decrease in rab6b in p110 δ KI samples was consistent, irrespective of the p-Akt level. The level of p-Akt in the p110 δ KI macrophages does not appear to be reduced. In fact, the trend in the three samples was towards increased p-Akt in p110 δ KI macrophages compared to the WT samples in the basal state. This is not consistent with previous publications in which p-Akt levels have been shown to be lower in p110 δ KI macrophages but all previous data that we are aware of was gained from macrophages deprived of CSF-1 for 12-24 h [1, 79]. In this experiment and all our other experiments with primary macrophages we have used normal growth conditions including CSF-1. We did note that in the p110 δ KI macrophages the induction of p-Akt in response to LPS appears to be less substantial than in the WT macrophages [Figure 5.16]. We also noted that in this experiment, the LPS-stimulated induction of p-p38 in the p110 δ KI macrophages was significantly repressed [Figure 5.16]. This reduction in LPS-induced p-p38 in p110 δ KI macrophages has previously been observed by another member of our laboratory in CSF-1-deprived macrophages [174]. In our experiments using immortalised macrophage cell lines we consistently observed that p110 δ -selective inhibition did not affect LPS-induced p-p38 [Chapter 4, Figure 4.1].

5.7.2. Normal expression of rab6b protein in whole brain tissue derived from p110 δ KI mice

As stated above rab6b was initially reported as a brain-specific rab6 isoform [172] and p110 δ is expressed in neurons[15]. We were therefore interested to determine whether brain tissue derived from p110 δ KI mice would express reduced levels of rab6b. We compared the expression of rab6b in brain tissue from three p110 δ KI mice and three WT mice. We probed for the expression of Rab6b and p110 δ as well as p-Akt. The results firstly confirm that rab6b is highly expressed in brain tissue as published by Opdam *et al.* [172][Figure 5.17]. Interestingly, we found that the expression of rab6b was unaffected in the p110 δ KI brain samples [Figure 5.17]. The p-Akt in the WT and p110 δ KI brain samples also appears to be consistent [Figure 5.17].

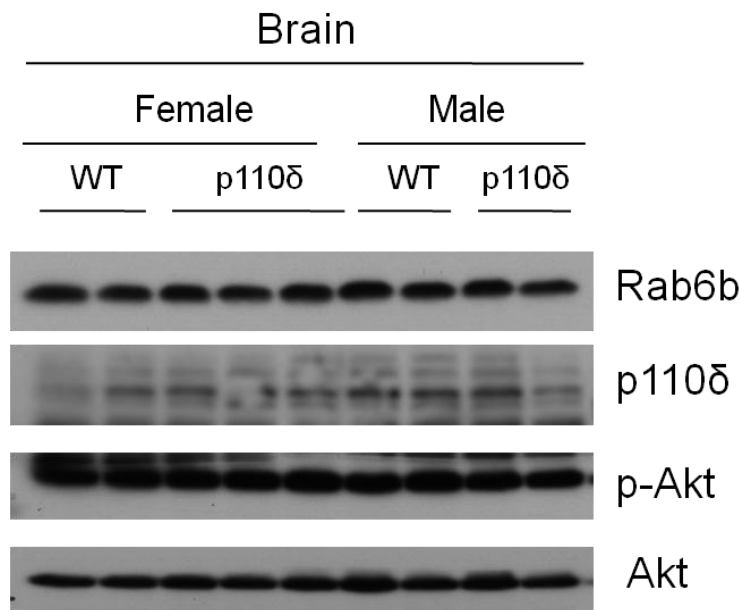


Figure 5.17. Expression of rab6b is unaffected in p110 δ KI brain tissue compared to expression in WT brain tissue. Brains were removed from culled mice and washed with PBS to remove excess blood before being immediately lysed in ice-cold lysis buffer. The expression of the indicated proteins was measured in the lysates using immunoblotting.

The normal expression of *Rab6b* in p110 δ KI whole brain suggests that our theory that the highly restricted *Rab6b* tissue expression that correlated with p110 δ expression could be regulated by p110 δ activity is incorrect. It instead points us towards a hypothesis that the regulation of Rab6b expression by p110 δ is leukocyte-specific. Interestingly one of the brain cell types in which rab6b is reported to be highly expressed was microglial cells. Microglial cells are in fact tissue-specific resident macrophages that are derived from leukocyte precursors. It would be interesting to assess whether p110 δ KI microglial cells express reduced levels of Rab6b, or whether other leukocytes from p110 δ KI mice express less *Rab6b*.

Indeed, shortly after we completed our LDA validation of our Affymetrix results another group published a study linking p110 δ inactivation to reduced levels of Rab6b. Patton *et al.* compared the genome-wide expression of p110 δ KI Tregs to WT Tregs and identified differential expression of 125 genes (1 logFC, $p \leq 0.01$) including *Rab6b*, which was decreased in the p110 δ KI Tregs [50]. Patton *et al.* did not confirm that this decreased expression of Rab6b translated into reduced rab6b protein [50]. Together the results of this publication and our data on *Rab6b* strongly support a role for p110 δ in the positive regulation of *Rab6b* expression in leukocytes.

5.7.3. Validation of the specificity of the commercial rab6b-specific antibody

Whilst rab6a is ubiquitously expressed, rab6b is reported to be highly expressed in brain but with no detectable expression in the liver amongst other tissues. At the time we took brains for the previous experiment we also removed livers from the mice. We therefore reasoned that if the rab6b-specific antibody is indeed specific to rab6b then we would observe a strong signal in brain but not in liver. We also probed for p110 δ which is also expressed in brain tissue but not in livers as a control and found higher p110 δ expression in the brain samples than the liver samples [Figure 5.18]. The rab6b antibody detected a strong signal in the brain and but detected no signal in the liver cells [Figure 5.18]. These results support the manufacturer's claims regarding the specificity of this antibody for rab6b and not rab6a [Figure 5.18]. These results do strongly support the specificity of the rab6b antibody but ideally we would confirm its specificity by testing its ability to detect recombinant rab6b and rab6a protein.

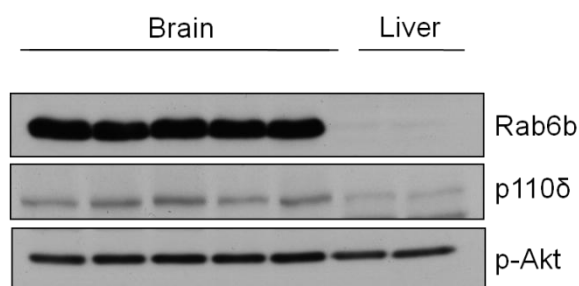


Figure 5.18 The Rab6b-selective antibody detects a signal in murine brain tissue but not liver tissue. Brain tissue was lysed as described in Figure 5.17 and livers were extracted and processed in the same way as the brains. The expression of rab6b, p110 δ and p-Akt in the samples was compared by immunoblotting.

5.8. Conclusion

Our genome-wide expression analysis of p110 δ KI macrophages compared to WT macrophages identified only twenty-five differentially regulated unique probe sets in the former cells. Specifically our Affymetrix data revealed that seventeen probe sets, interrogating fourteen known genes were differentially regulated in basal growing p110 δ KI macrophages compared to their counterparts. In LPS-stimulated p110 δ KI macrophages twenty probe sets were differentially regulated,

of which twelve were common to those affected in the basal state. This represents less than 0.1% of the genome and furthermore, a number of these genes are likely to represent false positives and therefore it is apparent that the role of p110 δ in the regulation of macrophage gene expression is restricted to a small number of genes. Even after LPS-stimulation only eight additional genes are regulated by p110 δ . This suggests that p110 δ plays a minimal role in the induction of transcriptional changes in response to LPS in macrophages. Yet, in fact we cannot conclude from this data that p110 δ plays a minimal role in LPS-stimulated gene regulation as we have merely taken a snapshot of the LPS-induced responses. It is possible that at either an earlier or a later time point after LPS-stimulation a much larger number of genes are affected by p110 δ inactivation. The role of p110 δ in LPS-driven responses was not our focus but if this had been our primary interest a time course experiment might be most suitable.

We have identified more than 100 less probe sets differentially regulation in p110 δ KI macrophages compared to the number the Okkenhaug group identified in p110 δ KI Tregs [50]. This could imply that p110 δ activity is less important in macrophages than it is in adaptive immune cells such as Tregs. Such theories would need further data analysis as the experiments were performed separately and the protocols used may not have been similar. Ideally a comparison across experiments requires normalisation across all chips and adjustment for inter-experiment batch effects [175].

The most relevant network identified by IPA which relates to three key functions integral to immune function (Inflammatory response, antimicrobial response and cell-to-cell contacts) is consistent with what is known about the impact of p110 δ loss on *in vivo* or *in vitro* immunity. Having said that, we did not identify any “classic inflammatory” genes and we identified just eight genes that were specifically affected by p110 δ activity downstream of LPS in the genome-wide expression analysis. We have confirmed that *Ube4b* and *Mthfr* expression are repressed in specifically in p110 δ KI macrophages stimulated with LPS and therefore it would be interesting to learn more about how this might impact upon LPS-driven responses.

We have found that the expression of *Rab6b* is reduced in p110 δ KI macrophages by Affymetrix and subsequently confirmed this finding in an additional set of RNA

using Taqman[®] LDAs. Importantly, we have confirmed that this differential expression translates to reduced levels of rab6b protein in p110 δ KI macrophages [Figure 5.16]. The fact that we and another independent group have both identified *Rab6b* downstream of p110 δ inactivation in primary leukocytes strongly supports our findings. We have also expanded on this finding by investigating the effect of the p110 δ KI mutation on the expression of rab6b in the brain, where it was reported to be highly enriched. Our data indicated that rab6b expression is unaffected in p110 δ KI brain tissue. We suggest based on these data that p110 δ may regulate *Rab6b* expression in a leukocyte specific manner.

There was no overlap between the genes affected by p110 δ inactivation in these primary macrophages and in our pilot study using RAW 264.7 macrophages. We were aware that there were two variables that might be responsible for this difference. First, this is a comparison between primary macrophages and a transformed macrophage cell line. Secondly, the method of p110 δ inactivation was different as in the RAW 264.7 study, p110 δ was inhibited using a selective p110 δ -inhibitor, whilst in this study p110 δ was genetically inactivated. In theory, the p110 δ KI mutation should have a very similar effect as pharmaceutical inactivation. We were curious to note that substantially more genes were found to be differentially regulated by p110 δ inactivated RAW 264.7 macrophages than in primary p110 δ KI macrophages. This is perhaps the converse of what we might have predicted based on data regarding the decreased dependence of macrophage cell lines on p110 δ activity at the signalling level. On the other hand, IC87114 may have off-target effects which could account for a number of the gene expression changes. We also must bear in mind that after the removal of outliers the RAW 264.7 macrophage pilot study was performed on just two samples per condition. This makes the results less reliable, and may have increased the number of genes that reached the statistical stringency threshold that we set, thereby increasing the number of false positives. Therefore, the difference in number of genes identified in RAW 264.7 macrophages chronically treated with IC87114 compared to those identified in the p110 δ KI macrophages should be treated with caution and no conclusions can reliably be drawn on this point. What we can perhaps say with greater confidence is that the genes identified as differentially regulated in p110 δ KI macrophages are not differentially regulated in RAW 264.7 macrophages chronically treated with a p110 δ -selective inhibitor. To be certain of this

conclusion we would need to confirm this with an additional batch of RAW 264.7 macrophages chronically treated with IC87114.

CHAPTER 6

6. INVESTIGATING THE EFFECTS OF PHARMACOLOGICAL INACTIVATION OF P110 DELTA ON THE PRIMARY MACROPHAGE TRANSCRIPTOME

6.1. Introduction

We chose to continue to pursue our objective of identifying potential biomarkers of p110 δ inactivation. We therefore decided to set aside the results of the pilot study and proceeded by determining which genes are differentially regulated in primary macrophages chronically treated with IC87114. We hoped that some of the genes identified in the p110 δ KI macrophages would also be affected in primary macrophages chronically treated with IC87114.

6.2. The effect of IC87114 treatment on Akt activation

Before proceeding with the microarray we confirmed that basal and LPS-induced p-Akt was indeed repressed by IC87114 in primary macrophages. Our results indicate a roughly twofold decrease in the p-Akt in both conditions [Figure 6.1].

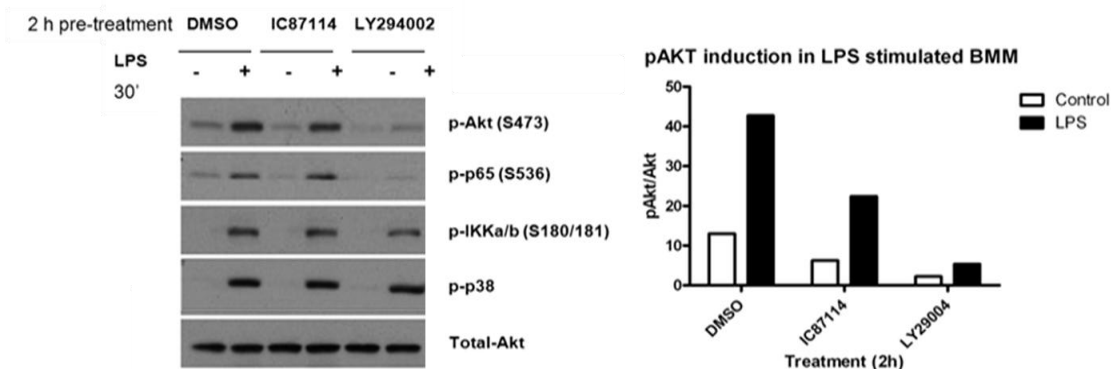


Figure 6.1. p110 δ -selective inhibition reduced basal and LPS-induced p-Akt. WT primary macrophages were plated in complete media containing 10% FBS and CSF-1 (20 ng/ml). The following day the cells were pre-treated with p110 δ -selective IC87114 (1 μ M), pan-PI3K inhibitor

LY294002 (5 μ M) or DMSO control for 2 h prior to 30' stimulation with LPS (1 μ g/ml). Lysates were analysed for the indicated antibodies using standard immunoblotting techniques.

6.2.1. Activation of Akt in macrophages differentiated in the presence of IC87114

We decided to compare the expression of macrophages that had been differentiated in the presence of IC87114 to those differentiated in the presence of DMSO. In doing so, we aimed to mimic the p110 δ null conditions during that exist during the differentiation period of p110 δ KI macrophages. As with the longer term inhibition used in the RAW 264.7 study, we felt that this was also more relevant to clinical use of p110 δ inhibitors than a brief post-differentiation treatment. We therefore assessed the levels of p-Akt in primary macrophages after differentiation in the presence of DMSO or IC87114, compared to macrophages treated with IC87114 or LY294002 for 2 h or 24 h [Figure 6.2].

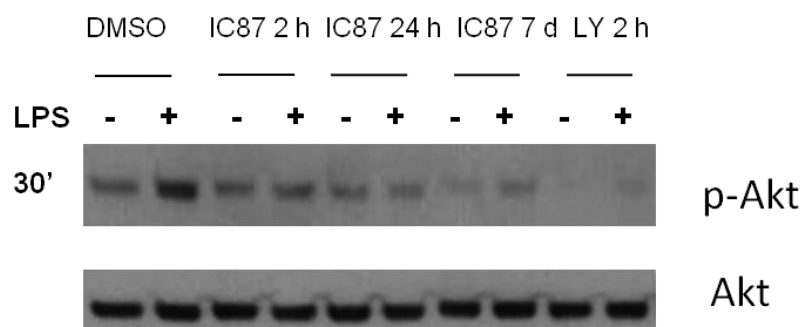


Figure 6.2. Long-term pharmacological inactivation of p110 δ in WT macrophages represses p-Akt. WT primary macrophages were extracted and cultured in the presence of DMSO or p110 δ -selective IC87114 (1 μ M) for the duration of the differentiation period (7 d). The cells were plated on day seven in complete medium containing 10% FBS and CSF-1 (20 ng/ml) and pre-treated with the indicated inhibitors. 24 h later the cells were stimulated with LPS (1 μ g/ml) for 30 min and cell lysates were obtained and analysed for the indicated proteins using immunoblotting.

6.3. Genome-wide expression analysis experimental design and implementation

We decided to obtain genome-wide expression data for WT macrophages that had been differentiated and cultured in the presence of either IC87114 (1 μ M) or DMSO for the duration of the differentiation period and during the final experiment [Figure 6.3]. As with the previous microarray experiment, we treated the two

groups with either control or LPS for 6 h prior to extracting total RNA for microarray analysis [Figure 6.3].

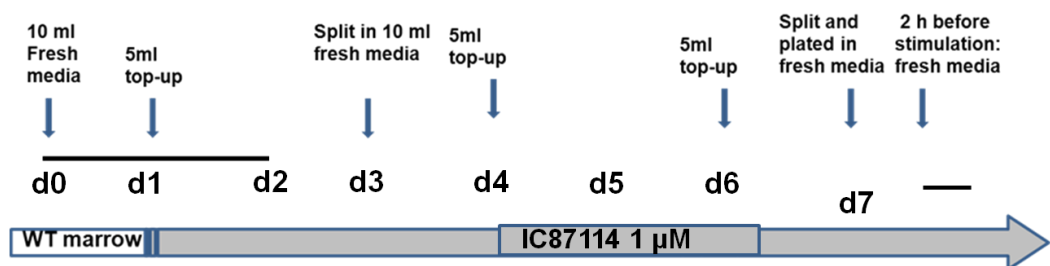


Figure 6.3. Schematic of the differentiation of WT macrophages in the presence of IC87114 or DMSO. Bone marrow derived macrophage precursor cells were extracted from WT mice and cultured in medium containing a starting concentration of p110 δ -selective 1 μ M IC87114. Plates were topped up with 5 ml of complete medium containing 10% FBS, CSF-1 (20-30 ng/ml) and IC87114 (1 μ M) on day 1 (d1), day 4 (d4) and day 6 (d6). The plates were split as per the modified protocol on day 3 (d3) and cells were replated in fresh complete medium containing 10% FBS, CSF-1 (20-30 ng/ml) and IC87114 (1 μ M).

6.4. Investigating the genome-wide expression impact of IC87114 treatment

6.4.1. Extraction of raw expression data and normalisation

The samples were analysed as described in Chapters 4 and 5. Briefly, labelled fragmented RNA samples were hybridised to GeneChips[®] before staining. Subsequently fluorescence data was obtained and extracted and processed to obtain raw expression values. The raw data was then extracted on our behalf by Dr H. Edwards, Dr P. Hales and Ms E. Gadaleta. Briefly the dataset was normalised using the standard GC-RMA normalisation algorithm and data for the top 10,000 most variable probe sets was then extracted.

6.4.2. Multivariate Analysis to determine sample clusters

First, we performed PCA, which indicated that the major differential factor in the data set was the treatment of LPS, as was the case with the p110 δ KI compared to WT study [Figure 6.4]. More in-depth analysis revealed that the samples did not cluster according to p110 δ activity status (IC87114 *versus* DMSO).

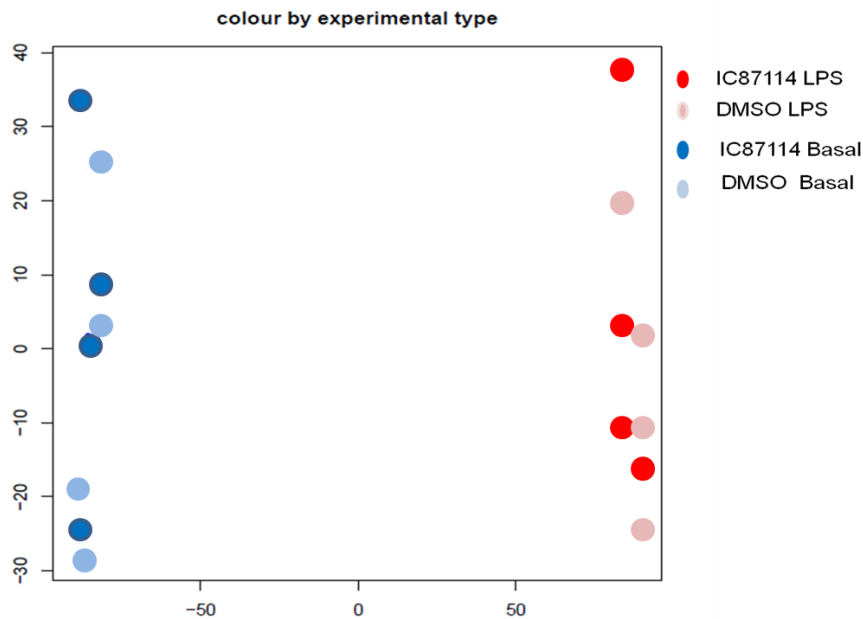


Figure 6.4. PCA analysis revealed samples clustered according to LPS stimulation status rather than genotype. PCA was performed on expression data to determine separation of samples. Samples separated according to stimulation status (unstimulated or LPS-stimulated but not according to genotype (WT or p110 δ KI).

6.4.3. The expression of the classifier probe sets was not sufficient to identify inactivation of p110 δ

The best way to confirm the validity of the set of computer-identified classifiers found to be most representative of the p110 δ KI state is to test the algorithms ability to assign a new data set to the appropriate categories. We were interested to find out whether the classifier algorithm would assign the IC87114-treated samples as p110 δ KI and the DMSO samples as WT. In fact, with the help of Dr P. Hales we found that the algorithm failed to assign the samples to the “correct” categories and assigned all samples to the WT genotype. The classifier set was sufficient to correctly identify whether or not samples were treated with LPS [Figure 6.5].

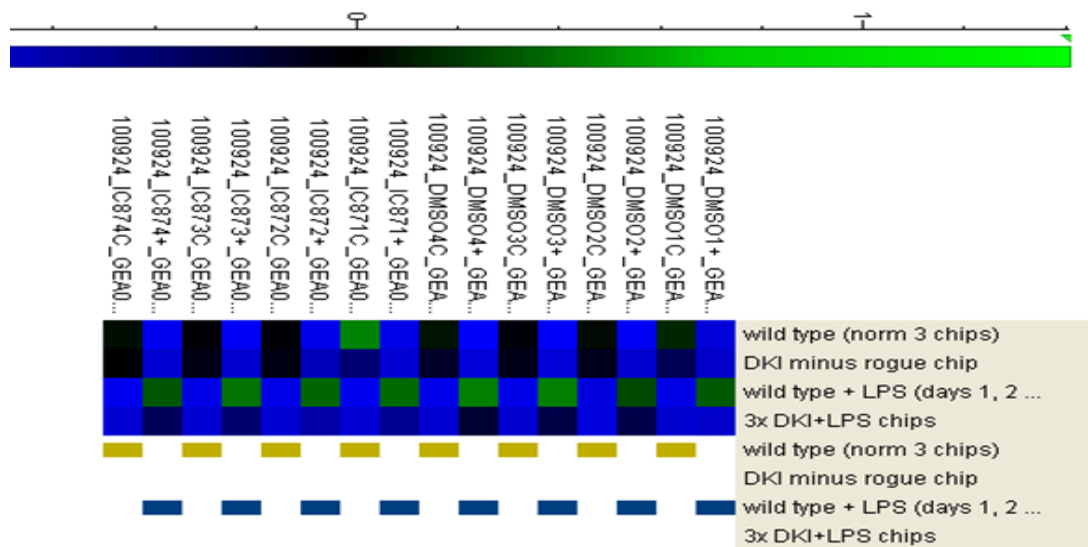


Figure 6.5. The classifier probe set produced by analysis of p110δ KI versus WT study did not classify WT IC87114 samples as p110δ KI. The data from the WT IC87114 study was entered ungrouped into the programme and the algorithm failed to assign the IC87114-treated samples to the p110δ KI group based on the expression of the six classifier probe sets.

6.4.4. Identification of genes differentially regulated in WT macrophages differentiated in IC87114

We next extracted a list of probe sets affected by differentiation in the presence of IC87114 in basal and or LPS-stimulated conditions with the help of Dr H. Edwards. Eight probe sets, or seven interrogating known genes, were differentially expressed in basal WT macrophages differentiated in the presence of IC87114 compared to in DMSO [Table 6.1]. In the LPS-stimulated state, just three probe sets were differentially regulated, interrogating two genes and one RIKEN sequence. The genes affected in the LPS and basal states were all different [Table 6.2].

Probe Set ID	Gene Symbol	Protein	Basal	
			logFC	adjP value
1418057_at	Tiam1	T-cell lymphoma invasion and metastasis 1	-1.448	2.02E-02
1456212_x_at	Socs3	suppressor of cytokine signaling 3	1.421	2.29E-02
1424727_at	Ccr5	chemokine (C-C motif) receptor 5	-1.367	4.54E-02
1424896_at	Grp85	G protein-coupled receptor 85	-1.363	2.29E-02
1426278_at	Ifi2712a	interferon, alpha-inducible protein 27 like 2A	-1.202	4.54E-02
1415949_at	NA	NA	-1.156	4.54E-02
1449799_s_at	Pkp2	plakophilin 2	-1.090	4.54E-02
1428663_at	Sgms2	sphingomyelin synthase 2	1.019	4.54E-02

Table 6.1. Probe sets differentially expressed in basal WT macrophages differentiated and cultured in the presence of IC87114. Genes are ranked according to magnitude of deregulation, known genes are highlighted in bold and genes increased or decreased in p110 δ KI macrophages are highlighted in red or green respectively.

Probe Set ID	Gene Symbol	Protein	LPS-stimulated	
			logFC	adjP value
1440047_at	Socs1	suppressor of cytokine signaling 1	-1.038	3.43E-03
1456509_at	1110032F04Rik	RIKEN cDNA 1110032F04 gene	-1.142	4.94E-02
1451322_at	Cmb1	carboxymethylenebutenolidase-like (Pseudomonas)	-1.462	3.82E-02

Table 6.2. Probe sets differentially regulated in LPS-stimulated WT macrophages differentiated and cultured in the presence of IC87114. Genes are ranked according to magnitude of deregulation and known genes are highlighted in bold and genes increased or decreased in p110 δ KI macrophages are highlighted in red or green respectively.

6.5. Comparison of pharmacological and genetic inactivation of p110 delta

We subsequently compared these lists to the list of probe sets found to be differentially regulated in p110 δ KI macrophages and were surprised to find that there was no overlap. The genes identified as differentially regulated in WT macrophages differentiated in IC87114 were not differentially regulated in p110 δ KI macrophages. Furthermore, the genes were also entirely dissimilar to those affected by IC87114-treatment in RAW 264.7 macrophages. We decided to attempt to investigate the unexpected finding that the genes identified in the two primary macrophages do not overlap with each other or with those identified in the pilot study using RAW 264.7 macrophages.

6.5.1. The genes differentially regulated in p110 δ KI macrophages were not affected by IC87114

We reasoned that when using the more sensitive TaqMan-based LDA cards we might observe some impact of IC87114 on the genes affected in p110 δ KI macrophages. We therefore obtained comparative expression data for the fifteen p110 δ KI validation genes [Chapter 5, Table 5.5] in WT macrophages differentiated in IC87114 (WT-IC87114) compared to those differentiated in DMSO (WT-DMSO). In fact, the results confirmed the Affymetrix results; these fifteen genes are not differentially regulated in WT-IC87114 macrophages [Data not shown]. These data are consistent with the results of the two Affymetrix arrays and thus, allow us to confirm with a greater degree of certainty, that the effects of genetic and pharmacological inactivation on macrophage transcription are distinct. Although, we only included genes identified in the p110 δ KI study on the LDA cards and were as such unable to perform the same analysis in reverse. We cannot therefore state as confidently that the genes affected by IC87114-treatment are indeed not affected by the p110 δ KI macrophages, but our genome-wide expression analysis suggests this is the case.

We formulated a number of theories to explain this surprising lack of overlap between the effects of IC87114 treatment of a cell line, primary macrophages and of genetic inactivation of p110 δ . We have addressed a number of them, but due to time constraints or resource limitations some of the theories have not been tested and are considered beyond the scope of this project/PhD. We first considered in what ways the WT IC87114-treated macrophages were different to the p110 δ KI macrophages. The first obvious difference is of course the mode of inactivation of p110 δ ; pharmacological compared to genetic. Secondly, the timing of the inactivation of p110 δ differs as the WT-IC87114 macrophages were differentiated from WT precursor cells extracted from the WT bone marrow environment of a WT mouse, whereas the p110 δ KI cells are cultured from p110 δ KI precursors extracted from a p110 δ KI environment.

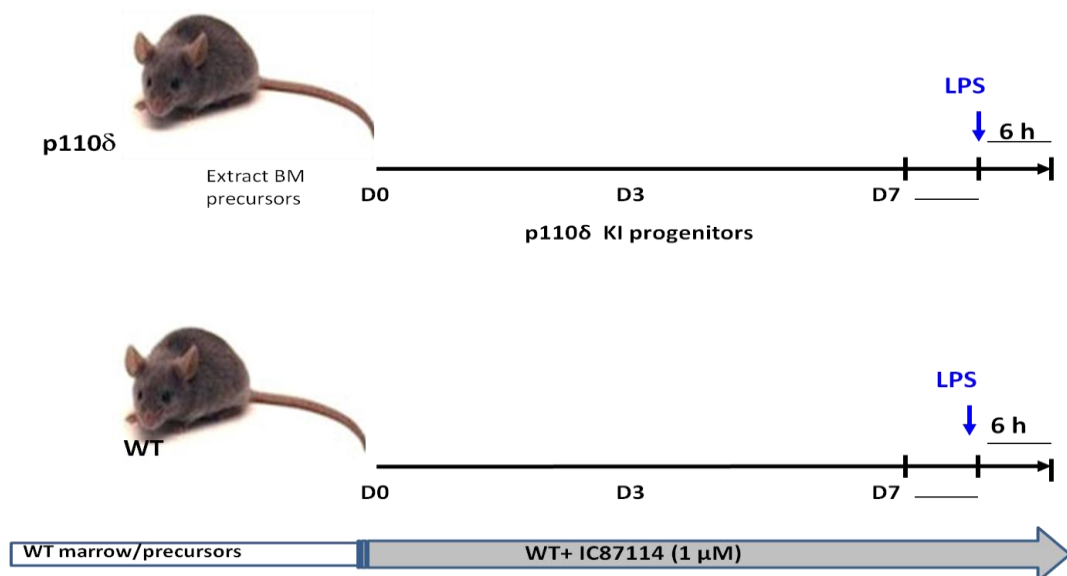


Figure 6.6. Comparison of the genome-wide expression analysis of the effects of genetic and pharmacological inactivation of p110 δ . The same macrophage extraction and differentiation protocol was followed for both studies. The major differences between the two studies are firstly, the precursor cells and marrow from which they are derived that are p110 δ KI or WT in the genetic and pharmacological study respectively. Secondly, the WT macrophages are of supplemented with IC87114 (1 μ M) to inhibit p110 δ activity throughout and after differentiation, whilst the p110 δ KI macrophages lack p110 δ activity as a result of the mutation.

6.5.1.1. Testing the concentration of IC87114 in the medium during differentiation

We first decided to address a potential technical issue that could be responsible for the lack of deregulation of the same genes in the WT-IC87114 macrophages as in the p110 δ KI macrophages. We reasoned that the IC87114 stability could have been insufficient to maintain an inhibitory concentration between fresh medium additions which contained the inhibitor. We therefore analysed the concentration of IC87114 in media samples that had been previously taken throughout the seven day differentiation process to test whether this was the case and whether the IC87114 was maintained throughout at a suitable inhibitory concentration. The mass spectrometry was kindly performed by Dr M. Jairaj at UCB. The samples were taken from the experiment used to generate the WT-IC87114 and WT-DMSO macrophages analysed on the LDA card as detailed above. The results indicate that the concentration of IC87114 was maintained at sufficient levels throughout the seven day differentiation period [Figure 6.7]. We therefore felt confident that insufficient concentration of IC87114 in the media was not responsible for the absence of overlapping effects of the genetic and pharmacological inactivation of p110 δ .

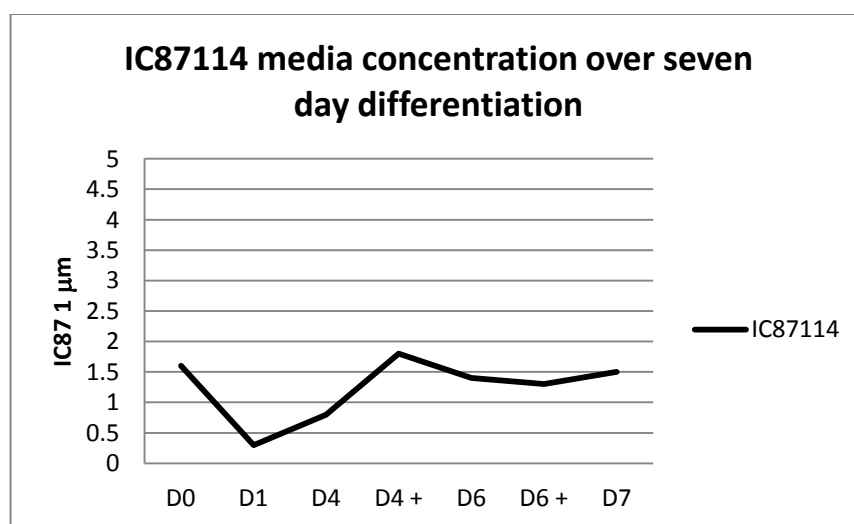


Figure 6.7. The concentration of IC87114 in the medium was within a suitable range throughout the course of the experiment. Medium samples were taken throughout the course of the experiment and the concentration of the IC87114 was then measured against a set of medium standards with IC87114 at concentrations from 0 μ M to 100 μ M [This analysis was performed by Dr. M. Jairaj, UCB].

6.5.2. Analysis of the chromosomal locations of the genes identified

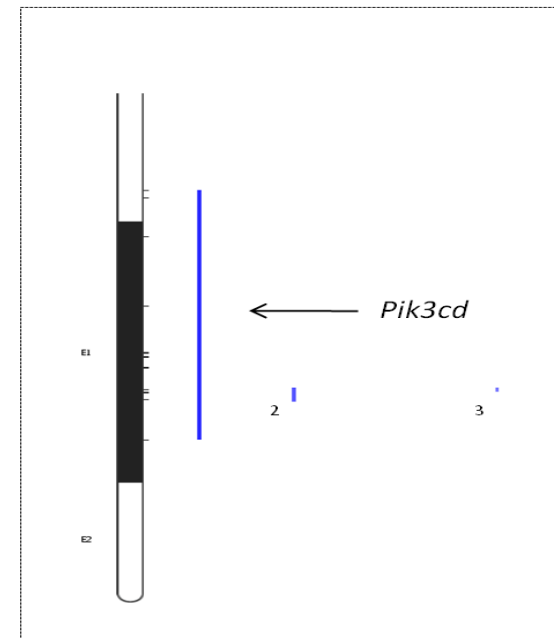
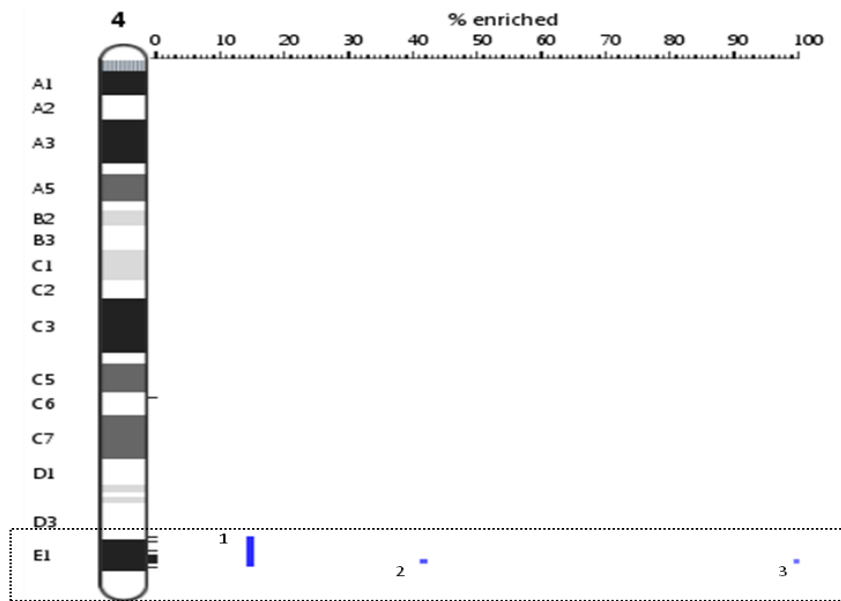
We decided to map the locations of the genes affected by the p110 δ KI mutation in primary macrophages. The results revealed that twelve of the nineteen probe sets that are mapped to chromosomal locations (63% of the genes) are located on chromosome four [Table 6.3].

Gene Symbol	Protein	Chromosome
<i>Fblim1</i>	filamin binding LIM protein 1	4
<i>Pdpn</i>	Podoplanin	4
<i>Kif1b</i>	Kinesin family member 1b	4
<i>Plod1</i>	procollagen-lysine, 2-oxoglutarate 5-dioxygenase 1	4
<i>Ubiad1</i>	UbiA prenyltransferase domain containing 1	4
<i>Efhd2</i>	EF hand domain containing 2	4
<i>Efcab7</i>	EF-hand calcium binding domain 7	4
<i>Vamp3</i>	vesicle-associated membrane protein 3	4
<i>Mthfr</i>	5,10-methylenetetrahydrofolate reductase	4
<i>Ube4b</i>	ubiquitination factor E4B, UFD2 homolog (S. cerevisiae)	4
<i>Clstn1</i>	calsyntenin 1	4
<i>Miip</i>	migration and invasion inhibitory protein	4
<i>Fst</i>	Follistatin	13
<i>Pacsin3</i>	protein kinase C and casein kinase substrate in neurons 3	2
<i>Htatsf1</i>	HIV TAT specific factor 1	X
<i>Sh2d1b1</i>	SH2 domain protein 1B1	1
<i>Paip1</i>	polyadenylate binding protein-interacting protein 1	13
<i>Rab6b</i>	RAB6B, member RAS oncogene family	9
<i>Nin</i>	Ninein	12

Table 6.3. Location of nineteen mapped probe sets differentially regulated in p110 δ KI macrophages. The chromosome on which each gene is located in the murine genome was identified using a genome browser. Genes found to be expressed at higher levels in p110 δ KI macrophages compared to WT macrophages are highlighted in red, those expressed at lower levels in these mutant macrophages are highlighted in green.

6.5.2.1. A cluster of the differentially regulated genes around the *Pik3cd* gene

Next, we performed positional gene enrichment (PGE) analysis to determine the statistical significance of the clustering of the genes found to be differentially regulated in p110 δ KI macrophages. To do this we employed an open access PGE web tool [176]. This analysis confirmed that the enrichment of genes differentially regulated in p110 δ KI macrophages on chromosome four was highly significant. Importantly this analysis also identified a specific locus (E1) in which this enrichment was concentrated. Indeed, the statistical significance of this enriched region was assigned an $\text{adj}p$ value of 1.74×10^{-25} [Figure 6.8]. The *Pik3cd* gene that encodes p110 δ is encoded within this same locus.



Region 1: $p = 1.74 \times 10^{-25}$ adjusted $p = < 0.002$ (12/76 genes)

Region 2: $p = 2.23 \times 10^{-8}$ adjusted $p = < 0.002$ (3/73 genes)

Region 3: $p = 7.79 \times 10^{-7}$ adjusted $p = < 0.002$ (2/2 genes)

Figure 6.8. Positional gene enrichment analysis revealed a very highly statistically significant cluster of genes enriched on chromosome four, locus E1. The list of probe sets differentially regulated in p110 δ KI macrophages was uploaded to the PGE analysis tool and the enrichment of those genes mapped to specific chromosome locations was calculated. The p value was adjusted to account for the multiple testing integral to the algorithm [176].

We also checked for PGE in the lists of genes identified in the WT-IC87114 study and the pilot RAW 264.7 study and found no significant PGE within either of these gene lists [data not shown].

6.5.3. Unlinked genes such as *Rab6b* are not affected by IC87114

This enrichment is in fact the final compelling reason why we chose to follow up the expression of *Rab6b* at the protein level. Unlike the other genes that we validated, *Rab6b* was found to be differentially regulated in p110 δ KI macrophages but importantly is not linked to *Pik3cd*. [Figure 6.8 & Table 6.3]. Nevertheless, despite its independence from the E1 locus, our LDA analysis of *Rab6b* mRNA expression in WT-IC87114 macrophages had confirmed that it was also not affected by pharmacological inactivation of p110 δ . This suggested to us that there may be multiple factors contributing to the differential effects of genetic and pharmacological inactivation of p110 δ on the transcriptome.

We reasoned that perhaps *Rab6b* expression required a more complete inhibition of p110 δ activity that was achieved by 1 μ M of IC87114 and we have performed two experiments to test this theory. We first compared the expression of the fifteen “p110 δ KI genes” represented on the LDA cards, including *Rab6b* in WT and heterozygous p110 δ KI macrophages. The preliminary data regarding the expression of these genes, including *Rab6b* indicated that they are not differentially regulated in heterozygous p110 δ KI macrophages [data not shown]. These data would need to be confirmed with an additional experiment before it could be presented confidently. Nevertheless, this apparent lack of differential regulation of *Rab6b* in heterozygous p110 δ KI macrophages supports the possibility that disruption of *Rab6b* expression requires a complete ablation of p110 δ activity. Consequently, we chose to test whether differentiation in the presence of a higher dose of IC87114 was sufficient to reduce *rab6b* protein levels. We extracted primary macrophages from three WT mice and differentiated them separately in the presence of either DMSO, 1 μ M IC87114 or 5 μ M IC87114 for the duration of the seven day differentiation period. Analysis of lysates obtained from these macrophages revealed that the repression of p-Akt was enhanced in the cells grown in the presence of 5 μ M IC87114 compared to those grown in 1 μ M IC87114

[Figure 6.9]. Rab6b was not reduced in macrophages differentiated in the presence of IC87114 at 1 μ M as expected based on our Affymetrix and LDA data and importantly, rab6b expression was also unaffected by differentiation in the presence of 5 μ M IC87114 [Figure 6.9].

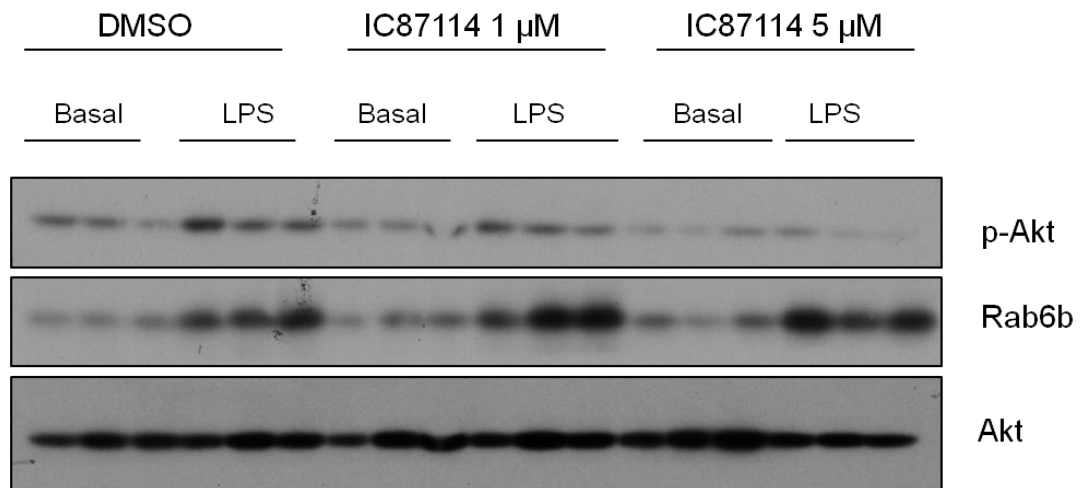


Figure 6.9. Expression of rab6b protein is unaffected in WT macrophages differentiated in either 1 μ M or 5 μ M IC87114 as indicated. Macrophage precursor cells were extracted from three WT mice and split into three groups that were differentiated in the presence of DMSO, p110 δ -selective IC87114 at 1 μ M or at 5 μ M as indicated. After seven days of differentiation cells were stimulated with LPS (1 μ g/ml) for 30 min prior to cell lysis. Total cell lysates were analysed for the expression of the indicated proteins using immunoblotting.

We note that in this experiment rab6b was induced by LPS-stimulation [Figure 6.9]. This was not observed in our previous experiment in which rab6b levels were compared in WT and p110 δ KI macrophages in basal and LPS-stimulated conditions [Chapter 5, Figure 5.16]. These data indicate that although increasing the dose of IC87114 reduced the activation of Akt this had no detectable impact on rab6b protein levels. These data would suggest that the reason behind the differential effects of genetic and pharmacological inactivation on *Rab6b* expression may not be incomplete inhibition of p110 δ in the later case.

6.6. Conclusion

Firstly, based on our Affymetrix data we have identified just nine genes that are differentially regulated in WT-IC87114 macrophages [Table 6.1 & 6.2]. We did not validate the effect of IC87114 on the expression of these genes and therefore the potential link between p110 δ activity and the expression of these genes is presented with caution. It is possible that they are false positive results or that they represent off-target effects of IC87114. It would be interesting to determine which of these genes stand-up to validation, and furthermore to check that they are not affected in p110 δ KI macrophages. In terms of a biomarker if the expression of any gene(s) is validated, it would then be necessary to determine whether the same effect is observed in human leukocytes such as readily accessible blood derived monocytes or macrophages differentiated from them.

Perhaps our most important and unexpected result was the identification of a potential problem with the p110 δ KI mouse model. PGE analysis has revealed a highly statistically significant enrichment of the genes differentially regulated in p110 δ KI macrophages on chromosome four. Their localisation specifically, within or proximal to the locus where *Pik3cd* lies is certainly a cause for concern. We proposed three possible explanations for this localisation of genes differentially regulated in p110 δ KI macrophages. First, it could indicate that disruption of epigenetic structure or modifications have occurred on the mutant chromosome. Alternatively we proposed that the genetic engineering may have interfered with a regulatory sequence such as a micro RNA (miRNA). Our third hypothesis is that the expression of these genes is not affected by the mutation *per se* but as the result of the retention of genetic material from the mouse strain in which the mutation was originally generated. To put this simply, the D910A mutation was first generated in embryonic stem cells derived from a 129 strain mouse, whereas the p110 δ KI mouse colony we now use is of the C57BL/6 background. The mice were backcrossed for at least nine generations to homogenise the genetic background to C57BL/6 genetic material but we suggest that by selecting for p110 δ KI mutants we may have selected those mice that have retained the 129 genetic material surrounding the *Pik3cd* gene. Finally we must acknowledge that the differential regulation of the genes linked to *Pik3cd* might genuinely occur as a result of inactivation of p110 δ in macrophages. The possible

explanations for the unexpected enrichment of genes differentially regulated in p110 δ KI macrophages are described and considered in detail in the discussion, which follows.

We also noted that macrophages differentiated in IC87114 had repressed p-Akt whilst this was not apparent in the p110 δ KI macrophages. Previous data regarding the reduced activation of Akt in p110 δ KI macrophages was always obtained from macrophages deprived of CSF-1 for 12-24 h [1, 79], whilst we have observed no decrease in the presence of CSF-1. We have also observed that a decrease in p-p38 occurred in p110 δ KI macrophages, but not in our experience in either primary macrophages or macrophage cell lines treated with IC87114. This result regarding p-p38 being affected by the mutation but not the drug could also be relevant to our findings but would first need to be confirmed with additional experiments.

CHAPTER 7

7. DISCUSSION

7.1. The effects of genetic and pharmacological inactivation of p110 delta on transcriptional regulation

The main conclusions of this study are:

1. p110 δ plays a minimal role in the regulation of transcription in primary macrophages
2. Expression of *Rab6b* is reduced in p110 δ KI macrophages but is unaffected in macrophages differentiated in the presence of IC87114
3. The effects of genetic and pharmacological inactivation of p110 δ in primary macrophages are entirely disparate
4. The expression of twelve genes proximal to the *Pik3cd* gene on chromosome four are differentially expressed in p110 δ KI macrophages

7.1.1. Genetic inactivation of p110 δ has a minimal effect on gene expression

When we set out to perform our genome-wide expression analyses of macrophages lacking p110 δ activity we had two key objectives in mind. First, we wanted to gain an insight into the role that p110 δ plays in transcriptional regulation in macrophages and which processes are regulated by p110 δ at this level. Secondly, by identifying individual genes affected by p110 δ inactivation we hoped to identify a unique signature of p110 δ inactivation, which could be used to develop biomarkers.

We initially chose to identify genes regulated by p110 δ in primary macrophages using the genetic p110 δ KI model. We reasoned that comparing the expression of p110 δ KI macrophages to WT macrophages was the cleanest system in which we could elucidate the specific effects of p110 δ inactivation on transcriptional

regulation. Specifically, we felt that starting our investigation using genetic inactivation was preferable to using pharmacological inactivation, as the latter method is likely to have off-target effects. Instead, we preferred to investigate the genes affected by the p110 δ KI mutation and subsequently identify which of these were also common to macrophages treated with p110 δ -selective inhibitors. An alternative to this strategy would have been to determine the effect of several different p110 δ -selective inhibitors on the genome-wide expression of primary macrophages. Those genes found to be affected by all of the drugs could be considered as most likely to be genuinely downstream of p110 δ -inactivation.

The comparison of the genome-wide expression of p110 δ KI and WT macrophages revealed that the regulation of transcription in growing macrophages is minimally affected by loss of p110 δ activity. The effects were restricted to just twenty-five probe sets that were differentially regulated in either basal or LPS-stimulated p110 δ KI macrophages. Specifically, in growing unstimulated p110 δ KI macrophages, just seventeen probe sets, or fourteen known genes were differentially regulated [Table 7.1 & 7.3]. Whilst in LPS-stimulated p110 δ KI macrophages twenty probe sets, or seventeen genes were affected, and strikingly, only eight of these genes were unique to the LPS-stimulated state [Table 7.2 & 7.3]. This data was obtained from four biological replicates per condition and statistical analysis identified these probe sets had p values of ≤ 0.05 which are considered very significant.

Gene Symbol	Protein	Basal	
		logFC	adjP value
<i>Rab6b</i>	RAB6B, member RAS oncogene family	-2.368	2.14E-05
<i>Nin</i>	Ninein	2.316	2.14E-05
<i>Clstn1</i>	calsyntenin 1	1.737	7.60E-03
<i>Sh2d1b1</i>	SH2 domain protein 1B1	1.286	4.02E-02
<i>Miip</i>	migration and invasion inhibitory protein	-1.092	3.05E-02

Table 7.1. The expression of five genes was found to be differentially regulated in p110δ KI macrophages compared to WT macrophages in unstimulated conditions only. Genes are ordered by magnitude of change irrespective of the direction of logFC and genes increased or decreased in p110δ KI macrophages are highlighted in red or green respectively. The expression of two genes *Rab6b* and *Miip* were decreased in basal p110δ KI macrophages. The expression of three genes (*Clstn1*, *Sh2d1b1* and *Nin*) was increased in basal p110δ KI macrophages.

Gene Symbol	Protein	LPS-stimulated	
		logFC	adjPValue
<i>Mthfr</i>	5,10-methylenetetrahydrofolate reductase	-2.194	1.70E-04
<i>Ube4b</i>	ubiquitination factor E4B, UFD2 homolog (S. cerevisiae)	-1.802	1.38E-04
<i>Kif1b</i>	Kinesin family member 1b	1.409	1.72E-02
<i>Mid1</i>	midline 1	1.408	1.64E-02
<i>Fst</i>	Follistatin	1.305	1.07E-03
<i>Pacsin3</i>	protein kinase C and casein kinase substrate in neurons 3	1.304	3.10E-03
<i>Tnn</i>	tenascin N	-1.083	3.47E-02
<i>Htatsf1</i>	HIV TAT specific factor 1	1.078	4.33E-02

Table 7.2. The expression of eight genes was found to be differentially regulated in LPS-stimulated p110δ KI macrophages compared to LPS-stimulated WT macrophages. Genes are ordered by magnitude of LogFC irrespective of the direction of change and genes increased or decreased in p110δ KI macrophages are highlighted in red or green respectively. Increased expression of four genes (*Htatsf1*, *Pacsin3*, *Fst* and *Mid1*) was identified in LPS-stimulated p110δ KI macrophages. The expression of four genes (*Mthfr*, *Ube4b*, *Kif1b* and *Tnn*) was reduced.

Gene Symbol	Protein	Basal		LPS-stimulated	
		logFC	adjpValue	logFC	adjpValue
<i>Fblim1</i>	filamin binding LIM protein 1	-2.927	3.61E-04	-3.892	4.42E-03
<i>Pdpm</i>	Podoplanin	-3.629	2.14E-05	-3.321	2.71E-05
<i>Paip1</i>	polyadenylate binding protein-interacting protein 1	3.110	6.79E-06	3.350	8.71E-07
<i>Pisd-ps3</i>	phosphatidylserine decarboxylase, pseudogene 3	2.230	2.24E-03	1.849	4.57E-03
9530053H05 Rik	RIKEN cDNA 9530053H05 gene	2.157	1.20E-02	1.329	2.04E-02
<i>Plod1</i>	procollagen-lysine, 2-oxoglutarate 5-dioxygenase 1	-1.886	5.93E-04	-1.771	4.08E-04
<i>Ubiad1</i>	UbiA prenyltransferase domain containing 1	1.811	9.11E-03	2.345	2.95E-04
<i>Efhd2</i>	EF hand domain containing 2	-1.782	4.66E-04	-1.541	7.10E-04
1700029I01 Rik	RIKEN cDNA 1700029I01 gene	-1.685	6.82E-03	-1.752	1.83E-03
3110007F17 Rik	RIKEN cDNA 3110007F17 gene	-1.662	2.24E-03	-1.230	1.33E-02
<i>Efcab7</i>	EF-hand calcium binding domain 7	-1.583	4.08E-03	-1.409	4.57E-03
<i>Vamp3</i>	vesicle-associated membrane protein 3	-1.088	3.05E-02	-1.121	1.11E-02

Table 7.3. The expression of twelve probe sets interrogating nine known genes and three RIKEN transcripts were differentially regulated in unstimulated as well as LPS-stimulated p110 δ KI macrophages. Probe sets are ordered by magnitude of logFC irrespective of the direction of change and known genes are in bold and genes increased or decreased in p110 δ KI macrophages are highlighted in red or green respectively. Six known genes and two RIKEN clones were found to be decreased in basal and LPS-p110 δ KI macrophages. Three known genes and one RIKEN were found to be increased in basal and LPS-stimulated p110 δ KI macrophages.

We have confirmed the differential expression of fifteen of the twenty-five unique probe sets identified in a validation study. We felt that it was important to obtain these confirmatory data using a new set of samples, as opposed to validating the observed changes in the original samples. We therefore, performed comparative expression analysis on three new sets of RNA samples derived from WT or p110 δ KI macrophages in the basal and LPS-stimulated state. Additionally, we included one of the four sets of original RNA samples, which we had analysed by microarray. In total, we have now analysed the expression of this sub-set of genes in seven biological replicates (p110 δ KI and WT macrophages in basal and LPS-stimulated

state) and thus we are confident of our findings regarding their differential regulation in p110 δ KI macrophages.

We have presented quantitative data supporting our Affymetrix findings regarding the differential regulation of seven genes in p110 δ KI macrophages. Specifically, we have confirmed that the expression of *Clstn1* is increased in p110 δ KI macrophages and the expression of *Rab6b*, *Fblim1*, *Pdpm* and *Plod 1* are decreased in p110 δ KI macrophages. We also confirmed that *Mthfr* and *Ube4b* expression is decreased in LPS-stimulated p110 δ KI macrophages. In the case of *Rab6b*, the Affymetrix results had indicated that it was only differentially expressed in the basal state whereas an effect in both basal and LPS-stimulated states was observed in the validation study. This highlights the benefit of utilising TaqMan for validation of Affymetrix results because of its increased sensitivity and dynamic range compared to a microarray. This increased sensitivity may explain why we observe a much greater fold change in *Rab6b* expression in the validation study, compared the fold change observed in the Affymetrix study. Below we have considered the implications of our results in terms of the role that p110 δ appears to play in the regulation of macrophage transcription. Subsequently, we discuss the data regarding the possible impact of decreased expression of *Rab6b* in p110 δ KI macrophages.

7.1.2. The genome-wide perspective

As well as aiming to identify individual genes regulated by p110 δ , we were also keen to gain insight into the extent to which p110 δ contributes to the regulation of the macrophages transcriptome as a whole. We knew that p110 δ has a significant role to play in signalling in macrophages and that macrophages lacking p110 δ display defective motility and migration as well as have defects in certain secretory pathways [1, 79, 114]. Yet what remained unclear was to what extent these and other processes regulated by p110 δ are modulated or controlled at the level of transcription. At the time we initiated this study there were no publications detailing the effects of either genetic or pharmacological inactivation of p110 δ on the transcriptome as a whole. We were therefore keen to observe, how many

genes overall were affected by p110 δ inactivation and which processes if any might be partially regulated at the level of transcription.

We had read several publications that indicated that a number of transcription factors can be affected by PI3K-Akt activity. These include the FOXO family of transcription factors, NF- κ B and CREB, which between them regulate the expression of hundreds of genes [35-36, 40, 42-43]. Therefore, one might expect that inactivation of p110 δ would affect the expression of hundreds of genes as a result of altered activity of these transcription factors in the absence of p110 δ . Having said that, the majority of this research into transcription factors downstream of PI3K-Akt has been performed using pan-PI3K inactivation or PI3K activation and thus the observed effects on transcription factor activity might be mediated by other PI3K isoform. Yet, even when we consider the impact of pan-PI3K modulation, Cook *et al.* identified just forty genes differentially regulated in cardiomyocytes expressing constitutively active Akt [46]. Thus it seems that distortion of PI3K activity in isolation may be insufficient to induce significant transcriptional deregulation.

In this thesis, we have presented data indicating that the contribution of p110 δ to the regulation of macrophage transcription is very limited in unstimulated growing murine macrophages. We make this assertion based on our observation that the expression of only fourteen known genes was found to be differentially regulated in unstimulated growing macrophages. We postulate that instead the fundamental regulation of the transcriptome might fall to one of the other ubiquitously expressed PI3K isoforms such as p110 α or p110 β . Alternatively, we recognise that it is possible that PI3K as a family does not play a central role in transcriptional regulation. Our results could indicate that whilst PI3K-Akt activity does, in some instances modulate transcription factor activity, it is one of many inputs into the regulation of transcription and thus its inactivation does not result in a dramatic shift. This would make sense in the context of the many feedback loops and regulatory controls that have evolved to ensure a single defect cannot drive a cell into malignancy. For example, we know that the loss of a single tumour-suppressor gene is rarely enough to induce oncogenesis, but instead an oncogene must generally also be deregulated [177]. In the same way, inactivation of p110 δ may not be able to deregulate transcription in the absence of other

cellular abnormalities. Perhaps, if p110 δ were to be inhibited alongside another canonical signalling pathway, a role in transcriptional regulation would become more apparent.

Whilst we have been investigating the effect of the p110 δ KI mutation on macrophage transcription, Patton *et al.* examined its effects on the transcriptome of Tregs [50]. The authors report that the effects of inactivating p110 δ in Tregs were also relatively restricted [50]. Specifically, 125 probe sets were found to be differentially regulated in p110 δ KI Tregs [50]. This represents a very small proportion of the entire genome, but is approximately 100 more than we identified in p110 δ KI macrophages [50]. In view of our results and those obtained by Patton *et al.* [50], we can suggest with greater confidence that the effects of p110 δ inactivation on transcription are not wide-spread. It is interesting that the transcriptome of Tregs appears to be more dependent upon p110 δ activity than the transcriptome in macrophages. We are tempted to speculate that in adaptive immune cells such as Tregs p110 δ may play a more significant, even if still limited, role in transcriptional regulation than it does in innate immune cells such as macrophages. Based purely on these two studies, this is of course nothing more than speculation, but we suggest that it might be interesting to compare the effects of p110 δ inactivation on the transcriptome of a panel of innate and adaptive immune cells.

Comparisons between two microarray studies, such as our own and that published by Patton *et al.* must always be made with caution, particularly as we have found that even on a single data set, the data analysis performed can impact upon the number and the list of genes identified. As such, if one were especially keen to compare and confidently draw conclusions from two studies, it would be wise to normalise the data across both studies and then analysis the data together. Of course, it is not just data analysis that can affect the results: the exact protocols applied and even the colony of mutant mice used, can affect microarray results. In this respect, we can compare the effects of the p110 δ KI mutation in macrophages and Tregs more confidently because we actually used mice from the same WT and p110 δ KI colonies as Patton *et al.* because of shortages in our own mouse colonies [50]. We were especially keen to identify any genes that were affected by p110 δ inactivation in both Tregs and macrophages. Just four genes were differentially

regulated in both p110 δ KI Tregs and p110 δ KI macrophages: *Vamp-3*, *Rab6b*, *Kif1* and *Ubiab1*. The identification of these genes in both studies supports the validity of our results regarding their differential expression and we speculate that they may be involved in a specialised function that is common to leukocytes.

Below we present a summary of the evidence that leads us to propose that *Rab6b* and also potentially *Vamp-3* are regulated by p110 δ in order to modulate a specialist leukocyte functions. Although we must point out that the linkage of *Vamp-3* to the E1 encoding *Pik3cd* locus, which is discussed in detail later, may indicate that this is a false lead. Alternatively, it is also possible that some of the disruption observed in p110 δ KI macrophage functions mentioned below in relation to *Rab6b* and *Vamp-3* might in fact be due to differential regulation of *Vamp-3* independent of p110 δ activity. With this caveat put temporarily to one side, we have considered the possible function implications of differential regulation of *Rab6b* and additional *Vamp-3* in p110 δ KI macrophages.

7.2. Investigating the effects of p110 delta activity on *Rab6b* expression

7.2.1. Reduced expression of *Rab6b* in p110 δ KI macrophages but not in p110 δ KI brain tissue

In this thesis, we have presented data that reveal that the expression of *Rab6b* is reduced in p110 δ KI macrophages. As described above, these data were obtained using two methods across a total of seven biological replicates, which increases our confidence in this finding. Importantly, we have also presented evidence that this decreased expression results in a decrease in rab6b protein in p110 δ KI macrophages. Our results at the protein level reveal that *Rab6b* expression is decreased in both unstimulated and stimulated p110 δ KI macrophages, which is consistent with our TaqMan[®] LDA results.

We were struck by two findings regarding *Rab6b*, first that the expression of *Rab6b* has also been found to be decreased in p110 δ KI Tregs, another type of leukocyte [50]. This independent identification of differential regulation of *Rab6b* in p110 δ

KI cells further enhanced our confidence in this result. Secondly, we noticed a remarkable degree of overlap between the tissues within which p110 δ and rab6b are reported to be expressed: leukocytes, neurons and melanocytes [50, 172-173]. Based on this observation, we postulated that p110 δ activity might regulate the tissue-specific distribution of rab6b. We tested this hypothesis by comparing the expression of rab6b in brain tissue derived from p110 δ KI and WT macrophages. Our results indicate that rab6b is expressed at WT levels in p110 δ KI brain tissue, which disproved our hypothesis. Together these data suggest that the regulation of *Rab6b* by p110 δ may instead be restricted to, but potentially common across, the haematopoietic cell lineage. It would be pertinent to compare the levels of rab6b in other WT and p110 δ KI leukocytes to determine whether this is correct. In summary, we have identified *Rab6b*, amongst other genes as a potential regulatory target of p110 δ activity and we have shown that this results in a reduced expression of rab6b protein in p110 δ KI macrophages.

7.2.2. Possible functional consequences of reduced rab6b in p110 δ KI macrophages

It was beyond the scope of this project to investigate the functional implications of this reduced expression of *Rab6b* in macrophages. Addressing this question potentially represents an entire project in itself, particularly in light of the very limited information regarding rab6b function. Nevertheless, we have considered the potential implications of our findings based on what is known about rab6b and our own knowledge regarding macrophages and p110 δ functions in them. We have identified two processes that are integral to the specialised functions of macrophages in which rab6b might function. Furthermore, we have found evidence supporting a potential involvement of *Vamp-3* (one of the other genes differentially regulated in p110 δ KI macrophages) in these processes.

7.2.2.1. The role of rab6b in the endomembrane trafficking network

We must consider what is known about the functions of rab6b and that of its family members in order to formulate informed hypotheses regarding the possible implications of reduced expression of *Rab6b*. We know that rab6b belongs to the

large rab family consisting of around fifty small-GTPase proteins, which perform regulatory functions within the endomembrane network. Within the rab family, rab6b is a member of a small sub-family alongside rab6a and its splice-variant rab6a', which are both ubiquitously expressed [172]. The endomembrane network facilitates the transport of proteins and lipids to and from appropriate intracellular organelles or membranes. Much of the flow through this network is devoted to the transport of new translated protein cargo from the endoplasmic reticulum (ER) to the Golgi apparatus and subsequently onwards within vesicular carriers to the organelle or endomembrane in which the cargo functions [Figure 7.1]. The ability to regulate the fusion of the vesicular carriers that pass between the compartments is crucial for the spatial regulation of proteins and lipids. The rab family of proteins are integral to this regulation of vesicular fusion. In their specific localisations, they form a sort of molecular signature or gatekeeper ensuring that only the appropriate vesicles are able to fuse and unload their protein/lipid cargo.

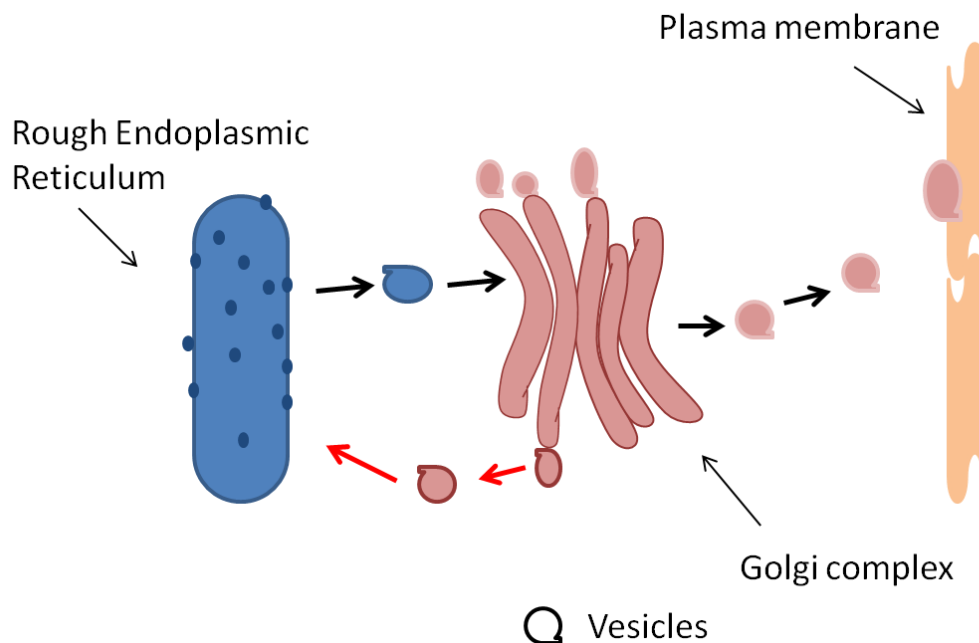


Figure 7.1. Schematic of vesicle trafficking in the endomembrane system. Transport of cargo from the ER to Golgi and on to the appropriate subcellular location is mediated through highly regulated vesicular transport. Opposing this flow is retrograde transport (red lines) which returns proteins to the Golgi and/or ER.

Retrograde transport moving against the predominant flow of newly-translated cargo is required to return the molecular machinery and lipids to the ER and Golgi in order to enable further cycles of transport to proceed. A large proportion of retrograde cargo including ER are recognised and bound by coatamer protein I (COP-I) which facilitates their vesicular transport back to the ER. Current data including subcellular localisation studies suggest that rab6a and rab6b perform non-identical functions within retrograde transport. Both were initially reported to be localised to the Golgi apparatus, and additionally to be enriched in specific peripheral sites [172, 178-179]. These peripheral sites are thought to be retrograde transport entry sites on the ER and thus this enrichment is consistent with a role for rab6a and rab6b in retrograde transport [172, 179]. Rab6a was found to perform retrograde transport independently of the COP-I-dependent pathway [178-179]. In contrast, rab6b has been localised to ERGIC-53-containing vesicular structures, which are associated with COP-I-dependent retrograde transport [172]. This indicates that rab6b, unlike rab6a, may function within the canonical COP-I-dependent retrograde transport pathway [172, 179]. An additional role for rab6b that might be relevant to its tissue-specific expression in neurons, macrophages and melanocytes has been uncovered. Bicaudal-D1 was found to interact with rab6b and both were then shown to co-localise to microtubule bound dynein-dynactin complexes [180]. Interestingly, the authors visualised live dynamic bi-directional movement of rab6b along microtubules [180]. This observation reveals that rab6b contributes to both anterograde and retrograde transport of vesicles containing unknown cargo along the extended microtubule network within neural cell processes.

Neural processes often extend long distances from the cell body and thus it seems plausible that the capacity to regulate bi-directional transport along extended microtubules tracks might require cell-specific components such as rab6b [Figure 7.2].

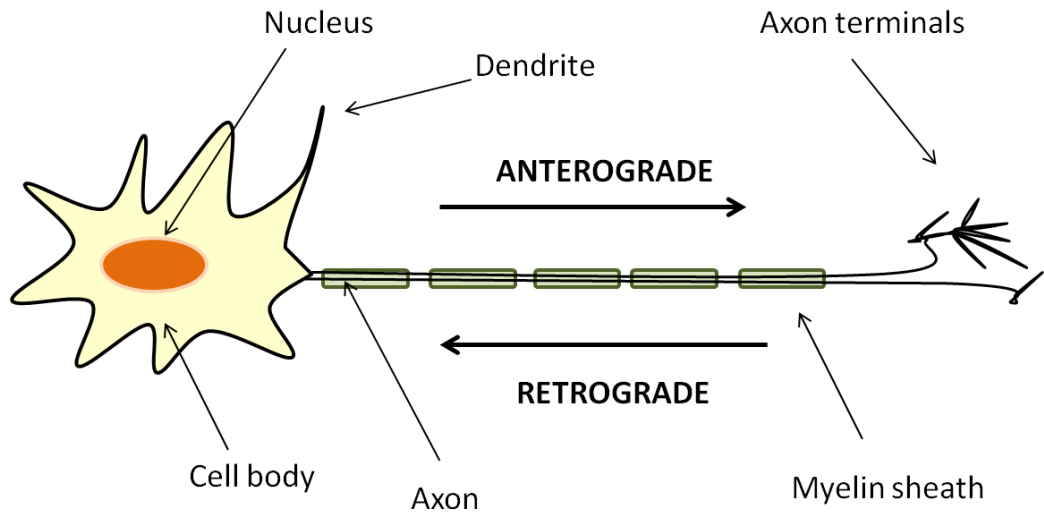


Figure 7.2. Schematic of a nerve cell with extended axon and dendrites along which numerous cargo must be transported. Anterograde transport away from the cell body utilises plus-end directed molecular motors such as Rabkinesin. Retrograde transport returns cargo to the cell body utilising minus-end directed molecular motors such as dynein-dynactin.

7.2.2.2. Rab6b function in macrophages?

There is no data regarding the function or even localisation of rab6b in macrophages therefore, one can only extrapolate these observations in neurons to predict what functions rab6b might perform in macrophages. Based on the limited expression of rab6b we propose that this is likely to be a cell-specific function. In terms of macrophage biology, we know that macrophages also form protrusions in order to fulfil two of their major functions. First, they form pseudopodia, which are membranous extensions with which they reach for and engulf pathogens by phagocytosis. Secondly, macrophages must be able to migrate efficiently across a wide-range of extracellular matrix in order to reach sites of infection. To do this macrophages, form broad membranous extensions known as lamellapodia at the leading edge of the cell. The protrusion of the leading edge is facilitated by the extension of actin networks and actin-rich adhesive structures known as podosomes. Podosomes bind integrin complexes to create the contractile force needed to move the cell forward across the extracellular matrix. The podosomes and their integrin partners must be repeatedly re-distributed to the leading edge of the cell as the migration progresses. The plasma membrane at the leading edge must also be continuously supplemented with lipids to allow the protrusion to extend. This re-distribution of lipids and protein components is thought to require both endocytic and exocytic transport mechanisms. It is therefore tempting to

propose that rab6b might be involved in this specialised recycling function transporting membranous vesicles to the leading edge of the migrating macrophages. In particular, the observed capacity of rab6b to support bi-directional trafficking along microtubule networks might be advantageous in this highly dynamic process.

Interestingly, we have found publications by the Murray group revealing that *Vamp-3*, which we have found to be down-regulated in p110 δ KI macrophages (not validated), contributes to macrophage migration by regulating this endocytic-exocytic process [181-182]. *Vamp-3* facilitates the recycling of integrin complexes to the leading edge via the long-loop recycling pathway, which diverts the cargo via recycling endosomes [182]. Consequently, reduction of *vamp-3* results in disorganisation of podosomes because the integrin partners of the actin structures are not re-distributed to the advancing leading edge. A more recent publication revealed that the passage of the integrin-containing *vamp-3*-positive vesicles via recycling endosomes allows the vesicles to deliver recycling endosome membrane to the leading edge [183]. Accordingly, *vamp-3* in association with other SNARE complexes, is necessary to facilitate appropriate adhesion through integrin-podosome structures and additionally to allow and membrane expansion.

The observed effects of suppressing *vamp-3* activity in macrophages include a reduced capacity to migrate, a more rounded phenotype due to a reduced adhesive area and a disorganisation of podosomes. This is particularly interesting because p110 δ KI macrophages have migratory defects and display a more rounded phenotype with a reduced adhesive surface [79]. Furthermore, p110 δ KI dendritic cells have been found to lack normal podosome structures [Dr Aksoy, Centre for Cell Signalling, unpublished data]. We suggest that it would be informative to test whether re-expression of *Vamp-3* in p110 δ KI macrophages rescues or improves the migratory and adhesion defects in these cells.

As rab6b has been shown to function in retrograde transport, and *vamp-3* is clearly implicated in this particular form of retrograde transport it is tempting to speculate that these two proteins rab6b and *vamp-3* both function in the same specialised process. Thereby, co-ordinated regulation of both *Rab6b* and *Vamp-3* expression by p110 δ might act to modulate this specialised intracellular trafficking function. If one were to investigate this possibility, one would need to investigate

the localisation of rab6b as suggested above but also to assess whether *Rab6b* null cells have a similar defect in migration. In fact, a functional association between rab6b and vamp-3 is supported by a publication that found both of these proteins in purified synaptic vesicle preparations [184]. We caution the reader that no co-localisation studies were performed and that these two proteins were identified alongside many other proteins [184]. Nevertheless, this could indicate that rab6b and vamp-3 both regulate secretion within neurons or more specifically contributes to the delivery and recycling of neurotransmitter release at neuronal synapses. This would be consistent with the observation of rab6b tracking in both directions along the microtubules of neuronal dendrites [180] and it is possible that vamp-3 is also involved in recycling the vesicles.

Furthermore, we propose that if rab6b is involved in neurotransmitter release in neurons, this might translate to an involvement in the release of inflammatory mediators by macrophages. The expression of *Rab6b* in these cells could be required to facilitate regulated secretion. In order to address this theory, it would first be pertinent to assess whether rab6b is associated with secretory vesicles in macrophages. Indeed, if one were to follow up the observed decrease of rab6b in p110 δ KI macrophages at the functional level, the most appropriate starting point might well be to determine where and with what rab6b co-localises in macrophages. This would help to elucidate which process or processes within macrophages involve rab6b activity and thus which might be affected by its inactivation. We know that p110 δ activity is directly involved in the regulation of secretion in macrophages [114]. Specifically, p110 δ is transiently recruited to the TGN where its localised activity appears to be essential to recruit dynactin-2 a regulator of vesicular fusion and release [114]. Hence, it seems plausible that as well as regulating the recruitment of regulatory proteins, p110 δ might also achieve an additional level of control over secretory processes by modulating the expression of regulatory proteins.

7.3. Comparing the effects of pharmacological and genetic inactivation of p110 delta on primary macrophage transcriptome

7.3.1. Pharmacological inactivation of p110 δ results in minimal changes to the transcriptome

We also investigated the effect of pharmacological inactivation of p110 δ . Comparing the results obtained from this experiment to the effects of genetic inactivation of p110 δ has been very interesting. In this study, we chose to compare the effects of pharmacological inactivation of p110 δ on primary macrophages. We decided to culture and differentiate bone marrow precursor cells to macrophages in the presence of IC87114, a p110 δ -selective inhibitor. We reasoned that differentiating these cells into macrophages in the presence of IC87114 was most comparable to the p110 δ KI macrophages. Furthermore, we reasoned this was more representative of chronic administration of a p110 δ -selective drug in the clinic than a short treatment. We predicted that we would observe a significant overlap between the genes affected by IC87114 and by the p110 δ KI mutation and we anticipated that some genes might be differentially affected by the drug or mutation. In particular, we hypothesised that we might see genes affected by the drug and not by the genetic inactivation as a result of off-target effects of IC87114. In fact, our assumptions were proved entirely wrong. First, we actually observed fewer genes affected by IC87114 than we found affected by the p110 δ KI mutation. We found just eleven probe sets or nine known genes affected [Table 7.4 & 7.5]. Specifically, seven known genes were affected in the unstimulated state [Table 7.4], whilst only two known genes were differentially regulated in LPS-stimulated p110 δ KI macrophages [Table 7.5]. Interestingly, the genes affected in the basal state were different to those that were affected in the LPS-stimulated macrophages. We have not validated these results and therefore the regulation of these genes in response to p110 δ inactivation is presented with caution.

Gene Symbol	Protein	Unstimulated	
		logFC	adjP value
<i>NA</i>	NA	-1.156	4.54E-02
<i>Tiam1</i>	T-cell lymphoma invasion and metastasis 1	-1.448	2.02E-02
<i>Ccr5</i>	chemokine (C-C motif) receptor 5	-1.367	4.54E-02
<i>Grp85</i>	G protein-coupled receptor 85	-1.363	2.29E-02
<i>Ifi2712a</i>	interferon, alpha-inducible protein 27 like 2A	-1.202	4.54E-02
<i>Sgms2</i>	sphingomyelin synthase 2	1.019	4.54E-02
<i>Plk2</i>	plakophilin 2	-1.090	4.54E-02
<i>Socs3</i>	suppressor of cytokine signaling 3	1.421	2.29E-02

Table 7.4. Differential expression of eight probe sets was observed in unstimulated WT macrophages differentiated and cultured in the presence of IC87114 compared to WT control macrophages.

Gene Symbol	Protein	LPS-stimulated	
		logFC	adjP value
<i>Socs1</i>	suppressor of cytokine signaling 1	-1.038	3.43E-03
1110032F04Rik	RIKEN cDNA 1110032F04 gene	-1.142	4.94E-02
<i>Cmb1</i>	carboxymethylenebutenolidase-like (Pseudomonas)	-1.462	3.82E-02

Table 7.5. Differential regulation of three probe sets was detected in LPS-stimulated WT macrophages differentiated and cultured in the presence of IC87114 compared to WT control macrophages.

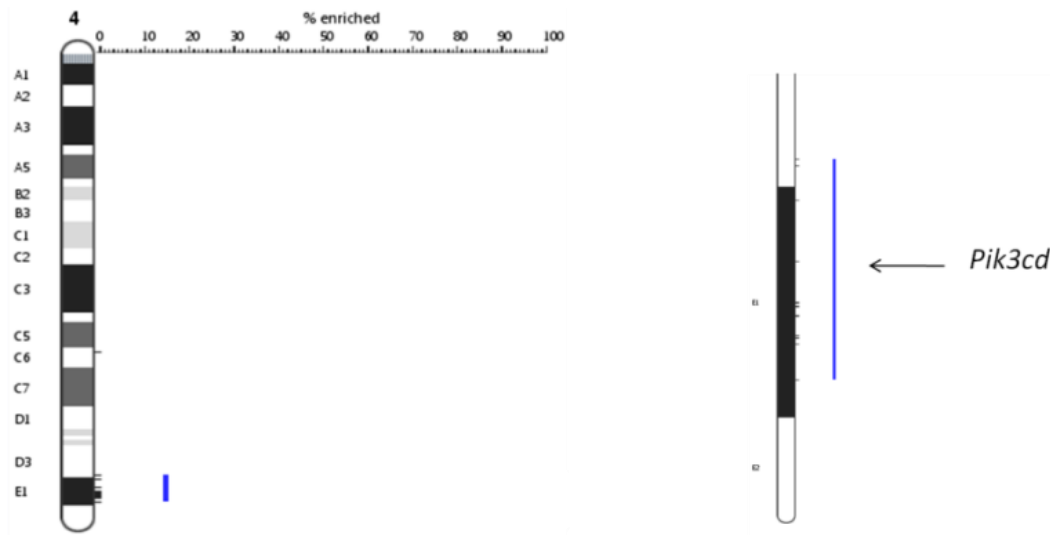
7.3.2. Comparison of genetic and pharmacological inactivation of p110 δ

Not only did we observe fewer genes affected by the pharmacological inactivation of p110 δ , but we also found that, contrary to our expectations, no genes were affected by both genetic and pharmacological inactivation. The results of our two genome-wide expression studies revealed that the genes affected by IC87114 and by the p110 δ KI mutation were entirely distinct at the transcriptional level. Thus, the effects of genetic inactivation of p110 δ in macrophages are more similar to the effects of genetic inactivation in Tregs than they are to pharmacological inactivation in macrophages! To our knowledge, this is the first instance in which the effects of genetic and pharmacological inactivation of p110 δ or, for that matter, any Class IA PI3K isoform have not been the same or similar. Of course, we were

concerned that this might have been due to a technical error or experimental design error such as insufficient addition of IC87114 to maintain an inhibitory dose. We decided to test the results and concurrently to obtain medium samples to assess the concentration of IC87114 in the medium throughout the experiment. We compared the expression of the genes affected by the p110 δ KI mutation in WT-IC87114 macrophages to their expression in WT-DMSO macrophages. The results of this experiment support the findings drawn from the Affymetrix data regarding expression of genes in p110 δ KI macrophages compared to WT macrophages. We recognise that ideally it would be informative to confirm the results of the Affymetrix experiment in which we compare the transcriptome of WT-IC87114 macrophages to that of WT-DMSO macrophages. Having done this, one could then additionally obtain the data in reverse, i.e. compare the expression of genes confirmed to be differentially regulated in WT-IC87114 macrophages in p110 δ KI macrophages. Assuming some or all of the genes affected by IC87114 were validated, it would also be pertinent to test whether other p110 δ -selective drugs have a similar effect. Additionally, we suggest that differentiating and culturing p110 δ KI macrophages in the absence and presence of IC87114 would be a useful control to discover whether these effects are p110 δ dependent.

7.3.3. Enrichment of genes differentially regulated in p110 δ KI macrophages flanking the *Pik3cd* locus

We have found one striking commonality between the majority of the genes that we found were differentially regulated in p110 δ KI macrophages in the Affymetrix experiment. The majority of the genes are located on chromosome four and, more precisely, are within or proximal to the E1 locus where the *Pik3cd* gene located. The enrichment was found to be highly significant by PGE analysis with a p value of 1.74×10^{-25} , which virtually rules out the possibility that these genes are clustered in this tiny region of the genome by chance [Figure 7.3][Table 6.3].



Region : $p = 1.74 \times 10^{-25}$ adjusted $p = < 0.002$ (12/76 genes)

Figure 7.3. PGE reveals a significant enrichment of genes differentially regulated in p110 δ KI macrophages in the region proximal to *Pik3cd*. The list of probe sets differentially regulated in p110 δ KI macrophages was uploaded to the PGE analysis tool and the enrichment of those genes mapped to specific chromosome locations was calculated. The p value was adjusted to account for the multiple testing integral to the algorithm. [176]

7.4. Explaining PGE of genes differentially regulated in p110 delta KI macrophages

This discovery was made towards the end of this project and, therefore, we have not been able to prove any one hypothesis explains this linkage, but we have found substantial amounts of literature and several publications supporting one particular hypothesis. We initially formulated a number of hypotheses as to why these differentially regulated genes might be clustered around the *Pik3cd* gene.

1. Genetic engineering of the D910A mutation has disrupted the expression of these genes in a manner independent of its effect on p110 δ activity
2. These genes are genuinely regulated by p110 δ activity by a mechanism which is unaffected by differentiation in IC87114
3. Differential regulation of these genes represents differential regulation of these genes in the mouse strain in which the D910A mutation was generated compared to the strain recipient strain into which the mutation has been backcrossed

7.4.1. Disruption to the expression of linked genes as an artefact of the D910A mutation

The engineering of the p110 δ KI mutation represented a step forward in the generation of mouse models because the p110 δ protein is still transcribed and translated at WT levels, just in an inactive form. The ability to engineer a gene to encode an inactive protein resulted in a cellular state that was predicted to closely mimic the effects of pharmacological inactivation. This circumvented a number of off-target effects occurring in earlier deletion techniques, which included the induction of compensatory changes to the other PI3K isoforms and regulatory subunits. Although the inactivation of p110 δ function was achieved by the introduction of a point mutation, other elements including a lox-p site and a myc-tag were also inserted into the region. We reasoned that either the process of introducing the point mutation or associated elements or alternatively the actual presence of these elements in the region, could disrupt expression of nearby genes. If the differential regulation of these linked genes is occurring as a result of the mutation or associated elements, we proposed two mechanisms that could be involved. Either a regulatory sequence such as a miRNA could have been disrupted or potentially the epigenetics of the region could have been disturbed. We do not consider these possibilities further here as we believe there is sufficient evidence to support an alternative hypothesis, so that these become highly unlikely.

7.4.2. Differential regulation represents the retention of 129-derived genetic material

It is well known that phenotypic variation between inbred mice strains and even between sub-strains occurs in part as a result of genetic polymorphisms which affect gene expression [185]. A visual example of genetic variation between mouse strains is coat colour; some mice strains are white (BALB/c), whilst others are agouti (129) and others are black (C57BL/6). Of course, it is not only visible phenotypes that are affected by genetic variation; behavioural traits and indeed cellular function can be affected by differential expression of genes. For instance, a recent publication detailed the investigation of the twofold lower expression of integrin- α 2 in the FVB mouse strain as compared to several other inbred strains, which amongst themselves had similar expression of this protein [186]. We

theorised that the differential regulation of genes flanking *Pik3cd* may represent a strain difference between the expression of these genes in the strain in which the mutation was first generated and the strain in which the mutation is maintained. This we reasoned could be the case if the region flanking *Pik3cd* had been maintained in its original form, which was derived from a 129 strain mouse, whilst this region in a WT mouse contains genetic material of the C57BL/6 mouse. In this case, the differential regulation of genes in this region would be entirely unrelated to the effects of inactivating p110 δ . In fact, after some research, it became apparent that this retention of ES cell derived genetic material flanking a mutation in a genetically engineered mouse line is a recognised phenomenon. Moreover, it is an almost unavoidable consequence of the strategy used to generate the p110 δ KI mice. If we consider the protocol used to generate these mice, this phenomenon becomes much clearer. The strategy will be described in generic terms for ease of explanation and has been described in detail in several publications [187].

7.4.2.1. Strategy used to generate mutant mice

The mutation is initially generated *in vitro* in an embryonic stem (ES) cell line derived from a 129 strain mouse using a targeting vector containing the gene of interest carrying the desired mutation and a neomycin selection cassette [Figure 7.4]. The targeting vector was cloned from 129 strain genetic material to ensure it was homologous to the region in the ES cell. This targeting vector is recombined into the ES cell DNA in the appropriate position as a result of homologous recombination [Figure 7.4a]. Those ES cells in which the targeting vector has been integrated are selected for using treatment with neomycin [Figure 7.4a]. The 129-derived ES cell carrying the point mutation is then microinjected into a blastocyst derived from a C57BL/6 mouse and the blastocyst is subsequently implanted in a C57BL/6 mouse for gestation [Figure 7.4b & c]. Within the resulting litter, some pups will be genetically heterogeneous because they will consist of cells derived from the donor ES cell (129 genetic material) and also cells derived from the original recipient blastocyst (C57BL/6 genetic material) [Figure 7.4d].

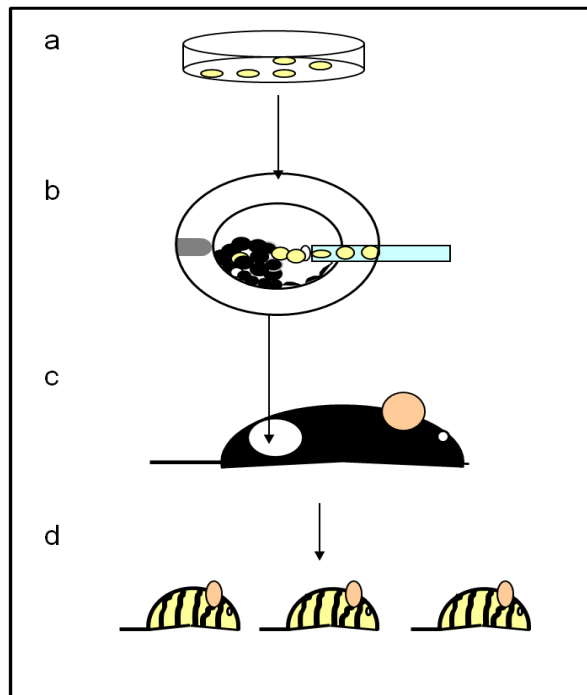


Figure 7.4. Schematic of the generation of genetically heterogenous/chimerical mice using 129-derived ES cell line and a C57BL/6 blastocyst. **a.** The 129-derived ES cells are electroporated with targeting construct, which is then integrated by homologous recombination. ES cells in which the construct has been integrated are selected by neomycin treatment. **b.** The selected ES cells are injected into a blastocyst derived from a C57BL/6 mouse **c.** The blastocyst is microinjected into a pseudopregnant C57BL/6 mouse. **d.** Chimeric progeny carrying both donor 129 genetic material and recipient C57BL/6 genetic material are born. [Figure reproduced and adapted with permission from Dr Martin-Berenjeno].

The crucial next step is to achieve germline transmission of the mutation. This is achieved by crossing the chimeric pups [Figure 7.5a]. The next generation will include mice that are homozygous, heterozygous and WT for the targeted locus in Mendelian ratios [Figure 7.5a]. Having transmitted the mutation to the germ line, the final stage is to purify or fix the genetic background, as the mice are currently heterogeneous for 129 and C57BL/6 genetic material. This mixed genetic background could confound phenotypic analysis of the effects of the mutation. Purification of the genetic background is performed by backcrossing the mutant mice to the recipient mouse strain (C57BL/6) for numerous generations [Figure 7.5b].

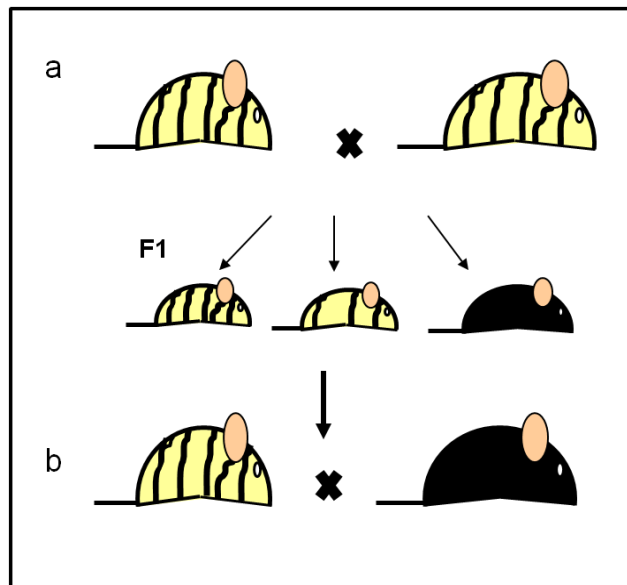


Figure 7.5. Schematic of strategy to generate congenic mutant mouse line. **a.** Cross the chimeric mice resulting germ line transmission of the mutation and an F1 generation consisting of pups heterozygous, homozygous and WT for the targeted gene. **b.** The homozygous mice must be backcrossed to inbred C57BL/6 mice for several generations to minimise 129-derived genetic material in the mice. [Figure reproduced and adapted with permission from Dr Martin-Berenjeno].

With every generation backcrossed to recipient homogenous C57BL/6 mice there is a logarithmic decrease in the donor (129) genetic material in the progeny due to meiotic recombination. As a result, the number of loci that are homozygous for C57BL/6 alleles will consistently increase every generation, whilst any loci heterozygous for the 129 alleles will diminish [Figure 7.6].

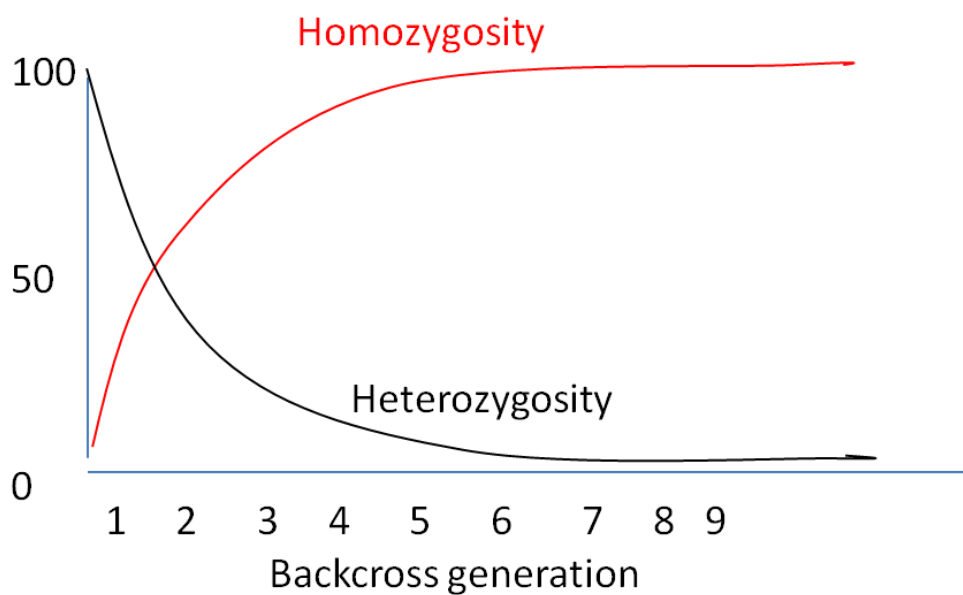


Figure 7.6. Increasing C57BL/6 allele homozygosity and concomitant decrease in heterozygosity for the donor 129 alleles with additional backcrosses. Mutant mice are backcrossed for multiple generations in order to reach genetic homozygosity. With each successive cross the mice reduce the number of 129 alleles remaining in the genome.

The ultimate aim of these backcrosses is to generate a congenic strain, allowing the effects of the mutation to be determined in a homogenous genetic background. The definition of a congenic strain is one in which all genetic material is identical with the exception of the target locus and its flanking region. Herein lies the crux of the problem: however many generations you backcross mice to the recipient strain, it is virtually impossible to eliminate the donor genetic material flanking the targeted locus. This region that is retained in the donor form is referred to as the differential chromosomal segment. Once the mice have been backcrossed for more than five generations, the approximate length of the differential chromosomal segment in centimorgans (cM) can be calculated using the equation $200/N$. This retention of donor genetic material occurs because continual selection for the genetically linked mutation causes linkage disequilibrium in the region surrounding a targeted locus. To be precise, the probability of recombination is inversely related to the distance between the site and the selected gene, which results in the preferential retention of donor 129 genetic material in the flanking region. This is therefore likely to account for the differential expression of the genes that we identified flanking *Pik3cd*. This assumes that these genes are differentially expressed in macrophages derived from WT 129 strain mice compared to those derived from WT strain C57BL/6 mice. We suggest that comparing the expression of these genes in the aforementioned macrophages would test if this were true. In addition, by utilising known DNA markers that vary between 129 and C57BL/6 strain mice the strain origin of the differential chromosomal segment in WT controls and in p110 δ KI mice could be determined.

7.4.2.2. Implications of retention of 129 genetic material flanking a targeted gene

The potential confusion that can be caused by the presence of these differential chromosomal segments has been reviewed in terms of its impact on behavioural and neuroscience studies [188-189]. In this field, the problem is confounded by the fact that the different mice strains have different behavioural traits, and moreover, the fact that the 129 donor strain is the most distinct strains in terms of behaviour and neuro-anatomy [190]. Gerlai points out that in a number of early

publications regarding the behavioural impact of null mutations, the null-mutant mouse phenotypes were actually similar to those observed in the mouse strain from which the donor ES cell line was derived (129) [189] & references herein]. This led Gerlai to suggest that the phenotypes are regulated by genes in the region flanking the targeted mutation rather than by the mutation itself [189]. When the strategy described above was used to generate a mouse line with a mutation in the K-Cl co-transporter, this phenomenon was very visible [187, 191]. The K-Cl co-transporter is encoded by *Kcc2* on chromosome two, close to the location of the gene which determines fur coat colour. In the 129 mice from which the donor ES cell line was derived the fur colour gene encodes the agouti allele, whilst in C57BL/6 mice in which the *Kcc2* mutation was maintained, the gene encodes the black allele. As a result of the proximity of the genes and the linkage disequilibrium induced by selecting the mutation, fur coat colour and the *Kcc2* mutation co-segregated. Had this gene affected a behavioural trait or a biochemical process, the authors would have very probably attributed the effects to the *Kcc2* mutation. It is probable that this was irrelevant to the function of the K-Cl co-transporter and investigated further because it caused such a visible effect. The authors of this publication report that even after eleven generations of backcrossing, fur coat colour still co-segregated with the mutation [187]. It is significant that in fact, the gene encoding fur coat colour and the *Kcc* gene are 5 cM apart on chromosome two, and importantly, there are many genes between them and also on the other side of *Kcc2*, which will presumably also be retained in the 129 form.

By some estimates, after as many as sixteen backcrosses the size of the flanking region retained in the donor form can be as large as 16 cM. Indeed, one publication reported a significantly larger flanking region [192]. This retention of donor strain genetic material surround a mutation appears to have been largely forgotten, at least in biochemical and cellular research. This is despite several publications that highlight the problem, including the rather scathing review by Crusio in 2004 [188-189]. Indeed, the assumption that phenotypic differences between mutants and WT controls are due to the mutation is pervasive in the world of mouse genetics and yet, in fact, there may be tens if not hundreds of genes also differing between the mutant and the WT control. This could account for, or contribute to, observed phenotypes of mutant mice. Thus, it is possible that there

are publications describing effects of mutations that are, in fact, independent of the mutation studied.

To our knowledge, there are no publications highlighting the impact that this retention of donor genetic material can have on the analysis of genome-wide expression analysis. Microarrays are now more affordable than ever and, furthermore, there is increasing pressure to maximise the insight gained from each mutant mouse strain generated. As such, we expect that the number of genome-wide expression studies analysing the effect of mutations on the transcriptome will continue to increase over the coming years. It is therefore imperative that scientists are made aware of this linkage disequilibrium, which results in retention of large regions of donor genetic material and its potential to lead to false positive results. Although the linkage of differentially regulated genes to *Pik3cd* was quite apparent in our data, we recognise that this was only by virtue of the limited number of genes affected by p110 δ , and to a lesser extent by the fact that these genes were not affected by IC87114. Hypothetically, if twelve out of 200 genes identified had been found located on chromosome four, we might not have taken this to be indicative of anything untoward. Assessment of the location of genes identified in a microarray study is not considered essential and we suspect that, more often than not, only the distribution across chromosomes rather than the specific location on the chromosomes is checked.

This of course is of concern as, we might have published the list of genes including the twelve linked to *Pik3cd*, as genes differentially regulated by p110 δ activity in macrophages. As a result, either the Centre for Cell Signalling or another laboratory could then have spent valuable resources and research time investigating a gene with absolutely no relationship to p110 δ activity. We propose that all analyses of the effects of a mutation generated in the described manner at the genome-wide expression level should include an assessment of the exact location of each of the genes identified, with a particular focus on whether any lie within the regions flanking the targeted locus. This is a trivial task thanks to the development of free online software that rapidly identifies significant enrichment of identified mapped probe sets across the entire genome or in a single locus with minimal user input [176].

Of course, we must also consider the implications this has for the results obtained in the genome-wide analysis of p110 δ KI macrophages compared to WT macrophages. First, based on the data and literature regarding genetics discussed above we conclude that it is highly likely that the genetic material flanking *Pik3cd* in the p110 δ KI mice is of 129 strain origin. Therefore based on this conclusion, we must assume that these twelve genes are not regulated by p110 δ activity. This suggests that, in fact, p110 δ inactivation has even less impact on transcription than our results initially suggested. This is consistent with the very limited effects that pharmacological inactivation of p110 δ has upon primary macrophage gene expression, although the genes identified differ. This conclusion does still need to be confirmed and we reason that comparing the expression of these linked differentially regulated genes in WT 129-derived macrophages and in WT C57BL/6 mice would resolve this.

Furthermore, the fact that this presumed retention of genetic material seems to result in differential regulation of twelve genes may have implications for data that has been obtained by studying the p110 δ KI mice. We should perhaps particularly scrutinise data regarding any phenotype(s) that are found to vary between mice strains, as this could be indicative of an independence from the actual mutation. In the case of the p110 δ KI mice, the only variable phenotype of which we are aware is the inflammatory colitis and the associated rectal prolapse. Inflammatory colitis is observed in p110 δ KI mice maintained in the C57BL/6 genetic background and results in rectal prolapse in female mice [123]. In BALB/c strain p110 δ KI mice the inflammatory colitis occurs at a later age and rectal prolapse is not observed [Unpublished data W. Pearce, Centre for Cell Signalling]. In this instance, the phenotype does occur but is observed at a later stage and, therefore, this may not be as a result of genes in the differential chromosomal segment. Instead, this may represent the effect of different alleles of modifier genes that affect the expression of the phenotype in C57BL/6 mice compared to in BALB/c mice as reviewed by Crusio in 2004 [188].

Characterisation of a PI3K mutant usually begins with observing *in vivo* phenotypes and subsequently the mechanism behind any dysfunction is investigated and delineated *ex vivo* using cells extracted from the mutant mice. This *ex vivo* analysis is usually carried out in conjunction with analysis of the

effects of isoform-selective inhibitors on WT cells, as was the case in this project. As a result, any effect on cell biology that is independent of the inactivation mutation would be highlighted by its absence in the drug treated WT cells. As such, in publications where the same effect is seen in response to treatment with a p110 δ -selective drug, one can be more confident that the effects are genuinely related to loss of p110 δ activity. To our knowledge this is the first instance in which genetic and pharmacological inactivation of a Class IA PI3K isoform have had dissimilar effects. There will, of course, be targets that are undruggable or targets for which drugs have not yet been developed, including the Class II PI3K isoforms for which comparisons to the effects of a selective inhibitor are not currently possible.

7.4.2.3. PGE of differentially regulated genes in p110 δ KI Tregs

Based on our data and assuming that our explanation is correct, we predicted that there would also be an enrichment of genes flanking *Pik3cd* in the list of genes found to be differentially regulated by Patton *et al.* in p110 δ KI Tregs [50]. We did indeed find an enrichment of genes in this region. Although it consisted of only four genes, *Vamp-3*, *Kif1b*, *Ubiad1* and *Slc25a33*, their proximity within a small area of chromosome four was found to be highly significant ($p = 3.1 \times 10^{-6}$). This finding certainly supports our theory that the region flanking *Pik3cd* may have been retained in the 129 form in the p110 δ KI mice. It is interesting that different genes were identified as differentially regulated in the p110 δ KI macrophages compared to in the p110 δ KI Tregs. We hypothesize that this may represent the different expression of genes in macrophages and Tregs, and suggest that in another cell

type the list of genes within this region that are differentially regulated might also be different.

7.4.2.4. Are linked genes in fact genuinely regulated by p110 δ activity?

Of course, until the above theory is proved we cannot exclude the seemingly unlikely possibility that these genes linked to *Pik3cd* are genuinely regulated downstream of p110 δ activity. To our knowledge, there are no examples of a protein regulating the expression of genes located proximal to its encoding gene. Nevertheless, it is not entirely inconceivable that some of these genes could be genuine targets and situated close to *Pik3cd* by chance.

7.5. Locus independent differential effects of genetic and pharmacological inactivation

We did not find that any of the genes differentially regulated in p110 δ KI macrophages were also differentially regulated in WT- IC87114 macrophages, including those that were independent of the *Pik3cd* locus. We confirmed this Affymetrix result by TaqMan[®], by checking that the expression of the seven of the genes found to be differentially regulated in the p110 δ KI macrophages were not significantly deregulated in WT-IC87114 macrophages. Importantly, we have confirmed by TaqMan and by western blot that the expression of *Rab6b*, a gene independent of *Pik3cd*, is not differentially expressed in WT-IC87114 macrophages. Hence, we conclude that there may well be multiple factors contributing to the different effects of pharmacological and genetic inactivation of p110 δ . At this stage, we cannot explain why the genes affected by IC87114 are not affected in p110 δ KI macrophages. It is possible that they are differentially expressed as a result of off-target effects of IC87114. To test this, it would be pertinent to differentiate p110 δ KI macrophages in the presence of IC87114 and, also to differentiate WT macrophages in the presence of other p110 δ selective inhibitors.

7.5.1. Why are unlinked genes also not affected by differentiation in IC87114?

We could conceive of a number of reasons why genes such as *Rab6b* are not differentially regulated macrophages differentiated in IC87114. We address the first possibility, which also relates to the generation of the original mutation in ES cells derived from 129 mice.

7.5.1.1. Are unlinked differentially regulated genes passenger loci in the p110 δ KI mouse line?

As well as retaining a large area flanking the targeted gene, congenic strains may also carry what are referred to as passenger loci, which are tiny sections of donor (129) genetic material at random positions dispersed throughout the genome. It is therefore possible that the allele of *Rab6b* that is carried within the p110 δ KI mutant mice is 129 in origin, whilst the allele in the WT control mice will of course be of C57BL/6 origin. This could be tested by comparing the expression of *Rab6b* in WT macrophages derived from 129 strain mice to expression in macrophages derived from C57BL/6 strain mice. Alternatively, if we took p110 δ KI mice and backcrossed them to the C57BL/6 inbred strain we should be able to obtain mice WT for p110 δ but with reduced expression of *Rab6b*, i.e. the expression of *Rab6b* would segregate independently of the *Pik3cd* mutant allele.

We set aside the first possibility to contemplate why else *Rab6b* expression might be differentially regulated in p110 δ KI macrophages but not in macrophages differentiated in IC87114. We noted that the main differences were the mode of inactivation and also the stage at which the inactivation of p110 δ occurred. This led us to generate two alternative hypotheses.

1. The regulation of the genes requires a minimal level of p110 δ activity which is absent in the p110 δ KI macrophages but is present in macrophages differentiated in IC87114

2. The regulation of *Rab6b* expression is pre-determined early in development prior to the bone marrow precursor stage at which we start IC87114 treatment

7.5.1.2. Is *Rab6b* developmentally regulated?

The activity of p110 δ may regulate the expression of *Rab6b* at an earlier stage in development within the bone marrow, prior to the formation of bone marrow precursor cells that we extract. If this is the case, then bone marrow precursor cells extracted from p110 δ KI macrophages will express lower levels of *Rab6b* than their WT counterparts. Potentially this regulation of *Rab6b* by p110 δ may not be cell-intrinsic; the activity of p110 δ in another cell type such as a stromal cell may be required to regulate its expression. In either instance, treatment of extracted bone marrow precursor cells with IC87114 would be ineffective. It would be interesting to observe whether bone marrow precursor cells or macrophages differentiated from them would have reduced expression of *Rab6b* if the mouse they were derived from was treated with IC87114 *in vivo*. It might be necessary to set up breeding pairs fed regularly with IC87114 and to continue to dose the mother with IC87114 throughout gestation and weaning.

7.5.1.3. Is *Rab6b* expression only affected by complete ablation of p110 δ activity?

Alternatively, we wonder if the key difference between the IC87114-treated macrophages and the p110 δ KI macrophages is simply the degree of residual p110 δ activity. Whilst genetic inactivation completely abrogates p110 δ activity, chronic treatment with IC87114 may well cause less than complete repression of p110 δ activity. It is plausible that the regulation of *Rab6b* requires only a minimal level of p110 δ activity. In which case, this could explain why IC87114 treatment does not suppress *Rab6b* expression. We reasoned that there was a logical way to begin investigating this hypothesis, by comparing the expression of *Rab6b* in macrophages derived from mice heterozygous for the D910A mutation. We reasoned that we could eliminate this possibility if these macrophages had reduced

levels of *Rab6b*, as they have only a fifty percent decrease in p110 δ activity. In fact, our preliminary data indicated that *Rab6b* expression is normal in heterozygous p110 δ KI macrophages. This is consistent with the possibility that complete ablation of p110 δ activity is necessary to repress *Rab6b* expression. In addition, this result is of relevance to our hypothesis that *Rab6b* expression may be developmentally regulated. Thus, the normal expression of *Rab6b* in heterozygous p110 δ KI macrophages supports the possibility that the transcription of *Rab6b* is only affected by more complete ablation of p110 δ activity, and is evidence against the developmental regulation of *Rab6b* but alone is insufficient to rule out this option. We also tested whether differentiation of macrophages in the presence of a higher dose of IC87114 (5 μ M instead of 1 μ M) would result in repression of *Rab6b* expression in WT macrophages. Our results at the protein level indicate that the expression of *Rab6b* was unaffected by differentiation in the presence of either 1 μ M or 5 μ M of IC87114. In order to fully investigate and eliminate this dose-dependent effect of p110 δ inactivation, several additional experiments would need to be performed. For example, we are interested to know whether *Rab6b* expression is reduced in p110 δ null macrophages or whether small interfering RNA (siRNA) targeting p110 δ would result in the repression of *Rab6b* expression. The latter would be challenging as primary macrophages are not readily permissive to siRNA techniques and the former is difficult as we do not have access to a p110 δ null mouse line at present.

7.6. Concluding remarks

The results of our investigation into the role of p110 δ in transcriptional regulation have been somewhat surprising. As a result of comparing the effects of genetic and pharmacological inactivation of p110 δ on the macrophage transcriptome, we have revealed that, at this level, these two modes of inactivation have entirely distinct effects. Furthermore, we have identified an enrichment of differentially regulated genes in p110 δ KI macrophages in the region flanking the *Pik3cd* gene. We currently support the hypothesis that the observed differences in the expression of these genes are representative of mouse strain-specific variation, caused by the retention of 129 mouse strain-derived genetic material. To the best of our knowledge, there are no publications revealing the impact of the retention of donor-mouse strain genetic material surrounding a mutation on genome-wide

expression analysis. We propose that our data highlights the need for mandatory assessment of the precise chromosomal location of genes found to be differentially regulated in mutant mice. This should ensure that differential regulation resulting from the retention of genetic material surrounding a mutation is not incorrectly associated with the direct effects of the mutation. The recent development of C57BL/6 ES cell lines that can be used to generate germline transmissible mutations, should also allow more mutations to be generated in ES cells of the same genetic background as the recipient mice. The mutant mice lines generated in this way will have homogenous genetic backgrounds and thus this problem should be circumvented.

We have found that *Rab6b* is differentially regulated in p110 δ KI macrophages, but is not differentially regulated in WT-IC87114 macrophages. Whilst another laboratory found that *Rab6b* was also reduced in p110 δ KI Tregs [50], we found that its expression was normal in p110 δ KI brain tissue. This suggests that the regulation of *Rab6b* expression by p110 δ might be restricted to leukocytes. We have confirmed that this differential regulation does result in a reduced expression of rab6b protein. We propose that this reduction of rab6b could contribute to the migratory defects in p110 δ KI macrophages. The mechanism by which genetic but not pharmacological inactivation affects *Rab6b* expression is currently unclear. As such, we are left with the uneasy question of whether the differential regulation of *Rab6b* in p110 δ KI macrophages is in fact genuinely related to inactivation of p110 δ .

Based on our data, we conclude that p110 δ inactivation by either genetic or pharmacological inactivation has a minimal effect on transcriptional regulation in growing macrophages and that very few (less than twelve genes) may be affected. This conclusion is based on the observation that less than twenty known genes are differentially regulated in either p110 δ KI macrophages or WT macrophages differentiated in the presence of IC87114. As a result of these unexpected findings, it has been difficult to identify a biomarker of p110 δ inactivation. Those genes differentially regulated in WT-IC87114 macrophages could, if validated, prove useful in this respect.

8. REFERENCES

1. Papakonstanti, E.A., *Distinct roles of class IA PI 3-kinase isoforms in primary and immortalised macrophages*, in *Journal of Cell Science*. 2008. **121**(pt24): p.4124-33.
2. Vanhaesebroeck, B. and M.D. Waterfield, *Signaling by distinct classes of phosphoinositide 3-kinases*. *Exp Cell Res*, 1999. **253**(1): p. 239-54.
3. Foster, F.M., C.J. Traer, S.M. Abraham, and M.J. Fry, *The phosphoinositide (PI) 3-kinase family*. *J Cell Sci*, 2003. **116**(Pt 15): p. 3037-40.
4. Vanhaesebroeck, B., J. Guillermet-Guibert, M. Graupera, and B. Bilanges, *The emerging mechanisms of isoform-specific PI3K signalling*. *Nat Rev Mol Cell Biol*, 2010. **11**(5): p. 329-41.
5. Dhand, R., K. Hara, I. Hiles, B. Bax, I. Gout, G. Panayotou, M.J. Fry, K. Yonezawa, M. Kasuga, and M.D. Waterfield, *PI 3-kinase: structural and functional analysis of intersubunit interactions*. *EMBO J*, 1994. **13**(3): p. 511-21.
6. Vanhaesebroeck, B., S.J. Leervers, G. Panayotou, and M.D. Waterfield, *Phosphoinositide 3-kinases: a conserved family of signal transducers*. *Trends Biochem Sci*, 1997. **22**(7): p. 267-72.
7. Stephens, L.R., A. Eguinoa, H. Erdjument-Bromage, M. Lui, F. Cooke, J. Coadwell, A.S. Smrcka, M. Thelen, K. Cadwallader, P. Tempst, and P.T. Hawkins, *The G beta gamma sensitivity of a PI3K is dependent upon a tightly associated adaptor, p101*. *Cell*, 1997. **89**(1): p. 105-14.
8. Krugmann, S., P.T. Hawkins, N. Pryer, and S. Braselmann, *Characterizing the interactions between the two subunits of the p101/p110gamma phosphoinositide 3-kinase and their role in the activation of this enzyme by G beta gamma subunits*. *J Biol Chem*, 1999. **274**(24): p. 17152-8.
9. Suire, S., J. Coadwell, G.J. Ferguson, K. Davidson, P. Hawkins, and L. Stephens, *p84, a new Gbetagamma-activated regulatory subunit of the type IB phosphoinositide 3-kinase p110gamma*. *Curr Biol*, 2005. **15**(6): p. 566-70.
10. Guillermet-Guibert, J., K. Bjorklof, A. Salpekar, C. Gonella, F. Ramadani, A. Bilancio, S. Meek, A.J. Smith, K. Okkenhaug, and B. Vanhaesebroeck, *The p110beta isoform of phosphoinositide 3-kinase signals downstream of G protein-coupled receptors and is functionally redundant with p110gamma*. *Proc Natl Acad Sci U S A*, 2008. **105**(24): p. 8292-7.
11. Hazeki, O., T. Okada, H. Kurosu, S. Takasuga, T. Suzuki, and T. Katada, *Activation of PI 3-kinase by G protein betagamma subunits*. *Life Sci*, 1998. **62**(17-18): p. 1555-9.
12. Bi, L., I. Okabe, D.J. Bernard, A. Wynshaw-Boris, and R.L. Nussbaum, *Proliferative defect and embryonic lethality in mice homozygous for a deletion in the p110alpha subunit of phosphoinositide 3-kinase*. *J Biol Chem*, 1999. **274**(16): p. 10963-8.

13. Vanhaesebroeck, B., M.J. Welham, K. Kotani, R. Stein, P.H. Warne, M.J. Zvelebil, K. Higashi, S. Volinia, J. Downward, and M.D. Waterfield, *P110delta, a novel phosphoinositide 3-kinase in leukocytes*. Proc Natl Acad Sci U S A, 1997. **94**(9): p. 4330-5.
14. Chantry, D., A. Vojtek, A. Kashishian, D.A. Holtzman, C. Wood, P.W. Gray, J.A. Cooper, and M.F. Hoekstra, *p110delta, a novel phosphatidylinositol 3-kinase catalytic subunit that associates with p85 and is expressed predominantly in leukocytes*. J Biol Chem, 1997. **272**(31): p. 19236-41.
15. Eickholt, B.J., A.I. Ahmed, M. Davies, E.A. Papakonstanti, W. Pearce, M.L. Starkey, A. Bilancio, A.C. Need, A.J. Smith, S.M. Hall, F.P. Hamers, K.P. Giese, E.J. Bradbury, and B. Vanhaesebroeck, *Control of axonal growth and regeneration of sensory neurons by the p110delta PI 3-kinase*. PLoS One, 2007. **2**(9): p. e869.
16. Sawyer, C., J. Sturge, D.C. Bennett, M.J. O'Hare, W.E. Allen, J. Bain, G.E. Jones, and B. Vanhaesebroeck, *Regulation of breast cancer cell chemotaxis by the phosphoinositide 3-kinase p110delta*. Cancer Res, 2003. **63**(7): p. 1667-75.
17. Carpenter, C.L., K.R. Auger, M. Chanudhuri, M. Yoakim, B. Schaffhausen, S. Shoelson, and L.C. Cantley, *Phosphoinositide 3-kinase is activated by phosphopeptides that bind to the SH2 domains of the 85-kDa subunit*. J Biol Chem, 1993. **268**(13): p. 9478-83.
18. Yu, J., C. Wjasow, and J.M. Backer, *Regulation of the p85/p110alpha phosphatidylinositol 3'-kinase. Distinct roles for the n-terminal and c-terminal SH2 domains*. J Biol Chem, 1998. **273**(46): p. 30199-203.
19. Czupalla, C., M. Culo, E.C. Muller, C. Brock, H.P. Reusch, K. Spicher, E. Krause, and B. Nurnberg, *Identification and characterization of the autophosphorylation sites of phosphoinositide 3-kinase isoforms beta and gamma*. J Biol Chem, 2003. **278**(13): p. 11536-45.
20. Schlessinger, J., *Cell signaling by receptor tyrosine kinases*. Cell, 2000. **103**(2): p. 211-25.
21. Mayer, B.J., R. Ren, K.L. Clark, and D. Baltimore, *A putative modular domain present in diverse signaling proteins*. Cell, 1993. **73**(4): p. 629-630.
22. Kholodenko, B.N., J.B. Hoek, and H.V. Westerhoff, *Why cytoplasmic signalling proteins should be recruited to cell membranes*. Trends in Cell Biology, 2000. **10**(5): p. 173-178.
23. Lee, J.O., H. Yang, M.M. Georgescu, A. Di Cristofano, T. Maehama, Y. Shi, J.E. Dixon, P. Pandolfi, and N.P. Pavletich, *Crystal structure of the PTEN tumor suppressor: implications for its phosphoinositide phosphatase activity and membrane association*. Cell, 1999. **99**(3): p. 323-34.
24. Wisniewski, D., A. Strife, S. Swendeman, H. Erdjument-Bromage, S. Geromanos, W.M. Kavanaugh, P. Tempst, and B. Clarkson, *A novel SH2-containing phosphatidylinositol 3,4,5-trisphosphate 5-phosphatase (SHIP2) is constitutively tyrosine phosphorylated and associated with src homologous and collagen gene (SHC) in chronic myelogenous leukemia progenitor cells*. Blood, 1999. **93**(8): p. 2707-20.
25. Muraille, E., X. Pesesse, C. Kuntz, and C. Erneux, *Distribution of the src-homology-2-domain-containing inositol 5-phosphatase SHIP-2 in both non-*

- haemopoietic and haemopoietic cells and possible involvement of SHIP-2 in negative signalling of B-cells.* Biochem J, 1999. **342 Pt 3**: p. 697-705.
26. Backers, K., D. Blero, N. Paternotte, J. Zhang, and C. Erneux, *The termination of PI3K signalling by SHIP1 and SHIP2 inositol 5-phosphatases.* Adv Enzyme Regul, 2003. **43**: p. 15-28.
 27. Alessi, D.R., M. Andjelkovic, B. Caudwell, P. Cron, N. Morrice, P. Cohen, and B.A. Hemmings, *Mechanism of activation of protein kinase B by insulin and IGF-1.* EMBO J, 1996. **15**(23): p. 6541-51.
 28. Alessi, D.R., S.R. James, C.P. Downes, A.B. Holmes, P.R. Gaffney, C.B. Reese, and P. Cohen, *Characterization of a 3-phosphoinositide-dependent protein kinase which phosphorylates and activates protein kinase Balpha.* Curr Biol, 1997. **7**(4): p. 261-9.
 29. Song, G., G. Ouyang, and S. Bao, *The activation of Akt/PKB signaling pathway and cell survival.* Journal of Cellular and Molecular Medicine, 2005. **9**(1): p. 59-71.
 30. Testa, J.R. and P.N. Tsichlis, *AKT signaling in normal and malignant cells.* Oncogene, 2005. **24**(50): p. 7391-7393.
 31. Engelman, J.A., J. Luo, and L.C. Cantley, *The evolution of phosphatidylinositol 3-kinases as regulators of growth and metabolism.* Nat Rev Genet, 2006. **7**(8): p. 606-19.
 32. Foukas, L.C., M. Claret, W. Pearce, K. Okkenhaug, S. Meek, E. Peskett, S. Sancho, A.J. Smith, D.J. Withers, and B. Vanhaesebroeck, *Critical role for the p110alpha phosphoinositide-3-OH kinase in growth and metabolic regulation.* Nature, 2006. **441**(7091): p. 366-70.
 33. Fang, X., S.X. Yu, Y. Lu, R.C. Bast, Jr., J.R. Woodgett, and G.B. Mills, *Phosphorylation and inactivation of glycogen synthase kinase 3 by protein kinase A.* Proc Natl Acad Sci U S A, 2000. **97**(22): p. 11960-5.
 34. Zoncu, R., A. Efeyan, and D.M. Sabatini, *mTOR: from growth signal integration to cancer, diabetes and ageing.* Nat Rev Mol Cell Biol, 2011. **12**(1): p. 21-35.
 35. Salih, D.A.M. and A. Brunet, *FoxO transcription factors in the maintenance of cellular homeostasis during aging.* Current Opinion in Cell Biology, 2008. **20**(2): p. 126-136.
 36. Pugazhenti, S., A. Nesterova, C. Sable, K.A. Heidenreich, L.M. Boxer, L.E. Heasley, and J.E. Reusch, *Akt/protein kinase B up-regulates Bcl-2 expression through cAMP-response element-binding protein.* J Biol Chem, 2000. **275**(15): p. 10761-6.
 37. Gilmore, T.D., *Introduction to NF-kappaB: players, pathways, perspectives.* Oncogene, 2006. **25**(51): p. 6680-4.
 38. Jacobs, M.D. and S.C. Harrison, *Structure of an IkappaBalpha/NF-kappaB complex.* Cell, 1998. **95**(6): p. 749-58.
 39. Wang, D. and A.S. Baldwin, *Activation of Nuclear Factor-kappaB-dependent Transcription by Tumor Necrosis Factor-kappa Is Mediated through Phosphorylation of RelA/p65 on Serine 529.* Journal of Biological Chemistry, 1998. **273**(45): p. 29411-29416.

40. Ozes, O.N., L.D. Mayo, J.A. Gustin, S.R. Pfeffer, L.M. Pfeffer, and D.B. Donner, *NF-kappaB activation by tumour necrosis factor requires the Akt serine-threonine kinase*. *Nature*, 1999. **401**(6748): p. 82-5.
41. Karin, M. and M. Delhase, *The I kappa B kinase (IKK) and NF-kappa B: key elements of proinflammatory signalling*. *Semin Immunol*, 2000. **12**(1): p. 85-98.
42. Sizemore, N., S. Leung, and G.R. Stark, *Activation of phosphatidylinositol 3-kinase in response to interleukin-1 leads to phosphorylation and activation of the NF-kappaB p65/RelA subunit*. *Mol Cell Biol*, 1999. **19**(7): p. 4798-805.
43. Madrid, L.V., C.Y. Wang, D.C. Guttridge, A.J. Schottelius, A.S. Baldwin, Jr., and M.W. Mayo, *Akt suppresses apoptosis by stimulating the transactivation potential of the RelA/p65 subunit of NF-kappaB*. *Mol Cell Biol*, 2000. **20**(5): p. 1626-38.
44. Wirleitner, B., G. Baier-Bitterlich, G. Hoffmann, W. Schobersberger, H. Wachter, and D. Fuchs, *Neopterin derivatives to activate NF-kappa B*. *Free Radic Biol Med*, 1997. **23**(1): p. 177-9.
45. Loi, S., B. Haibe-Kains, S. Majjaj, F. Lallemand, V. Durbecq, D. Larsimont, A.M. Gonzalez-Angulo, L. Pusztai, W.F. Symmans, A. Bardelli, P. Ellis, A.N. Tutt, C.E. Gillett, B.T. Hennessy, G.B. Mills, W.A. Phillips, M.J. Piccart, T.P. Speed, G.A. McArthur, and C. Sotiriou, *PIK3CA mutations associated with gene signature of low mTORC1 signaling and better outcomes in estrogen receptor-positive breast cancer*. *Proc Natl Acad Sci U S A*, 2010. **107**(22): p. 10208-13.
46. Cook, S.A., T. Matsui, L. Li, and A. Rosenzweig, *Transcriptional effects of chronic Akt activation in the heart*. *J Biol Chem*, 2002. **277**(25): p. 22528-33.
47. Dos Santos, S., A.I. Delattre, F. De Longueville, H. Bult, and M. Raes, *Gene expression profiling of LPS-stimulated murine macrophages and role of the NF-kappaB and PI3K/mTOR signaling pathways*. *Ann N Y Acad Sci*, 2007. **1096**: p. 70-7.
48. Dos Santos Mendes, S., A. Candi, M. Vansteenbrugge, M.-R. Pignon, H. Bult, K.Z. Boudjeltia, C. Munaut, and M. Raes, *Microarray analyses of the effects of NF-[kappa]B or PI3K pathway inhibitors on the LPS-induced gene expression profile in RAW264.7 cells: Synergistic effects of rapamycin on LPS-induced MMP9-overexpression*. *Cellular Signalling*, 2009. **21**(7): p. 1109-1122.
49. Ulici, V., C.G. James, K.D. Hoenselaar, and F. Beier, *Regulation of gene expression by PI3K in mouse growth plate chondrocytes*. *PLoS One*, 2010. **5**(1): p. e8866.
50. Patton, D.T., M.D. Wilson, W.C. Rowan, D.R. Soond, and K. Okkenhaug, *The PI3K p110delta regulates expression of CD38 on regulatory T cells*. *PLoS One*, 2011. **6**(3): p. e17359.
51. Graupera, M., J. Guillermet-Guibert, L.C. Foukas, L.K. Phng, R.J. Cain, A. Salpekar, W. Pearce, S. Meek, J. Millan, P.R. Cutillas, A.J. Smith, A.J. Ridley, C. Ruhrberg, H. Gerhardt, and B. Vanhaesebroeck, *Angiogenesis selectively requires the p110alpha isoform of PI3K to control endothelial cell migration*. *Nature*, 2008. **453**(7195): p. 662-6.
52. Marone, R., V. Cmiljanovic, B. Giese, and M.P. Wymann, *Targeting phosphoinositide 3-kinase: moving towards therapy*. *Biochim Biophys Acta*, 2008. **1784**(1): p. 159-85.

53. Samuels, Y., L.A. Diaz, Jr., O. Schmidt-Kittler, J.M. Cummins, L. Delong, I. Cheong, C. Rago, D.L. Huso, C. Lengauer, K.W. Kinzler, B. Vogelstein, and V.E. Velculescu, *Mutant PIK3CA promotes cell growth and invasion of human cancer cells*. *Cancer Cell*, 2005. **7**(6): p. 561-73.
54. Okkenhaug, K. and B. Vanhaesebroeck, *PI3K in lymphocyte development, differentiation and activation*. *Nat Rev Immunol*, 2003. **3**(4): p. 317-30.
55. Kharas, M.G., R. Okabe, J.J. Ganis, M. Gozo, T. Khandan, M. Paktinat, D.G. Gilliland, and K. Gritsman, *Constitutively active AKT depletes hematopoietic stem cells and induces leukemia in mice*. *Blood*, 2010. **115**(7): p. 1406-1415.
56. Park, S., N. Chapuis, J. Tamburini, V. Bardet, P. Cornillet-Lefebvre, L. Willems, A. Green, P. Mayeux, C. Lacombe, and D. Bouscary, *Role of the PI3K/AKT and mTOR signalling pathways in acute myeloid leukemia*. *Haematologica*, 2009: p. haematol.2009.013797.
57. Terauchi, Y., Y. Tsuji, S. Satoh, H. Minoura, K. Murakami, A. Okuno, K. Inukai, T. Asano, Y. Kaburagi, K. Ueki, H. Nakajima, T. Hanafusa, Y. Matsuzawa, H. Sekihara, Y. Yin, J.C. Barrett, H. Oda, T. Ishikawa, Y. Akanuma, I. Komuro, M. Suzuki, K. Yamamura, T. Kodama, H. Suzuki, S. Koyasu, S. Aizawa, K. Tobe, Y. Fukui, Y. Yazaki, and T. Kadowaki, *Increased insulin sensitivity and hypoglycaemia in mice lacking the p85 alpha subunit of phosphoinositide 3-kinase*. *Nat Genet*, 1999. **21**(2): p. 230-5.
58. Vlahos, C.J., W.F. Matter, K.Y. Hui, and R.F. Brown, *A specific inhibitor of phosphatidylinositol 3-kinase, 2-(4-morpholinyl)-8-phenyl-4H-1-benzopyran-4-one (LY294002)*. *J Biol Chem*, 1994. **269**(7): p. 5241-8.
59. Arcaro, A. and M.P. Wymann, *Wortmannin is a potent phosphatidylinositol 3-kinase inhibitor: the role of phosphatidylinositol 3,4,5-trisphosphate in neutrophil responses*. *Biochem J*, 1993. **296** (Pt 2): p. 297-301.
60. Gharbi, S.I., M.J. Zvelebil, S.J. Shuttleworth, T. Hancox, N. Saghir, J.F. Timms, and M.D. Waterfield, *Exploring the specificity of the PI3K family inhibitor LY294002*. *Biochem J*, 2007. **404**(1): p. 15-21.
61. Brunn, G.J., J. Williams, C. Sabers, G. Wiederrecht, J.C. Lawrence, Jr., and R.T. Abraham, *Direct inhibition of the signaling functions of the mammalian target of rapamycin by the phosphoinositide 3-kinase inhibitors, wortmannin and LY294002*. *EMBO J*, 1996. **15**(19): p. 5256-67.
62. Sadhu, C., B. Masinovsky, K. Dick, C.G. Sowell, and D.E. Staunton, *Essential role of phosphoinositide 3-kinase delta in neutrophil directional movement*. *J Immunol*, 2003. **170**(5): p. 2647-54.
63. Lee, K.S., S.J. Park, S.R. Kim, K.H. Min, S.M. Jin, K.D. Puri, and Y.C. Lee, *Phosphoinositide 3-kinase-[delta] inhibitor reduces vascular permeability in a murine model of asthma*. *Journal of Allergy and Clinical Immunology*, 2006. **118**(2): p. 403-409.
64. Sujobert, P., V. Bardet, P. Cornillet-Lefebvre, J.S. Hayflick, N. Prie, F. Verdier, B. Vanhaesebroeck, O. Muller, F. Pesce, N. Ifrah, M. Hunault-Berger, C. Berthou, B. Villemagne, E. Jourdan, B. Audhuy, E. Solary, B. Witz, J.L. Harousseau, C. Himmerlin, T. Lamy, B. Lioure, J.Y. Cahn, F. Dreyfus, P. Mayeux, C. Lacombe, and D. Bouscary, *Essential role for the p110delta isoform in phosphoinositide 3-kinase activation and cell proliferation in acute myeloid leukemia*. *Blood*, 2005. **106**(3): p. 1063-6.

65. Knight, Z.A., B. Gonzalez, M.E. Feldman, E.R. Zunder, D.D. Goldenberg, O. Williams, R. Loewith, D. Stokoe, A. Balla, B. Toth, T. Balla, W.A. Weiss, R.L. Williams, and K.M. Shokat, *A pharmacological map of the PI3-K family defines a role for p110alpha in insulin signaling*. *Cell*, 2006. **125**(4): p. 733-47.
66. Williams, O., B.T. Houseman, E.J. Kunkel, B. Aizenstein, R. Hoffman, Z.A. Knight, and K.M. Shokat, *Discovery of dual inhibitors of the immune cell PI3Ks p110delta and p110gamma: a prototype for new anti-inflammatory drugs*. *Chem Biol*, 2010. **17**(2): p. 123-34.
67. Suzuki, H., Y. Terauchi, M. Fujiwara, S. Aizawa, Y. Yazaki, T. Kadowaki, and S. Koyasu, *Xid-like immunodeficiency in mice with disruption of the p85alpha subunit of phosphoinositide 3-kinase*. *Science*, 1999. **283**(5400): p. 390-2.
68. Fruman, D.A., S.B. Snapper, C.M. Yballe, F.W. Alt, and L.C. Cantley, *Phosphoinositide 3-kinase knockout mice: role of p85alpha in B cell development and proliferation*. *Biochem Soc Trans*, 1999. **27**(4): p. 624-9.
69. Vanhaesebroeck, B., K. Ali, A. Bilancio, B. Geering, and L.C. Foukas, *Signalling by PI3K isoforms: insights from gene-targeted mice*. *Trends Biochem Sci*, 2005. **30**(4): p. 194-204.
70. Vanhaesebroeck, B., J.L. Rohn, and M.D. Waterfield, *Gene targeting: attention to detail*. *Cell*, 2004. **118**(3): p. 274-6.
71. Sasaki, T., J. Irie-Sasaki, R.G. Jones, A.J. Oliveira-dos-Santos, W.L. Stanford, B. Bolon, A. Wakeham, A. Itie, D. Bouchard, I. Kozieradzki, N. Joza, T.W. Mak, P.S. Ohashi, A. Suzuki, and J.M. Penninger, *Function of PI3Kgamma in thymocyte development, T cell activation, and neutrophil migration*. *Science*, 2000. **287**(5455): p. 1040-6.
72. Mijimolle, N., J. Velasco, P. Dubus, C. Guerra, C.A. Weinbaum, P.J. Casey, V. Campuzano, and M. Barbacid, *Protein farnesyltransferase in embryogenesis, adult homeostasis, and tumor development*. *Cancer Cell*, 2005. **7**(4): p. 313-24.
73. Cristofano, A.D., B. Pesce, C. Cordon-Cardo, and P.P. Pandolfi, *Pten is essential for embryonic development and tumour suppression*. *Nat Genet*, 1998. **19**(4): p. 348-355.
74. Stambolic, V., A. Suzuki, J.L. de la Pompa, G.M. Brothers, C. Mirtsos, T. Sasaki, J. Ruland, J.M. Penninger, D.P. Siderovski, and T.W. Mak, *Negative Regulation of PKB/Akt-Dependent Cell Survival by the Tumor Suppressor PTEN*. *Cell*, 1998. **95**(1): p. 29-39.
75. Ali, K., A. Bilancio, M. Thomas, W. Pearce, A.M. Gilfillan, C. Tkaczyk, N. Kuehn, A. Gray, J. Giddings, E. Peskett, R. Fox, I. Bruce, C. Walker, C. Sawyer, K. Okkenhaug, P. Finan, and B. Vanhaesebroeck, *Essential role for the p110delta phosphoinositide 3-kinase in the allergic response*. *Nature*, 2004. **431**(7011): p. 1007-11.
76. Jou, S.T., N. Carpino, Y. Takahashi, R. Piekorz, J.R. Chao, D. Wang, and J.N. Ihle, *Essential, nonredundant role for the phosphoinositide 3-kinase p110delta in signaling by the B-cell receptor complex*. *Mol Cell Biol*, 2002. **22**(24): p. 8580-91.
77. Leverrier, Y., K. Okkenhaug, C. Sawyer, A. Bilancio, B. Vanhaesebroeck, and A.J. Ridley, *Class I phosphoinositide 3-kinase p110beta is required for apoptotic cell and Fcgamma receptor-mediated phagocytosis by macrophages*. *J Biol Chem*, 2003. **278**(40): p. 38437-42.

78. Marques, M., A. Kumar, I. Cortes, A. Gonzalez-Garcia, C. Hernandez, M.C. Moreno-Ortiz, and A.C. Carrera, *Phosphoinositide 3-kinases p110alpha and p110beta regulate cell cycle entry, exhibiting distinct activation kinetics in G1 phase*. Mol Cell Biol, 2008. **28**(8): p. 2803-14.
79. Papakonstanti, E.A., A.J. Ridley, and B. Vanhaesebroeck, *The p110delta isoform of PI 3-kinase negatively controls RhoA and PTEN*. EMBO J, 2007. **26**(13): p. 3050-61.
80. Vanhaesebroeck, B., G.E. Jones, W.E. Allen, D. Zicha, R. Hooshmand-Rad, C. Sawyer, C. Wells, M.D. Waterfield, and A.J. Ridley, *Distinct PI(3)Ks mediate mitogenic signalling and cell migration in macrophages*. Nat Cell Biol, 1999. **1**(1): p. 69-71.
81. Bi, L., I. Okabe, D.J. Bernard, and R.L. Nussbaum, *Early embryonic lethality in mice deficient in the p110beta catalytic subunit of PI 3-kinase*. Mamm Genome, 2002. **13**(3): p. 169-72.
82. Hirsch, E., E. Ciruolo, A. Ghigo, and C. Costa, *Taming the PI3K team to hold inflammation and cancer at bay*. Pharmacol Ther, 2008. **118**(2): p. 192-205.
83. Jackson, S.P., S.M. Schoenwaelder, I. Goncalves, W.S. Nesbitt, C.L. Yap, C.E. Wright, V. Kenche, K.E. Anderson, S.M. Dopheide, Y. Yuan, S.A. Sturgeon, H. Prabakaran, P.E. Thompson, G.D. Smith, P.R. Shepherd, N. Daniele, S. Kulkarni, B. Abbott, D. Saylik, C. Jones, L. Lu, S. Giuliano, S.C. Hughan, J.A. Angus, A.D. Robertson, and H.H. Salem, *PI 3-kinase p110beta: a new target for antithrombotic therapy*. Nat Med, 2005. **11**(5): p. 507-14.
84. Okkenhaug, K., A. Bilancio, G. Farjot, H. Priddle, S. Sancho, E. Peskett, W. Pearce, S.E. Meek, A. Salpekar, M.D. Waterfield, A.J. Smith, and B. Vanhaesebroeck, *Impaired B and T cell antigen receptor signaling in p110delta PI 3-kinase mutant mice*. Science, 2002. **297**(5583): p. 1031-4.
85. Rolf, J., S.E. Bell, D. Kovessi, M.L. Janas, D.R. Soond, L.M.C. Webb, S. Santinelli, T. Saunders, B. Hebeis, N. Killeen, K. Okkenhaug, and M. Turner, *Phosphoinositide 3-Kinase Activity in T Cells Regulates the Magnitude of the Germinal Center Reaction*. The Journal of Immunology, 2010. **185**(7): p. 4042-4052.
86. Patton, D.T., O.A. Garden, W.P. Pearce, L.E. Clough, C.R. Monk, E. Leung, W.C. Rowan, S. Sancho, L.S. Walker, B. Vanhaesebroeck, and K. Okkenhaug, *Cutting edge: the phosphoinositide 3-kinase p110 delta is critical for the function of CD4+CD25+Foxp3+ regulatory T cells*. J Immunol, 2006. **177**(10): p. 6598-602.
87. Costa, C. and E. Hirsch, *More Than Just Kinases: The Scaffolding Function of PI3K*. Curr Top Microbiol Immunol, 2010. **346**: p. 171-81.
88. Thomas, M.S., J.S. Mitchell, C.C. DeNucci, A.L. Martin, and Y. Shimizu, *The p110gamma isoform of phosphatidylinositol 3-kinase regulates migration of effector CD4 T lymphocytes into peripheral inflammatory sites*. J Leukoc Biol, 2008. **84**(3): p. 814-23.
89. Alcazar, I., M. Marques, A. Kumar, E. Hirsch, M. Wymann, A.C. Carrera, and D.F. Barber, *Phosphoinositide 3-kinase gamma participates in T cell receptor-induced T cell activation*. J Exp Med, 2007. **204**(12): p. 2977-87.
90. Hume, D.A., *The mononuclear phagocyte system*. Current Opinion in Immunology, 2006. **18**(1): p. 49-53.

91. Mackay, C.R., *Chemokines: immunology's high impact factors*. Nat Immunol, 2001. **2**(2): p. 95-101.
92. Kamperdijk, E.W., M.A. Verdaasdonk, and R.H. Beelen, *Expression and function of MHC class II antigens on macrophages and dendritic cells*. Adv Exp Med Biol, 1988. **237**: p. 789-93.
93. Akira, S., K. Takeda, and T. Kaisho, *Toll-like receptors: critical proteins linking innate and acquired immunity*. Nat Immunol, 2001. **2**(8): p. 675-80.
94. Beutler, B., I.W. Milsark, and A.C. Cerami, *Passive immunization against cachectin/tumor necrosis factor protects mice from lethal effect of endotoxin*. Science, 1985. **229**(4716): p. 869-71.
95. Tracey, K.J., Y. Fong, D.G. Hesse, K.R. Manogue, A.T. Lee, G.C. Kuo, S.F. Lowry, and A. Cerami, *Anti-cachectin/TNF monoclonal antibodies prevent septic shock during lethal bacteraemia*. Nature, 1987. **330**(6149): p. 662-4.
96. Li, M.H., S.C. Seatter, R. Manthei, M. Bubrick, and M.A. West, *Macrophage Endotoxin Tolerance: Effect of TNF or Endotoxin Pretreatment*. Journal of Surgical Research, 1994. **57**(1): p. 85-92.
97. Karima, R., S. Matsumoto, H. Higashi, and K. Matsushima, *The molecular pathogenesis of endotoxic shock and organ failure*. Mol Med Today, 1999. **5**(3): p. 123-32.
98. Poltorak, A., X. He, I. Smirnova, M.Y. Liu, C. Van Huffel, X. Du, D. Birdwell, E. Alejos, M. Silva, C. Galanos, M. Freudenberg, P. Ricciardi-Castagnoli, B. Layton, and B. Beutler, *Defective LPS signaling in C3H/HeJ and C57BL/10ScCr mice: mutations in Tlr4 gene*. Science, 1998. **282**(5396): p. 2085-8.
99. Qureshi, S.T., L. Lariviere, G. Leveque, S. Clermont, K.J. Moore, P. Gros, and D. Malo, *Endotoxin-tolerant mice have mutations in Toll-like receptor 4 (Tlr4)*. J Exp Med, 1999. **189**(4): p. 615-25.
100. Hoshino, K., O. Takeuchi, T. Kawai, H. Sanjo, T. Ogawa, Y. Takeda, K. Takeda, and S. Akira, *Cutting edge: Toll-like receptor 4 (TLR4)-deficient mice are hyporesponsive to lipopolysaccharide: evidence for TLR4 as the Lps gene product*. J Immunol, 1999. **162**(7): p. 3749-52.
101. Haziot, A., E. Ferrero, F. Köntgen, N. Hijiya, S. Yamamoto, J. Silver, C.L. Stewart, and S.M. Goyert, *Resistance to Endotoxin Shock and Reduced Dissemination of Gram-Negative Bacteria in CD14-Deficient Mice*. Immunity, 1996. **4**(4): p. 407-414.
102. Moore, K.J., L.P. Andersson, R.R. Ingalls, B.G. Monks, R. Li, M.A. Arnaout, D.T. Golenbock, and M.W. Freeman, *Divergent Response to LPS and Bacteria in CD14-Deficient Murine Macrophages*. J Immunol, 2000. **165**(8): p. 4272-4280.
103. Nagai, Y., S. Akashi, M. Nagafuku, M. Ogata, Y. Iwakura, S. Akira, T. Kitamura, A. Kosugi, M. Kimoto, and K. Miyake, *Essential role of MD-2 in LPS responsiveness and TLR4 distribution*. Nat Immunol, 2002. **3**(7): p. 667-72.
104. Kawai, T., O. Adachi, T. Ogawa, K. Takeda, and S. Akira, *Unresponsiveness of MyD88-deficient mice to endotoxin*. Immunity, 1999. **11**(1): p. 115-22.

105. Li, S., A. Strelow, E.J. Fontana, and H. Wesche, *IRAK-4: a novel member of the IRAK family with the properties of an IRAK-kinase*. Proc Natl Acad Sci U S A, 2002. **99**(8): p. 5567-72.
106. Akira, S., *Toll-like receptors: lessons from knockout mice*. Biochem Soc Trans, 2000. **28**(5): p. 551-6.
107. Guha, M. and N. Mackman, *LPS induction of gene expression in human monocytes*. Cell Signal, 2001. **13**(2): p. 85-94.
108. Martin, M., R.E. Schifferle, N. Cuesta, S.N. Vogel, J. Katz, and S.M. Michalek, *Role of the phosphatidylinositol 3 kinase-Akt pathway in the regulation of IL-10 and IL-12 by Porphyromonas gingivalis lipopolysaccharide*. J Immunol, 2003. **171**(2): p. 717-25.
109. Arbibe, L., J.-P. Mira, N. Teusch, L. Kline, M. Guha, N. Mackman, P.J. Godowski, R.J. Ulevitch, and U.G. Knaus, *Toll-like receptor 2-mediated NF-[kappa]B activation requires a Rac1-dependent pathway*. Nat Immunol, 2000. **1**(6): p. 533-540.
110. Ojaniemi, M., V. Glumoff, K. Harju, M. Liljeroos, K. Vuori, and M. Hallman, *Phosphatidylinositol 3-kinase is involved in Toll-like receptor 4-mediated cytokine expression in mouse macrophages*. Eur J Immunol, 2003. **33**(3): p. 597-605.
111. Park, Y.C., C.H. Lee, H.S. Kang, H.T. Chung, and H.D. Kim, *Wortmannin, a specific inhibitor of phosphatidylinositol-3-kinase, enhances LPS-induced NO production from murine peritoneal macrophages*. Biochem Biophys Res Commun, 1997. **240**(3): p. 692-6.
112. Tengku-Muhammad, T.S., T.R. Hughes, A. Cryer, and D.P. Ramji, *Involvement of both the tyrosine kinase and the phosphatidylinositol-3' kinase signal transduction pathways in the regulation of lipoprotein lipase expression in J774.2 macrophages by cytokines and lipopolysaccharide*. Cytokine, 1999. **11**(7): p. 463-468.
113. Thomas, K.W., M.M. Monick, J.M. Staber, T. Yarovinsky, A.B. Carter, and G.W. Hunninghake, *Respiratory syncytial virus inhibits apoptosis and induces NF-kappa B activity through a phosphatidylinositol 3-kinase-dependent pathway*. J Biol Chem, 2002. **277**(1): p. 492-501.
114. Low, P.C., R. Misaki, K. Schroder, A.C. Stanley, M.J. Sweet, R.D. Teasdale, B. Vanhaesebroeck, F.A. Meunier, T. Taguchi, and J.L. Stow, *Phosphoinositide 3-kinase delta regulates membrane fission of Golgi carriers for selective cytokine secretion*. J Cell Biol, 2010. **190**(6): p. 1053-65.
115. Manderson, A.P., J.G. Kay, L.A. Hammond, D.L. Brown, and J.L. Stow, *Subcompartments of the macrophage recycling endosome direct the differential secretion of IL-6 and TNF α* . The Journal of Cell Biology, 2007. **178**(1): p. 57-69.
116. Martin, M., K. Rehani, R.S. Jope, and S.M. Michalek, *Toll-like receptor-mediated cytokine production is differentially regulated by glycogen synthase kinase 3*. Nat Immunol, 2005. **6**(8): p. 777-84.
117. Braat, H., P. Rottiers, D.W. Hommes, N. Huyghebaert, E. Remaut, J.P. Remon, S.J. van Deventer, S. Neiryck, M.P. Peppelenbosch, and L. Steidler, *A phase I trial with transgenic bacteria expressing interleukin-10 in Crohn's disease*. Clin Gastroenterol Hepatol, 2006. **4**(6): p. 754-9.

118. Virca, G.D., S.Y. Kim, K.B. Glaser, and R.J. Ulevitch, *Lipopolysaccharide induces hyporesponsiveness to its own action in RAW 264.7 cells*. Journal of Biological Chemistry, 1989. **264**(36): p. 21951-21956.
119. Bowling, W.M., M.W. Flye, Y.Y. Qiu, and M.P. Callery, *Inhibition of phosphatidylinositol-3'-kinase prevents induction of endotoxin tolerance in vitro*. J Surg Res, 1996. **63**(1): p. 287-92.
120. Davidson, A. and B. Diamond, *Autoimmune diseases*. N Engl J Med, 2001. **345**(5): p. 340-50.
121. Hisamatsu, T., H. Ogata, and T. Hibi, *Innate immunity in inflammatory bowel disease: state of the art*. Curr Opin Gastroenterol, 2008. **24**(4): p. 448-54.
122. Munkholm, P., *Review article: the incidence and prevalence of colorectal cancer in inflammatory bowel disease*. Aliment Pharmacol Ther, 2003. **18 Suppl 2**: p. 1-5.
123. Uno, J.K., K.N. Rao, K. Matsuoka, S.Z. Sheikh, T. Kobayashi, F. Li, E.C. Steinbach, A.R. Sepulveda, B. Vanhaesebroeck, R.B. Sartor, and S.E. Plevy, *Altered Macrophage Function Contributes to Colitis in Mice Defective in the Phosphoinositide-3 Kinase Subunit p110[delta]*. Gastroenterology, 2010. **139**(5): p. 1642-1653.e6.
124. Arteaga, C.L., *Clinical development of phosphatidylinositol-3 kinase pathway inhibitors*. Curr Top Microbiol Immunol, 2010. **347**: p. 189-208.
125. Samuels, Y., Z. Wang, A. Bardelli, N. Silliman, J. Ptak, S. Szabo, H. Yan, A. Gazdar, S.M. Powell, G.J. Riggins, J.K. Willson, S. Markowitz, K.W. Kinzler, B. Vogelstein, and V.E. Velculescu, *High frequency of mutations of the PIK3CA gene in human cancers*. Science, 2004. **304**(5670): p. 554.
126. Courtney, K.D., R.B. Corcoran, and J.A. Engelman, *The PI3K Pathway As Drug Target in Human Cancer*. Journal of Clinical Oncology, 2010. **28**(6): p. 1075-1083.
127. Smith, A., J. Blois, H. Yuan, E. Aikawa, C. Ellson, J.L. Figueiredo, R. Weissleder, R. Kohler, M.B. Yaffe, L.C. Cantley, and L. Josephson, *The antiproliferative cytostatic effects of a self-activating viridin prodrug*. Mol Cancer Ther, 2009. **8**(6): p. 1666-75.
128. Cosemans, J.M., I.C. Munnix, R. Wetzker, R. Heller, S.P. Jackson, and J.W. Heemskerk, *Continuous signaling via PI3K isoforms beta and gamma is required for platelet ADP receptor function in dynamic thrombus stabilization*. Blood, 2006. **108**(9): p. 3045-52.
129. Edgar, K.A., J.J. Wallin, M. Berry, L.B. Lee, W.W. Prior, D. Sampath, L.S. Friedman, and M. Belvin, *Isoform-specific phosphoinositide 3-kinase inhibitors exert distinct effects in solid tumors*. Cancer Res, 2010. **70**(3): p. 1164-72.
130. Wee, S., D. Wiederschain, S.M. Maira, A. Loo, C. Miller, R. deBeaumont, F. Stegmeier, Y.M. Yao, and C. Lengauer, *PTEN-deficient cancers depend on PIK3CB*. Proc Natl Acad Sci U S A, 2008. **105**(35): p. 13057-62.
131. Cully, M., H. You, A.J. Levine, and T.W. Mak, *Beyond PTEN mutations: the PI3K pathway as an integrator of multiple inputs during tumorigenesis*. Nat Rev Cancer, 2006. **6**(3): p. 184-92.
132. Saal, L.H., K. Holm, M. Maurer, L. Memeo, T. Su, X. Wang, J.S. Yu, P.O. Malmstrom, M. Mansukhani, J. Enoksson, H. Hibshoosh, A. Borg, and R.

- Parsons, *PIK3CA mutations correlate with hormone receptors, node metastasis, and ERBB2, and are mutually exclusive with PTEN loss in human breast carcinoma*. *Cancer Res*, 2005. **65**(7): p. 2554-9.
133. Okkenhaug, K. and B. Vanhaesebroeck, *PI3K-signalling in B- and T-cells: insights from gene-targeted mice*. *Biochem Soc Trans*, 2003. **31**(Pt 1): p. 270-4.
 134. Ji, H., F. Rintelen, C. Waltzinger, D. Bertschy Meier, A. Bilancio, W. Pearce, E. Hirsch, M.P. Wymann, T. Ruckle, M. Camps, B. Vanhaesebroeck, K. Okkenhaug, and C. Rommel, *Inactivation of PI3Kgamma and PI3Kdelta distorts T-cell development and causes multiple organ inflammation*. *Blood*, 2007. **110**(8): p. 2940-7.
 135. Ali, K., M. Camps, W.P. Pearce, H. Ji, T. Ruckle, N. Kuehn, C. Pasquali, C. Chabert, C. Rommel, and B. Vanhaesebroeck, *Isoform-Specific Functions of Phosphoinositide 3-Kinases: p110δ but Not p110γ Promotes Optimal Allergic Responses In Vivo*. *The Journal of Immunology*, 2008. **180**(4): p. 2538-2544.
 136. Randis, T.M., K.D. Puri, H. Zhou, and T.G. Diacovo, *Role of PI3Kdelta and PI3Kgamma in inflammatory arthritis and tissue localization of neutrophils*. *Eur J Immunol*, 2008. **38**(5): p. 1215-24.
 137. Muller, C.I., C.W. Miller, W.K. Hofmann, M.E. Gross, C.S. Walsh, N. Kawamata, Q.T. Luong, and H.P. Koeffler, *Rare mutations of the PIK3CA gene in malignancies of the hematopoietic system as well as endometrium, ovary, prostate and osteosarcomas, and discovery of a PIK3CA pseudogene*. *Leuk Res*, 2007. **31**(1): p. 27-32.
 138. Rommel, C., B. Vanhaesebroeck, P.K. Vogt, and A. Khwaja, *PI3K as a Target for Therapy in Haematological Malignancies*, in *Phosphoinositide 3-kinase in Health and Disease*. 2011, Springer Berlin Heidelberg. p. 169-188.
 139. Kubota, Y., H. Ohnishi, A. Kitanaka, T. Ishida, and T. Tanaka, *Constitutive activation of PI3K is involved in the spontaneous proliferation of primary acute myeloid leukemia cells: direct evidence of PI3K activation*. *Leukemia*, 2004. **18**(8): p. 1438-1440.
 140. Min, Y.H., J.I. Eom, J.W. Cheong, H.O. Maeng, J.Y. Kim, H.K. Jeung, S.T. Lee, M.H. Lee, J.S. Hahn, and Y.W. Ko, *Constitutive phosphorylation of Akt/PKB protein in acute myeloid leukemia: its significance as a prognostic variable*. *Leukemia*, 2003. **17**(5): p. 995-997.
 141. Herman, S.E., R. Lapalombella, A.L. Gordon, A. Ramanunni, K.A. Blum, J. Jones, X. Zhang, B.J. Lannutti, K.D. Puri, N. Muthusamy, J.C. Byrd, and A.J. Johnson, *The role of phosphatidylinositol 3-kinase-delta in the immunomodulatory effects of lenalidomide in chronic lymphocytic leukemia*. *Blood*, 2011. **117**(16): p. 4323-7.
 142. Lannutti, B.J., S.A. Meadows, S.E. Herman, A. Kashishian, B. Steiner, A.J. Johnson, J.C. Byrd, J.W. Tyner, M.M. Loriaux, M. Deininger, B.J. Druker, K.D. Puri, R.G. Ulrich, and N.A. Giese, *CAL-101, a p110delta selective phosphatidylinositol-3-kinase inhibitor for the treatment of B-cell malignancies, inhibits PI3K signaling and cellular viability*. *Blood*, 2011. **117**(2): p. 591-4.
 143. Hoellenriegel, J., S.A. Meadows, M. Sivina, W.G. Wierda, H. Kantarjian, M.J. Keating, N. Giese, S. O'Brien, A. Yu, L.L. Miller, B.J. Lannutti, and J.A. Burger, *The phosphoinositide 3'-kinase delta inhibitor, CAL-101, inhibits B-cell*

- receptor signaling and chemokine networks in chronic lymphocytic leukemia.* Blood, 2011. **118**(13): p. 3603-12.
144. Jarvis, L.M., *PI3K At The Clinical Crossroads.* Chemical and Engineering News, 2011. **89**(15): p. 15-19.
 145. Morgan, C., J.W. Pollard, and E.R. Stanley, *Isolation and characterization of a cloned growth factor dependent macrophage cell line, BAC1.2F5.* J Cell Physiol, 1987. **130**(3): p. 420-7.
 146. Kaplan, G.a.M., B., *Properties of a murine monocytic tumour cell line J-774in vitro : Morphology and Endocytosis.* Experimental Cell Research, 1978. **115**: p. 53-61.
 147. Mauel, J. and V. Defendi, *Infection and transformation of mouse peritoneal macrophages by simian virus 40.* J Exp Med, 1971. **134**(2): p. 335-50.
 148. Raschke, W.C., S. Baird, P. Ralph, and I. Nakoinz, *Functional macrophage cell lines transformed by Abelson leukemia virus.* Cell, 1978. **15**(1): p. 261-7.
 149. Donahue, A.C., M.G. Kharas, D.A. Fruman, and H.A. Brown, *Measuring Phosphorylated Akt and Other Phosphoinositide 3-kinase-Regulated Phosphoproteins in Primary Lymphocytes,* in *Methods in Enzymology.* 2007, Academic Press. p. 131-154.
 150. Schroeder, A., O. Mueller, S. Stocker, R. Salowsky, M. Leiber, M. Gassmann, S. Lightfoot, W. Menzel, M. Granzow, and T. Ragg, *The RIN: an RNA integrity number for assigning integrity values to RNA measurements.* BMC Mol Biol, 2006. **7**: p. 3.
 151. Benjamini, Y. and Y. Hochberg, *Controlling the False Discovery Rate: A Practical and Powerful Approach to Multiple Testing.* Journal of the Royal Statistical Society. Series B (Methodological), 1995. **57**(1): p. 289-300.
 152. Bilancio, A., K. Okkenhaug, M. Camps, J.L. Emery, T. Ruckle, C. Rommel, and B. Vanhaesebroeck, *Key role of the p110delta isoform of PI3K in B-cell antigen and IL-4 receptor signaling: comparative analysis of genetic and pharmacologic interference with p110delta function in B cells.* Blood, 2006. **107**(2): p. 642-50.
 153. Foukas, L.C. and K. Okkenhaug, *Gene-targeting reveals physiological roles and complex regulation of the phosphoinositide 3-kinases.* Arch Biochem Biophys, 2003. **414**(1): p. 13-8.
 154. Nock, G., *Investigating the isoform-specific role of phosphoinositide 3-kinase p110delta,* in *Department of Biochemistry and Molecular Biology.* 2008, University College London: London. p. 288.
 155. Dunant, N. and K. Ballmer-Hofer, *Signalling by Src family kinases: lessons learnt from DNA tumour viruses.* Cell Signal, 1997. **9**(6): p. 385-93.
 156. Gottlieb, K.A. and L.P. Villarreal, *Natural biology of polyomavirus middle T antigen.* Microbiol Mol Biol Rev, 2001. **65**(2): p. 288-318 ; second and third pages, table of contents.
 157. Ichaso, N. and S.M. Dilworth, *Cell transformation by the middle T-antigen of polyoma virus.* Oncogene, 2001. **20**(54): p. 7908-16.
 158. Randle, D.H., F. Zindy, C.J. Sherr, and M.F. Roussel, *Differential effects of p19(Arf) and p16(Ink4a) loss on senescence of murine bone marrow-derived*

- preB cells and macrophages*. Proc Natl Acad Sci U S A, 2001. **98**(17): p. 9654-9.
159. Pollard, J.W., C.J. Morgan, P. Dello Sbarba, C. Cheers, and E.R. Stanley, *Independently arising macrophage mutants dissociate growth factor-regulated survival and proliferation*. Proc Natl Acad Sci U S A, 1991. **88**(4): p. 1474-8.
 160. Shlens, J., *A Tutorial on Principal Component Analysis*. 2005, Institute for Nonlinear Science, UCSD.
 161. Yeung, K.Y. and W.L. Ruzzo, *Principal component analysis for clustering gene expression data*. Bioinformatics, 2001. **17**(9): p. 763-774.
 162. Duxbury, M.S. and E.E. Whang, *RRM2 induces NF-kappaB-dependent MMP-9 activation and enhances cellular invasiveness*. Biochem Biophys Res Commun, 2007. **354**(1): p. 190-6.
 163. Mann, A.P., A. Verma, G. Sethi, B. Manavathi, H. Wang, J.Y. Fok, A.B. Kunnumakkara, R. Kumar, B.B. Aggarwal, and K. Mehta, *Overexpression of tissue transglutaminase leads to constitutive activation of nuclear factor-kappaB in cancer cells: delineation of a novel pathway*. Cancer Res, 2006. **66**(17): p. 8788-95.
 164. Shishodia, S., S. Majumdar, S. Banerjee, and B.B. Aggarwal, *Ursolic acid inhibits nuclear factor-kappaB activation induced by carcinogenic agents through suppression of IkappaBalpha kinase and p65 phosphorylation: correlation with down-regulation of cyclooxygenase 2, matrix metalloproteinase 9, and cyclin D1*. Cancer Res, 2003. **63**(15): p. 4375-83.
 165. Volanti, C., N. Hendrickx, J. Van Lint, J.Y. Matroule, P. Agostinis, and J. Piette, *Distinct transduction mechanisms of cyclooxygenase 2 gene activation in tumour cells after photodynamic therapy*. Oncogene, 2005. **24**(18): p. 2981-91.
 166. Gines, S., E. Ivanova, I.-S. Seong, C.A. Saura, and M.E. MacDonald, *Enhanced Akt Signaling Is an Early Pro-survival Response That Reflects N-Methyl-D-aspartate Receptor Activation in Huntington's Disease Knock-in Striatal Cells*. Journal of Biological Chemistry, 2003. **278**(50): p. 50514-50522.
 167. Du, K., S. Herzig, R.N. Kulkarni, and M. Montminy, *TRB3: A tribbles Homolog That Inhibits Akt/PKB Activation by Insulin in Liver*. Science, 2003. **300**(5625): p. 1574-1577.
 168. Bocko, D., A. Kosmaczewska, L. Ciszak, R. Teodorowska, and I. Frydecka, *CD28 costimulatory molecule--expression, structure and function*. Arch Immunol Ther Exp (Warsz), 2002. **50**(3): p. 169-77.
 169. Bansal, K., N. Kapoor, Y. Narayana, G. Puzo, M. Gilleron, and K.N. Balaji, *PIM2 Induced COX-2 and MMP-9 Expression in Macrophages Requires PI3K and Notch1 Signaling*. PLoS One, 2009. **4**(3): p. e4911.
 170. Xie, B., Z. Dong, and I. Fidler, *Regulatory mechanisms for the expression of type IV collagenases/gelatinases in murine macrophages*. The Journal of Immunology, 1994. **152**(7): p. 3637-3644.
 171. Srivastava, A.K., X. Qin, N. Wedhas, M. Arnush, T.A. Linkhart, R.B. Chadwick, and A. Kumar, *Tumor Necrosis Factor-beta Augments Matrix Metalloproteinase-9 Production in Skeletal Muscle Cells through the Activation of Transforming Growth Factor-activated Kinase 1 (TAK1)-dependent Signaling Pathway*. Journal of Biological Chemistry, 2007. **282**(48): p. 35113-35124.

172. Opdam, F., A. Echard, H. Croes, J. van den Hurk, R. van de Vorstenbosch, L. Ginsel, B. Goud, and J. Fransen, *The small GTPase Rab6B, a novel Rab6 subfamily member, is cell-type specifically expressed and localised to the Golgi apparatus*. J Cell Sci, 2000. **113**(15): p. 2725-2735.
173. Chen, D., J. Guo, T. Miki, M. Tachibana, and W.A. Gahl, *Molecular cloning and characterization of rab27a and rab27b, novel human rab proteins shared by melanocytes and platelets*. Biochem Mol Med, 1997. **60**(1): p. 27-37.
174. Kok, K., *Expression, action and function of phosphoinositide 3-kinase p110delta*, in *University Medical Centre*. 2006, Groningen University: Groningen. p. 125.
175. Scherer, A., *Batch effects and noise in microarray experiments : sources and solutions*. Wiley series in probability and statistics. 2009, Chichester, U.K.: J. Wiley.
176. De Preter, K., R. Barriot, F. Speleman, J. Vandesompele, and Y. Moreau, *Positional gene enrichment analysis of gene sets for high-resolution identification of overrepresented chromosomal regions*. Nucleic Acids Res, 2008. **36**(7): p. e43.
177. Knudson, A.G., Jr., *Mutation and cancer: statistical study of retinoblastoma*. Proc Natl Acad Sci U S A, 1971. **68**(4): p. 820-3.
178. Martinez, O., A. Schmidt, J. Salamero, B. Hoflack, M. Roa, and B. Goud, *The small GTP-binding protein rab6 functions in intra-Golgi transport*. J Cell Biol, 1994. **127**(6 Pt 1): p. 1575-88.
179. White, J., L. Johannes, F.d.r. Mallard, A. Girod, S. Grill, S. Reinsch, P. Keller, B. Tzschaschel, A. Echard, B. Goud, and E.H.K. Stelzer, *Rab6 Coordinates a Novel Golgi to ER Retrograde Transport Pathway in Live Cells*. The Journal of Cell Biology, 1999. **147**(4): p. 743-760.
180. Wanschers, B.F.J., R. van de Vorstenbosch, M.A. Schlager, D. Splinter, A. Akhmanova, C.C. Hoogenraad, B. Wieringa, and J.A.M. Fransen, *A role for the Rab6B Bicaudal-D1 interaction in retrograde transport in neuronal cells*. Experimental Cell Research, 2007. **313**(16): p. 3408-3420.
181. Luftman, K., N. Hasan, P. Day, D. Hardee, and C. Hu, *Silencing of VAMP3 inhibits cell migration and integrin-mediated adhesion*. Biochem Biophys Res Commun, 2009. **380**(1): p. 65-70.
182. Veale, K.J., C. Offenhauser, S.P. Whittaker, R.P. Estrella, and R.Z. Murray, *Recycling endosome membrane incorporation into the leading edge regulates lamellipodia formation and macrophage migration*. Traffic, 2010. **11**(10): p. 1370-9.
183. Veale, K.J., C. Offenhauser, and R.Z. Murray, *The role of the recycling endosome in regulating lamellipodia formation and macrophage migration*. Commun Integr Biol, 2011. **4**(1): p. 44-7.
184. Takamori, S., M. Holt, K. Stenius, E.A. Lemke, M. Gronborg, D. Riedel, H. Urlaub, S. Schenck, B. Brugger, P. Ringler, S.A. Muller, B. Rammner, F. Grater, J.S. Hub, B.L. De Groot, G. Mieskes, Y. Moriyama, J. Klingauf, H. Grubmuller, J. Heuser, F. Wieland, and R. Jahn, *Molecular anatomy of a trafficking organelle*. Cell, 2006. **127**(4): p. 831-46.

185. Simpson, E.M., C.C. Linder, E.E. Sargent, M.T. Davisson, L.E. Mobraaten, and J.J. Sharp, *Genetic variation among 129 substrains and its importance for targeted mutagenesis in mice*. Nat Genet, 1997. **16**(1): p. 19-27.
186. Li, T.-T., S. Larrucea, S. Souza, S.M. Leal, J.A. Lapez, E.M. Rubin, B. Nieswandt, and P.F. Bray, *Genetic variation responsible for mouse strain differences in integrin IL2 expression is associated with altered platelet responses to collagen*. Blood, 2004. **103**(9): p. 3396-3402.
187. Silver, L.M., *Mouse genetics : concepts and applications*. 1995, New York: Oxford University Press.
188. Crusio, W.E., *Flanking gene and genetic background problems in genetically manipulated mice*. Biol Psychiatry, 2004. **56**(6): p. 381-5.
189. Gerlai, R., *Gene-targeting studies of mammalian behavior: is it the mutation or the background genotype?* Trends Neurosci, 1996. **19**(5): p. 177-81.
190. Wolfer, D.P., U. Müller, M. Stagliar, and H.-P. Lipp, *Assessing the effects of the 129/Sv genetic background on swimming navigation learning in transgenic mutants: a study using mice with a modified [beta]-amyloid precursor protein gene*. Brain Research, 1997. **771**(1): p. 1-13.
191. Woo, N.S., J. Lu, R. England, R. McClellan, S. Dufour, D.B. Mount, A.Y. Deutch, D.M. Lovinger, and E. Delpire, *Hyperexcitability and epilepsy associated with disruption of the mouse neuronal-specific K-Cl cotransporter gene*. Hippocampus, 2002. **12**(2): p. 258-68.
192. Bolivar, V.J., M.N. Cook, and L. Flaherty, *Mapping of quantitative trait loci with knockout/congenic strains*. Genome Res, 2001. **11**(9): p. 1549-52.